Altered Vitamin D Metabolism in Health and Disease

Mackenzie Camille Bergagnini-Kolev

A dissertation

submitted in partial fulfillment of the

requirements for the degree of

Doctor of Philosophy

University of Washington

2020

Reading Committee:

Yvonne S. Lin, Chair

Kenneth E. Thummel

Edward J. Kelly

Program Authorized to Offer Degree:

Pharmaceutics

University of Washington

Abstract

Altered Vitamin D Metabolism in Health and Disease

Mackenzie Camille Bergagnini-Kolev

Chair of the Supervisory Committee:

Yvonne S. Lin

Department of Pharmaceutics

Vitamin D (cholecalciferol or ergocalciferol) is essential for regulating serum calcium and maintaining bone integrity. As vitamin D is not biologically active, it must undergo two sequential enzyme-catalyzed hydroxylations to form the active metabolite, 1α,25-hydroxyvitamin D ($1\alpha,25(OH)_2D$), via the intermediate, 25-hydroxyvitamin D (25(OH)D). The predominant circulating form of 25(OH)D, $25(OH)D_3$, is metabolized to other metabolites, including 24,25-dihydroxyvitamin D_3 ($24,25(OH)_2D_3$), 4β,25-dihydroxyvitamin D_3 ($4\beta,25(OH)_2D_3$), 25-hydroxyvitamin D-3-O-sulfate ($25(OH)D_3$-S), and 25-hydroxyvitamin D-3-O-glucuronide ($25(OH)D_3$-G). Changes in enzyme expression due to disease, ontogeny, or drug interactions may alter the circulating concentrations of $25(OH)D_3$ and its metabolites, and contribute to an increased risk of vitamin D deficiency. The aim of this dissertation was to explore mechanisms of altered vitamin D homeostasis in patients with cystic fibrosis (CF) and in pregnant women, and to evaluate $4\beta,25(OH)_2D_3$ as an endogenous biomarker of CYP3A4 activity. Chapter 2 describes the development and validation of a liquid chromatography-tandem mass spectrometry (LC-MS/MS) method for the simultaneous quantification of vitamin D_2, vitamin D_3,

25(OH)D_2, 25(OH)D_3, 1α,25(OH)$_2D_2$, 1α,25(OH)$_2D_3$, 24R,25(OH)$_2D_3$, 4β,25(OH)$_2D_3$, 1β,25(OH)$_2D_3$, and 1α,24,25(OH)$_3D_3$. We measured the serum concentration of 25(OH)D_3 and selected metabolites in a cohort of patients with CF (n = 83) and age-, sex-, and race-matched healthy controls (n=82) (Chapter 3). Patients with CF had 15%, 35%, and 40% lower circulating concentrations of 1α,25(OH)$_2D_3$, 4β,25(OH)$_2D_3$, and 25(OH)D_3-S, respectively. We found no difference in the clearance or half-life of d_6-25(OH)D_3 in patients with CF compared to healthy controls (n = 5 per group) after IV bolus administration of d_6-25(OH)D_3. To assess changes in 25(OH)D_3 metabolism during pregnancy, we measured 25(OH)D_3 and selected metabolites in a longitudinal study of healthy women (n = 15) before, during, and after pregnancy (Chapter 4). The change in the concentration of 25(OH)D_3 and its metabolites were evaluated using linear mixed-effects, modeling. The model predicted increase in the concentration of 25(OH)D_3 was 45% during pregnancy. Serum concentrations of 1α,25(OH)$_2D_3$, 4β,25(OH)$_2D_3$, and 25(OH)D_3-G increased by 200%, 14%, and 38%, respectively, as estimated by the linear mixed-effects model from pre-pregnancy to 36 weeks of gestation ($p < 0.001$). Additionally, 25(OH)D_3-S concentrations decreased 25% from pre-pregnancy to 36 weeks of gestation ($p < 0.001$ for all). Protein binding was altered during pregnancy; vitamin D binding protein (VDBP) serum concentrations increased by 190% and albumin concentrations decreased 26% from pre-pregnancy to 36 weeks of gestation, resulting in a 20% decrease in the percent unbound of 25(OH)D_3. To evaluate the potential of 4β,25(OH)$_2D_3$ as a biomarker of CYP3A4 activity, we developed semi-mechanistic pharmacokinetic-pharmacodynamic models for midazolam, clarithromycin, rifampin, 25(OH)D_3, and 4β,25(OH)$_2D_3$. The midazolam, clarithromycin, and rifampin models were developed using published clinical data. Model parameters for 25(OH)D_3 and 4β,25(OH)$_2D_3$ were estimated using clinical data following administration of placebo (control), clarithromycin, rifampin, or clarithromycin and rifampin in combination for 14 days. The sensitivity of 4β,25(OH)$_2D_3$ to detect induction or mechanism-based inhibition of CYP3A4 was compared to midazolam, a sensitive probe drug for CYP3A4 activity. For mechanism-based

inhibition, we found that a 5.4-fold increase in midazolam AUC corresponded with a 46% decrease in the serum concentration 4β,25$(OH)_2D_3$. For induction, we found that an 44% decrease in midazolam AUC corresponded with a 200% increase in 4β,25$(OH)_2D_3$ activity. Further clinical studies are necessary to validate 4β,25$(OH)_2D_3$ as a biomarker of CYP3A4 activity. Although there are still many unanswered questions, the research presented in this dissertation furthers our understanding of vitamin D disposition in health and disease, and provides more insight into the complexity of vitamin D homeostasis.

Dedication

To my family – for constant love, support, and encouragement. You are my cheerleaders; none of this would be possible without you.

Acknowledgements

To my doctoral advisor, Dr. Yvonne Lin, thank you for your mentorship and encouragement. Thank you for giving me the pushes I needed to keep moving forward, even when I felt lost and discouraged. You taught me to think critically, thoroughly review my data, and the power of detailed proofreading.

To my doctoral committee – Dr. Kenneth Thummel, Dr. Jashvant Unadkat, Dr. Edward Kelly, and Dr. Cathy Yeung – thank you for your dedication and guidance. Your thoughtful questions and discussion pushed me to think critically of my work.

To those who have assisted with all of my mass spec troubles, completing all of my work would not have been possible without your support. Dale and Tauri, thank you for patience and encouragement as I learned how to use a mass spec. The PK lab – Brian Phillips, Dr. Laura Shireman, Calder Brauchla, and Alex Menn – thank you for maintaining the instruments and labs, listening to me complain about the Sciex, and celebrating my successes.

To my wonderful classmates – Dr. Lindsay Henderson, Dr. Lyrialle Han, and Kevin Lidberg, you have supported and encouraged me from the very beginning. My fellow lab members, Dr. Brice Thompson and Dr. Freddy Chen, thank you for the many laughs and thoughtful lab meetings. To all of my collaborators, thank you for the opportunity to work with you, for sharing your precious clinical samples, and for your scientific insights.

To the SWOSU Department of Chemistry and Physics, thank for always challenging me in my coursework. You encouraged me to explore research careers and apply for graduate programs outside of my comfort zone.

To my family, I would not be who I am without all of you in my life. I have learned so much from each and every one of you. Dad, you taught me to never be afraid of getting messy and to passionately pursue the things you love. Mom, you taught me hard work and the power of being a strong, educated woman. Grandpa Mike, from a young age you encouraged hard

work, critical thinking, and problem solving. Lastly, to my loving husband, Nikolche, you are my biggest supporter. I could not have done this without you in my corner.

Table of Contents

Chapter 1.

Introduction

1.1. Background

Vitamin D is a fat-soluble hormone, derived from a steroid precursor, that plays an essential role in the human endocrine system (1-6). Vitamin D works with parathyroid hormone (PTH) to regulate calcium homeostasis (2-5). Low levels of vitamin D result in bone disorders such as rickets and osteoporosis (1, 2, 7-13). However, more recent literature suggests that adequate levels of vitamin D are also key in overall health (7, 14-18). Low levels of vitamin D have been linked to decreased immune function, increased risk of cardiovascular disease, and can exacerbate chronic health conditions like chronic kidney disease (19-21). It is estimated that only 40-60% of adults in the United States are vitamin D sufficient (6, 22-25). As a result, current research is focused on understanding the contributors to vitamin D deficiency and insufficiency, apart from low vitamin D intake.

1.2. Vitamin D

Vitamin D exists in two forms, vitamin D_2, ergocalciferol, and vitamin D_3, cholecalciferol. These molecules have the same backbone and differ only in the side chain with the addition of a methyl group on carbon 24 and a double bond between carbon 22 and 23 (Figure 1.1) (3). Vitamin D_3 can be synthesized endogenously from 7-dehydrocholesterol (3, 5, 26-28). Upon exposure to ultraviolet (UVB) light, keratinocytes in the skin photolytically convert 7-dehydrocholesertol to pre-vitamin D_3, followed by thermal isomerization to form vitamin D_3 (2, 3). Although both vitamin D_3 and vitamin D_2 can be absorbed from dietary sources, there are only a few foods which are a natural source of the hormone (3, 29). These foods include eggs, mushrooms and fatty cold-water fish like salmon (3-5). Many processed foods containing high levels of calcium are also fortified with either vitamin D_2 or vitamin D_3 (e.g., dairy products, bread, and cereal) (29-31). In addition, vitamin D is sold as a standalone supplement or as a

component in most multivitamins with doses ranging from 400-10,000 international units (IU) (29, 30, 32).

1.3. Mechanism of Action of Vitamin D

Vitamin D regulates serum calcium homeostasis through its binding of the active form, 1α,25$(OH)_2$D, to the vitamin D receptor (VDR) (3, 28, 33). When serum calcium is low, PTH is released from the parathyroid gland and stimulates the formation of 1α,25$(OH)_2$D from 25(OH)D in the kidney by cytochrome P450 27B1 (CYP27B1) (33, 34). Together PTH and 1α,25$(OH)_2$D increase calcium absorption in the gut, increase calcium reabsorption from bone, and decrease phosphate reabsorption in the kidney (33, 34). Some of these effects are mediated by transcriptional activation of calcium transport and binding proteins (35, 36). The release of fibroblast growth factor 23 (FGF23) from bone is also stimulated by increased levels of 1α,25$(OH)_2$D (33, 34). FGF23 can downregulate CYP27B1 and induce the catabolism of 1α,25$(OH)_2$D, thereby decreasing the circulating levels of 1α,25$(OH)_2$D after it has exerted its biological effect (33, 37). VDR is also expressed in immune cells, intestines, skin, and placenta (29). 1α,25$(OH)_2$D is known to directly and indirectly regulate more than 200 genes, including genes that control cell differentiation, apoptosis, and endogenous and exogenous metabolism (29, 38).

1.4. Definition of Vitamin D Deficiency and Insufficiency

The half-life of 1α,25$(OH)_2$D, determined after oral administration, is approximately 4-6 hours (39). Due to the short half-life of 1α,25$(OH)_2$D, 25(OH)D is typically used as a biomarker of vitamin D status (24, 34, 40, 41). With an estimated half-life of 2 weeks, 25(OH)D better reflects long-term exposure to vitamin D and can be rapidly converted to 1α,25$(OH)_2$D as needed (24, 34, 41). Although vitamin D_2 and D_3 have differing biological activities, total 25(OH)D (i.e., the summed concentrations of 25$(OH)D_2$ and 25$(OH)D_3$) are used for clinical assessment of vitamin D status (24, 34, 41). Prior to the 1990s, vitamin D sufficiency was based

on a serum 25(OH)D concentration greater than 10 ng/mL (25 nM), which was thought to be the minimum 25(OH)D concentration needed to prevent rickets (41, 42). Over the last 20 years, a new reference range for vitamin D sufficiency was established based on the concentration of 25(OH)D required to minimize serum PTH (41). Currently, the Endocrine Society defines vitamin D sufficiency as serum 25(OH)D concentrations greater than 30 ng/mL (41, 43). Vitamin D insufficiency is defined as serum 25(OH)D concentrations between 20 to 29 ng/mL and vitamin D deficiency as concentrations below 20 ng/mL (43, 44). In contrast, the Institute of Medicine (IOM) defines vitamin D sufficiency as 25(OH)D concentration greater than 20 ng/mL (45).

1.5. Bound versus Unbound Vitamin D

The free hormone hypothesis proposes that only the unbound portion of circulating hormones are able to enter the cell and exert a biological effect (46-48). The remaining bound fraction is restricted to blood and is too large to pass through the cell membrane (46-48). Since greater than 99% of 25(OH)D and 1α,25$(OH)_2$D circulate bound to vitamin D binding protein (VDBP) and albumin, researchers have long questioned whether total or unbound concentrations of 25(OH)D better represent vitamin D status (47, 48). Only 0.02 – 0.09% of 25(OH)D and 0.4% of 1α,25$(OH)_2$D circulate unbound to plasma proteins, with ~85% bound to VDBP and the remaining ~15% bound to albumin (49, 50). In a direct comparison, the dissociation constant of 25(OH)D_3 for VDBP was half of that for 25(OH)D_2, suggesting that the unbound fraction of 25(OH)D_2 is higher than 25(OH)D_3, which leads to a greater fraction of 25(OH)D_2 circulating unbound to plasma proteins (51).

Polymorphisms in *VDBP* can affect the circulating concentration of VDBP as well as the affinity of the protein for the hormone and, hence, total and free concentrations of 25(OH)D. In a study of more than 500 non-pregnant women, subjects homozygous for the *GC1* haplotype had serum concentrations of VDBP approximately 20% higher than subjects homozygous for the *GC2* haplotype (52). Additionally, Schwartz et al. found that the total and unbound

concentrations of 25(OH)D_3 were lowest in participants homozygous for the *GC2* haplotype (53).

1.6. Biological Differences Between Vitamin D_2 and Vitamin D_3

The structural differences between vitamin D_2 and vitamin D_3 result in differences in the distribution and clearance of 25(OH)D. Supplementation with vitamin D_3 is more effective at raising serum levels of total 25(OH)D. In a study by Armas et al., 30 men were followed for 28 days to evaluate the difference in pharmacokinetics of 25(OH)D after high dose supplementation (50,000 IU) of either vitamin D_2 or vitamin D_3 (54). Both vitamin D_2 and vitamin D_3 were absorbed at the same rate (54). However, the subjects treated with vitamin D_2 achieved a peak 25(OH)D concentration ~4 ng/mL higher than baseline on day 3. In contrast, subjects treated with vitamin D_3 reached a peak 25(OH)D concentration ~7 ng/mL higher than baseline on day 14 (54). Concentrations of 25(OH)D remained elevated above baseline on day 28 for subjects treated with vitamin D_3, whereas subjects treated with vitamin D_2 had 25(OH)D concentrations that dropped below baseline by day 21 (54). Additionally, the area under the plasma vs. concentration time curve from day 0 to day 28 of 25(OH)D was 3.3 times higher in subjects that received vitamin D_3 compared to subjects that received vitamin D_2 (54). A similar study saw a 70% higher increase in 25(OH)D concentrations after treatment with vitamin D_3 compared with vitamin D_2 (55).

In 2015, Jones et al. published a pharmacokinetic study comparing the half-lives of deuterium-labeled vitamin D_2 and vitamin D_3 following oral administration (40). The mean observed half-life of 25(OH)D_3 was 15.1 days compared to 13.9 days for 25(OH)D_2 (40). The observed difference in the half-life of 25(OH)D_2 and 25(OH)D_3 was attributed to the difference in binding affinity to VDBP (40, 54, 55). It is hypothesized that as a higher percentage of 25(OH)D_2 circulates unbound to VDBP and albumin, more 25(OH)D_2 is available for metabolism and elimination (1, 46, 48).

1.7. Vitamin D Metabolism

As previously discussed, vitamin D is not biologically active and must undergo a series of enzyme-catalyzed hydroxylations to form the active metabolite, 1α,25(OH)$_2$D. In addition to forming the active metabolite, 25(OH)D_3 is metabolized to several inactive metabolites (3-5, 28, 56). The specific metabolites studied in this dissertation are discussed in more detail below. Partial metabolic schemes for vitamin D_2 and vitamin D_3 are presented in Figure 1.2 and Figure 1.3, respectively.

1.7.1. Formation of 25-Hydroxyvitamin D

The conversion of vitamin D to 25(OH)D occurs primarily in the liver, catalyzed by multiple microsomal and mitochondrial CYP isoforms (3, 5, 28). The primary enzyme of 25(OH)D formation is CYP2R1, first identified in the microsomal fraction of mouse livers (3, 57-62). CYP2R1 is able to hydroxylate both vitamin D_2 and vitamin D_3 with similar efficiency (58, 62). In CYP2R1-null mouse models, 25(OH)D concentrations were reduced more than 50% without large effects on serum calcium and phosphate (61, 62). In humans, a rare genetic *CYP2R1* variant was identified in Nigerians with severe bone disorders (57, 58, 60). *In vitro* kinetic experiments conducted in transfected HEK293T cells showed that the *CYP2R1* variants resulted in misfolded, inactive CYP2R1 protein and a nearly 2-fold decrease in the intrinsic clearance for 25-hydroxylation (60). Generally, individuals with “genetic rickets” (i.e., *CYP2R1* variants) present with serum 25(OH)D concentrations below 15 ng/mL; indeed, one individual was reported to have a 25(OH)D concentration of 1.5 ng/mL (60). These individuals must be treated with high dose (> 50,000 IU monthly) vitamin D_3 and calcium to resolve symptoms of rickets (57, 60).

The enzyme with the second largest contribution to formation of 25(OH)D formation is CYP27A1 (2, 3, 56, 61, 62). Unlike CYP2R1, CYP27A1 is expressed in the mitochondria of the liver and only hydroxylates vitamin D_3 (56, 59, 61, 62). Surprisingly, mouse knock-out models of

CYP27A1 have serum 25(OH)D_3 concentrations 2- to 3-times higher than wild-type mice, suggesting that other CYP enzymes are able to compensate for the absence of *CYP27A1* (3, 4, 56, 59, 61, 62). In individuals with *CYP27A1* variants that result in inactive CYP27A1, plasma/serum 25(OH)D concentrations are about half that of healthy controls (14.6 ± 6.6 ng/mL compared to 30.4 ± 8.0 ng/mL), but in general, these individuals do not present with rickets or other bone disorders (3, 63). Instead, these patients are diagnosed with cerebrotendinous xanthomatosis, a condition characterized by abnormal bile and cholesterol metabolism, reflecting the more critical role of the enzyme in maintaining cholesterol homeostasis (3, 63-66).

1.7.2. Formation of 1α,25-dihydroxyvitamin D

Further hydroxylation of 25(OH)D to 1α,25$(OH)_2$D is performed exclusively by CYP27B1, primarily in the proximal tubule of the kidney (56, 59, 67). With a reference range for 1α,25$(OH)_2D_3$ concentrations of 24 to 66 pg/mL, 1α,25$(OH)_2$D circulates at concentrations approximately 1000-fold lower than 25(OH)D (68). Unlike 25(OH)D, the concentration of 1α,25$(OH)_2$D is tightly regulated by PTH, FGF23, and autoregulatory mechanisms (33). PTH induces the expression of CYP27B1, while FGF and 1α,25$(OH)_2$D downregulates CYP27B1 synthesis (33). While the kidney is the primary source of circulating 1α,25$(OH)_2$D, other organs (e.g., small intestine, skin, bone, immune cells, and placenta) can contribute to the local formation of 1α,25$(OH)_2$D, which may drive local biological effects (27).

1.7.3. Formation of 24,25-dihydroxyvitamin D

Located in the kidney mitochondria, CYP24A1 converts 25(OH)D to 24,25-dihydroxyvitamin D (24,25$(OH)_2$D) (3, 56, 59, 67). In a study of 1,996 subjects, the mean serum concentrations of 24,25$(OH)_2$D was reported to be 5.7 ± 3.4 ng/mL (69). Humans with *CYP24A1* mutations resulting in inactive protein develop idiopathic infantile hypercalcemia (IIH) in

childhood (3, 70). In contrast to CYP27B1, FGF23 stimulates CYP24A1 activity, whereas PTH and 1α,25$(OH)_2D_3$ downregulate CYP24A1 expression (33).

1.7.4. Formation of 4β,25-dihydroxyvitamin D_3

More recently, 4β,25-dihydroxyvitamin D_3 (4β,25$(OH)_2D_3$) has been identified as an additional elimination pathway of 25$(OH)D_3$. The search for an alternative CYP3A4-dependent pathway began after Brodie et al. reported that 25$(OH)D_3$ concentrations were reduced after extended treatment with rifampin, a potent inducer of CYP activity (71, 72). In 2012, Wang et al. reported that 4β,25$(OH)_2D_3$ is a metabolite of 25$(OH)D_3$ following enzymatic incubations with CYP3A4 Supersomes and human liver microsomes (73). Additionally, they determined that 25$(OH)D_3$ was not converted to 4β,25$(OH)_2D_3$ by CYP24A1 or other P450 enzymes (74). Clinical studies confirmed that serum concentrations of 4β,25$(OH)_2D_3$ increased after treatment with rifampin (38, 70, 73, 74). In 2017, Hawkes et al. tested rifampin as a treatment for IIH (70). In the two patients that received rifampin, serum calcium, PTH and 1α,25$(OH)_2D_3$ concentrations were reduced; the reduction was hypothesized to be due to the induction of CYP3A4 and increased formation of 4β,25$(OH)_2D_3$ (70). Additionally, there is potential that 4β,25$(OH)_2D_3$ could serve as a biomarker of CYP3A4 activity *in vivo*.

1.7.5. Formation of 25-hydroxyvitamin D_3-3-O-Sulfate

A major metabolite of 25$(OH)D_3$ is 25-hydroxyvitamin D_3-O-sulfate (25$(OH)D_3$-S), which circulates at plasma concentrations similar to 25$(OH)D_3$ (10 to 40 ng/mL) (75-80). Using *in vitro* incubations with human liver cytosol, recombinant sulfotransferase (SULT) enzymes and human hepatocytes, investigators identified SULT2A1 as the liver enzyme responsible for the formation of 25$(OH)D_3$-S from 25$(OH)D_3$ (75, 81). 25$(OH)D_3$-S was detected in human bile at a concentration of approximately 1.3 ng/mL, which supports the hypothesis that 25$(OH)D_3$-S undergoes enterohepatic recirculation and may serve as an additional source of 25$(OH)D_3$ once

deconjugated (75). Additionally, 25(OH)D_3-S circulates tightly bound to VDBP and is not excreted into the urine (75).

1.7.6. Formation of 25-hydroxyvitamin D_3-3-O-Glucuronide

In 1975, glucuronidated metabolites of 25(OH)D_3 were detected in human bile after IV administration of ^{3}H-25(OH)D_3 (82). Subsequently, two isomers of 25-hydroxyvitamin D_3-O-glucuronides, at the 3- and 25- positions, were identified in rat and human bile (83, 84). 25-hydroxyvitamin D_3-3-O-glucuronide (25(OH)D_3-G) is formed primarily from 25(OH)D_3 by uridine 5'-diphospho-glucuronosyltransferase (UGT) 1A4, with a smaller contribution from UGT1A3 (85). Similar to 25(OH)D_3-S, 25(OH)D_3-G is thought to undergo enterohepatic recirculation after biliary excretion into the small intestine (82, 84-86).

1.8. Bone Health

Vitamin D plays an essential role in bone growth and development in children (10, 13, 23, 87). Children who are vitamin D deficient develop rickets, a bone disorder characterized by pain in extremities, short stature, bowed legs, and deformed teeth (88). Children with rickets are also at an increased risk of bone fractures (88). Children with rickets can be treated with high doses of vitamin D and calcium and frequently, with early detection and proper treatment, bone deformities improve or are reversed (88).

In addition, low serum levels of 25(OH)D are associated with poor bone mineral density (BMD), osteoporosis, and increased risk of bone fractures in adults (89, 90). In a study of more than 13,000 adults 20 years of age and older, bone mineralization was strongly associated with circulating levels of 25(OH)D (89). Participants in the upper quintile of 25(OH)D concentrations had a 4% higher BMD compared to those in the lowest quintile (89). In a meta-analysis of 12 randomized-control trials, subjects treated with 700 to 800 IU of vitamin D_3 daily had a 23% and 26% reduction in the relative risk of hip fractures and non-vertebral fractions, respectively,

compared to subjects treated with 400 IU of vitamin D_3 per day (90). Subjects receiving 400 IU of vitamin D_3 per day had no significant benefit compared to untreated subjects (90). A meta-analysis published in 2017 found that supplementation with vitamin D and calcium reduced the risk of falls in the elderly compared to those not receiving supplements (odds ratio: 0.87 95% CI, 0.80-0.94) (91).

1.9. Beyond Bone Health

While vitamin D is traditionally known for its role in bone health, other biological effects related to systemic 25(OH)D is an area of active research. CYP27B1 and VDR are expressed in immune cells, lung, intestines, skin, and reproductive organs, suggesting that 1α,25$(OH)_2$D is synthesized outside of the control of the parathyroid endocrine system (7, 15-17, 26, 27). For example, production of 1α,25$(OH)_2$D stimulates the expression of antibacterial proteins in macrophages (14, 16, 92, 93). Expression of these antibacterial proteins are triggered by pathogens and recruit additional immune cells to the site of infection (14, 16, 92, 93). Clinical studies of tuberculosis, upper respiratory infections, and influenza reported that lower levels of 25(OH)D were associated with longer duration of illness, as well as increased risk of hospitalization and mortality (14, 15).

Additionally, vitamin D deficiency and insufficiency have been linked to a severity of various autoimmune disorders, including Type 1 Diabetes, rheumatoid arthritis, and multiple sclerosis (14, 18, 20, 22, 94-96). Individuals with lower levels of 25(OH)D were at increased risk of coronary heart disease and cardiac mortality (21, 22, 96-98). Epidemiological studies found that lower circulating levels of 25(OH)D were associated with an increased risk of cancer, most notably in the colon (15, 17, 21, 22, 87, 96). In a study with 193 women diagnosed with colorectal cancer, the relative risk of developing colorectal cancer was 0.53 for subjects in the upper quintile of serum 25(OH)D (median: 35.2 ng/mL) compared to those in the lowest quintile (median: 15 ng/mL) (90, 99). Individuals with low levels of 25(OH)D were found to be at an

increased risk of being diagnosed with polycystic ovary syndrome (PCOS) or endometriosis, and had higher rates of infertility (100). Although epidemiology studies found associations between serum levels of 25(OH)D and risk of disease, clinical studies in which subjects were treated with vitamin D frequently fail to confirm these associations in patients with diabetes and pregnant women (101, 102).

1.10. Dissertation Aims

The aim of this dissertation was to explore mechanisms of altered vitamin D homeostasis in several specific populations. As discussed previously, vitamin D undergoes a series of metabolic steps for biological activation, inactivation, and storage. The circulating concentration of 25(OH)D_3 and its metabolites, and thereby risk of vitamin D deficiency, may be altered by changes in enzyme expression caused by disease, ontogeny, or drug interactions. An additional mechanism of altered vitamin D homeostasis could be as a result of changes in the plasma concentration of VDBP and albumin due to disease or pregnancy. Many conditions, such as pregnancy and chronic kidney disease, result in altered concentrations of serum proteins (20, 26, 93, 103-105).

This dissertation focuses on understanding altered 25(OH)D metabolism in pregnancy, in patients with cystic fibrosis, and following drug interactions. In Chapter 2, we developed a method to accurately and reproducibly measure 25(OH)D and its hydroxylated metabolites in human plasma and serum. In Chapter 3, we characterized the changes in 25(OH)D_3 metabolism and pharmacokinetics in patients with cystic fibrosis (CF) compared to age- and gender-matched healthy controls. In Chapter 4, we studied the longitudinal effects of pregnancy on 25(OH)D_3 metabolism and plasma proteins. Lastly, in Chapter 5, we investigated 4β,25(OH)$_2D_3$ as a potential biomarker of CYP3A4 activity by using a semi-mechanistic pharmacokinetic model to describe CYP3A4 induction by rifampin and CYP3A4 inhibition by clarithromycin. A brief rationale for each chapter is presented below.

1.10.1. Cystic Fibrosis

Cystic fibrosis (CF) is an autosomal recessive genetic disorder that affects more than 33,000 people in the U.S (106-109). CF is caused by a mutation in the cystic fibrosis transmembrane conductance regulator (*CFTR*) gene (107, 108). Although CFTR is expressed throughout the body, CF primarily affects epithelial cells and results in mucus retention and chronic lung infections (107, 110-112). The prevalence of vitamin D deficiency and insufficiency in CF patients was estimated to be as high as 90% (113, 114). Consequently, many investigators are trying to understand the underlying causes of low vitamin D levels in patients with CF.

Vitamin D deficiency in patients with CF increases the risk of lung infections and lower bone mass density (106, 115-121). While the majority of research in the last two decades has focused on the development of new vitamin D supplement formulations and alternative dosing strategies to increase plasma concentrations of $25(OH)D_3$, some researchers have suggested that decreased formation or increased metabolism of $25(OH)D_3$ may contribute to vitamin D deficiency in patients with CF (113, 117, 120, 122-125). Additionally, a more complete profile of $25(OH)D_3$ metabolites has yet to be determined in patients with CF. In Chapter 3, we characterized the circulating levels of $25(OH)D_3$ and five of its metabolites in patients with CF and paired healthy control subjects. Additionally, we assessed the pharmacokinetics of a single intravenous dose of deuterium-labeled 25-hydroxyvitamin D_3 (d_6-$25(OH)D_3$) in patients with CF and healthy controls to evaluate whether increased $25(OH)D_3$ clearance contributes to low $25(OH)D_3$ levels in patients with CF.

1.10.2. Pregnancy

Adequate levels of vitamin D during pregnancy are essential for fetal bone development and maternal health. Low maternal levels of 25(OH)D are associated with pre-eclampsia, preterm delivery, low birthweight, and childhood asthma (100, 126-131). Although 50-90% of

women take prenatal vitamins, 45% of white women and 83% of black women in the northeastern United States were classified as vitamin D deficient or insufficient at the time of delivery, and only 34% of white and 7.6% of black newborns were vitamin D sufficient at birth (132, 133). Physiological changes that occur in pregnancy (i.e., changes in enzyme expression, cardiac output, protein binding, and placental enzyme expression) may contribute to altered concentrations of $25(OH)D_3$ and its metabolites (134). In Chapter 4, we measured $25(OH)D_3$ and five of its metabolites in a cohort of pregnant women to assess longitudinal changes from pre-pregnancy, through gestation, and postpartum. This observational study was unique in that subjects were recruited prior to becoming pregnant, pregnancy samples were collected as early as 4 weeks of gestation, and up to 11 samples were collected from each woman during pregnancy and postpartum. Plasma concentrations of specific metabolites that have not been previously reported in pregnant women (i.e., $4\beta,25(OH)_2D_3$, $25(OH)D_3$-S, and $25(OH)D_3$-G) were measured during pregnancy and postpartum. Additionally, we characterized the plasma concentrations of VDBP and albumin to assess changes in the free concentrations of $25(OH)D_3$ and $1\alpha,25(OH)_2D_3$ during the first trimester of pregnancy.

1.10.3. 4β,25-Dihydroxyvitamin D_3 as a Biomarker of CYP3A4 Activity

Endogenous biomarkers of drug metabolizing enzymes and transporters are useful tools early in clinical development for evaluating the potential of new molecular entities to cause drug interactions. Understanding the sensitivity, specificity, and half-life of a biomarker is essential for implementation into clinical development. In Chapter 5, we used semi-mechanistic pharmacokinetic modeling to investigate $4\beta,25(OH)_2D_3$ as an endogenous biomarker of CYP3A4 activity. Plasma concentrations of $4\beta,25(OH)_2D_3$ and $25(OH)D_3$ were measured before, during, and after treatment with water (control arm), rifampin, clarithromycin, or rifampin and clarithromycin in combination. The data from the study and published *in vitro* and *in vivo* studies were used to build semi-mechanistic models of midazolam, rifampin, clarithromycin, $25(OH)D_3$

and 4β,25(OH)$_2$D$_3$. To assess the duration of treatment and sample size required to detect significant changes in the plasma concentration of 4β,25(OH)$_2$D$_3$, simulations of clinical trials were conducted. Additionally, we simulated the effects of strong, moderate, and weak inhibitors of CYP3A4 to probe the *in vivo* sensitivity of 4β,25(OH)$_2$D$_3$ as a biomarker of CYP3A4 activity.

1.11. References

(1) Bikle, D.D., Gee, E., Halloran, B., Kowalski, M.A., Ryzen, E. & Haddad, J.G. Assessment of the free fraction of 25-hydroxyvitamin D in serum and its regulation by albumin and the vitamin D-binding protein. *J Clin Endocrinol Metab* **63**, 954-9 (1986).

(2) Bikle, D.D. Vitamin D and bone. *Curr Osteoporos Rep* **10**, 151-9 (2012).

(3) Bikle, D.D. Vitamin D metabolism, mechanism of action, and clinical applications. *Chem Biol* **21**, 319-29 (2014).

(4) Gallagher, J.C. & Bikle, D.D. Vitamin D: Mechanisms of Action and Clinical Applications. *Endocrinol Metab Clin North Am* **46**, xvii-xviii (2017).

(5) Bikle, D. Vitamin D: Production, Metabolism, and Mechanisms of Action. In: *Endotext* (eds. Feingold, K.R., Anawalt, B., Boyce, A., Chrousos, G., Dungan, K., Grossman, A. *et al.*) (South Dartmouth (MA), 2000).

(6) Nair, R. & Maseeh, A. Vitamin D: The "sunshine" vitamin. *Journal of pharmacology & pharmacotherapeutics* **3**, 118-26 (2012).

(7) Bikle, D.D. & Bouillon, R. Vitamin D and bone and beyond. *Bone Rep* **9**, 120-1 (2018).

(8) Aris, R.M., Lester, G.E., Dingman, S. & Ontjes, D.A. Altered calcium homeostasis in adults with cystic fibrosis. *Osteoporosis international : a journal established as result of cooperation between the European Foundation for Osteoporosis and the National Osteoporosis Foundation of the USA* **10**, 102-8 (1999).

(9) Holick, M.F. The role of vitamin D for bone health and fracture prevention. *Curr Osteoporos Rep* **4**, 96-102 (2006).

(10) Holick, M.F. Resurrection of vitamin D deficiency and rickets. *The Journal of clinical investigation* **116**, 2062-72 (2006).

(11) Holick, M.F. Vitamin D and bone health. *J Nutr* **126**, 1159s-64s (1996).

(12) Karaguzel, G. & Holick, M.F. Diagnosis and treatment of osteopenia. *Reviews in endocrine & metabolic disorders* **11**, 237-51 (2010).

(13) Palermo, N.E. & Holick, M.F. Vitamin D, bone health, and other health benefits in pediatric patients. *Journal of pediatric rehabilitation medicine* **7**, 179-92 (2014).

(14) Bartley, J. Vitamin D: emerging roles in infection and immunity. *Expert review of anti-infective therapy* **8**, 1359-69 (2010).

(15) Bikle, D. Nonclassic actions of vitamin D. *J Clin Endocrinol Metab* **94**, 26-34 (2009).

(16) Christakos, S., Dhawan, P., Ajibade, D., Benn, B.S., Feng, J. & Joshi, S.S. Mechanisms involved in vitamin D mediated intestinal calcium absorption and in non-classical actions of vitamin D. *J Steroid Biochem Mol Biol* **121**, 183-7 (2010).

(17) Christakos, S. *et al.* Vitamin D: beyond bone. *Ann N Y Acad Sci* **1287**, 45-58 (2013).

(18) Grant, W.B. & Holick, M.F. Benefits and requirements of vitamin D for optimal health: a review. *Alternative medicine review : a journal of clinical therapeutic* **10**, 94-111 (2005).

(19) Bizzaro, G., Antico, A., Fortunato, A. & Bizzaro, N. Vitamin D and Autoimmune Diseases: Is Vitamin D Receptor (VDR) Polymorphism the Culprit? *The Israel Medical Association journal : IMAJ* **19**, 438-43 (2017).

(20) Holick, M.F. Sunlight and vitamin D for bone health and prevention of autoimmune diseases, cancers, and cardiovascular disease. *Am J Clin Nutr* **80**, 1678s-88s (2004).

(21) Holick, M.F. Vitamin D: important for prevention of osteoporosis, cardiovascular heart disease, type 1 diabetes, autoimmune diseases, and some cancers. *Southern medical journal* **98**, 1024-7 (2005).

(22) Holick, M.F. The vitamin D deficiency pandemic and consequences for nonskeletal health: mechanisms of action. *Molecular aspects of medicine* **29**, 361-8 (2008).

(23) Hossein-nezhad, A. & Holick, M.F. Vitamin D for health: a global perspective. *Mayo Clinic proceedings* **88**, 720-55 (2013).

(24) Holick, M.F. Vitamin D status: measurement, interpretation, and clinical application. *Annals of epidemiology* **19**, 73-8 (2009).

(25) Liu, X., Baylin, A. & Levy, P.D. Vitamin D deficiency and insufficiency among US adults: prevalence, predictors and clinical implications. *Br J Nutr* **119**, 928-36 (2018).

(26) Ardawi, M.S., Nasrat, H.A. & HS, B.A.A. Calcium-regulating hormones and parathyroid hormone-related peptide in normal human pregnancy and postpartum: a longitudinal study. *Eur J Endocrinol* **137**, 402-9 (1997).

(27) Bikle, D.D. Vitamin D metabolism and function in the skin. *Mol Cell Endocrinol* **347**, 80-9 (2011).

(28) Christakos, S., Ajibade, D.V., Dhawan, P., Fechner, A.J. & Mady, L.J. Vitamin D: metabolism. *Endocrinol Metab Clin North Am* **39**, 243-53, table of contents (2010).

(29) Holick, M.F. Vitamin D deficiency. *N Engl J Med* **357**, 266-81 (2007).

(30) Tangpricha, V. Vitamin D in food and supplements. *Am J Clin Nutr* **95**, 1299-300 (2012).

(31) Holden, J.M., Lemar, L.E. & Exler, J. Vitamin D in foods: development of the US Department of Agriculture database. *Am J Clin Nutr* **87**, 1092s-6s (2008).

(32) Cashman, K.D. *et al.* Relative effectiveness of oral 25-hydroxyvitamin D3 and vitamin D3 in raising wintertime serum 25-hydroxyvitamin D in older adults. *Am J Clin Nutr* **95**, 1350-6 (2012).

(33) Goodman, L.S., Brunton, L.L., Chabner, B. & Knollmann, B.r.C. *Goodman & Gilman's pharmacological basis of therapeutics*. 12th edn. (McGraw-Hill: New York, 2011).

(34) Herrmann, M., Farrell, C.L., Pusceddu, I., Fabregat-Cabello, N. & Cavalier, E. Assessment of vitamin D status - a changing landscape. *Clinical chemistry and laboratory medicine* **55**, 3-26 (2017).

(35) Haussler, M.R. *et al.* Molecular mechanisms of vitamin D action. *Calcified tissue international* **92**, 77-98 (2013).

(36) van de Graaf, S.F., Boullart, I., Hoenderop, J.G. & Bindels, R.J. Regulation of the epithelial Ca2+ channels TRPV5 and TRPV6 by 1alpha,25-dihydroxy Vitamin D3 and dietary Ca2+. *J Steroid Biochem Mol Biol* **89-90**, 303-8 (2004).

(37) Farrell, C.J., Martin, S., McWhinney, B., Straub, I., Williams, P. & Herrmann, M. State-of-the-art vitamin D assays: a comparison of automated immunoassays with liquid chromatography-tandem mass spectrometry methods. *Clin Chem* **58**, 531-42 (2012).

(38) Wang, Z., Schuetz, E.G., Xu, Y. & Thummel, K.E. Interplay between vitamin D and the drug metabolizing enzyme CYP3A4. *J Steroid Biochem Mol Biol* **136**, 54-8 (2013).

(39) Jin, S.E., Park, J.S. & Kim, C.K. Pharmacokinetics of oral calcitriol in healthy human based on the analysis with an enzyme immunoassay. *Pharmacological research* **60**, 57-60 (2009).

(40) Jones, K.S. *et al.* 25(OH)D2 half-life is shorter than 25(OH)D3 half-life and is influenced by DBP concentration and genotype. *J Clin Endocrinol Metab* **99**, 3373-81 (2014).

(41) Holick, M.F. *et al.* Guidelines for preventing and treating vitamin D deficiency and insufficiency revisited. *J Clin Endocrinol Metab* **97**, 1153-8 (2012).

(42) Holick, M.F. The vitamin D deficiency pandemic: Approaches for diagnosis, treatment and prevention. *Reviews in endocrine & metabolic disorders* **18**, 153-65 (2017).

(43) Pramyothin, P. & Holick, M.F. Vitamin D supplementation: guidelines and evidence for subclinical deficiency. *Current opinion in gastroenterology* **28**, 139-50 (2012).

(44) Binkley, N., Krueger, D.C., Morgan, S. & Wiebe, D. Current status of clinical 25-hydroxyvitamin D measurement: an assessment of between-laboratory agreement. *Clin Chim Acta* **411**, 1976-82 (2010).

(45) Rosen, C.J. *et al.* IOM committee members respond to Endocrine Society vitamin D guideline. *J Clin Endocrinol Metab* **97**, 1146-52 (2012).

(46) Jassil, N.K., Sharma, A., Bikle, D. & Wang, X. Vitamin D Binding Protein and 25-Hydroxyvitamin D Levels: Emerging Clinical Applications. *Endocr Pract* **23**, 605-13 (2017).

(47) Chun, R.F., Peercy, B.E., Orwoll, E.S., Nielson, C.M., Adams, J.S. & Hewison, M. Vitamin D and DBP: the free hormone hypothesis revisited. *J Steroid Biochem Mol Biol* **144 Pt A**, 132-7 (2014).

(48) Bikle, D., Bouillon, R., Thadhani, R. & Schoenmakers, I. Vitamin D metabolites in captivity? Should we measure free or total 25(OH)D to assess vitamin D status? *J Steroid Biochem Mol Biol* **173**, 105-16 (2017).

(49) Olerod, G., Hulten, L.M., Hammarsten, O. & Klingberg, E. The variation in free 25-hydroxy vitamin D and vitamin D-binding protein with season and vitamin D status. *Endocrine connections* **6**, 111-20 (2017).

(50) Bikle, D.D. & Schwartz, J. Vitamin D Binding Protein, Total and Free Vitamin D Levels in Different Physiological and Pathophysiological Conditions. *Front Endocrinol (Lausanne)* **10**, 317 (2019).

(51) Nilsson, S.F., Ostberg, L. & Peterson, P.A. Binding of vitamin D to its human carrier plasma protein. *Biochemical and biophysical research communications* **46**, 1380-7 (1972).

(52) Lauridsen, A.L., Vestergaard, P. & Nexo, E. Mean serum concentration of vitamin D-binding protein (Gc globulin) is related to the Gc phenotype in women. *Clin Chem* **47**, 753-6 (2001).

(53) Schwartz, J.B. *et al.* Determination of Free 25(OH)D Concentrations and Their Relationships to Total 25(OH)D in Multiple Clinical Populations. *J Clin Endocrinol Metab* **103**, 3278-88 (2018).

(54) Armas, L.A., Hollis, B.W. & Heaney, R.P. Vitamin D2 is much less effective than vitamin D3 in humans. *J Clin Endocrinol Metab* **89**, 5387-91 (2004).

(55) Trang, H.M., Cole, D.E., Rubin, L.A., Pierratos, A., Siu, S. & Vieth, R. Evidence that vitamin D3 increases serum 25-hydroxyvitamin D more efficiently than does vitamin D2. *Am J Clin Nutr* **68**, 854-8 (1998).

(56) Sakaki, T., Kagawa, N., Yamamoto, K. & Inouye, K. Metabolism of vitamin D3 by cytochromes P450. *Front Biosci* **10**, 119-34 (2005).

(57) Cheng, J.B., Levine, M.A., Bell, N.H., Mangelsdorf, D.J. & Russell, D.W. Genetic evidence that the human CYP2R1 enzyme is a key vitamin D 25-hydroxylase. *Proc Natl Acad Sci U S A* **101**, 7711-5 (2004).

(58) Cheng, J.B., Motola, D.L., Mangelsdorf, D.J. & Russell, D.W. De-orphanization of cytochrome P450 2R1: a microsomal vitamin D 25-hydroxilase. *J Biol Chem* **278**, 38084-93 (2003).

(59) Jones, G., Prosser, D.E. & Kaufmann, M. Cytochrome P450-mediated metabolism of vitamin D. *J Lipid Res* **55**, 13-31 (2014).

(60) Thacher, T.D., Fischer, P.R., Singh, R.J., Roizen, J. & Levine, M.A. CYP2R1 Mutations Impair Generation of 25-hydroxyvitamin D and Cause an Atypical Form of Vitamin D Deficiency. *J Clin Endocrinol Metab* **100**, E1005-13 (2015).

(61) Zhu, J. & DeLuca, H.F. Vitamin D 25-hydroxylase - Four decades of searching, are we there yet? *Arch Biochem Biophys* **523**, 30-6 (2012).

(62) Zhu, J.G., Ochalek, J.T., Kaufmann, M., Jones, G. & Deluca, H.F. CYP2R1 is a major, but not exclusive, contributor to 25-hydroxyvitamin D production in vivo. *Proc Natl Acad Sci U S A* **110**, 15650-5 (2013).

(63) Berginer, V.M. *et al.* Osteoporosis and increased bone fractures in cerebrotendinous xanthomatosis. *Metabolism: clinical and experimental* **42**, 69-74 (1993).

(64) Bjorkhem, I. Cerebrotendinous xanthomatosis. *Current opinion in lipidology* **24**, 283-7 (2013).

(65) Koyama, S. & Kato, T. Pathophysiology of cerebrotendinous xanthomatosis. *Rinsho shinkeigaku = Clinical neurology* **56**, 821-6 (2016).

(66) Salen, G. & Steiner, R.D. Epidemiology, diagnosis, and treatment of cerebrotendinous xanthomatosis (CTX). *Journal of inherited metabolic disease* **40**, 771-81 (2017).

(67) Inouye, K. & Sakaki, T. Enzymatic studies on the key enzymes of vitamin D metabolism; 1 alpha-hydroxylase (CYP27B1) and 24-hydroxylase (CYP24). *Biotechnol Annu Rev* **7**, 179-94 (2001).

(68) Dirks, N.F. *et al.* Determination of human reference values for serum total 1,25-dihydroxyvitamin D using an extensively validated 2D ID-UPLC-MS/MS method. *J Steroid Biochem Mol Biol* **164**, 127-33 (2016).

(69) Tang, J.C.Y. *et al.* Reference intervals for serum 24,25-dihydroxyvitamin D and the ratio with 25-hydroxyvitamin D established using a newly developed LC-MS/MS method. *The Journal of nutritional biochemistry* **46**, 21-9 (2017).

(70) Hawkes, C.P., Li, D., Hakonarson, H., Meyers, K.E., Thummel, K.E. & Levine, M.A. CYP3A4 Induction by Rifampin: An Alternative Pathway for Vitamin D Inactivation in Patients With CYP24A1 Mutations. *J Clin Endocrinol Metab* **102**, 1440-6 (2017).

(71) Brodie, M.J. *et al.* Effect of rifampicin and isoniazid on vitamin D metabolism. *Clin Pharmacol Ther* **32**, 525-30 (1982).

(72) Brodie, M.J. *et al.* Rifampicin and vitamin D metabolism. *Clin Pharmacol Ther* **27**, 810-4 (1980).

(73) Wang, Z. *et al.* An inducible cytochrome P450 3A4-dependent vitamin D catabolic pathway. *Mol Pharmacol* **81**, 498-509 (2012).

(74) Wang, Z. *et al.* Enhancement of hepatic 4-hydroxylation of 25-hydroxyvitamin D3 through CYP3A4 induction in vitro and in vivo: implications for drug-induced osteomalacia. *J Bone Miner Res* **28**, 1101-16 (2013).

(75) Wong, T. *et al.* Polymorphic Human Sulfotransferase 2A1 Mediates the Formation of 25-Hydroxyvitamin D3-3-O-Sulfate, a Major Circulating Vitamin D Metabolite in Humans. *Drug Metab Dispos* **46**, 367-79 (2018).

(76) Gao, C. *et al.* Simultaneous quantification of 25-hydroxyvitamin D3-3-sulfate and 25-hydroxyvitamin D3-3-glucuronide in human serum and plasma using liquid chromatography-tandem mass spectrometry coupled with DAPTAD-derivatization. *J Chromatogr B Analyt Technol Biomed Life Sci* **1060**, 158-65 (2017).

(77) Higashi, T. *et al.* Levels of 24,25-dihydroxyvitamin D3, 25-hydroxyvitamin D3 and 25-hydroxyvitamin D3 3-sulphate in human plasma. *Ann Clin Biochem* **36 (Pt 1)**, 43-7 (1999).

(78) Higashi, T. *et al.* A Method for Simultaneous Determination of 25-Hydroxyvitamin D3 and Its 3-Sulfate in Newborn Plasma by LC/ESI-MS/MS after Derivatization with a Proton-Affinitive Cookson-Type Reagent. *Mass spectrometry (Tokyo, Japan)* **5**, S0051 (2016).

(79) Ogawa, S., Ooki, S., Morohashi, M., Yamagata, K. & Higashi, T. A novel Cookson-type reagent for enhancing sensitivity and specificity in assessment of infant vitamin D status using liquid chromatography/tandem mass spectrometry. *Rapid Commun Mass Spectrom* **27**, 2453-60 (2013).

(80) Axelson, M. 25-Hydroxyvitamin D3 3-sulphate is a major circulating form of vitamin D in man. *FEBS letters* **191**, 171-5 (1985).

(81) Kurogi, K., Sakakibara, Y., Suiko, M. & Liu, M.C. Sulfation of vitamin D3 -related compounds-identification and characterization of the responsible human cytosolic sulfotransferases. *FEBS letters* **591**, 2417-25 (2017).

(82) Arnaud, S.B., Goldsmith, R.S., Lambert, P.W. & Go, V.L. 25-Hydroxyvitamin D3: evidence of an enterohepatic circulation in man. *Proceedings of the Society for Experimental Biology and Medicine Society for Experimental Biology and Medicine (New York, NY)* **149**, 570-2 (1975).

(83) Shimada, K., Nakatani, I., Saito, K. & Mitamura, K. Separation and characterization of monoglucuronides of vitamin D(3) and25-hydroxyvitamin D(3) in rat bile by high-performance liquid chromatography. *Biological & pharmaceutical bulletin* **19**, 491-4 (1996).

(84) Yoshimura, Y. *et al.* Identification of conjugation positions of urinary glucuronidated vitamin D3 metabolites by LC/ESI-MS/MS after conversion to MS/MS-fragmentable derivatives. *Biomedical chromatography : BMC* **33**, e4538 (2019).

(85) Wang, Z. *et al.* Human UGT1A4 and UGT1A3 conjugate 25-hydroxyvitamin D3: metabolite structure, kinetics, inducibility, and interindividual variability. *Endocrinology* **155**, 2052-63 (2014).

(86) Shimada, K., Mitamura, K., Saito, K., Ohtake, Y. & Nakatani, I. Enzymatic hydrolysis of the conjugate of vitamin D and related compounds. *Journal of pharmaceutical and biomedical analysis* **15**, 1207-14 (1997).

(87) Holick, M.F. & Chen, T.C. Vitamin D deficiency: a worldwide problem with health consequences. *Am J Clin Nutr* **87**, 1080s-6s (2008).

(88) Creo, A.L., Thacher, T.D., Pettifor, J.M., Strand, M.A. & Fischer, P.R. Nutritional rickets around the world: an update. *Paediatrics and international child health* **37**, 84-98 (2017).

(89) Bischoff-Ferrari, H.A., Dietrich, T., Orav, E.J. & Dawson-Hughes, B. Positive association between 25-hydroxy vitamin D levels and bone mineral density: a population-based study of younger and older adults. *The American journal of medicine* **116**, 634-9 (2004).

(90) Bischoff-Ferrari, H.A., Giovannucci, E., Willett, W.C., Dietrich, T. & Dawson-Hughes, B. Estimation of optimal serum concentrations of 25-hydroxyvitamin D for multiple health outcomes. *Am J Clin Nutr* **84**, 18-28 (2006).

(91) Wu, H. & Pang, Q. The effect of vitamin D and calcium supplementation on falls in older adults : A systematic review and meta-analysis. *Der Orthopade* **46**, 729-36 (2017).

(92) Holick, M.F. Noncalcemic actions of 1,25-dihydroxyvitamin D3 and clinical applications. *Bone* **17**, 107s-11s (1995).

(93) Theodoratou, E., Tzoulaki, I., Zgaga, L. & Ioannidis, J.P. Vitamin D and multiple health outcomes: umbrella review of systematic reviews and meta-analyses of observational studies and randomised trials. *BMJ (Clinical research ed)* **348**, g2035 (2014).

(94) Holick, M.F. Vitamin D: a d-lightful solution for health. *Journal of investigative medicine : the official publication of the American Federation for Clinical Research* **59**, 872-80 (2011).

(95) Holick, M.F. High prevalence of vitamin D inadequacy and implications for health. *Mayo Clinic proceedings* **81**, 353-73 (2006).

(96) Holick, M.F. Vitamin D: importance in the prevention of cancers, type 1 diabetes, heart disease, and osteoporosis. *Am J Clin Nutr* **79**, 362-71 (2004).

(97) Cannell, J.J., Grant, W.B. & Holick, M.F. Vitamin D and inflammation. *Dermato-endocrinology* **6**, e983401 (2014).

(98) Lee, J.H., O'Keefe, J.H., Bell, D., Hensrud, D.D. & Holick, M.F. Vitamin D deficiency an important, common, and easily treatable cardiovascular risk factor? *Journal of the American College of Cardiology* **52**, 1949-56 (2008).

(99) Feskanich, D. *et al.* Plasma vitamin D metabolites and risk of colorectal cancer in women. *Cancer epidemiology, biomarkers & prevention : a publication of the American Association for Cancer Research, cosponsored by the American Society of Preventive Oncology* **13**, 1502-8 (2004).

(100) Mousa, A., Abell, S., Scragg, R. & de Courten, B. Vitamin D in Reproductive Health and Pregnancy. *Semin Reprod Med* **34**, e1-13 (2016).

(101) Pittas, A.G. *et al.* Vitamin D Supplementation and Prevention of Type 2 Diabetes. *N Engl J Med* **381**, 520-30 (2019).

(102) Mirzakhani, H. *et al.* Early pregnancy vitamin D status and risk of preeclampsia. *The Journal of clinical investigation* **126**, 4702-15 (2016).

(103) Figueiredo, A.C.C. *et al.* Changes in plasma concentrations of 25-hydroxyvitamin D and 1,25-dihydroxyvitamin D during pregnancy: a Brazilian cohort. *Eur J Nutr* **57**, 1059-72 (2018).

(104) Gustafsson, M.K. *et al.* Alterations in the vitamin D endocrine system during pregnancy: A longitudinal study of 855 healthy Norwegian women. *PLoS One* **13**, e0195041 (2018).

(105) Karras, S.N., Koufakis, T., Fakhoury, H. & Kotsa, K. Deconvoluting the Biological Roles of Vitamin D-Binding Protein During Pregnancy: A Both Clinical and Theoretical Challenge. *Front Endocrinol (Lausanne)* **9**, 259 (2018).

(106) Tsuprykov, O., Chen, X., Hocher, C.F., Skoblo, R., Lianghong, Y. & Hocher, B. Why should we measure free 25(OH) vitamin D? *J Steroid Biochem Mol Biol* **180**, 87-104 (2018).

(107) Drumm, M.L. & Collins, F.S. Molecular biology of cystic fibrosis. *Molecular genetic medicine* **3**, 33-68 (1993).

(108) Jaffe, A. & Bush, A. Cystic fibrosis: review of the decade. *Monaldi archives for chest disease = Archivio Monaldi per le malattie del torace* **56**, 240-7 (2001).

(109) Strausbaugh, S.D. & Davis, P.B. Cystic fibrosis: a review of epidemiology and pathobiology. *Clinics in chest medicine* **28**, 279-88 (2007).

(110) Radlovic, N. Cystic fibrosis. *Srpski arhiv za celokupno lekarstvo* **140**, 244-9 (2012).

(111) Ratjen, F. & Doring, G. Cystic fibrosis. *Lancet (London, England)* **361**, 681-9 (2003).

(112) Wolfenden, L.L., Judd, S.E., Shah, R., Sanyal, R., Ziegler, T.R. & Tangpricha, V. Vitamin D and bone health in adults with cystic fibrosis. *Clin Endocrinol (Oxf)* **69**, 374-81 (2008).

(113) Loukou, I., Boutopoulou, B., Fouzas, S. & Douros, K. Vitamin D and Cystic Fibrosis Lung Disease. *Mini reviews in medicinal chemistry* **15**, 974-83 (2015).

(114) Rana, M. *et al.* Fat-soluble vitamin deficiency in children and adolescents with cystic fibrosis. *Journal of clinical pathology* **67**, 605-8 (2014).

(115) Konstantinidis, I. *et al.* Vitamin D(3) deficiency and its association with nasal polyposis in patients with cystic fibrosis and patients with chronic rhinosinusitis. *American journal of rhinology & allergy* **31**, 395-400 (2017).

(116) Pincikova, T., Paquin-Proulx, D., Sandberg, J.K., Flodstrom-Tullberg, M. & Hjelte, L. Vitamin D treatment modulates immune activation in cystic fibrosis. *Clinical and experimental immunology* **189**, 359-71 (2017).

(117) Pincikova, T., Paquin-Proulx, D., Sandberg, J.K., Flodstrom-Tullberg, M. & Hjelte, L. Clinical impact of vitamin D treatment in cystic fibrosis: a pilot randomized, controlled trial. *Eur J Clin Nutr* **71**, 203-5 (2017).

(118) Schechter, M.S. & Gutierrez, H.H. Improving the quality of care for patients with cystic fibrosis. *Current opinion in pediatrics* **22**, 296-301 (2010).

(119) Stevens, D.P. & Marshall, B.C. A decade of healthcare improvement in cystic fibrosis: lessons for other chronic diseases. *BMJ quality & safety* **23 Suppl 1**, i1-2 (2014).

(120) Tangpricha, V. *et al.* An update on the screening, diagnosis, management, and treatment of vitamin D deficiency in individuals with cystic fibrosis: evidence-based recommendations from the Cystic Fibrosis Foundation. *J Clin Endocrinol Metab* **97**, 1082-93 (2012).

(121) Tangpricha, V. *et al.* The Vitamin D for Enhancing the Immune System in Cystic Fibrosis (DISC) trial: Rationale and design of a multi-center, double-blind, placebo-controlled trial of high dose bolus administration of vitamin D3 during acute pulmonary exacerbation of cystic fibrosis. *Contemporary clinical trials communications* **6**, 39-45 (2017).

(122) Douros, K. Cystic fibrosis and vitamin D: the quest for more pieces of the puzzle. *Acta paediatrica (Oslo, Norway : 1992)* **105**, 854 (2016).

(123) Ferguson, J.H. & Chang, A.B. Vitamin D supplementation for cystic fibrosis. *The Cochrane database of systematic reviews*, Cd007298 (2014).

(124) Norton, L., Page, S., Sheehan, M., Mazurak, V., Brunet-Wood, K. & Larsen, B. Prevalence of inadequate vitamin d status and associated factors in children with cystic fibrosis. *Nutrition in clinical practice : official publication of the American Society for Parenteral and Enteral Nutrition* **30**, 111-6 (2015).

(125) Regalado Lam Chew Tun, R., Porhownik, N., Taback, S. & Oleschuk, C. Effect of high dose vitamin D3 therapy on serum vitamin D3 levels in vitamin D insufficient adults with cystic fibrosis. *Clinical nutrition ESPEN* **23**, 84-8 (2018).

(126) Brannon, P.M. Vitamin D and adverse pregnancy outcomes: beyond bone health and growth. *Proc Nutr Soc* **71**, 205-12 (2012).

(127) Brannon, P.M. & Picciano, M.F. Vitamin D in pregnancy and lactation in humans. *Annu Rev Nutr* **31**, 89-115 (2011).

(128) Kiely, M., Hemmingway, A. & O'Callaghan, K.M. Vitamin D in pregnancy: current perspectives and future directions. *Ther Adv Musculoskelet Dis* **9**, 145-54 (2017).

(129) Perez-Lopez, F.R. *et al.* Effect of vitamin D supplementation during pregnancy on maternal and neonatal outcomes: a systematic review and meta-analysis of randomized controlled trials. *Fertil Steril* **103**, 1278-88 e4 (2015).

(130) Sablok, A. *et al.* Supplementation of vitamin D in pregnancy and its correlation with feto-maternal outcome. *Clin Endocrinol (Oxf)* **83**, 536-41 (2015).

(131) Zhang, J.Y., Lucey, A.J., Horgan, R., Kenny, L.C. & Kiely, M. Impact of pregnancy on vitamin D status: a longitudinal study. *Br J Nutr* **112**, 1081-7 (2014).

(132) Bodnar, L.M., Simhan, H.N., Powers, R.W., Frank, M.P., Cooperstein, E. & Roberts, J.M. High prevalence of vitamin D insufficiency in black and white pregnant women residing in the northern United States and their neonates. *J Nutr* **137**, 447-52 (2007).

(133) Branum, A.M., Bailey, R. & Singer, B.J. Dietary supplement use and folate status during pregnancy in the United States. *J Nutr* **143**, 486-92 (2013).

(134) Isoherranen, N. & Thummel, K.E. Drug metabolism and transport during pregnancy: how does drug disposition change during pregnancy and what are the mechanisms that cause such changes? *Drug Metab Dispos* **41**, 256-62 (2013).

1.12. Figures

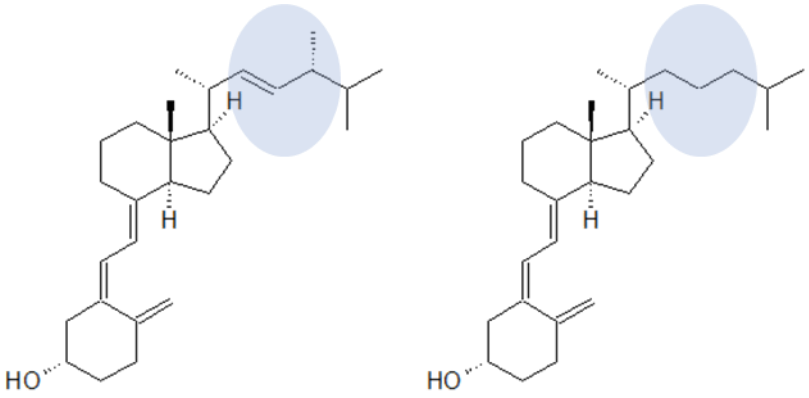

Vitamin D_2 (Ergocalciferol) **Vitamin D_3 (Cholecalciferol)**

Figure 1.1: Chemical structures of vitamin D_2 and vitamin D_3. The blue shaded regions highlight the structural differences between vitamin D_2 and vitamin D_3.

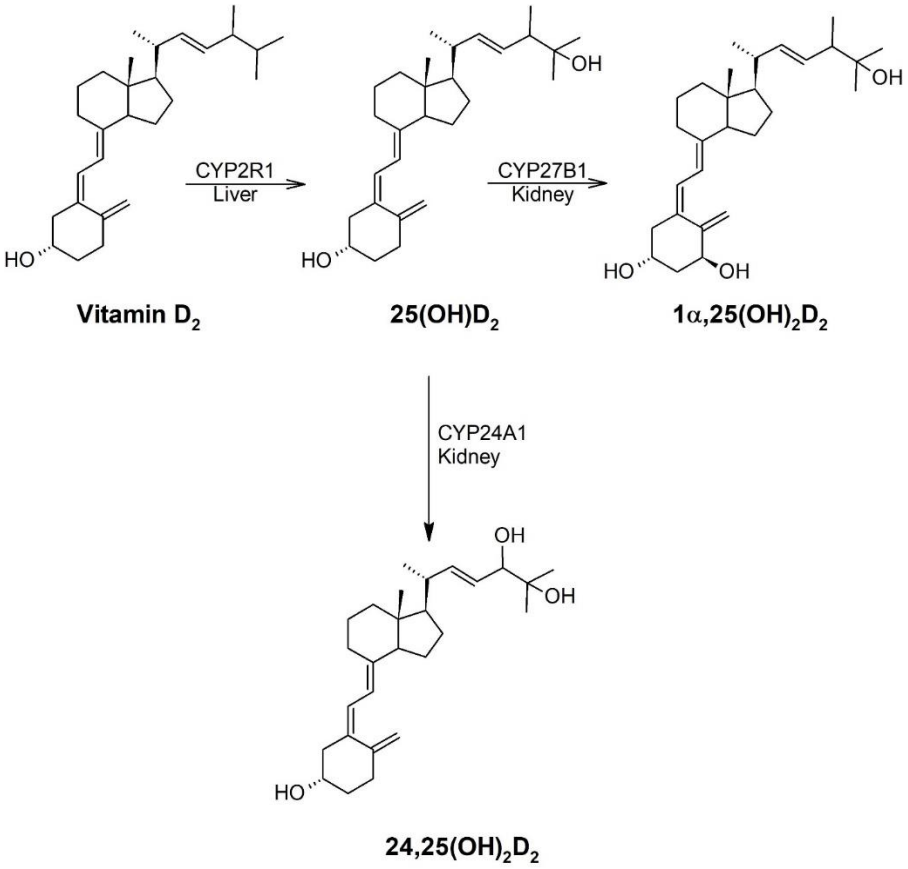

Figure 1.2: Partial metabolic scheme of vitamin D_2 and 25-hydroxyvitamin D_2.

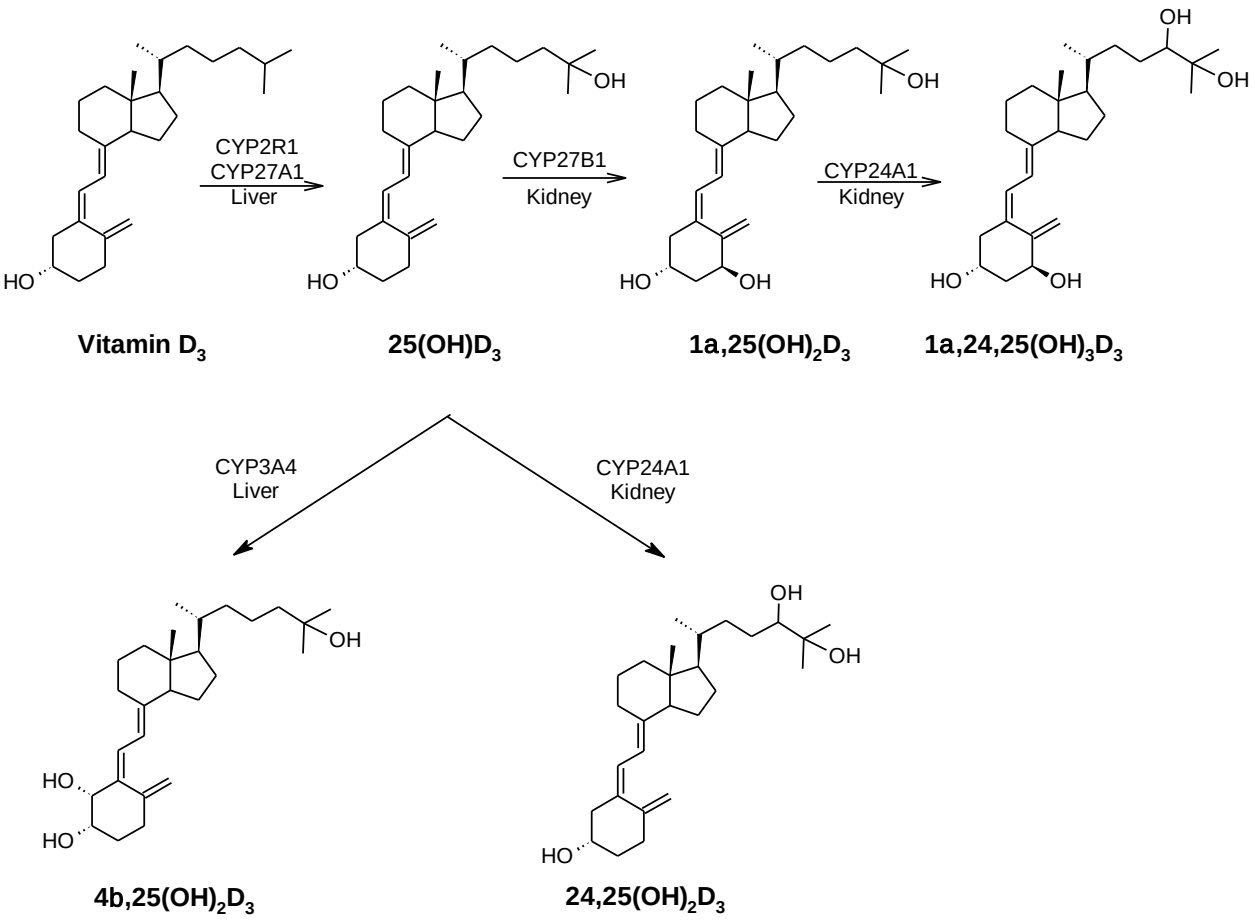

Figure 1.3: Partial metabolic scheme of vitamin D_3 and 25-hydroxyvitamin D_3.

Chapter 2.

Simultaneous Quantification of Vitamin D_2, Vitamin D_3 and Eight Hydroxylated Vitamin D Metabolites in Human Serum and Plasma by LC-MS/MS

2.1. Abstract

In recent decades, research supports an essential role of vitamin D in multiple aspects of human health, in addition to maintaining bone integrity. There are numerous methods to quantify 25-hydroxyvitamin D, the primary circulating metabolite of vitamin D. However, vitamin D metabolism is complex and produces multiple metabolites that may be useful for understanding the effects of genetic variation, drugs or disease on vitamin D disposition and health outcomes. To evaluate these additional metabolites, we developed a liquid chromatography-tandem mass spectrometry (LC-MS/MS) method that simultaneously quantifies vitamin D_2, vitamin D_3, 25-hydroxyvitamin D_2, 25-hydroxyvitamin D_3, 24R,25-dihydroxyvitamin D_3, 1α,25-dihydroxyvitamin D_2, 1α,25-dihydroxyvitamin D_3, 1β,25-dihydroxyvitamin D_3, 4β,25-dihydroxyvitamin D_3, and 1α,24R,25-trihydroxyvitamin D_3. Solid-phase extraction was used to isolate vitamin D metabolites of interest from human plasma and serum samples. The isolated metabolites were derivatized with (4'-dimethylaminophenyl)-1,2,4-triazoline-3,5-dione (DAPTAD) to improve analytical sensitivity. The method was found suitable for the quantification of all metabolites in serum and plasma samples. This method should be useful for comprehensively assessing vitamin D metabolite status in one assay.

2.2. Introduction

Recent evidence suggests that vitamin D plays an essential role in overall human health, in addition to bone health. (1-5) As such, there has been increased interest in developing assays to accurately quantify vitamin D and its many metabolites for clinical and research purposes. However, accurate quantification of vitamin D and its metabolites presents a range of

challenges, including high plasma protein binding, isomeric products of metabolism, and low plasma concentrations. (6-8)

Vitamin D exists in two primary forms: vitamin D_2 (ergocalciferol) and vitamin D_3 (cholecalciferol) (Figure 2.1). Both forms of vitamin D regulate calcium and phosphate homeostasis in the body and follow similar pathways of metabolism. (9, 10) In the liver, vitamin D is converted to the major circulating metabolite, 25-hydroxyvitamin D (25(OH)D), by cytochromes P450 (CYP) 2R1 and 27A1. (9-12) Given the long plasma half-life of 25(OH)D (2 to 3 weeks), 25(OH)D is used as a biomarker of long-term vitamin D exposure. In the kidney, 25(OH)D undergoes metabolism by CYP27B1 to form the biologically active 1α,25-dihydroxyvitamin D (1α,25$(OH)_2$D) and the inactive 24R,25-dihydroxyvitamin D (24R,25$(OH)_2$D) by CYP24A1. (9-12) The active metabolite, 1α,25$(OH)_2$D, can be rendered inactive by CYP24A1, resulting in 1α,24R,25-trihydroxyvitamin D (1α,24R,25$(OH)_3$D). (9, 10) Additional metabolites, which are thought to be inactive include, 4β,25-dihydroxyvitamin D (4β,25$(OH)_2$D) and 1β,25-dihydroxyvitamin D (1β,25$(OH)_2$D). (13-15) Since 4β,25$(OH)_2D_3$ is formed by the drug-metabolizing enzyme CYP3A4, it is currently under investigation as a potential biomarker for drug interactions involving CYP3A4. (13)

Most commonly, quantification of 25(OH)D and other metabolites is conducted by immunoassay and LC-MS/MS, both of which have advantages and limitations. (6, 8) Immunoassays allow for sensitive and rapid quantification of 25(OH)D and are often high throughput methods that are easily automated. (6, 7) However, antibody-based assays cannot distinguish between 25(OH)D_2 and 25(OH)D_3, and cross-reactivity with other vitamin D metabolites may contribute to inaccurate and irreproducible results. (6-8) Sequestration by plasma binding proteins can limit sensitivity and accuracy. (8, 16) Additionally, specific 1α,25(OH)D kits must be purchased as immunoassays cannot simultaneously measure 25(OH)D and 1αα,25$(OH)_2$D.

In contrast, LC-MS/MS assays can provide simultaneous quantification of multiple metabolites using multiple reaction monitoring (MRM). Quantification of low abundance metabolites, including active species, is challenging because of picomolar concentrations in plasma or serum and weak ionization. However, these issues can be partially overcome through derivatization with compounds like 4-phenyl-1,2,4-triazoline-3,5-dione (PTAD) or 4-(4'-dimethylaminophenyl)-1,2,4-triazoline-3,5-dione (DAPTAD). (17-20) Quantification of 1α,25$(OH)_2$D is also challenging due to structural isomers with the same precursor and product ionization pattern, such as for 1α,25$(OH)_2D_3$ and 4β,25$(OH)_2D_3$. In this case, additional efforts must be made to ensure the chromatographic separation of the analytes for accurate quantification of vitamin D and all its metabolites. Two previously published methods used LC-MS/MS to separate and quantify epimers of vitamin D_3 and to separate 1α,25$(OH)_2D_3$ from 4β,25$(OH)_2D_3$. (21, 22)

In this paper, we describe an LC-MS/MS assay developed for the quantification of vitamin D_2, vitamin D_3, and eight of their metabolites in either serum or plasma samples. This method may prove useful for simultaneously monitoring the circulating concentrations of vitamin D and its metabolites in patients with vitamin D deficiency or in clinical studies where metabolic changes in vitamin D metabolism are anticipated.

2.3. Materials and Methods

2.3.1. Chemicals and Materials

d_7-vitamin D_3, *d_6*-25(OH)D_2, 24R,25$(OH)_2D_3$, *d_6*-24R,25$(OH)_2D_3$, *d_6*-1α,25$(OH)_2D_3$, and 4β,25$(OH)_2D_3$ were purchased from Toronto Research Chemicals (North York, Ontario, Canada). Vitamin D_2, *d_3*-vitamin D_2, Vitamin D_3, 25(OH)D_2, 25(OH)D_3, *d_6*-25(OH)D_3, 1α,25$(OH)_2D_2$, 1α,25$(OH)_2D_3$, and 1α,24R,25$(OH)_3D_3$ were purchased from Cerilliant Corporation (Round Rock, TX). 1β,25$(OH)_2D_3$ was purchases from MedChemExpress, LLC

(Monmouth Junction, NJ). Bovine serum albumin (BSA) and iodobenzene I,I-diacetate were purchased from Sigma-Aldrich Corp. (St. Louis, MO). 4-(4'-dimethylaminophenyl)-1,2,4-triazolidine-3,5-dione (DAPTAD precursor) was purchased from Santa Cruz Biotechnology, Inc. (Dallas, TX). HPLC grade acetonitrile, ethyl acetate, methanol, methyl tert-butyl ether (MTBE), heptane, isopropanol, hexanes, formic acid, acetic acid, and dichloromethane were purchased from Fisher Scientific (Pittsburgh, PA). Vitamin D-free serum was purchased from Golden West Biologicals (Temecula, CA).

2.3.2. Preparation of DAPTAD Solution

The DAPTAD solution was prepared by combining 6 mg of iodobenzene I,I-diacetate with 4 mg of DAPTAD precursor in 4 mL of ethyl acetate. (19) The solution was stirred for 3 hours at room temperature until the color of the mixture changed to red. A fresh DAPTAD solution was prepared for each day of sample preparation.

2.3.3. Preparation of Working Solutions

Standards for vitamin D_2, vitamin D_3, 25(OH)D_3, 1α,25(OH)$_2D_2$, 1α,25(OH)$_2D_3$, 1β,25(OH)$_2D_3$, and 1,24R,25(OH)$_3D_3$ were purchased as stock solutions in methanol. Stock solutions of 24R,25(OH)$_2D_3$ and 4β,25(OH)$_2D_3$ were prepared by dissolving solid in ethanol to a final concentration of 0.1 ng/mL and 0.02 ng/mL, respectively. A single working calibration standard in ethanol was prepared by diluting the appropriate amount of each stock solution to final concentrations of 160 pg/µL, 220 pg/µL, 250 pg/µL, 500 pg/µL, 150 pg/µL, 8 pg/µL, 8 pg/µL, 8 pg/µL, 8 pg/µL, and 8 pg/µL for vitamin D_2, vitamin D_3, 25(OH)D_2, 25(OH)D_3, 24R,25(OH)$_2D_3$, 1α,25(OH)$_2D_2$, 1α,25(OH)$_2D_3$, 4β,25(OH)$_2D_3$, 1β,25(OH)$_2D_3$, and 1,24R,25(OH)$_3D_3$, respectively (total volume of 25 mL). The working calibration standard was aliquoted into amber vials and stored at -80°C until use.

Similarly, stock deuterium-labeled internal standards were purchased as solutions in methanol for d_7-vitamin D_3, d_3-vitamin D_2, and d_6-25(OH)D_3. Internal standard stock solutions of d_6-25(OH)D_2, d_6-24R,25(OH)$_2D_3$ and d_6-1α,25(OH)$_2D_3$ were prepared by dissolving solid in ethanol to a final concentration of 0.1 ng/mL. A single working internal standard solution in ethanol was prepared by diluting appropriate volumes of each internal standard stock solution to final concentrations of 200 pg/µL, 200 pg/µL, 200 pg/µL, 500 pg/µL, 250 pg/µL, and 60 pg/µL for d_3-vitamin D_2, d_7-vitamin D_3, d_6-25(OH)D_2, d_6-25(OH)D_3, d_6-24R,25(OH)$_2D_3$ and d_6-1α,25(OH)$_2D_3$, respectively (total volume of 100 mL). The working internal standard solution was aliquoted into amber vials and stored at -80°C until use.

2.3.4. Preparation of Quality Control Samples

Quality control samples were prepared by adding the appropriate volume of working standard solution into 150 mL of 30 mg/mL BSA solution. Low, mid, and high QC samples were prepared to span the expected physiological concentrations in human plasma and serum. The final metabolite concentrations in the QC samples are listed in Table 2.2.

2.3.5. Chromatographic Conditions

Liquid chromatography-mass spectrometry (LC-MS/MS) analysis was performed on a Sciex QTRAP 6500 hybrid triple quadrupole/linear ion trap mass spectrometer (Framingham, MA) coupled with a Shimadzu liquid chromatography system (Kyoto, Japan). An Ascentis Express RP-Amide column (2.1 mm x 150 mm x 2.7 µm) (Sigma-Aldrich Corp, St. Louis, MO), attached to a SecurityGuard™ ULTRA cartridge (2.1 mm x 2 µm) guard column (Phenomenex, Torrance, CA) was used for chromatographic separation.

The column temperature was maintained at 20°C with a mobile phase flowing at a rate of 0.275 mL/min. The mobile phase consisted of a mixture of 0.1% formic acid in water (A) and 100% methanol (B). Initial conditions were set to 55% B. Between 1 and 6 minutes, B was

increased linearly from 55% to 65% and maintained at 65% from 6 to 8 minutes. Between 8 and 15 minutes, B was increased linearly from 65% to 75% and maintained at 75% until 15.5 minutes. Between 15.5 and 17 minutes, B was increased from 75% to 90%. B was maintained at 90% until 23 minutes, and then B was returned to initial conditions. The total run time was 26 minutes. The autosampler was maintained at 4°C, and the injection volume was 10 µL.

2.3.6. Mass Spectrometric Conditions

Mass spectrometric conditions are summarized in Table 2.1. The electrospray ionization (ESI) source of the mass spectrometer was operated in the positive ion mode. Multiple reaction monitoring (MRM) was used for quantitation. The following MS parameters were selected for optimal quantitation: curtain gas, 30 psi; nebulizer gas (GS1) and turbo gas (GS2), 75 psi; ion spray voltage, 5500 V; source temperature, 350°C. The retention time, precursor and product ions, declustering potential, entrance potential, collision energy, and collision cell exit potential for each analyte are presented in Table 2.1.

2.3.7. Quantification and Data Analysis

Peak integration was performed using MultiQuant software (version 3.0.2) from AB Sciex. Peak heights of vitamin D_2 and vitamin D_3 were normalized to d_3-vitamin D_2 and d_7-vitamin D_3, respectively. 25(OH)D_3 and 24R,25$(OH)_2D_3$ were normalized to d_6-25(OH)D_3 and d_6-24R,25$(OH)_2D_3$, respectively. Peak heights of 1α,25$(OH)_2D_2$, 1α,25$(OH)_2D_3$, 4β,25$(OH)_2D_3$, 1β,25$(OH)_2D_3$, and 1α,24R,25$(OH)_3D_3$ were normalized to d_6-1α,25$(OH)_2D_3$. A quadratic equation with $1/x^2$ weighting was used to estimate the relationship between peak height ratios and concentration. The lower limit of detection (LLOD) was set at 5 times above background and the concentration range for each analyte is presented in Table 2.1.

2.3.8. Sample Preparation

The calibration curve was prepared by adding 500 µL of 30 mg/mL BSA solution to nine 2 mL polypropylene micro-centrifuge tubes. Increasing volumes (0, 0.2, 0.5, 1, 2.5, 5, 10, 25, and 50 µL) of the working calibration standard were added. After thawing, low, mid, and high QC samples were vortexed for 15 seconds and 500 µL was aliquoted into 2 mL polypropylene micro-centrifuge tubes. After thawing, serum or plasma samples were vortexed for 15 seconds and centrifuged at 20,000 *g* for 5 minutes at 4°C. Sample aliquots of 500 µL serum or plasma were transferred into 2 mL polypropylene micro-centrifuge tubes.

2.3.9. Extraction of Analytes from Samples

After the addition of 20 µL of the internal standard solution, samples were vortexed and allowed to equilibrate at room temperature for 25 minutes. Proteins were precipitated with 1 mL of acetonitrile and samples centrifuged at 13,362 *g* for 10 min at 4°C. The supernatant was transferred to silanized glass tubes and 1.5 mL of 0.1 M phosphate buffer (pH 10.5) was added. Analytes were extracted using two SPE steps. First, the Agilent Bond Elut C18 OH solid-phase extraction (SPE) cartridges (500 mg, 3 mL) were equilibrated with 2 mL of acetonitrile, 2 mL of methanol, and 2 mL of deionized water. After the addition of the sample, the column was washed with 5 mL of 70% methanol and eluted with 6 mL of 10% isopropanol in hexanes (v/v). The eluants were collected into silanized glass culture tubes. Samples were dried under N_2 gas at 37°C and reconstituted in 1 mL of 10% dichloromethane in heptane (v/v). For the second SPE step, samples were processed using Agilent Bond Elut SI cartridges (100 mg, 1 mL). The cartridge was conditioned with 1 mL of dichloromethane and 1 mL of heptanes. After loading the sample, the cartridge was washed with 3 mL of 10% dichloromethane in heptane, 3 mL of 30% dichloromethane in heptane (v/v), and 2 mL of 40% dichloromethane in heptane (v/v). Samples were eluted with 5% isopropanol in MTBE (v/v) into silanized glass culture tubes. Samples were dried under N_2 gas at 37°C and reconstituted in 50 µL of acetonitrile. DAPTAD (50 µL) was

added and samples were shaken at room temperature for 45 minutes. The derivatization reaction was stopped by drying under N_2 gas at 37°C. The residue was reconstituted in 45 µL of methanol and 20 µL of water. The derivatized samples were centrifuged at 13,362 *g* for 5 min to remove insoluble particulates and excess DAPTAD. The supernatant was transferred to a 96-well plate for LC-MS/MS analysis.

2.3.10. Method Validation

2.3.10.1. Selectivity

Selectivity was assessed by evaluating MRM chromatograms under the following conditions: 1) Blank BSA, 2) BSA spiked with each analyte individually, 3) BSA spiked with all analytes and internal standards. Representative chromatograms are shown in Figure 2.2.

2.3.10.2. Assessment of Calibration Curve

To determine the linearity of the calibration curve for each analyte, BSA was spiked with eight volumes of the working calibration solution (0.2, 0.5, 1, 2.5, 5, 15, 25, 50 µL). The range of the standard curve for each analyte is presented in Table 2.1. Calibration curves were plotted as the peak height ratio of each analyte versus the spiked concentration and fit with a quadratic equation and $1/x^2$ weighting.

2.3.10.3. Accuracy and Precision

Intra-day accuracy and precision were evaluated by preparing six replicates of the low, mid, and high QC samples in one day (concentrations for each analyte are listed in Table 2.2). Inter-day accuracy and precision were evaluated by the preparation of low, mid, and high QC in triplicate on three separate days. The accuracy was calculated as the percent relative error (%RE = mean observed concentration / actual concentration). The precision was calculated as

the percent relative standard deviation (%RSD = standard deviation / mean observed concentration).

2.3.10.4. Stability

The stability of analytes in human serum was assessed by spiking known amounts of the standard solution in vitamin D-free serum and subjecting them to the following conditions: 1) leaving samples at room temperature for 2 hours, 2) three freeze-thaw cycles (RT to -80°C), and 3) held in the autosampler at 4°C for 24 hours prior to LC-MS/MS analysis. Blank vitamin D-free serum was also prepared in triplicate to correct for residual analytes in the matrix.

2.3.10.5. Application to plasma samples

The application of the extraction method to plasma samples was investigated by spiking the standard solution at three concentrations into blank plasma in triplicate. Blank plasma was also prepared in triplicate to correct for residual analytes in the matrix. Samples were extracted and analyzed using the methods described above.

2.4. Results and Discussion

2.4.1. Optimization of Extraction Methods and LC-MS/MS Conditions

2.4.1.1. Optimization of Sample Preparation

In a previous report, Takeuchi et al. quantified 25(OH)D_3 and 1α,25$(OH)_2D_3$ from 0.5 mL of plasma by precipitating plasma proteins with acetonitrile and extracting the supernatant with Agilent Bond Elut C18 OH cartridges and used HPLC with UV detection for quantification. (22, 23)

Upon screening, we achieved sufficient recovery of 25(OH)D_3, 1α,25$(OH)_2D_3$, and the additional analytes of interest from this method; however, contaminants increased the noise levels and raised the limits of detection. A second SPE step with an Agilent Bond Elut SI

cartridge was added to reduce the contaminants. The best recovery of analytes from the second SPE was achieved with a gradient of dichloromethane and heptane, with 3 mL of 10% dichloromethane in heptane, 3 mL of 30% dichloromethane in heptane (v/v), and 2 mL of 40% dichloromethane in heptane (v/v) (data not shown). Optimal derivatization was achieved with 50 µL of DAPTAD solution and 50 µL of acetonitrile (data not shown).

2.4.1.2. Optimization of LC-MS/MS Conditions for 1α,25$(OH)_2D_3$, 1β,25$(OH)_2D_3$, and 4β,25$(OH)_2D_3$

In 2011, Wang et al. published a method to quantify 25$(OH)D_3$, 24R,25$(OH)_2D_3$, 1α,25$(OH)_2D_3$, and 4β,25$(OH)_2D_3$ by LC-MS/MS. The optimized LC-MS/MS conditions for each analyte are presented in Table 2.1. Due to previous reports of positional isomers (i.e., 3-epi-25-hydroxyvitamin D_3) eluting simultaneously and reducing the accuracy of the quantification of 1α,25$(OH)_2D_3$, efforts were made to separate 1α,25$(OH)_2D_3$ from interfering analytes by HPLC. Chromatographic separation was achieved by using an Ascentis Express RP-Amide column and a gradient of 0.1% formic acid in water and 100% methanol over 26 minutes. The column was cooled to 20°C to increase separation. Since complete baseline separation of 1α,25$(OH)_2D_3$ and 4β,25$(OH)_2D_3$ was not achieved, peak height was used for quantification of all analytes rather than peak area. Representative chromatograms demonstrating separation of 1α,25$(OH)_2D_3$, 1β,25$(OH)_2D_3$, 4β,25$(OH)_2D_3$, and all other analytes are presented in Figure 2.2.

2.4.2. Method validation

2.4.2.1. Precision and Accuracy

Table 2.2 summarizes the precision and accuracy of the assay for all analytes. Intra-day precision and accuracy were assessed by the extraction of independent replicates of the low, mid, and high QC samples in a single run (n = 6). For all analytes, the intra-assay variation was less than 10%. All analytes were within 11% of their target concentration. Inter-day precision

and accuracy were determined by the extraction of the low, mid, and high QC replicates prepared on three separate days (n = 9). For all analytes, the variation was less than 13%, and the calculated concentrations were within 11% of their target concentrations.

2.4.2.2. Stability in human serum

Analyte stability was assessed in triplicate by spiking vitamin D-free serum with standards to achieve the low, mid, and high QC concentrations. The untreated serum and spiked serum were subjected to resting at room temperature for 2 hours or three freeze-thaw cycles. Additionally, the stability of the prepared samples was tested by leaving derivatized samples in the autosampler at 4°C for 24 hours. The results from each test are reported in Table 2.3. The accuracy of all analytes was within 15% for all three concentrations after leaving samples at room temperature for 2 hours and after three freeze-thaw cycles. All analytes were with 15% of the target concentration for samples prepared and stored in the autosampler at 4°C for 24 hours. These data suggest that the analytes are stable under the studied conditions.

2.4.2.3. Application of methods to plasma samples

Applicability of the extraction and analytical methods to plasma samples was investigated by preparing control plasma and spiked plasma at low, mid, and QC concentrations in triplicate in a single day. The measured concentrations of each analyte were corrected for the endogenous vitamin D metabolites in plasma by subtracting the mean concentrations of the control samples from each replicate of the spiked samples. As reported in Table 2.3, all analytes were within 15% of their target concentration after correction for endogenous vitamin D levels.

2.5. Conclusions

We developed and validated an LC-MS/MS method for the simultaneous quantification of vitamin D_2, vitamin D_3, and eight metabolites. We optimized chromatographic separation of $1\alpha,25(OH)_2D_3$ from its isomers. This method can be applied to both human serum and plasma

samples accurately and reproducibly. While this assay can simultaneously quantify the numerous metabolites, it requires a relatively large sample volume (0.5 mL), is labor-intensive, and requires long run times on the LC-MS/MS. However, this method can be used to simultaneously quantify vitamin D and multiple metabolites in plasma or serum samples from clinical studies to investigate changes in vitamin D metabolic pathways that may result from genetic variation, drug therapy, pregnancy, or disease.

2.6. References

(1) Hossein-nezhad, A. & Holick, M.F. Vitamin D for health: a global perspective. Mayo Clinic proceedings 88, 720-55 (2013).

(2) Theodoratou, E., Tzoulaki, I., Zgaga, L. & Ioannidis, J.P. Vitamin D and multiple health outcomes: umbrella review of systematic reviews and meta-analyses of observational studies and randomised trials. *BMJ (Clinical research ed)* **348**, g2035 (2014).

(3) Wei, S.Q. Vitamin D and pregnancy outcomes. *Current opinion in obstetrics & gynecology* **26**, 438-47 (2014).

(4) Wranicz, J. & Szostak-Wegierek, D. Health outcomes of vitamin D. Part II. Role in prevention of diseases. *Roczniki Panstwowego Zakladu Higieny* **65**, 273-9 (2014).

(5) Bikle, D.D. & Bouillon, R. Vitamin D and bone and beyond. *Bone Rep* **9**, 120-1 (2018).

(6) Carter, G.D. 25-Hydroxyvitamin D assays: the quest for accuracy. *Clin Chem* **55**, 1300-2 (2009).

(7) Carter, G.D. Accuracy of 25-hydroxyvitamin D assays: confronting the issues. *Curr Drug Targets* **12**, 19-28 (2011).

(8) Farrell, C.J., Martin, S., McWhinney, B., Straub, I., Williams, P. & Herrmann, M. State-of-the-art vitamin D assays: a comparison of automated immunoassays with liquid chromatography-tandem mass spectrometry methods. *Clin Chem* **58**, 531-42 (2012).

(9) Bikle, D.D. Vitamin D metabolism, mechanism of action, and clinical applications. *Chem Biol* **21**, 319-29 (2014).

(10) Bikle, D. Vitamin D: Production, Metabolism, and Mechanisms of Action. In: *Endotext* (eds. Feingold, K.R., Anawalt, B., Boyce, A., Chrousos, G., Dungan, K., Grossman, A. *et al.*) (South Dartmouth (MA), 2000).

(11) Cheng, J.B., Motola, D.L., Mangelsdorf, D.J. & Russell, D.W. De-orphanization of cytochrome P450 2R1: a microsomal vitamin D 25-hydroxilase. *J Biol Chem* **278**, 38084-93 (2003).

(12) Cheng, J.B., Levine, M.A., Bell, N.H., Mangelsdorf, D.J. & Russell, D.W. Genetic evidence that the human CYP2R1 enzyme is a key vitamin D 25-hydroxylase. *Proc Natl Acad Sci U S A* **101**, 7711-5 (2004).

(13) Wang, Z. *et al.* Enhancement of hepatic 4-hydroxylation of 25-hydroxyvitamin D3 through CYP3A4 induction in vitro and in vivo: implications for drug-induced osteomalacia. *J Bone Miner Res* **28**, 1101-16 (2013).

(14) Wang, Z. *et al.* An inducible cytochrome P450 3A4-dependent vitamin D catabolic pathway. *Mol Pharmacol* **81**, 498-509 (2012).

(15) Wang, Z., Schuetz, E.G., Xu, Y. & Thummel, K.E. Interplay between vitamin D and the drug metabolizing enzyme CYP3A4. *J Steroid Biochem Mol Biol* **136**, 54-8 (2013).

(16) Nguyen, V.T., Li, X., Castellanos, K.J., Fantuzzi, G., Mazzone, T. & Braunschweig, C.A. The accuracy of vitamin D assays of circulating 25-hydroxyvitamin D values: influence of 25-hydroxylated ergocalciferol concentration. *J AOAC Int* **97**, 1048-55 (2014).

(17) Muller, M.J. & Volmer, D.A. Mass spectrometric profiling of vitamin D metabolites beyond 25-hydroxyvitamin D. *Clin Chem* **61**, 1033-48 (2015).

(18) Higashi, T., Shimada, K. & Toyo'oka, T. Advances in determination of vitamin D related compounds in biological samples using liquid chromatography-mass spectrometry: a review. *J Chromatogr B Analyt Technol Biomed Life Sci* **878**, 1654-61 (2010).

(19) Ogawa, S., Ooki, S., Morohashi, M., Yamagata, K. & Higashi, T. A novel Cookson-type reagent for enhancing sensitivity and specificity in assessment of infant vitamin D status using liquid chromatography/tandem mass spectrometry. *Rapid Commun Mass Spectrom* **27**, 2453-60 (2013).

(20) El-Khoury, J.M., Reineks, E.Z. & Wang, S. Progress of liquid chromatography-mass spectrometry in measurement of vitamin D metabolites and analogues. *Clin Biochem* **44**, 66-76 (2011).

(21) Jenkinson, C. *et al.* High throughput LC-MS/MS method for the simultaneous analysis of multiple vitamin D analytes in serum. *J Chromatogr B Analyt Technol Biomed Life Sci* **1014**, 56-63 (2016).

(22) Wang, Z. *et al.* Simultaneous measurement of plasma vitamin D(3) metabolites, including 4beta,25-dihydroxyvitamin D(3), using liquid chromatography-tandem mass spectrometry. *Analytical biochemistry* **418**, 126-33 (2011).

(23) Takeuchi, A. *et al.* Simplified method for the determination of 25-hydroxy and 1alpha,25-dihydroxy metabolites of vitamins D2 and D3 in human plasma. Application to nutritional studies. *Journal of chromatography B, Biomedical sciences and applications* **691**, 313-9 (1997).

2.7. Tables

Table 2.1. Retention time, precursor molecular ion/product ion for quantification and detection parameters for each analyte

Analyte	Retention Time (min)	Precursor Ion	Product Ion	DP[a] (V)	EP[b] (V)	CE[c] (V)	CXP[d] (V)	LLOD	Standard Curve Range
Vitamin D_2	22.0	615.2	163.2	276	10	51	10	0.06 ng/mL	0.06 – 16 ng/mL
d_3-vitamin D_2	21.9	618.3	163.2	276	10	51	10	-	-
Vitamin D_3	22.2	603.2	163.1	276	10	53	10	0.06 ng/mL	0.09 – 22 ng/mL
d_7-vitamin D_3	22.1	610.2	163.1	276	10	53	10	-	-
25(OH)D_2	18.4	631.2	341.1	156	10	31	20	0.1 ng/mL	0.1 – 25 ng/mL
d_6-25(OH)D_2	18.4	637.3	341.1	156	10	31	20	-	-
25(OH)D_3	18.3	619.2	601.1	196	10	27	22	0.1 ng/mL	0.2 – 50 ng/mL
d_6-25(OH)D_3	18.2	625.4	341.1	196	10	31	22	-	-
24R,25$(OH)_2D_3$	13.9	635.2	341.1	66	10	35	20	0.03 ng/mL	0.06 – 15 ng/mL
d_6-24R,25$(OH)_2D_3$	13.7	641.2	341.1	66	10	35	20	-	-
1α,25$(OH)_2D_2$	16.4	647.2	357.2	51	10	33	18	1.6 pg/mL	2 – 800 pg/mL
1α,25$(OH)_2D_3$	15.7	635.2	357.1	146	5	33	21	1.6 pg/mL	2 – 800 pg/mL
1β,25$(OH)_2D_3$	16.8	635.2	357.1	146	5	33	21	1.6 pg/mL	2 – 800 pg/mL
4β,25$(OH)_2D_3$	15.5	635.2	357.1	146	5	33	21	1.6 pg/mL	2 – 800 pg/mL
d_6-1α,25$(OH)_2D_3$	15.6	641.2	357.1	146	5	33	21	-	-
1α,24R,25$(OH)_3D_3$	10.2	651.3	357.0	221	10	35	24	1.6 pg/mL	2 – 800 pg/mL

[a] declustering potential
[b] entrance potential
[c] collision energy
[d] collision cell exit potential

Table 2.2. Intra- and Inter-day accuracy and precision of vitamin D metabolites

Analyte	Concentration	Intra-day Variability (n = 6)[a]			Inter-day Variability (n = 9)[b]		
		Measured[c]	%RE[d]	%RSD[e]	Measured[c]	%RE[d]	%RSD[e]
Vitamin D_2 (ng/mL)	0.16	0.16 ± 0.01	2.13	6.02	0.16 ± 0.01	3.60	9.71
	1.6	1.69 ± 0.08	5.42	4.44	1.78 ± 0.18	10.35	9.98
	8	7.84 ± 0.50	2.11	6.37	8.38 ± 0.25	4.52	3.01
Vitamin D_3 (ng/mL)	0.22	0.12 ± 0.01	9.59	3.06	0.12 ± 0.01	10.75	7.97
	2.2	2.16 ± 0.07	1.93	3.18	2.24 ± 0.21	1.95	9.52
	11	10.1 ± 0.7	8.75	6.60	10.7 ± 1.2	2.45	10.84
$25(OH)D_2$ (ng/mL)	0.25	0.24 + 0.02	4.90	7.03	0.23 ± 0.02	6.94	6.91
	2.5	2.43 ± 0.22	2.88	9.01	2.44 ± 0.22	2.55	9.12
	12.5	11.5 ± 0.26	8.40	2.27	12.0 ± 0.50	4.07	4.45
$25(OH)D_3$ (ng/mL)	0.5	0.54 ± 0.04	6.83	7.88	0.51 ± 0.06	2.60	12.18
	5	4.92 ± 0.27	1.73	5.52	5.12 ± 0.31	2.32	6.02
	25	22.8 ± 1.05	9.64	4.60	23.6 ± 1.60	5.92	6.84
$24R,25(OH)_2D_3$ (ng/mL)	0.15	0.17 ± 0.01	9.46	7.16	0.17 ± 0.01	9.40	6.44
	1.5	1.37 ± 0.12	9.76	8.97	1.61 ± 0.16	6.90	10.14
	7.5	7.05 ± 0.44	6.38	6.23	7.14 ± 0.64	4.99	9.02
$1\alpha,25(OH)_2D_2$ (pg/mL)	8	8.85 ± 0.82	9.57	9.28	8.34 ± 0.76	4.13	9.13
	80	82.4 ± 3.5	2.95	4.19	83.0 ± 5.4	3.65	6.48
	400	405 ± 17	1.29	4.27	380 ± 15	5.39	3.89
$1\alpha,25(OH)_2D_3$ (pg/mL)	8	8.95 ± 0.81	10.61	9.06	8.26 ± 0.49	3.16	7.17
	80	82.4 ± 8.0	2.95	9.68	82.4 ± 7.8	2.93	9.49
	400	388 ± 21	3.09	5.42	380 ± 37	5.24	9.79

$1\beta,25(OH)_2D_3$ (pg/mL)	8	8.32 ± 0.24	3.87	2.93	8.56 ± 0.67	6.51	7.79
	80	87.8 ± 5.1	8.85	5.84	82.5 ± 6.04	3.03	7.32
	400	396 ± 13	1.13	3.19	385 ± 34	3.93	8.90
$4\beta,25(OH)_2D_3$ (pg/mL)	8	8.53 ± 0.74	6.25	8.64	8.35 ± 0.67	4.19	8.02
	80	78.1 ± 7.4	2.40	9.51	79.7 ± 6.0	0.36	7.47
	400	400 ± 30	0.10	7.40	388 ± 35	3.15	8.93
$1\alpha,24R,25(OH)_3D_3$ (pg/mL)	8	7.73 ± 0.66	3.49	8.59	8.24 ± 0.6	2.87	7.30
	80	80.8 ± 7.9	0.94	9.83	81.2 ± 5.6	1.45	6.89
	400	408 ± 15	2.01	3.75	419 ± 15	4.60	3.65

[a] Intra-day precision was calculated from 6 replicates measured in a single run.
[b] Inter-day precision was calculated from 3 replicates samples prepared on each of 3 days.
[c] Values = Mean ± SD of measured concentrations
[d] %RE = mean overserved calculations / actual concentration
[e] %RSD = standard deviation / mean overserved calculations

Table 2.3: Stability of serum after 2 hours at room temperature, after 3 free-thaw cycles, prepared and stored at 4°C for 24 hours and applicability of extraction method to plasma

Analyte	Concentration	% Accuracy[a]			
		Serum at room temperature for 2 hours[b]	Serum after 3 freeze-thaw cycles[b]	Prepared serum samples stored at 4°C for 24 hours[b]	Spiked plasma[b]
Vitamin D_2 (ng/mL)	0.16	0.17 ± 0.03	0.15 ± 0.02	0.18 ± 0.01	0.18 ± 0.06
	1.6	1.39 ± 0.04	1.75 ± 0.13	1.78 ± 0.05	1.81 ± 0.20
	8	8.47 ± 0.14	7.83 ± 0.11	8.64 ± 0.12	8.36 ± 0.19
Vitamin D_3 (ng/mL)	0.22	0.24 ± 0.03	0.20 ± 0.01	0.25 ± 0.03	0.21 ± 0.05
	2.2	2.44 ± 0.11	2.34 ± 0.17	2.41 ± 0.09	2.42 ± 0.33
	11	11.5 ± 0.9	11.2 ± 0.2	10.2 ± 0.3	10.2 ± 0.7
$25(OH)D_2$ (ng/mL)	0.25	0.26 ± 0.02	0.27 ± 0.04	0.24 ± 0.03	0.28 ± 0.14
	2.5	2.36 ± 0.02	2.41 ± 0.24	2.61 ± 0.19	2.29 ± 0.25
	12.5	13.3 ± 0.6	12.5 ± 0.3	13.3 ± 0.4	12.0 ± 0.5
$25(OH)D_3$ (ng/mL)	0.5	0.51 ± 0.06	0.56 ± 0.06	0.53 ± 0.03	0.57 ± 0.07
	5	5.46 ± 1.00	2.41 ± 0.34	5.11 ± 0.34	5.18 ± 0.20
	25	22.2 ± 0.9	23.4 ± 0.5	26.2 ± 1.6	25.3 ± 0.9
$24R,25(OH)_2D_3$ (ng/mL)	0.15	0.14 ± 0.01	0.14 ± 0.01	0.16 ± 0.03	0.16 ± 0.01
	1.5	1.44 ± 0.17	1.32 ± 0.07	1.58 ± 0.21	1.37 ± 0.09
	7.5	7.54 ± 0.25	7.85 ± 0.26	7.73 ± 0.47	7.04 ± 0.34
$1\alpha,25(OH)_2D_2$ (pg/mL)	8	7.27 ± 0.26	8.53 ± 0.16	8.09 ± 0.29	7.82 ± 0.30
	80	75.7 ± 3.6	85.0 ± 1.8	83.4 ± 1.2	84.2 ± 5.2
	400	382 ± 22	395 ± 14	384 ± 4	393 ± 14

$1\alpha,25(OH)_2D_3$ (pg/mL)	8	8.54 ± 0.92	8.46 ± 0.01	7.97 ± 0.48	8.24 ± 1.01
	80	78.2 ± 6.3	82.8 ± 1.7	84.3 ± 2.4	82.2 ± 2.1
	400	376 ± 15	401 ± 19	396 ± 14	395 ± 9
$1\beta,25(OH)_2D_3$ (pg/mL)	8	8.76 ± 1.16	9.04 ± 0.28	8.23 ± 0.52	8.68 ± 3.08
	80	84.9 ± 6.8	85.5 ± 3.6	84.4 ± 2.2	83.3 ± 5.5
	400	413 ± 14	359 ± 8	385 ± 9	387 ± 14
$4\beta,25(OH)_2D_3$ (pg/mL)	8	7.96 ± 0.19	8.16 ± 0.44	8.67 ± 0.25	8.31 ± 0.59
	80	84.9 ± 4.1	81.3 ± 2.0	82.2 ± 3.5	80.6 ± 2.9
	400	372 ± 17	408 ± 6	412 ± 27	392 ± 8
$1\alpha,24R,25(OH)_3D_3$ (pg/mL)	8	7.88 ± 0.45	9.15 ± 1.11	8.23 ± 0.53	8.27 ± 0.80
	80	83.7 ± 5.7	76.5 ± 6.70	87.1 ± 2.0	88.0 ± 2.9
	400	392 ± 17	377 ± 21	390 ± 13	415 ± 10

[a] Corrected for residual analyte in blank serum or plasma
[b] Mean ± SD reported

2.8. Figures

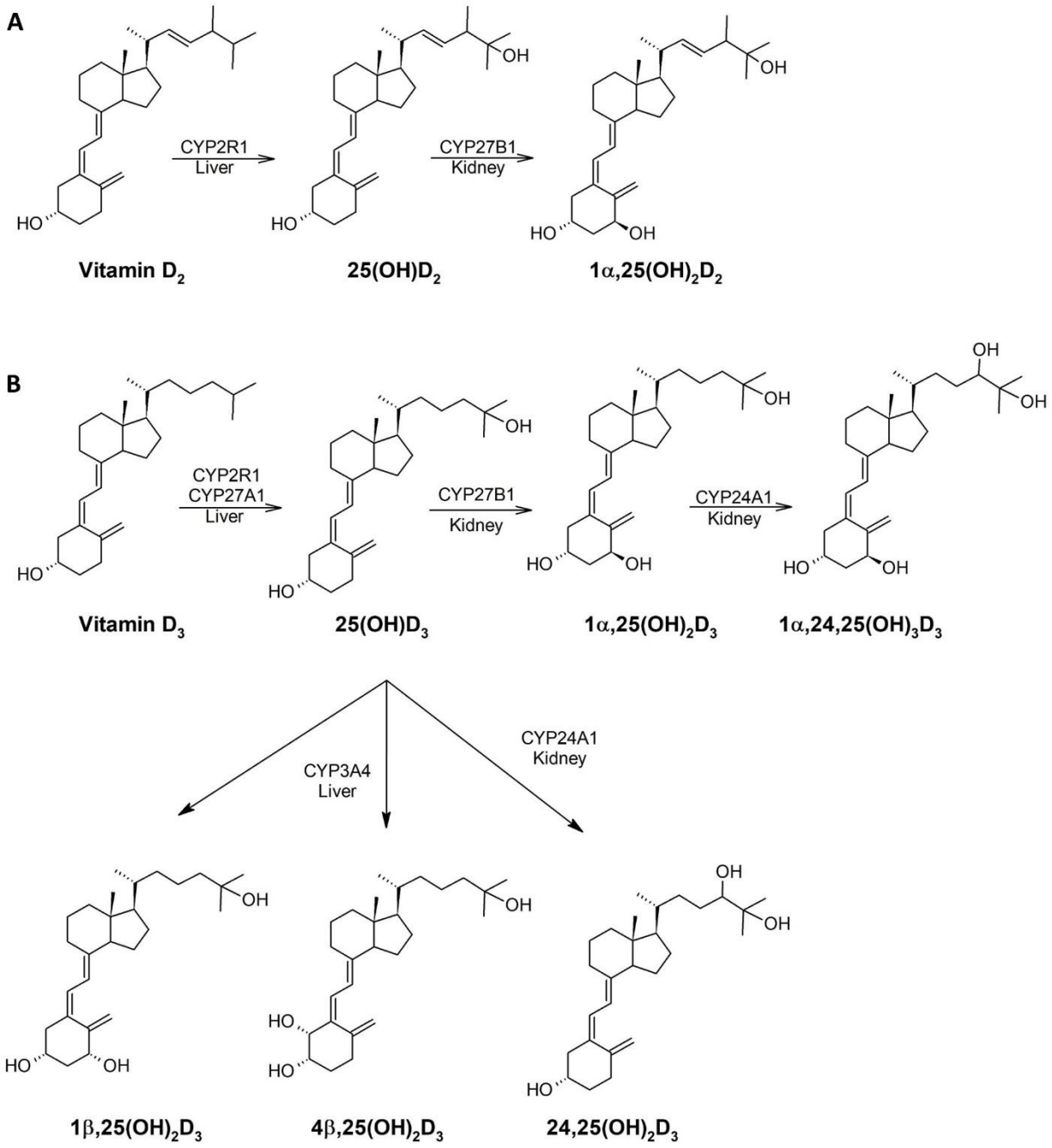

Figure 2.1: Metabolic scheme of A) vitamin D_2 and B) vitamin D_3 and metabolites analyzed in this assay.

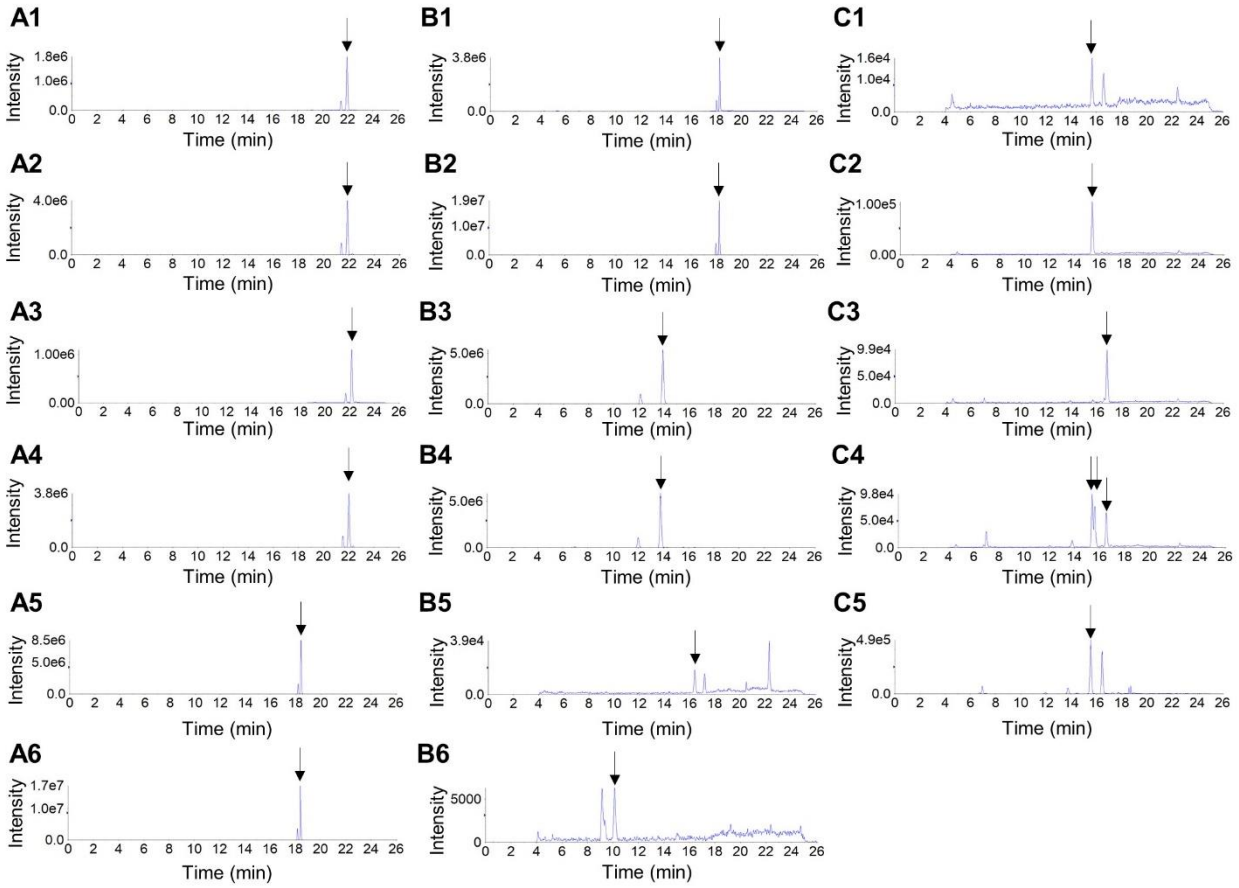

Figure 2.2: Representative chromatograms of vitamin D_2, vitamin D_3, metabolites of interest and their internal standards. A1) Vitamin D_2; A2) d_3-vitamin D_2; A3) Vitamin D_3; A4) d_7-vitamin D_3; A5) 25-hydroxyvitamin D_2, A6) d_6-25-hydroxyvitamin D_2, B1) 25-hydroxyvitamin D_3, B2) d_6-25-hydroxyvitamin D_3; B3) 24R,25-dihydroxyvitamin D_3; B4) d_6-24R,25-dihydroxyvitamin D_3; B5) 1α,25-dihydroxyvitamin D_2; B6) 1α,24R,25-trihydroxyvitamin D_3; C1) 1α,25-dihydroxyvitamin D_3; C2) 4β,25-dihydroxyvitamin D_3; C3) 1β,25-dihydroxyvitamin D_3; C4) 4β,25-dihydroxyvitamin D_3, 1α,25-dihydroxyvitamin D_3, and 1β,25-dihydroxyvitamin D_3, respectively; C5) d_6-1α,25-dihydroxyvitamin D_3.

Chapter 3.

Altered Vitamin D Metabolism in Patients with Cystic Fibrosis

3.1. Abstract

Historically, patients with cystic fibrosis (CF) have lower circulating levels of 25-hydroxyvitamin D (25(OH)D), the major circulating metabolite of vitamin D, compared to healthy individuals. Lower 25(OH)D is associated with an increased risk of osteoporosis, decreased lung function, and a higher risk of lung infections. In this chapter, we investigated whether patients with CF had increased metabolism of 25(OH)D in an observational cohort study and a pharmacokinetic study. In the observational cohort study, single blood samples were analyzed for 25(OH)D and its metabolites, including 1α,25-dihydroxyvitamin D (1α,25$(OH)_2$D), 24,25-dihydroxyvitamin D_3 (24,25$(OH)_2D_3$), 4β,25-dihydroxyvitamin D_3 (4β,25$(OH)_2D_3$), 25-hydroxyvitamin D_3-3-sulfate (25$(OH)D_3$-S), and 25-hydroxyvitamin D_3-3-glucuronide (25$(OH)D_3$-G) by liquid chromatography with tandem mass spectrometry (LC-MS/MS) in 83 patients with CF and 82 age-, race-, and sex-matched healthy controls. Although serum 25(OH)D were similar in healthy controls and CF patients, both serum 4β,25$(OH)_2D_3$ and 25$(OH)D_3$-S were 40% lower in patients with CF compared to healthy controls. In the pharmacokinetic study, deuterium-labeled 25$(OH)D_3$ (d_6-25$(OH)D_3$) was administered intravenously to 5 patients with CF and 5 healthy controls to study the disposition of 25$(OH)D_3$. We observed no difference in the clearance of d_6-25$(OH)D_3$ in patients with CF compared to healthy controls, however, this study was underpowered to detect small changes in clearance. Larger studies would need to be conducted to determine if the kinetics of d_6-25$(OH)D_3$ or d_6-24,25$(OH)_2D_3$ is altered in patients with CF.

3.2. Introduction

Cystic Fibrosis (CF) affects an estimated 30,000 individuals in the United States and 70,000 individuals worldwide (1). Occurring at a rate of approximately 1:3200 births in

Caucasians, CF is one of the most prevalent, lethal genetic disorders (1, 2). CF is caused by defects in the cystic fibrosis transmembrane conductance regulator (CFTR) protein (1-3). CFTR is a chloride channel protein, important in balancing the osmolarity in epithelial cells (1-3). CFTR is expressed at the apical membrane of epithelial cells in the lungs, skin, kidney, pancreas, digestive tract, and reproductive organs (1-3). A loss of CFTR function results in the accumulation of mucus in the lumen of the affected tissues, most notably the lungs (1-3). The buildup of mucus in the lungs allows for the colonization of bacteria, resulting in frequent lung infections and a decrease in lung function (1-3). Approximately 2,000 *CFTR* variants have been identified in patients with CF (4). While the majority of these variants are rare, 85% of patients carry a three-base deletion in *CFTR* that encodes the phenylalanine 508 deletion (*F508del*). Half of CF patients are homozygous for *F508del* and the remaining patients carry one *F508del* and another reduced or loss of function genetic variant (4).

Vitamin D deficiency increases the risk of bone disorders, including rickets, osteomalacia, osteopenia, and osteoporosis in healthy children and adults (5-12). However, these effects on bone health are further compounded in patients with CF (13, 14). Bone strength in patients with CF is affected by a decreased ability to exercise and from malnutrition due to poor absorption of nutrients (13, 14). Additionally, the use of medications, especially corticosteroids, commonly used to manage the symptoms of CF, can further impair bone health (13, 15). In 2013, 21% of young adults in the Cystic Fibrosis Foundation Patient Registry reported having osteopenia. Globally, other studies have shown that up to 50% of adults with CF have osteopenia, while 10-34% report having osteoporosis (15-17). Additionally, a meta-analysis of bone health in patients with CF found that the prevalence of vertebral fractures was 38%, while the prevalence of non-vertebral fractures was 23.5% (13, 18). Supplementation with calcium and vitamin D have been shown to be effective at reducing bone loss in patients with CF (19).

Apart from bone health, there is also evidence suggesting that higher levels of vitamin D in CF patients are associated with better immune function and health outcomes (20). In a randomized, placebo-controlled trial of adult patients with CF hospitalized with pulmonary exacerbations, subjects that received a single high dose of vitamin D_3 (250,000 IU orally) spent 36 fewer days in the hospital in the 6 months following treatment. Additionally, the subjects treated with high dose vitamin D had higher 1-year survival rates compared to subjects receiving the placebo control (21). However, there is mixed evidence as to whether serum concentrations of 25-hydroxyvitamin D (25(OH)D) are positively associated with forced expiratory volume (FEV), a measure of pulmonary function (22, 23).

The Cystic Fibrosis Foundation (CFF) published guidelines for testing and monitoring vitamin D levels in patients with CF, strategies for optimizing supplementation, and recommendations for the daily supplementation of vitamin D in pediatric and adult patients (24). Despite the awareness of vitamin D deficiency and routine supplementation, researchers in the U.S. and Europe have found that vitamin D deficiency is still a critical issue in patients with CF (14, 25). Multiple studies have reported that up to 90% of children and adults with CF have 25(OH)D concentrations lower than 30 ng/mL (75 nM) recommended by the Cystic Fibrosis Foundation and Endocrine Society (18, 22, 24, 26, 27). However, Hall et al. reported gradual improvement in serum levels of 25(OH)D in children and adults since the CFF guidelines were implemented in the early 2000s (28).

There are numerous potential causes of vitamin D deficiency in patients with CF. Approximately 85-90% of patients with CF have exocrine pancreatic insufficiency due to the accumulation of mucus blocking the secretion of pancreatic enzymes into the small intestine, a process similar to how the disease prevents appropriate air flow in the lungs (1, 2, 29). The accumulation of mucus, and subsequent reduction in secreted pancreatic enzymes, reduces the intestinal absorption of fat and fat-soluble vitamins (1). Although the absorption of fat-soluble vitamins, such as vitamin D, can be increased when supplemented with pancreatic enzymes,

absorption is still reduced in patients with CF compared to healthy controls (14). Many formulations of vitamin D have been developed specifically to overcome the malabsorption of vitamin D in patients with CF (23, 30-32). Other factors that may contribute to vitamin D insufficiency in patients with CF including: reduced sun exposure, increased use of sunscreen, and decreased fat storage, a site for sequestering vitamin D for future needs following sunlight production or dietary consumption (28, 33, 34).

The elimination of 25(OH)D is primarily through metabolism, either to oxidation or conjugated products (Figure 3.1). The biologically active 1α,25-dihydroxyvitamin D ($1\alpha,25(OH)_2D$) and inactive 24R,25-dihydroxyvitamin D ($24,25(OH)_2D$) metabolites are formed predominantly in the kidney by cytochrome P450 (CYP) 27B1 and 24A1, respectively (35-39). In the liver, 4β,25-dihydroxyvitamin D ($4\beta,25(OH)_2D$) is formed by the major drug metabolizing enzyme, CYP3A4 (40-42). The major hepatic conjugated metabolites are 25-hydroxyvitamin D_3-3-sulfate ($25(OH)D_3$-S), formed by sulfotransferase (SULT) 2A1, and 25-hydroxyvitamin D_3-3-glucuronide ($25(OH)D_3$-G), formed by uridine 5'-diphospho-glucuronosyltransferase (UGT) 1A3 and 1A4 (43, 44). The high prevalence of liver disease in CF populations, especially in adulthood, may further reduce the capacity of the liver to metabolize vitamin D.

25(OH)D circulates more than 99% bound to plasma proteins. Approximately 85% of 25(OH)D is bound to the vitamin D binding protein (VDBP), while the remaining 15% is bound to albumin (45, 46). It has been reported that patients with CF have decreased serum concentrations of both VDBP and albumin (47). Decreased concentrations of plasma proteins can potentially contribute to the increased elimination of vitamin D and result in lower steady-state levels of total 25(OH)D, without altering unbound 25(OH)D levels (48). Binding of $25(OH)D_3$ to VDBP is essential for $25(OH)D_3$ reabsorption in the kidney. $25(OH)D_3$ bound to VDBP is endocytosed by the proximal tubule cells via the megalin-cubilin system (49).

Vitamin D works in tandem with parathyroid hormone (PTH) and fibroblast growth factor 23 (FGF) to regulate serum calcium (50). Low concentrations of 1α,25(OH)D stimulate the

release of PTH from the parathyroid (50). Concentrations of PTH are more variable in patients with CF compared to healthy populations. There is also evidence to suggest that higher concentrations of 25(OH)D are required to suppress the release of PTH in patients with CF (13). In contrast, when concentrations of 1α,25$(OH)_2$D are elevated, FGF is released from the bones and reduces the circulating concentration of 1α,25$(OH)_2$D (50). It is unknown if CF affects the release of FGF23.

To better understand the contribution of altered 25(OH)D metabolism to vitamin D deficiency in patients with CF, we conducted an observational cohort study and a pharmacokinetic study. In the observational cohort study, serum samples were collected from patients with CF and age-, race-, and sex-matched healthy controls to investigate differences in basal levels of 25$(OH)D_3$ and its metabolites. In the pharmacokinetic study, healthy controls and patients with CF were administered deuterium-labeled 25$(OH)D_3$ (d_6-25$(OH)D_3$) intravenously to compare the pharmacokinetics of d_6-25$(OH)D_3$ and d_6-24,25$(OH)_2D_3$. Together, these studies provide insights into the metabolism and elimination of 25$(OH)D_3$ in patients with CF.

3.3. Materials and Methods

3.3.1. Chemicals and materials

25$(OH)D_3$-S, 25$(OH)D_3$-G and d_6-25$(OH)D_3$ were purchased from Toronto Research Chemicals (North York, Ontario, Canada). (Diacetoxyiodo)benzene, 3'-phosphoadenosine-5'-phosphosulfate (PAPS), uridine 5′-diphosphoglucuronic acid trisodium salt (UDPGA), alamethacin, 2-amino-2-(hydroxymethyl)-1,3-propanediol hydrochloride (Tris HCl), and bovine serum albumin (BSA) were purchased from Sigma-Aldrich Corp. (St. Louis, MO). 4-(4'-dimethylaminophenyl)-1,2,4-triazolidine-3,5-dione (DAPTAD precursor) was purchased from Santa Cruz Biotechnology, Inc. (Dallas, TX). HPLC grade acetonitrile, ethyl acetate, sodium acetate, ammonium hydroxide (28% w/w), methanol, methyl tert-butyl ether (MTBE), heptane,

isopropanol, hexanes, formic acid, acetic acid, dichloromethane, and magnesium chloride were purchased from Fisher Scientific (Pittsburgh, PA). Vitamin D free serum (Seratrol™) was purchased from Golden West Biologicals, Inc. (Temecula, CA). Human liver microsomes and human liver cytosol were generated at the University of Washington.

3.3.2. Basal Vitamin D and Metabolite Levels in Healthy Controls and Patients with Cystic Fibrosis

3.3.2.1. Study Population

Patients with CF were recruited into a study to better understand the catabolism of $25(OH)D_3$ in patients with CF. A single blood sample was collected from each patient with CF. Healthy controls with banked blood samples were matched by age, sex, and race to patients with CF.

3.3.2.2. Quantification of vitamin D metabolites

Vitamin D metabolites (i.e., $25(OH)D_3$, $1\alpha,25(OH)_2D_3$, $24,25(OH)_2D_3$, $25(OH)D_2$, and $1\alpha,25(OH)_2D_2$) and circulating levels of fibroblast growth factor 23 (FGF), parathyroid hormone (PTH), albumin, and VDBP were measured in serum samples by liquid chromatography and tandem mass spectrometry (LC-MS/MS) by the Department of Laboratory Medicine at the University of Washington. *VDBP* haplotype was determined from DNA samples by the Department of Laboratory Medicine at the University of Washington.

The concentrations of $4\beta,25(OH)_2D_3$ were measured as described in Chapter 2. In brief, a $4\beta,25(OH)_2D_3$ calibration curve was prepared in BSA. After thawing, 500 µL of serum was aliquoted and an internal standard solution (20 µL of 60 pg/mL of d_6-$1\alpha,25(OH)_2D_3$) was added to each sample. Samples were vortexed, allowed to rest at room temperature for 25 minutes to allow for equilibration of the internal standard and centrifuged at 13,362 *g* for 10 min at 4°C following the addition of 1 mL of acetonitrile to precipitate soluble proteins. The supernatant was

transferred to silanized glass tubes. After the addition of 1.5 mL of 0.1 M phosphate buffer (pH 10.5), analytes were extracted using two solid phase extraction (SPE) steps using Agilent (Santa Clara, CA) Bond Elut C18 OH SPE cartridges (500 mg, 3 mL) and Agilent Bond Elut SI cartridges (100 mg, 1 mL). Sample analytes were eluted with 5% isopropanol in MTBE (v/v) into silanized glass culture tubes and dried under N_2 gas at 37°C. The residue was reconstituted in 50 µL of acetonitrile, followed by the addition of DAPTAD (50 µL). Samples were shaken at room temperature for 45 minutes before the reaction was quenched by drying under N_2 gas at 37°C. Following reconstitution in 45 µL of methanol and 20 µL of water, the derivatized samples were centrifuged at 13,362 *g* for 5 min to remove insoluble particulates and excess DAPTAD. The supernatant was transferred to a 96-well plate for LC-MS/MS analysis.

Liquid chromatography-mass spectrometry (LC-MS/MS) analysis was performed on a Sciex QTRAP 6500 hybrid triple quadrupole/linear ion trap mass spectrometer (Framingham, MA) coupled with a Shimadzu liquid chromatography system (Kyoto, Japan). Chromatographic separation was achieved using an Ascentis Express RP-Amide column (2.1 mm x 150 mm x 2.7 µm) (Sigma-Aldrich Corp.), attached to a SecurityGuard™ ULTRA cartridge (2.1 mm x 2 µm) guard column (Phenomenex, Torrance, CA). The column temperature was maintained at 20°C with a mobile phase flowing at a rate of 0.275 mL/min. The autosampler was maintained at 4°C and the injection volume was 10 µL. A gradient was used to elute the analytes with a mobile phase consisting of 0.1% formic acid in water (A) and 100% methanol (B). The total run time was 26 minutes. Mass spectrometric conditions are summarized in Table 3.1. The electrospray ionization (ESI) source of the mass spectrometer was operated in the positive ion mode. Multiple reaction monitoring (MRM) was used for quantitation. The retention time, precursor and product ions, declustering potential, entrance potential, collision energy, and collision cell exit potential for each analyte are presented in Table 3.1.

Peak integration was performed using MultiQuant software (version 3.0.2) from AB Sciex. The peak height of 4β,25$(OH)_2D_3$ was normalized to d_6-1α,25$(OH)_2D_3$. A quadratic

equation with $1/x^2$ weighting was used to estimate the relationship between the peak height ratio and concentration. The lower limit of detection (LLOD) was set at 5 times above background.

The conjugated metabolites, 25(OH)D_3-S and 25(OH)D_3-G, were quantified by the LC-MS/MS method described by Gao et al. (51). In brief, the calibration curve and QC samples were prepared in vitamin D-free serum. The internal standards, *d*$_6$-25(OH)D_3-S and *d*$_6$-25(OH)D_3-G, were generated by enzymatic incubations with *d*$_6$-25(OH)D_3. The *d*$_6$-25(OH)D_3-S internal standard was prepared by incubating 25 µM of *d*$_6$-25(OH)D_3, 0.1 M PAPS, and 4 mg/mL of pooled human liver cytosol in 50 mM Tris HCl buffer (pH: 7.5) (final volume 1 mL) at 37°C. The reaction was quenched after 3 to 5 hours with the addition of 1 mL of cold acetonitrile. The *d*$_6$-25(OH)D_3-G internal standard was prepared by incubating with 25 µM *d*$_6$-25(OH)D_3, 50 µg/mL alamethacin, 5 mM $MgCl_2$, 5 mM UDPGA, and 1 mg/mL pooled human liver microsomes in 50 mM Tris HCl buffer (pH 7.5) (final volume 1 mL) at 37°C. The reaction was quenched after 3 to 5 hours with 1 mL of cold acetonitrile. Precipitated proteins were removed from the internal standard products by centrifuging the samples at 13,000 g for 10 min at 4°C. Following derivatization with DAPTAD as described below, the abundance of *d*$_6$-25(OH)D_3-S and *d*$_6$-25(OH)D_3-G in the internal standard solutions was estimated by comparing LC-MS/MS peak heights with undeuterated 25(OH)D_3-S and 25(OH)D_3-G standards.

Human serum (200 µL) was combined with approximately 4 pmol of *d*$_6$-25(OH)D_3-S and 1.6 pmol of *d*$_6$-25(OH)D_3-G. Proteins were precipitated with 1 mL of acetonitrile and centrifuged at 13,000 *g* for 10 min at 4°C. The supernatants were combined with 1 mL of 0.1 M sodium acetate (pH 3.2). The samples were subjected to SPE using Waters Oasis WAX (1 cc, 30 mg, 60 µm) anion exchange cartridges (Waters (Milford, MA). The analytes were eluted from the column with the addition of 28% w/w ammonium hydroxide in methanol (3:97 v/v). Samples were dried under N_2 at 37°C and reconstituted in 50 µL of acetonitrile and derivatized with 50 µL of DAPTAD solution for 1 hour. Solutions were dried under N_2 at 37°C, reconstituted in 100 µL

of 30% acetonitrile in water and centrifuged at 20,000 *g* at 4°C for 5 min to remove excess DAPTAD.

Chromatographic separation was achieved using a Hypersil Gold (2.1 × 100 mm, 1.9 µm) column (Thermo Fisher Scientific, Waltham, MA) maintained at 45°C. LC-MS/MS analysis was performed on a Sciex QTRAP 6500 hybrid triple quadrupole/linear ion trap mass spectrometer with ESI operated in the positive mode coupled with a Shimadzu liquid chromatography system. The MRM transitions used for quantification, standard curve range, and the limits of quantification are presented in Table 3.2.

Peak integration was performed by MultiQuant software (version 3.0.2). Peak area ratios were determined by taking the peak areas of 25(OH)D_3-S or 25(OH)D_3-G and normalizing to the respective deuterated metabolite peak areas. A linear equation with $1/x^2$ weighting was fit to estimate the relationship between peak area ratios and concentrations of 25(OH)D_3-S or 25(OH)D_3-G.

3.3.2.3. Estimation of unbound concentrations of 25-hydroxyvitamin D_3 and 1α,25-dihydroxyvitamin D_3

Unbound concentrations of 25(OH)D_3 and 1α,25$(OH)_2D_3$ were calculated using the equations previously published by Bikle et al. (Equation 3.1),

$$D_{free} = \frac{D_{total}}{\left(1 + (k_{ALB} \cdot [ALB]) + (k_{VDBP} \cdot [VDBP])\right)} \quad (3.1)$$

where D_{free} is the calculated free concentration of 25(OH)D_3 or 1α,25$(OH)_2D_3$. D_{total} is the measured serum concentration of 25(OH)D_3 or 1α,25$(OH)_2D_3$. [ALB] and [VDBP] are the measured serum albumin and VDBP concentrations, respectively. k_{ALB} and k_{VDPB} are the binding constants for albumin and VDBP, respectively (46, 52, 53). The values of the 25(OH)D_3 binding constants for albumin and VDBP are 6×10^5 M^{-1} and 7×10^8 M^{-1}, respectively. The values of the

1α,25(OH)$_2$D$_3$ binding constants for albumin and VDBP are 5.4 x 10^4 M^{-1} and 3.7 x 10^7 M^{-1}, respectively.

The percent unbound of 25(OH)D$_3$ and 1α,25(OH)$_2$D$_3$ was estimated by Equation 3.2.

$$\% \text{ Unbound} = \frac{\text{D}_{\text{free}}}{\text{D}_{\text{total}}} \cdot 100\% \quad (3.2)$$

3.3.2.4. Statistical Analysis

The parent-to-metabolite molar ratio was calculated as (molar concentration of metabolite)/(molar concentration of parent)·1000, where the parent was 25(OH)D, 25(OH)D$_2$ or 25(OH)D$_2$, where appropriate.

Concentrations of vitamin D, its metabolites, parent-to-metabolite ratios, unbound concentrations, PTH, FGF, VDBP, and albumin were compared between healthy controls and patients with CF using a Wilcoxon test. Due to the small sample size, seasons were grouped as spring/summer and fall/winter. The comparison of total 25(OH)D concentrations between healthy controls and patients with CF was performed using linear regression, adjusted by season. Comparison between 25(OH)D$_3$ and gender was performed using linear regression, adjusted by season. Separate linear regressions were performed for healthy controls and patients with CF. Comparisons of 25(OH)D between seasons, *VDBP* haplotypes, and *CFTR* haplotypes were done using a Wilcoxon test. Correlations of 25(OH)D with its metabolites were calculated with a Spearman's Correlation. Correlations of 25(OH)D and 1α,25(OH)$_2$D to FGF and PTH were assessed using a Spearman's Correlation. A value of $p < 0.05$ was considered statistically significant.

3.3.3. Pharmacokinetics of d_6-25-hydroxyvitamin D_3 in Healthy Controls and Patients with CF

3.3.3.1. Study Design

A single bolus dose of d_6-25(OH)D_3 was administered intravenously to healthy controls and patients with CF. All study participants were required to be 18 years or older and have a screening serum 25(OH)D concentration between 10 to 50 ng/mL. Participants were excluded if they had taken supplements of more than 400 IU of vitamin D_2 or vitamin D_3 within 3 months of enrollment or used vitamin D receptor agonists or cinacalcet within 4 weeks of enrollment. In addition, participants were excluded if they used cytochrome P450 inhibitors or inducers within 4 weeks of enrollment.

The dose of d_6-25(OH)D_3 was individualized for each study participant and calculated to target a maximum initial concentration of 5 ng/mL. Estimated blood volume (EBV) was calculated using the equation by Nadler et al. (54) and the dose was estimated as 5 ng/mL * EBV. Serum samples were collected at 15 minutes, 4 hours, 1, 4, 7, 14, 21, 28, 42, and 56 days after d_6-25(OH)D_3 administration.

3.3.3.2. Analysis of d_6-25-hydroxyvitamin D_3 and d_6-24,25-dihydroxyvitamin D_3

The vitamin D metabolites, d_6-25(OH)D_3, and d_6-24,25$(OH)_2D_3$, were measured by liquid chromatography with tandem mass spectrometry (LC-MS/MS) by the Department of Laboratory Medicine at the University of Washington.

3.3.3.3. Non-Compartmental Analysis of d_6-25-hydroxyvitamin D_3 and d_6-24,25-dihydroxyvitamin D_3

Serum concentrations of d_6-25(OH)D_3 and d_6-24,25$(OH)_2D_3$ were analyzed using non-compartmental analysis (NCA) with Phoenix software (version 8.0.0). Since the administered dose of d_6-25(OH)D_3 was calculated from EBVs, the concentration-time profiles were dose-

normalized and scaled to a 25 µg dose of d_6-25(OH)D_3 to compare the pharmacokinetic parameters between the patients with CF and healthy controls.

For d_6-25(OH)D_3, C_{max} and T_{max} were the observed dose-normalized peak d_6-25(OH)D_3 concentration and the time when the concentration was observed, respectively. The elimination rate constant (k) was estimated using uniform weighting of the timepoints after 14 days. The elimination half-life of d_6-25(OH)D_3 was calculated as $t_{1/2} = \ln(2)/k$. For d_6-25(OH)D_3, the area under the concentration-time curve ($AUC_{0-\infty}$) was calculated as $AUC_{0\text{-}last} + C_{last}/k$, where the trapezoidal rule was used to calculate $AUC_{0\text{-}last}$ (AUC from t = 0 to the last observed timepoint) and added to the extrapolated AUC from the last observed concentration (C_{last}) to time = infinity. Clearance (CL) of d_6-25(OH)D_3 was calculated as dose/$AUC_{0-\infty}$. The volume of distribution (V_{ss}) was calculated using Equation 3.3, where AUMC is the area under the first moments curve.

$$V_{ss} = \frac{\text{dose} \cdot \text{AUMC}}{(AUC_{0-\infty})^2} \tag{3.3}$$

Concentrations of d_6-24,25(OH)$_2D_3$ were not dose-normalized for group comparisons. For d_6-24,25(OH)$_2D_3$, C_{max} and T_{max} were the observed peak d_6-24,25(OH)$_2D_3$ concentration and the time when the peak concentration was observed, respectively. There were not enough data to determine the elimination rate constant of d_6-24,25(OH)$_2D_3$ due to its long half-life and measured concentrations being near the lower limit of quantification. The area under the concentration-time curve from time = 0 to the last observed serum sample ($AUC_{0\text{-}last}$) was calculated using the trapezoidal rule.

3.3.3.4. Statistical Analysis

Pharmacokinetic parameters of patients with CF were compared to healthy controls using a Mann-Whitney test. A value of $p < 0.05$ was considered statistically significant.

3.4. Results

3.4.1. Survey of Vitamin D and Metabolite Levels in Patients with CF Matched to Healthy Controls

3.4.1.1. Demographics

A total of 83 study patients with CF and 82 healthy controls were recruited. The demographics for the participants are provided in Table 3.3. While an effort was made to match healthy controls to patients with CF by age, gender, and race, participants were not matched by the season during which the sample was collected. The mean age for both groups was comparable (Healthy: 32.5 ± 11.2 years, CF: 32.3 ± 11.1 years). The percentage of males in the healthy controls (38% male) was lower than that of the CF group (55% male). Nearly all of the participants self-identified as Caucasian in both groups (96%). More than 85% of patients with CF were diagnosed with pancreatic insufficiency. About 50% and 40% of the patients with CF were homozygous and heterozygous for the *F508del CFTR* mutation, respectively. The remaining 10% were not carriers of the *F508del CFTR* mutation. Serum VDBP concentrations were similar between healthy controls and patients with CF (274 ± 56 µg/mL and 264 ± 41 µg/mL, respectively). The most frequent *VDBP* haplotype in healthy controls and patients with CF was the *Gc1s/Gc1s* haplotype (healthy controls = 67%, patients with CF = 49%). Serum albumin concentrations were 10% lower in the patients with CF compared to healthy controls (healthy controls = 4.3 ± 0.3, patients with CF = 3.9 ± 0.4, $p < 0.001$). FGF and PTH concentrations were similar between healthy controls and patients with CF.

3.4.1.2. Basal Levels of Total 25-hydroxyvitamin D and 1α,25-dihydroxyvitamin D

The concentrations of total 25(OH)D and 1α,25$(OH)_2$D are presented in Table 3.4. Vitamin D sufficiency, insufficiency and deficiency are defined as 25(OH)D concentrations greater than 30 ng/mL, 20 to 30 ng/mL, and less than 20 ng/mL, respectively (25). The

distribution of vitamin D status in healthy controls and patients with CF is shown in Figure 3.2. Less than 40% of participants in both groups were vitamin D sufficient. In the healthy controls, 41% of participants were vitamin D insufficient and 21% were vitamin D deficient. Similarly, 34% of patients with CF were vitamin D insufficient and 33% were vitamin D deficient. Mean basal levels of 25(OH)D in healthy controls and patients with CF were 27.7 ± 9.9 ng/mL and 26.7 ± 12.3 ng/mL, respectively. However, the total concentration of 1α,25$(OH)_2$D was 14% lower in patients with CF compared to healthy controls (Healthy Controls = 50.7 ± 13.0 pg/mL, patients with CF = 43.6 ± 12.7 pg/mL, $p < 0.001$). In contrast, the molar ratios of 1α,25$(OH)_2$D to 25(OH)D were comparable between the two groups (Healthy Controls = 1.97 ± 0.90 pg/mL; Patients with CF = 2.10 ± 1.57).

The mean concentration of 25(OH)D by season was similar between the two groups (Figure 3.3). For patients with CF, concentrations of 25(OH)D were significantly lower in the fall and winter compared to the spring and summer ($p < 0.01$, Figure 3.3). The concentrations of 25(OH)D in healthy women were 22% lower than in healthy men ($p < 0.05$, Figure 3.4). In patients with CF, there was no difference in 25(OH)D concentrations between men and women (Figure 3.4). Concentrations of total and unbound 25(OH)D did not vary by *VDBP* haplotype (data not shown). In the patients with CF, 25(OH)D concentrations were not affected by pancreatic insufficiency or the number of *F508del* alleles (data not shown).

3.4.2. Basal levels of 25-hydroxyvitamin D_3 and its metabolites

The concentrations of 25$(OH)D_3$ and its metabolites are presented in Table 3.4 and Figure 3.5. The basal 25$(OH)D_3$ concentrations were comparable between healthy controls and patients with CF (Healthy Controls = 26.8 ± 10.1 ng/mL, Patients with CF = 25.3 ± 12.5 ng/mL). The concentrations of 1α,25$(OH)_2D_3$ were 15% higher in healthy controls compared patients with CF (Healthy Controls = 49.5 ± 12.8 pg/mL, Patients with CF = 42.3 ± 13.3; $p < 0.001$). In contrast, the molar ratio of 1α,25$(OH)_2D_3$ to 25$(OH)D_3$ was comparable between the two groups

(Healthy Controls = 2.01 ± 0.92, Patients with CF = 2.14 ± 1.57) (Table 3.4 and Figure 3.6A). The circulating concentrations of 24,25$(OH)_2D_3$ and the 24,25$(OH)_2D_3$ to 25$(OH)D_3$ molar ratio were comparable between the two cohorts (Figures 3.5B and 3.6B). Concentrations of 24,25$(OH)_2D_3$ were highly corelated with 25$(OH)D_3$ in both cohorts (Figure 3.7B). The basal concentrations of 4β,25$(OH)_2D_3$ were 35% lower in patients with CF (52.1 ± 38.9 pg/mL) compared to healthy controls (79.9 ± 60.2 pg/mL, $p < 0.001$, Figure 3.5C). Similarly, the molar ratios of 4β,25$(OH)_2D_3$ to 25$(OH)D_3$ were 30% lower in the patients with CF (2.09 ± 1.49) compared to healthy controls (2.94 ± 1.79, $p < 0.001$) (Figure 3.6C). Concentrations of 4β,25$(OH)_2D_3$ were weakly correlated with 25$(OH)D_3$ in both the healthy controls and patients with CF (Figure 3.7C).

For the conjugated metabolites, 25$(OH)D_3$-S concentrations were 40% lower in the patients with CF compared to the healthy controls (52.1 ± 38.9 and 79.9 ± 60.2, respectively, $p < 0.001$, Figure 3.5E). Similarly, the 25$(OH)D_3$-S to 25$(OH)D_3$ molar ratio in patients with CF (587 ± 274) was 40% lower than in the healthy controls (985 ± 426, $p < 0.001$, Figure 3.6D). The 25$(OH)D_3$-G concentrations were similar between the healthy controls and patients with CF (2.2 ± 1.6 and 1.9 ± 1.2, respectively, Figure 3.5F) as were the 25$(OH)D_3$-G to 25$(OH)D_3$ molar ratios (Figure 3.6E). Levels of 25OHD_3-S and 25$(OH)D_3$-G were both moderately correlated with 25$(OH)D_3$ (Figures 3.7D and 3.7E).

3.4.2.1. Basal Levels of 25-hydroxyvitamin D_2 and 1α,25-dihydroxy vitamin D_2

The concentrations of 25$(OH)D_2$ and 1α,25$(OH)_2D_2$ are presented in Table 3.4 and Figure 3.8. In general, concentrations of 25$(OH)D_2$ were more than 20-fold lower than concentrations of 25$(OH)D_3$. In healthy controls, the mean 25$(OH)D_2$ concentration was 0.9 ± 1.9 ng/mL compared to 1.3 ± 5.4 ng/mL in patients with CF ($p < 0.001$). Concentrations of 1α,25$(OH)_2D_2$ were 30% lower in healthy controls compared to patients with CF ($p < 0.001$). However, when normalized to 25$(OH)D_2$ concentrations, the molar ratios of 1α,25$(OH)_2D_2$ to

25(OH)D_2 were comparable between the two groups. Concentrations of 1α,25(OH)$_2D_2$ were not correlated with 25(OH)D_2 concentrations (data not shown).

3.4.2.2. Basal levels of unbound 25-hydroxyvitamin D_3 and 1α,25-dihydroxyvitamin D_3

Mean unbound concentrations and percent unbound of 25(OH)D_3 and 1α,25(OH)$_2D_3$ are presented in Table 3.5. The unbound concentrations of 25(OH)D_3 and 1α,25(OH)$_2D_3$ were estimated using 25(OH)D_3 or 1α,25(OH)$_2D_3$ concentrations, serum concentrations of VDBP and albumin, and their respective binding constants. The unbound concentrations and percent unbound of 25(OH)D_3 were unchanged between healthy controls (18.2 ± 6.8 ng/mL and 0.0693 ± 0.001%, respectively) and patients with CF (17.9 ± 8.4 ng/mL and 0.0716 ± 0.009%, respectively). The unbound concentration of 1α,25(OH)$_2D_3$ was 10% lower in patients with CF (0.508 ± 0.151 pg/mL) compared to healthy controls (0.566 ± 0.126 pg/mL, $p < 0.05$). In contrast, the fraction unbound of 1α,25(OH)$_2D_3$ was 4% higher in patients with CF compared to the healthy controls ($p = 0.03$).

3.4.2.3. Correlation of fibroblast growth factor 23 and parathyroid hormone with 25-hydroxyvitamin D and 1α,25-dihydroxyvitamin D

FGF concentrations were not associated with total 25(OH)D concentrations, but were weakly negatively associated with 1α,25(OH)D concentrations (Healthy: $R^2 = 0.132$, $p < 0.001$; CF: $R^2 = 0.288$, $p < 0.001$) (Figure 3.9). In contrast, PTH was not associated with 25(OH)$_2$D 1α,25(OH)$_2$D concentrations (Figure 3.9).

3.4.3. Pharmacokinetics of d_6-25-hydroxyvitamin D_3 in Healthy Controls and Patients with CF

3.4.3.1. Demographics

A total of 10 participants, 5 patients with CF and 5 healthy controls were recruited to receive d_6-25(OH)D_3 intravenously. The demographics for the participants are presented in

Table 3.6. The mean age of patients with CF were 38.8 ± 13.3 compared to 24.8 ± 3.3 in healthy controls. A higher percentage of males were enrolled in the CF cohort (4 of 5) compared to the healthy controls (1 of 5).

3.4.3.2. Pharmacokinetics of d_6-25-hydroxyvitamin D_3

A single bolus dose of d_6-25(OH)D_3 was administered intravenously to five healthy controls and five patients with CF. The chemical structure of the d_6-25(OH)D_3 with the location of the deuterium labels is presented in Figure 3.10. The mean dose of d_6-25(OH)D_3 was 22.0 µg (range: 18 to 26 µg) in the healthy controls and 26.4 µg (range: 22 to 30 µg) for the patients with CF. Pharmacokinetics of d_6-25(OH)D_3 were determined after concentrations were dose-normalized and scaled to a 25 µg dose of d_6-25(OH)D_3. The mean and representative concentration vs. time profiles are presented in Figure 3.11. The mean d_6-25(OH)D_3 estimated pharmacokinetic parameters are presented in Table 3.7. No differences were noted between healthy controls and patients with CF for the dose-normalized C_{max} and $AUC_{0-\infty}$ following intravenous administration of d_6-25(OH)D_3. In addition, clearance, terminal half-life and V_{SS} were comparable between healthy controls and patients with CF.

3.4.3.3. Pharmacokinetics of d_6-24,25-dihydroxyvitamin D_3

The serum d_6-24,25$(OH)_2D_3$ concentrations were measured after intravenous administration of d_6-25(OH)D_3. The mean and representative d_6-24,25$(OH)_2D_3$ concentration vs. time profiles are presented in Figure 3.10. Mean d_6-24,25$(OH)_2D_3$ estimated pharmacokinetic parameters are presented in Table 3.8. The peak d_6-24,25$(OH)_2D_3$ concentration was observed between 4 to 21 days and the peak concentrations were comparable between the two groups (Healthy = 0.13 ± 0.02 ng/mL, CF = 0.16 ± 0.02 ng/mL). The $AUC_{0\text{-last}}$ was calculated to the last observed concentration for each subject and was comparable in healthy controls and patients with CF. Due to variability in the data, the terminal half-life and $AUC_{0-\infty}$ could not be estimated.

3.5. Discussion

Optimizing vitamin D levels in patients with CF is essential for maintaining bone strength and immune function. Low levels of vitamin D in patients with CF has been attributed to poor intestinal absorption, reduced time outdoors, and reduced storage capacity due to low body fat (28). While many factors can contribute to vitamin D deficiency in patients with CF, in this chapter, we investigated the hypothesis that altered $25(OH)D_3$ metabolism in patients with CF contributes to low circulating levels of $25(OH)D_3$.

In our study, approximately 70% of the 83 patients with CF were vitamin D insufficient or deficient, as defined by the Cystic Fibrosis Foundation (25). The prevalence of vitamin D insufficiency and deficiency was similar to the healthy controls, however 50% of patients with CF were taking supplements compared to 22% in healthy controls. The dose of vitamin D supplements was not recorded. A chart review at Emory University Hospital showed a near doubling of the dose of vitamin D supplementation between 2008 and 2012 and a concomitant increase in 25(OH)D levels in patients with CF (18). Hall et al. reported an increase in 25(OH)D concentrations in patients with CF over the last 15 years (28). The results from our study, as well as studies conducted at other institutions, suggest that recent efforts to increase vitamin D supplementation in patients with CF have resulted in improved 25(OH)D levels.

Although concentrations of 25(OH)D in healthy controls was lower in the fall and winter months compared to the spring and summer months, no difference was noted among the patients with CF. Larger cohort studies in both patients with CF and healthy controls have reported that serum concentrations of 25(OH)D are lower in winter compared to summer, which is attributed to the change in sun exposure throughout the year. In a study of 185 patients with CF, Wolfenden et al. reported that concentrations 25(OH)D were nearly 40% lower in the winter compared to summer and fall (22). Similarly, a study of 540 healthy blood donors in Sweden found that 25(OH)D concentrations were 40% lower in the winter compared to the summer (55). The current recommendation of the Cystic Fibrosis Foundation is to test serum levels of

25(OH)D annually late in the fall or during the winter to assess 25(OH)D levels at their lowest point of the year (25).

We observed no differences in 25(OH)D concentrations between sexes in patients with CF, though healthy women had lower levels than healthy men. In contrast, Wolfenden et al. reported the prevalence of vitamin D deficiency was higher in men with CF (84%) compared to women with CF (70%) in a cohort of 185 patients with CF (22). Although *VDBP* haplotype is reported to affect the binding of affinity of 25(OH)D, we found no difference in the total 25(OH)D concentrations by *VDBP* haplotype, which may be due to the small sample size in our study (53, 56).

We did not find an association of the number of *F508del* alleles with $25(OH)D_3$ concentrations. The number of patients with CF in our study may not have been sufficient to detect differences in the number of *F508del* alleles. In additional, pancreatic insufficiency did not appear to be associated with lower levels of $25(OH)D_3$. Dorlochter et al. also reported no difference in $25(OH)D_3$ levels between subjects with CF with and without pancreatic insufficiency compared to those that were pancreatic sufficient, if adequately supplemented (57).

Serum concentrations of $25(OH)D_3$ were correlated with the serum concentrations of its metabolites. To compare the concentration of $25(OH)D_3$ metabolites in patients with CF, the metabolite to parent ratios were calculated to account for interindividual variability $25(OH)D_3$ concentrations. We observed lower basal serum $1\alpha,25(OH)_2D_3$, however, the $1\alpha,25(OH)_2D_3$ to $25(OH)D_3$ ratios were similar between patients with CF and healthy controls, which suggests that the lower concentration of $1\alpha,25(OH)_2D_3$ in patients with CF is likely due to the variability it the concentration of $25(OH)D_3$. Greer et al. also reported that $1\alpha,25(OH)_2D$ was lower in adults with CF compared to healthy controls (58).

Unlike $1\alpha,25(OH)_2D_3$, serum concentrations of $4\beta,25(OH)_2D_3$, and $25(OH)D_3$-S were lower in patients with CF compared to healthy controls, even with adjusting for the concentration

of 25(OH)D_3. The activity of CYP3A4 and SULT2A1 have not been directly evaluated in patients with CF compared to healthy controls. However, in a pharmacokinetic study of R-warfarin in patients with CF, the elimination of 10-hydroxywarfarin, formed primarily by CYP3A4, was similar to that of healthy controls, which suggests that CYP3A4 activity is not significantly altered in patients with CF (59). In contrast, sulfation was increased in patients with CF compared to healthy controls after dosing with acetaminophen (60), but dehydroepiandrosterone-sulfate (DHEAS), an endogenous metabolite formed by SULT2A1, was lower in patients with CF compared to standard reference ranges, indicating SULT2A1 activity may be decreased in patients with CF (61). Additionally, 25(OH)D_3-S is transported by breast cancer resistance protein (BCRP) and organic-anion-transporting polypeptide (OATP) 2B1 and 1B3 in the liver (62). Changes in the expression or function OATP2B1 on the apical membrane of enterocytes in CF patients may disrupt the reabsorption of 25(OH)D from the gut lumen following biliary excretion. To better understand the impact of altered drug metabolism in patients with CF, clinical studies on the pharmacokinetics of a conventional CYP3A4 probe substrate, such as midazolam, should be conducted in patients with CF and healthy controls to clarify whether CYP3A4 activity is altered at the intestinal or hepatic level in patients with CF.

Since vitamin D circulates up to 99% bound to plasma proteins, primarily to VDBP (80-85%) and albumin (10-15%), changes in the circulating concentration VDBP or albumin concentrations could alter the metabolism of 25(OH)D in patients with CF (63-65). Additionally, a CF mouse model has decreased cubilin expression in the proximal tubule, defective receptor-mediated endocytosis, increased cubilin excretion in the urine compared to wild-type mice (66). While we found albumin concentrations were on average 9% lower in patients with CF compared to healthy subjects, we observed no difference in VDBP concentrations between the cohorts. Aris et al. reported that concentrations of VDBP and albumin were lower in patients with patients with CF compared to healthy individuals (67). Additionally, we found no difference in the unbound concentration of 25(OH)D_3 between healthy controls and patients with CF.

However, the unbound 25(OH)D_3 concentrations in our study were estimated using published equations rather than direct measurement. While direct measurement of unbound 25(OH)D is highly correlated with calculated estimates in healthy subjects, we could find no study in which this was evaluated in patients with CF. The unbound 1α,25$(OH)_2D_3$ concentrations were lower in patients with CF compared to healthy controls, however, this is expected as serum concentrations of 1α,25$(OH)_2D_3$ were lower in patients with CF.

Markers of the biological response to vitamin D status, FGF and PTH, were comparable between the healthy controls and patients with CF. However, these hormones are variable throughout the day and a single sample may not accurately represent daily exposure. Nonetheless, our results are consistent with a study by Greer et al. reporting comparable PTH concentrations between 291 adults with CF that were age- and gender-matched to healthy controls (58). Previous studies reported that PTH is elevated in patients with CF (15, 27, 67, 68).

It is hypothesized that patients with CF have a reduced capacity to hydroxylate vitamin D in the liver and a limited intestinal absorption of fat-soluble vitamins (29, 67). Others have hypothesized that elimination of 25(OH)D is increased in patients with CF due to decreased plasma protein binding and reduced enterohepatic recirculation (48). We probed the kinetics of 25(OH)D_3 elimination by administering an intravenous bolus dose of deuterium-labeled 25(OH)D_3. To avoid any uncontrolled variability in vitamin D absorption and bioavailability following an oral dose, we opted to administer the dose intravenously. Moreover, low doses of d_6-25(OH)D_3 were targeted to reduce the likelihood of CYP27B1 downregulation and CYP24A1 induction with higher 25(OH)D_3.

There was no difference in the half-life of d_6-25(OH)D_3 between the patients with CF and healthy controls. The estimated half-life of 16 days was similar to previously reported estimates of 16 days (50, 69). The clearance and volume of distribution of d_6-25(OH)D_3 were comparable between healthy controls and patients with CF. With only five participants in each group, our

study was underpowered to detect changes in these parameters. Although, d_6-24,25(OH)D_3 concentrations were measurable, the concentrations were close to the limit of detection resulting in a high degree of variability. Higher doses of d_6-25(OH)D_3 and/or more sensitive analytical methods are required to more accurately quantify d_6-24,25$(OH)_2D_3$ and measure additional metabolites. The exposure of d_6-24,25$(OH)_2D_3$ was comparable between groups indicating that this metabolic pathway is likely unaltered in patients with CF. Although the sample size was small, these data and the lack of difference in 25(OH)D half-life, suggest that lower circulating levels of 25(OH)D is not due to large changes in the elimination of 25(OH)D_3.

The pharmacokinetic study was limited by the small number of subjects in enrolled and the low dose of d_6-25(OH)D_3 administered. More extensive studies, with a larger number of participants are required to make conclusions about the effects of CF on 25(OH)D_3 disposition and metabolism. Higher doses of d_6-25(OH)D_3 are required to detect other metabolites of d_6-25(OH)D_3, unless more sensitive quantification methods are developed. Additionally, investigators should probe the hypothesis that decreased 25-hydroxylation of vitamin D contributes low levels of 25(OH)D_3 in patients with CF. Finally, previous studies have demonstrated that vitamin D absorption is greatly reduced in patients with CF (70), by administering deuterium-labeled vitamin D_3 both intravenously and orally, the difference in the bioavailability and 25-hydroxylation of vitamin D_3 between healthy individuals and patients with CF can be evaluated.

3.6. Conclusions

While these data suggest that the CF patients are receiving sufficient supplementation to match average 25(OH)D concentrations in healthy controls, the majority of the patients with CF in this study still do not have sufficient levels, as defined by the Endocrine Society and Cystic Fibrosis Foundation. The ratios of 4β,25$(OH)_2D_3$ and 25(OH)D_3-S normalized to 25(OH)D_3 were decreased in patients with CF compared to healthy controls, suggesting down-regulation of

hepatic CYP3A4 and UGT. By using deuterium-labeled 25(OH)D_3, we were able to directly assess the disposition of 25(OH)D_3 in healthy controls and patients with CF. In our pharmacokinetic study, we found no difference in the clearance or half-life of d_6-25(OH)D_3 between healthy and patients with CF. While the pharmacokinetic study was small, our data suggest that patients with CF do not have altered 25(OH)D elimination and that other factors such as altered absorption of vitamin D or hepatic 25-hydroxylation contribute to higher risk of vitamin D deficiency in patients with CF.

3.7. References

(1) Strausbaugh, S.D. & Davis, P.B. Cystic fibrosis: a review of epidemiology and pathobiology. *Clinics in chest medicine* **28**, 279-88 (2007).

(2) Radlovic, N. Cystic fibrosis. *Srpski arhiv za celokupno lekarstvo* **140**, 244-9 (2012).

(3) Ratjen, F. & Doring, G. Cystic fibrosis. *Lancet (London, England)* **361**, 681-9 (2003).

(4) Maiuri, L., Raia, V. & Kroemer, G. Strategies for the etiological therapy of cystic fibrosis. *Cell death and differentiation* **24**, 1825-44 (2017).

(5) Holick, M.F. Vitamin D: a d-lightful solution for health. *Journal of investigative medicine : the official publication of the American Federation for Clinical Research* **59**, 872-80 (2011).

(6) Holick, M.F. High prevalence of vitamin D inadequacy and implications for health. *Mayo Clinic proceedings* **81**, 353-73 (2006).

(7) Holick, M.F. Vitamin D status: measurement, interpretation, and clinical application. *Annals of epidemiology* **19**, 73-8 (2009).

(8) Palermo, N.E. & Holick, M.F. Vitamin D, bone health, and other health benefits in pediatric patients. *Journal of pediatric rehabilitation medicine* **7**, 179-92 (2014).

(9) Holick, M.F. & Chen, T.C. Vitamin D deficiency: a worldwide problem with health consequences. *Am J Clin Nutr* **87**, 1080s-6s (2008).

(10) Karaguzel, G. & Holick, M.F. Diagnosis and treatment of osteopenia. *Reviews in endocrine & metabolic disorders* **11**, 237-51 (2010).

(11) Grant, W.B. & Holick, M.F. Benefits and requirements of vitamin D for optimal health: a review. *Alternative medicine review : a journal of clinical therapeutic* **10**, 94-111 (2005).

(12) Holick, M.F. Resurrection of vitamin D deficiency and rickets. *The Journal of clinical investigation* **116**, 2062-72 (2006).

(13) Litonjua, A.A. *Vitamin D and the lung : mechanisms and disease associations* (Humana Press: New York, 2012).

(14) Putman, M.S., Anabtawi, A., Le, T., Tangpricha, V. & Sermet-Gaudelus, I. Cystic fibrosis bone disease treatment: Current knowledge and future directions. *Journal of cystic fibrosis : official journal of the European Cystic Fibrosis Society* **18 Suppl 2**, S56-s65 (2019).

(15) Donovan, D.S., Jr. *et al.* Bone mass and vitamin D deficiency in adults with advanced cystic fibrosis lung disease. *American journal of respiratory and critical care medicine* **157**, 1892-9 (1998).

(16) Chedevergne, F. & Sermet-Gaudelus, I. Prevention of osteoporosis in cystic fibrosis. *Current opinion in pulmonary medicine* **25**, 660-5 (2019).

(17) Buntain, H.M. *et al.* Bone mineral density in Australian children, adolescents and adults with cystic fibrosis: a controlled cross sectional study. *Thorax* **59**, 149-55 (2004).

(18) Siwamogsatham, O., Alvarez, J.A. & Tangpricha, V. Diagnosis and treatment of endocrine comorbidities in patients with cystic fibrosis. *Current opinion in endocrinology, diabetes, and obesity* **21**, 422-9 (2014).

(19) Hillman, L.S., Cassidy, J.T., Popescu, M.F., Hewett, J.E., Kyger, J. & Robertson, J.D. Percent true calcium absorption, mineral metabolism, and bone mineralization in children with cystic fibrosis: effect of supplementation with vitamin D and calcium. *Pediatric pulmonology* **43**, 772-80 (2008).

(20) Pincikova, T., Paquin-Proulx, D., Sandberg, J.K., Flodstrom-Tullberg, M. & Hjelte, L. Vitamin D treatment modulates immune activation in cystic fibrosis. *Clinical and experimental immunology* **189**, 359-71 (2017).

(21) Grossmann, R.E. *et al.* Pilot study of vitamin D supplementation in adults with cystic fibrosis pulmonary exacerbation: A randomized, controlled trial. *Dermato-endocrinology* **4**, 191-7 (2012).

(22) Wolfenden, L.L., Judd, S.E., Shah, R., Sanyal, R., Ziegler, T.R. & Tangpricha, V. Vitamin D and bone health in adults with cystic fibrosis. *Clin Endocrinol (Oxf)* **69**, 374-81 (2008).

(23) Pincikova, T., Paquin-Proulx, D., Sandberg, J.K., Flodstrom-Tullberg, M. & Hjelte, L. Clinical impact of vitamin D treatment in cystic fibrosis: a pilot randomized, controlled trial. *Eur J Clin Nutr* **71**, 203-5 (2017).

(24) Li, L. & Somerset, S. Dietary intake and nutritional status of micronutrients in adults with cystic fibrosis in relation to current recommendations. *Clinical nutrition (Edinburgh, Scotland)* **35**, 775-82 (2016).

(25) Tangpricha, V. *et al.* An update on the screening, diagnosis, management, and treatment of vitamin D deficiency in individuals with cystic fibrosis: evidence-based recommendations from the Cystic Fibrosis Foundation. *J Clin Endocrinol Metab* **97**, 1082-93 (2012).

(26) Chavasse, R.J., Francis, J., Balfour-Lynn, I., Rosenthal, M. & Bush, A. Serum vitamin D levels in children with cystic fibrosis. *Pediatric pulmonology* **38**, 119-22 (2004).

(27) Rovner, A.J., Stallings, V.A., Schall, J.I., Leonard, M.B. & Zemel, B.S. Vitamin D insufficiency in children, adolescents, and young adults with cystic fibrosis despite routine oral supplementation. *Am J Clin Nutr* **86**, 1694-9 (2007).

(28) Hall, W.B., Sparks, A.A. & Aris, R.M. Vitamin d deficiency in cystic fibrosis. *International journal of endocrinology* **2010**, 218691 (2010).

(29) Hahn, T.J., Squires, A.E., Halstead, L.R. & Strominger, D.B. Reduced serum 25-hydroxyvitamin D concentration and disordered mineral metabolism in patients with cystic fibrosis. *The Journal of pediatrics* **94**, 38-42 (1979).

(30) Hermes, W.A. *et al.* Prospective, Randomized, Double-Blind, Parallel-Group, Comparative Effectiveness Clinical Trial Comparing a Powder Vehicle Compound of Vitamin D With an Oil Vehicle Compound in Adults With Cystic Fibrosis. *JPEN Journal of parenteral and enteral nutrition* **41**, 952-8 (2017).

(31) Bertolaso, C. *et al.* Fat-soluble vitamins in cystic fibrosis and pancreatic insufficiency: efficacy of a nutrition intervention. *Journal of pediatric gastroenterology and nutrition* **58**, 443-8 (2014).

(32) Regalado Lam Chew Tun, R., Porhownik, N., Taback, S. & Oleschuk, C. Effect of high dose vitamin D3 therapy on serum vitamin D3 levels in vitamin D insufficient adults with cystic fibrosis. *Clinical nutrition ESPEN* **23**, 84-8 (2018).

(33) Robberecht, E., Vandewalle, S., Wehlou, C., Kaufman, J.M. & De Schepper, J. Sunlight is an important determinant of vitamin D serum concentrations in cystic fibrosis. *Eur J Clin Nutr* **65**, 574-9 (2011).

(34) Lansing, A.H. *et al.* Vitamin D deficiency in pediatric patients with cystic fibrosis: associated risk factors in the northern United States. *Southern medical journal* **108**, 164-9 (2015).

(35) Jones, G., Prosser, D.E. & Kaufmann, M. Cytochrome P450-mediated metabolism of vitamin D. *J Lipid Res* **55**, 13-31 (2014).

(36) Inouye, K. & Sakaki, T. Enzymatic studies on the key enzymes of vitamin D metabolism; 1 alpha-hydroxylase (CYP27B1) and 24-hydroxylase (CYP24). *Biotechnol Annu Rev* **7**, 179-94 (2001).

(37) Sakaki, T., Kagawa, N., Yamamoto, K. & Inouye, K. Metabolism of vitamin D3 by cytochromes P450. *Front Biosci* **10**, 119-34 (2005).

(38) Christakos, S., Ajibade, D.V., Dhawan, P., Fechner, A.J. & Mady, L.J. Vitamin D: metabolism. *Endocrinol Metab Clin North Am* **39**, 243-53, table of contents (2010).

(39) Bikle, D. Vitamin D: Production, Metabolism, and Mechanisms of Action. In: *Endotext* (eds. Feingold, K.R., Anawalt, B., Boyce, A., Chrousos, G., Dungan, K., Grossman, A. *et al.*) (South Dartmouth (MA), 2000).

(40) Wang, Z. *et al.* Enhancement of hepatic 4-hydroxylation of 25-hydroxyvitamin D3 through CYP3A4 induction in vitro and in vivo: implications for drug-induced osteomalacia. *J Bone Miner Res* **28**, 1101-16 (2013).

(41) Wang, Z. *et al.* An inducible cytochrome P450 3A4-dependent vitamin D catabolic pathway. *Mol Pharmacol* **81**, 498-509 (2012).

(42) Wang, Z., Schuetz, E.G., Xu, Y. & Thummel, K.E. Interplay between vitamin D and the drug metabolizing enzyme CYP3A4. *J Steroid Biochem Mol Biol* **136**, 54-8 (2013).

(43) Wang, Z. *et al.* Human UGT1A4 and UGT1A3 conjugate 25-hydroxyvitamin D3: metabolite structure, kinetics, inducibility, and interindividual variability. *Endocrinology* **155**, 2052-63 (2014).

(44) Wong, T. *et al.* Polymorphic Human Sulfotransferase 2A1 Mediates the Formation of 25-Hydroxyvitamin D3-3-O-Sulfate, a Major Circulating Vitamin D Metabolite in Humans. *Drug Metab Dispos* **46**, 367-79 (2018).

(45) Bikle, D., Bouillon, R., Thadhani, R. & Schoenmakers, I. Vitamin D metabolites in captivity? Should we measure free or total 25(OH)D to assess vitamin D status? *J Steroid Biochem Mol Biol* **173**, 105-16 (2017).

(46) Bikle, D.D., Gee, E., Halloran, B., Kowalski, M.A., Ryzen, E. & Haddad, J.G. Assessment of the free fraction of 25-hydroxyvitamin D in serum and its regulation by albumin and the vitamin D-binding protein. *J Clin Endocrinol Metab* **63**, 954-9 (1986).

(47) Chesdachai, S. & Tangpricha, V. Treatment of vitamin D deficiency in cystic fibrosis. *J Steroid Biochem Mol Biol* **164**, 36-9 (2016).

(48) Coppenhaver, D. *et al.* Serum concentrations of vitamin D-binding protein (group-specific component) in cystic fibrosis. *Human genetics* **57**, 399-403 (1981).

(49) Chapron, B.D. *et al.* Reevaluating the role of megalin in renal vitamin D homeostasis using a human cell-derived microphysiological system. *ALTEX* **35**, 504-15 (2018).

(50) Bikle, D.D. Vitamin D metabolism, mechanism of action, and clinical applications. *Chem Biol* **21**, 319-29 (2014).

(51) Gao, C. *et al.* Simultaneous quantification of 25-hydroxyvitamin D3-3-sulfate and 25-hydroxyvitamin D3-3-glucuronide in human serum and plasma using liquid chromatography-tandem mass spectrometry coupled with DAPTAD-derivatization. *J Chromatogr B Analyt Technol Biomed Life Sci* **1060**, 158-65 (2017).

(52) Bikle, D.D., Malmstroem, S. & Schwartz, J. Current Controversies: Are Free Vitamin Metabolite Levels a More Accurate Assessment of Vitamin D Status than Total Levels? *Endocrinol Metab Clin North Am* **46**, 901-18 (2017).

(53) Schwartz, J.B. *et al.* Variability in free 25(OH) vitamin D levels in clinical populations. *J Steroid Biochem Mol Biol* **144 Pt A**, 156-8 (2014).

(54) Nadler, S.B., Hidalgo, J.H. & Bloch, T. Prediction of blood volume in normal human adults. *Surgery* **51**, 224-32 (1962).

(55) Klingberg, E., Oleröd, G., Konar, J., Petzold, M. & Hammarsten, O. Seasonal variations in serum 25-hydroxy vitamin D levels in a Swedish cohort. *Endocrine* **49**, 800-8 (2015).

(56) Lauridsen, A.L., Vestergaard, P. & Nexo, E. Mean serum concentration of vitamin D-binding protein (Gc globulin) is related to the Gc phenotype in women. *Clin Chem* **47**, 753-6 (2001).

(57) Dorlochter, L., Aksnes, L. & Fluge, G. Faecal elastase-1 and fat-soluble vitamin profiles in patients with cystic fibrosis in Western Norway. *Eur J Nutr* **41**, 148-52 (2002).

(58) Greer, R.M. *et al.* Abnormalities of the PTH-vitamin D axis and bone turnover markers in children, adolescents and adults with cystic fibrosis: comparison with healthy controls. *Osteoporosis international : a journal established as result of cooperation between the European Foundation for Osteoporosis and the National Osteoporosis Foundation of the USA* **14**, 404-11 (2003).

(59) Wang, J.P. *et al.* Disposition of drugs in cystic fibrosis. VI. In vivo activity of cytochrome P450 isoforms involved in the metabolism of (R)-warfarin (including P450 3A4) is not enhanced in cystic fibrosis. *Clin Pharmacol Ther* **55**, 528-34 (1994).

(60) Hutabarat, R.M., Unadkat, J.D., Kushmerick, P., Aitken, M.L., Slattery, J.T. & Smith, A.L. Disposition of drugs in cystic fibrosis. III. Acetaminophen. *Clin Pharmacol Ther* **50**, 695-701 (1991).

(61) Gordon, C.M., Binello, E., LeBoff, M.S., Wohl, M.E., Rosen, C.J. & Colin, A.A. Relationship between insulin-like growth factor I, dehydroepiandrosterone sulfate and proresorptive cytokines and bone density in cystic fibrosis. *Osteoporosis international : a journal established as result of cooperation between the European Foundation for Osteoporosis and the National Osteoporosis Foundation of the USA* **17**, 783-90 (2006).

(62) Gao, C., Liao, M.Z., Han, L.W., Thummel, K.E. & Mao, Q. Hepatic Transport of 25-Hydroxyvitamin D3 Conjugates: A Mechanism of 25-Hydroxyvitamin D3 Delivery to the Intestinal Tract. *Drug Metab Dispos* **46**, 581-91 (2018).

(63) Nilsson, S.F., Ostberg, L. & Peterson, P.A. Binding of vitamin D to its human carrier plasma protein. *Biochemical and biophysical research communications* **46**, 1380-7 (1972).

(64) Chun, R.F., Peercy, B.E., Orwoll, E.S., Nielson, C.M., Adams, J.S. & Hewison, M. Vitamin D and DBP: the free hormone hypothesis revisited. *J Steroid Biochem Mol Biol* **144 Pt A**, 132-7 (2014).

(65) Jassil, N.K., Sharma, A., Bikle, D. & Wang, X. Vitamin D Binding Protein and 25-Hydroxyvitamin D Levels: Emerging Clinical Applications. *Endocr Pract* **23**, 605-13 (2017).

(66) Jouret, F. & Devuyst, O. CFTR and defective endocytosis: new insights in the renal phenotype of cystic fibrosis. *Pflugers Archiv : European journal of physiology* **457**, 1227-36 (2009).

(67) Aris, R.M., Lester, G.E., Dingman, S. & Ontjes, D.A. Altered calcium homeostasis in adults with cystic fibrosis. *Osteoporosis international : a journal established as result of cooperation between the European Foundation for Osteoporosis and the National Osteoporosis Foundation of the USA* **10**, 102-8 (1999).

(68) West, N.E. *et al.* Appropriate goal level for 25-hydroxyvitamin D in cystic fibrosis. *Chest* **140**, 469-74 (2011).

(69) Bikle, D.D. Vitamin D and bone. *Curr Osteoporos Rep* **10**, 151-9 (2012).

(70) Lark, R.K. *et al.* Diminished and erratic absorption of ergocalciferol in adult cystic fibrosis patients. *Am J Clin Nutr* **73**, 602-6 (2001).

3.8. Tables

Table 3.1: Retention time, precursor molecular ion/product ion for quantification and detection parameters for 4β,25$(OH)_2D_3$ and its internal standard

Analyte	Retention Time (min)	Precursor Ion	Product Ion	DP[a] (V)	CE[b] (V)	LLOQ[c] (pg/mL)	Standard Curve Range (pg/mL)
4β,25$(OH)_2D_3$	15.5	635.2	357.1	146	33	1.6	2-800
d_6-1α,25$(OH)_2D_3$	15.6	641.2	357.1	146	33	-	-

[a] declustering potential
[b] collision energy
[c] lower limit of quantification

Table 3.2: Retention time, precursor molecular ion/product ion for quantification and detection parameters for 25-dihydroxyvitamin D_3-sulfate, 25-dihydroxyvitamin D_3-glucuronide, and their internal standards

Analyte	Retention Time (min)	Precursor Ion	Product Ion	DP[a] (V)	CE[b] (V)	LLOQ[c] (ng/mL)	Standard Curve Range (ng/mL)
25(OH)D_3-S	10.78	699.5	323.0	100	45	0.5	2.4 – 96
d_6-25(OH)D_3-S	10.72	705.5	323.0	100	45	-	-
25(OH)D_3-G	9.59	795.5	341.1	100	42.5	0.2	0.3 – 11.5
d_6-25(OH)D_3-G	9.56	801.5	341.1	100	42.5	-	-

[a] declustering potential
[b] collision energy
[c] lower limit of quantification

Table 3.3: Demographics of participants in the cohort of healthy controls and patients with CF to study basal levels of 25-hydroxyvitamin D and its metabolites

	Healthy Controls (n = 82)	Patients with CF (n = 83)
Age (years)	32.5 ± 11.2	32.3 ± 11.1
Male	31 (38%)	45 (55%)
BMI (kg/m^2)	25.5 ± 4.9	23.0 ± 3.4
Race		
White	79 (96%)	80 (96%)
Other	3 (4%)	3 (4%)
Season of Sample Collection		
Winter	37 (45%)	23 (37%)
Spring	31 (38%)	14 (17%)
Summer	10 (12%)	11 (13%)
Fall	4 (5%)	35 (42%)
Pancreatic Insufficient	0 (0%)	71 (86%)
Vitamin D Supplementation	18 (22)	44 (53)
CFTR Genotype[a]		
Homozygous *F508del*	ND	33 (40%)
Heterozygous *F508del*	ND	42 (51%)
Other	ND	8 (10%)
VDBP Diplotype		
Gc1f/Gc1f	7 (9%)	10 (12%)
Gc1f/Gc1s	15 (18%)	24 (29%)
Gc1s/Gc1s	55 (67%)	41 (49%)
Gc1f/Gc2	1 (1%)	5 (6%)
Gc1s/Gc2	0 (0%)	1 (1%)
Gc2/Gc2	4 (5%)	2 (2%)
Protein or Hormone Levels		
VDBP (µg/mL)	274 ± 56	264 ± 41
Albumin (g/dL)	4.3 ± 0.3	3.9 ± 0.4***
FGF (pg/mL)	41.4 ± 11.8	44.4 ± 18.3
PTH (pg/mL)	40.6 ± 15.4	43.1 ± 19.0

Results are reported as mean ± SD or count (%). ND = not determined.
***p < 0.001 compared to healthy controls
[a] *CFTR* genotype was not determined in healthy controls

Table 3.4: Basal levels of 25-hydroxyvitamin D and its metabolites in healthy controls and patients with cystic fibrosis

Metabolite	Healthy Controls (n = 82)		Patients with CF (n = 83)	
	Concentration	Ratio[a]	Concentration	Ratio[a]
Total				
25(OH)D (ng/mL)	27.7 ± 9.9	-	26.7 ± 12.3	-
1α,25(OH)$_2$D (pg/mL)	50.7 ± 13.0	1.97 ± 0.90	43.6 ± 12.7 ***	2.10 ± 1.57
Vitamin D$_3$ Metabolites				
25(OH)D$_3$ (ng/mL)	26.8 ± 10.1	-	25.3 ± 12.0	-
1α,25(OH)$_2$D$_3$ (pg/mL)	49.5 ± 12.8	2.01 ± 0.92	42.3 ± 13.3 ***	2.14 ± 1.57
24,25(OH)$_2$D$_3$ (ng/mL)	1.7 ± 1.0	59.3 ± 16.4	1.7 ± 1.2	58.6 ± 19.9
4β,25(OH)$_2$D$_3$ (pg/mL)[b]	79.9 ± 60.2	2.94 ± 1.79	52.1 ± 38.9 ***	2.09 ± 1.49 ***
25(OH)D$_3$-S (ng/mL)	30.1 ± 12.3	985 ± 426	17.7 ± 11.6 ***	587 ± 274 ***
25(OH)D$_3$-G (ng/mL)	2.2 ± 1.6	55.2 ± 24.9	1.9 ± 1.2	51.0 ± 17.7
Vitamin D$_2$ Metabolites				
25(OH)D$_2$ (ng/mL)	0.9 ± 1.9	-	1.3 ± 5.4 ***	-
1α,25(OH)$_2$D$_2$ (pg/mL)	1.2 ± 2.5	1.37 ± 1.07	1.3 ± 4.2 ***	1.52 ± 1.26

Values = mean ± SD. - = not applicable.
*p < 0.05, **p < 0.01, ***p < 0.001 compared to healthy controls

[a] Molar ratio calculated as (molar concentration of metabolite)/(molar concentration of parent)·1000, where parent is 25(OH)D, 25(OH)D$_2$ or 25(OH)D$_2$, where appropriate

[b] For the CF group, n = 82 due to insufficient sample volume for one study participant

Table 3.5: Basal unbound serum concentrations and percent unbound of 25-hydroxyvitamin D_3 and 1α,25-dihydroxyvitamin D_3 in healthy controls and patients with cystic fibrosis

	Healthy Controls (n = 82)	Patients with CF (n = 83)
25(OH)D_3		
Total 25(OH)D_3 (ng/mL)	26.8 ± 10.1	25.3 ± 12.0
Unbound 25(OH)D_3 (pg/mL)	18.2 ± 6.8	17.9 ± 8.4
Percent Free 25(OH)D_3 (%)	0.0693 ± 0.0010	0.0716 ± 0.0092
1,25(OH)D_3		
Total 1α,25$(OH)_2D_3$ (pg/mL)	49.5 ± 12.8	42.3 ± 13.3 ***
Unbound 1α,25$(OH)_2D_3$ (pg/mL)	0.566 ± 0.126	0.508 ± 0.151 *
Percent Free 1α,25$(OH)_2D_3$ (%)	0.486 ± 0.065	0.504 ± 0.061

Values = mean ± SD
*p < 0.05, **p < 0.01, ***p < 0.001 compared to healthy controls

Table 3.6: Demographics of participants in the pharmacokinetic study of d_6-25-hydroxyvitamin D_3

	Healthy Controls (n = 5)	Patients with CF (n = 5)
Age (years)	24.8 ± 3.3	38.8 ± 14.3
Male	1 (20%)	4 (80%)
Weight	65.7 ± 9.9	78.7 ± 13.3
BMI (kg/m^2)	22.4 ± 3.0	25.0 ± 3.1
Race		
White	5 (100%)	5 (100%)
Season at Start of Study		
Winter	0 (0%)	2 (40%)
Spring	4 (80%)	1 (20%)
Summer	1 (20%)	2 (40%)
Fall	0 (0%)	0 (0%)
Pancreatic Insufficiency	ND	3 (60%)
CFTR Genotype *F508del*[a]	ND	3 (60%)

Values given as mean ± standard deviation or count (%) . ND = not determined

[a] *CFTR* genotype was not determined in healthy controls

Table 3.7: Mean pharmacokinetic parameters after intravenous administration of d_6-25-hydroxyvitamin D_3.

Parameter	Healthy Controls (n=5)	Patients with CF (n=5)
***d_6*-25(OH)D_3**		
Dose (µg)	22.0 ± 3.2	26.4 ± 3.6
C_{max}[a] (ng/mL)	9.4 ± 1.9	8.8 ± 1.4
$AUC_{0\text{-}last}$ (ng·day/mL)	67.2 ± 8.3	58.3 ± 9.7
$AUC_{0\text{-}\infty}$ (ng·day/mL)	73.9 ± 9.0	65.1 ± 12.5
Extrapolated AUC (%)	8.9 ± 1.6	10.0 ± 3.6
CL (mL/day)	342 ± 41	397 ± 73
V_{SS} (L)	7.2 ± 1.1	8.4 ± 1.4
Half-life (day)	15.8 ± 1.6	16.2 ± 3.3
***d_6*-24,25$(OH)_2D_3$**		
C_{max} (ng/mL)	0.13 ± 0.02	0.16 ± 0.02
T_{max} (day)	14 (7 – 28)	21 (4 – 21)
$AUC_{0\text{-}last}$ (ng·day/mL)	4.8 ± 0.9	5.9 ± 1.2

d_6-25(OH)D_3 serum concentrations were adjusted to a 25 µg dose of d_6-25(OH)D_3.
[a] d_6-25(OH)D_3 C_{max} and AUCs were the dose-normalized concentration after the completion of the d_6-25(OH)D_3 bolus.

3.9. Figures

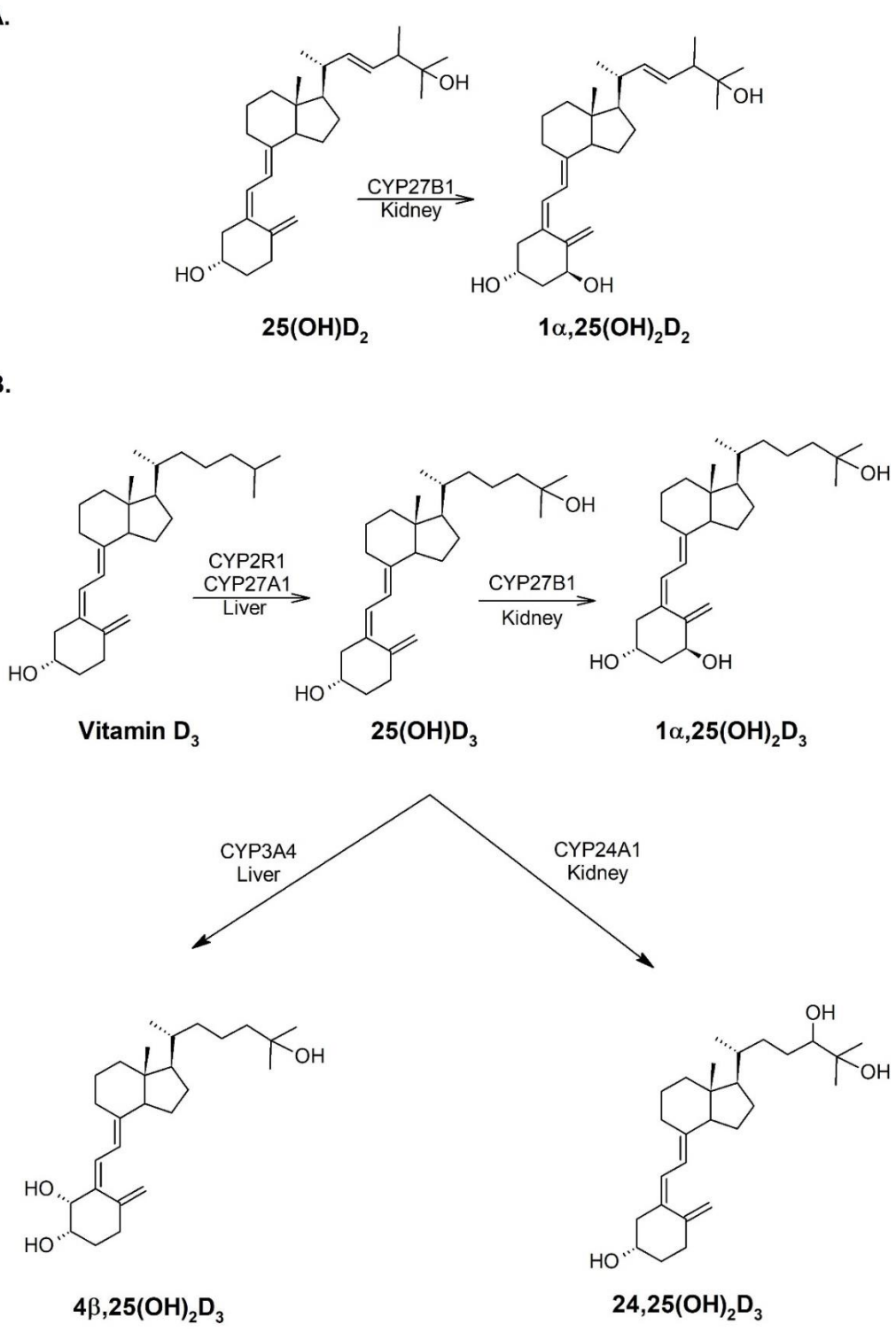

Figure 3.1: Partial metabolic schemes of A) vitamin D_2 and B) vitamin D_3.

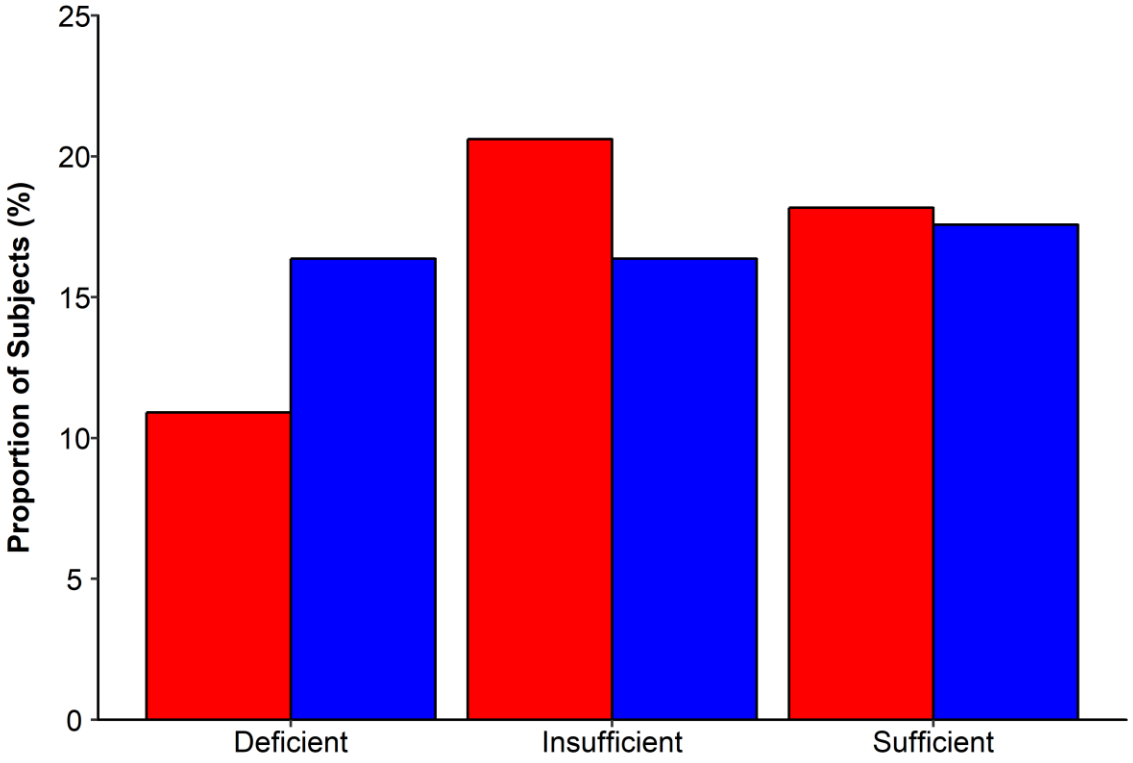

Figure 3.2: Vitamin D deficiency (less than 20 ng/mL), insufficiency (20 to 30 ng/mL), and sufficiency (greater than 30 ng/mL), as defined by the Endocrine Society and Cystic Fibrosis Foundation, in healthy controls (red) and patients with CF (blue).

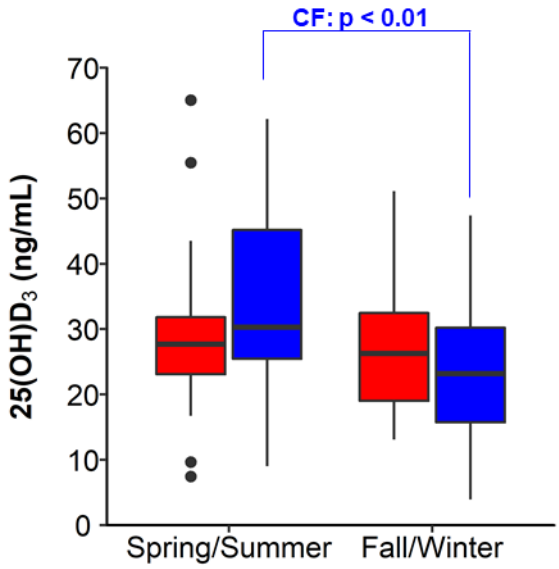

Figure 3.3: Boxplot of total 25(OH)D by season in healthy controls (red) and patients with CF (blue). For each boxplot, the center line represents the median. The shaded region is the 25th to 75th percentile (interquartile range). The whiskers are the largest value within 1.5 times interquartile range above the 75th percentile and smallest value within 1.5 times the interquartile range below the 25th percentile. The black circles are data points that are not within the 1.5 times the interquartile range.

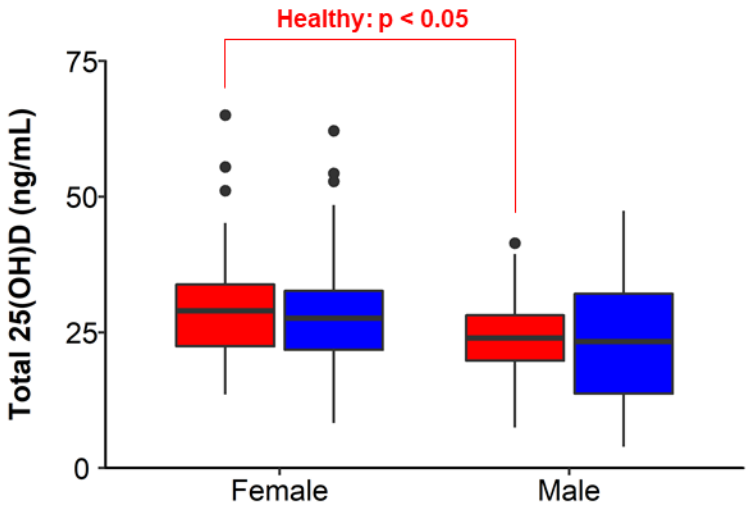

Figure 3.4: Total serum concentrations 25(OH)D by gender in healthy controls (red) and patients with CF (blue). For each boxplot, the center line represents the median. The shaded region is the 25th to 75th percentile (interquartile range). The whiskers are the largest value within 1.5 times the interquartile range above the 75th percentile and smallest value within 1.5 times the interquartile range below the 25th percentile. The black circles are data points that are not within the 1.5 times the interquartile range. Linear regression including gender and season was used to analyze the data separately for healthy controls and patients with CF.

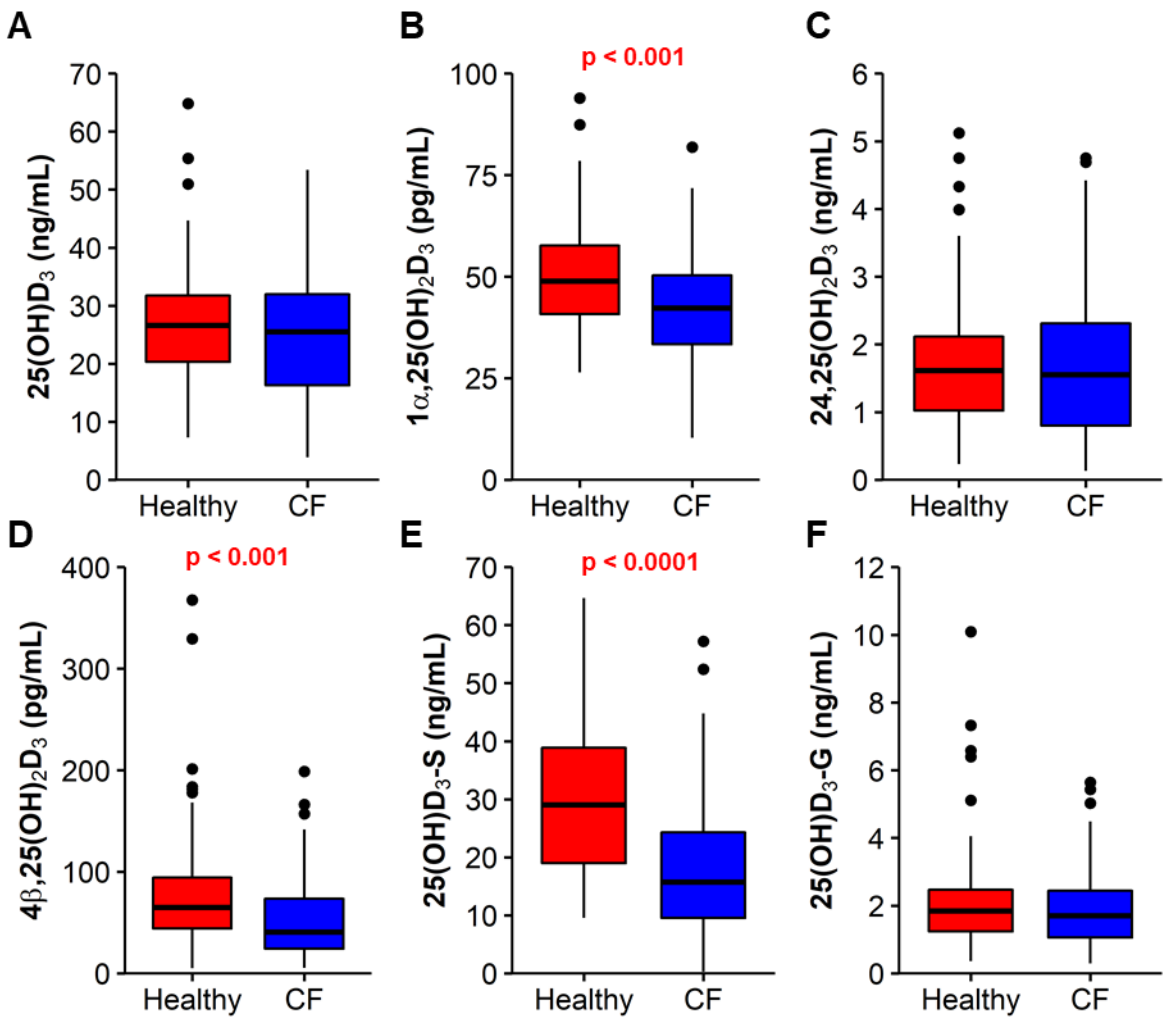

Figure 3.5: Basal levels of A) $25(OH)D_3$, B) $1\alpha,25(OH)_2D_3$, C) $24,25(OH)_2D_3$, D) $4\beta,25(OH)_2D_3$, E) $25(OH)D_3$-S, and F) $25(OH)D_3$-G in healthy controls (red) and patients with CF (blue). For each boxplot, the center line represents the median. The shaded region is the 25^{th} to 75^{th} percentile (interquartile range). The whiskers are the largest value within 1.5 times the interquartile range above the 75^{th} percentile and smallest value within 1.5 times the interquartile range below the 25^{th} percentile. The black circles are data points that are not within the 1.5 times the interquartile range.

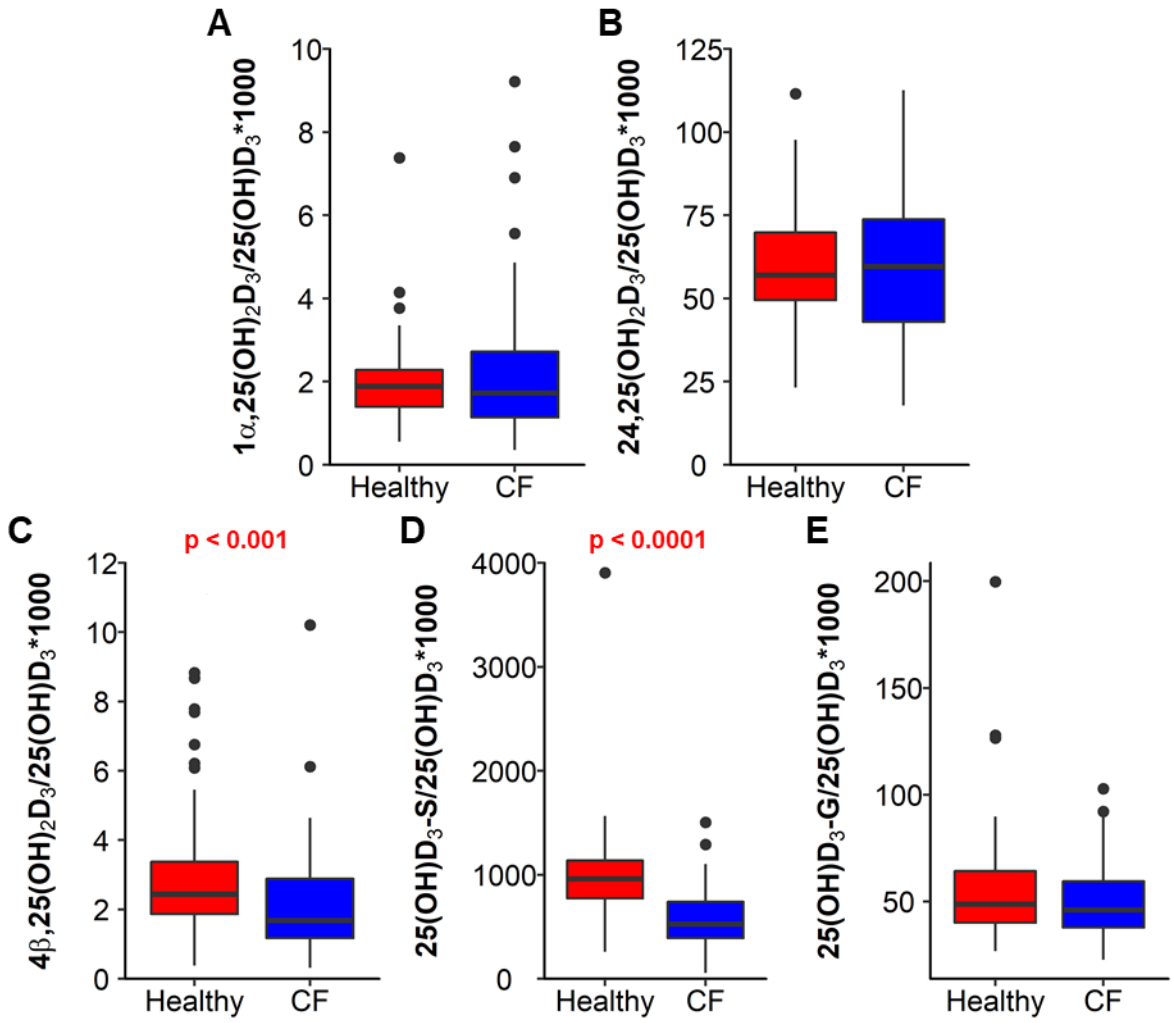

Figure 3.6: Molar concentration ratios of A) 1α,25$(OH)_2D_3$, B) 24,25$(OH)_2D_3$, C) 4β,25$(OH)_2D_3$, D) 25$(OH)D_3$-S, and E) 25$(OH)D_3$-G to 25$(OH)D_3$ in healthy controls (red) and patients with CF (blue). For each boxplot, the center line represents the median. The shaded region is the 25th to 75th percentile (interquartile range). The whiskers are the largest value within 1.5 times the interquartile range above the 75th percentile and smallest value within 1.5 times the interquartile range below the 25th percentile. The black circles are data points that are not within the 1.5 times the interquartile range.

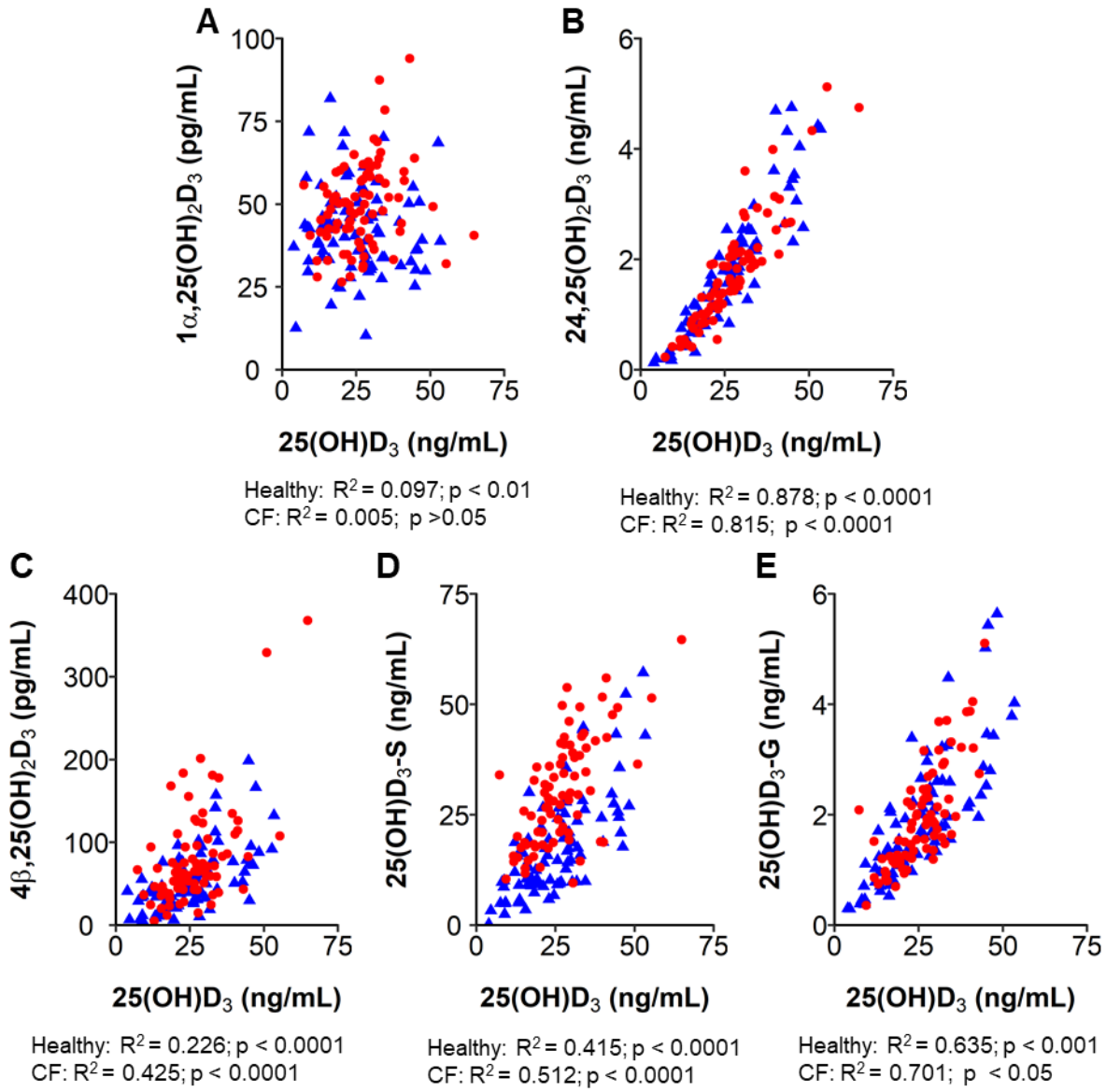

Figure 3.7: Correlation of serum concentrations of $25(OH)D_3$ with A) $1\alpha,25(OH)_2D_3$, B) $24,25(OH)_2D_3$, C) $4\beta,25(OH)_2D_3$, D) $25(OH)D_3$-S, and E) $25(OH)D_3$-G in healthy controls (red) and patients with CF (blue).

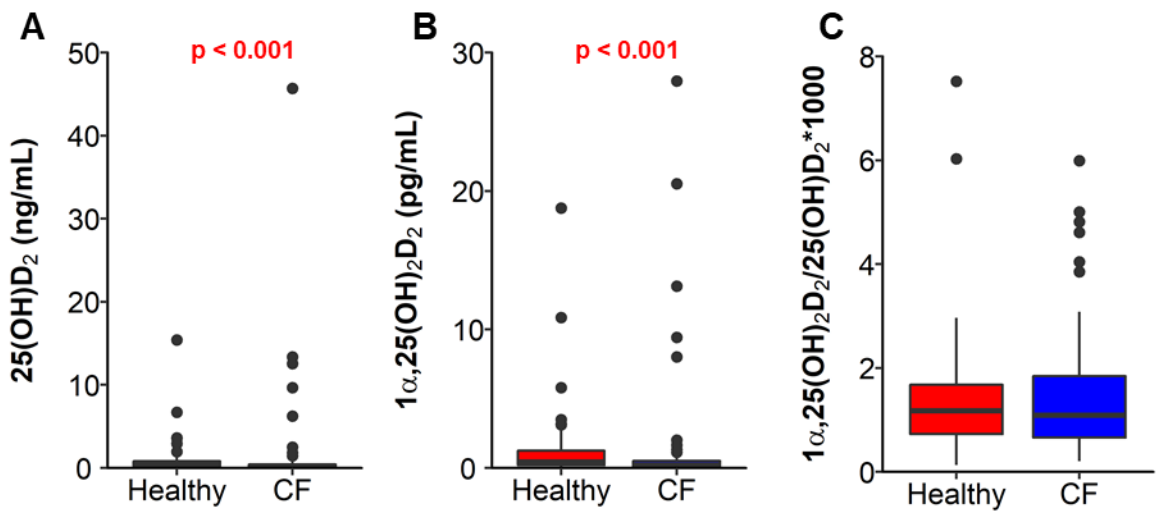

Figure 3.8: Basal serum concentrations of A) $25(OH)D_2$, B) $1\alpha,25(OH)_2D_2$, and C) the molar concentration ratio of $1\alpha,25(OH)_2D_2$ to $25(OH)D_2$ in healthy controls (red) and patients with CF (blue). For each boxplot, the center line represents the median. The shaded region is the 25th to 75th percentile (interquartile range). The whiskers are the largest value within 1.5 times the interquartile range above the 75th percentile and smallest value within 1.5 times the interquartile range below the 25th percentile. The black circles are data points that are not within the 1.5 times the interquartile range.

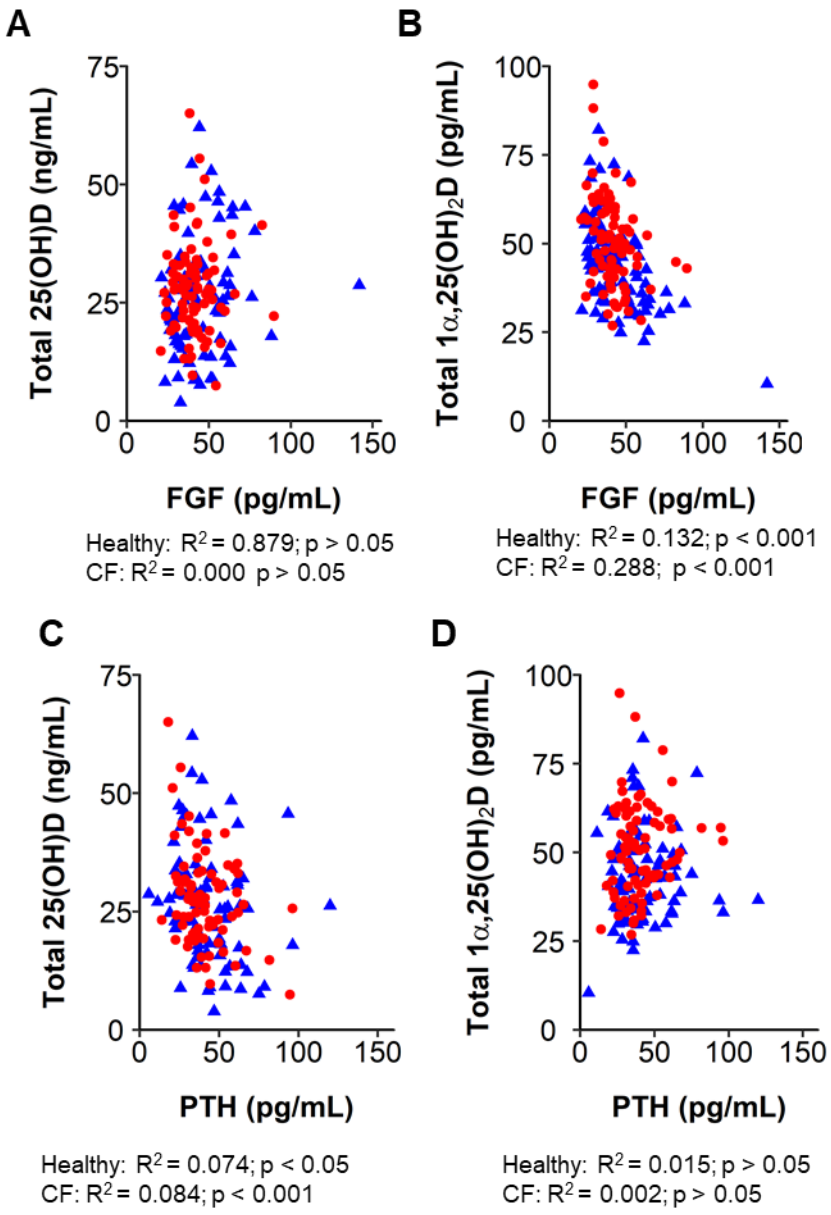

Figure 3.9: Correlation of serum concentrations of FGF with total concentrations of A) 25(OH)D and B) 1α,25$(OH)_2$D and PTH with total concentrations of C) 25(OH)D and D) 1α,25$(OH)_2$D in healthy controls (red circles) and patients with CF (blue triangles).

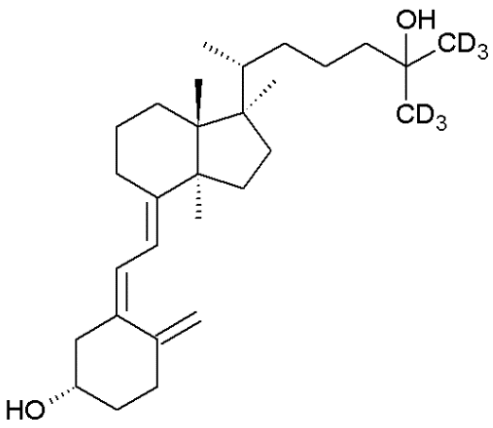

Figure 3.10: Chemical structure of d_6-25-hydroxyvitamin D_3 used in the pharmacokinetic study.

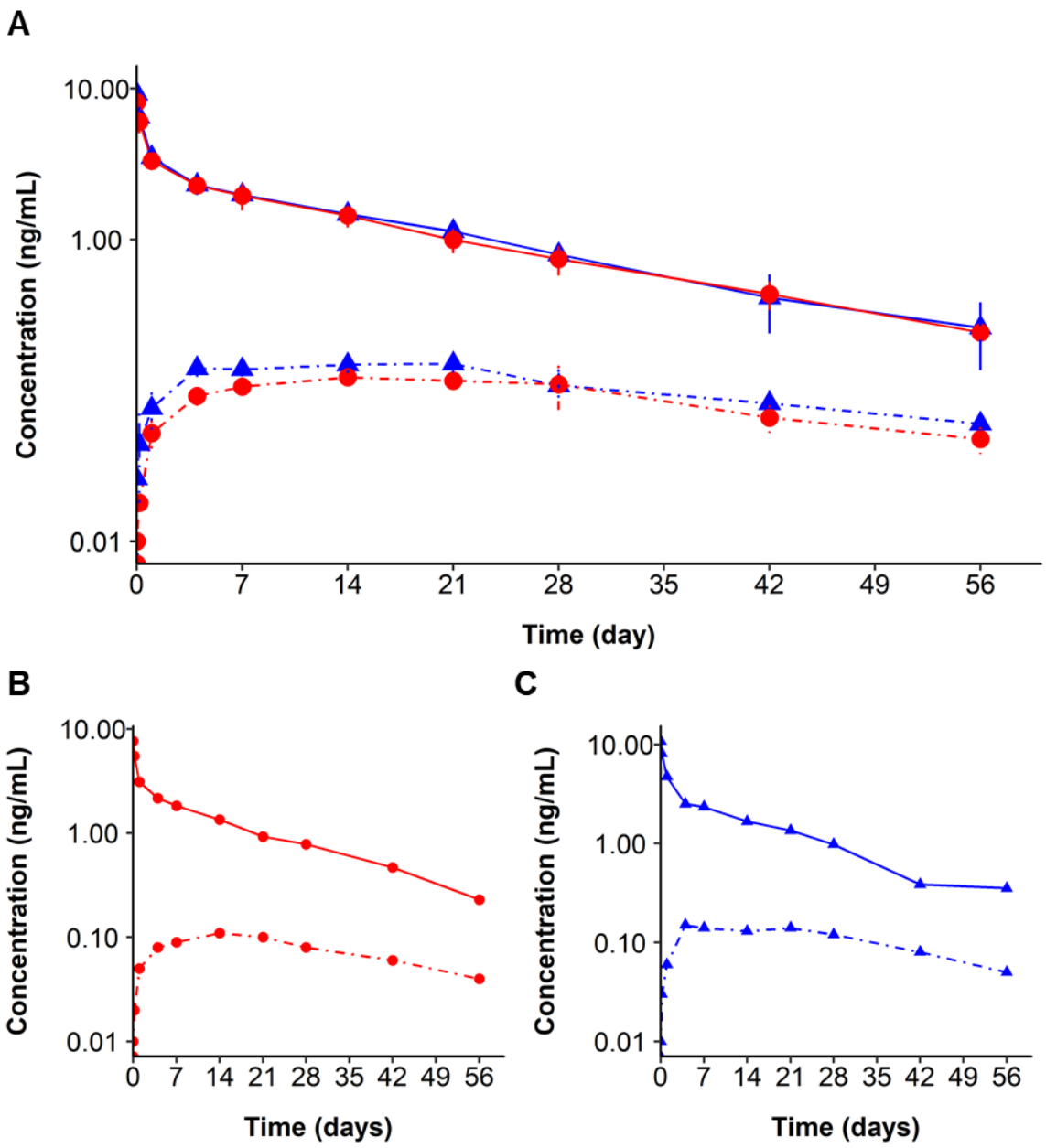

Figure 3.11 A) Dose normalized serum concentration versus time curves of d_6-25(OH)D_3 and d_6-24,25$(OH)_2D_3$ after intravenous administration of d_6-25(OH)D_3 in healthy controls (red circles) and patients with CF (blue triangles). A) Group mean and standard deviation, B) a representative healthy control, and C) a representative patient with CF shown for d_6-25(OH)D_3 (solid line) and d_6-24,25$(OH)_2D_3$ (dashed line).

Chapter 4.

An Observational Study of Longitudinal Changes in 25-Hydroxyvitamin D_3 and its Metabolites During Pregnancy and Postpartum

4.1. Abstract

Although more than 90% of pregnant women take prenatal supplements during pregnancy, the prevalence of vitamin D deficiency and insufficiency is high in pregnant women. Low maternal levels of vitamin D are associated with poor birth outcomes, such as preterm delivery and low weight for gestational age. Physiological changes that occur in pregnancy, including changes in blood flow, organ enzyme expression and plasma protein concentrations, may affect the circulating concentrations of 25-hydroxyvitamin D_3 ($25(OH)D_3$) and its metabolites. Fifteen healthy nulliparous women between the ages of 18-45 years were recruited for a longitudinal observational study of vitamin D and its metabolites in plasma. Samples were collected pre-pregnancy, during pregnancy, and postpartum. When possible, maternal and fetal samples were collected at delivery. The following metabolites were measured by liquid chromatography-mass spectrometry: $25(OH)D_3$, 1α,25-dihydroxyvitamin D_3 ($1\alpha,25(OH)_2D_3$), 24R,25-hydroxyvitamin D_3 ($24,25(OH)_2D_3$), 4β,25-dihydroxyvitamin D_3 ($4\beta,25(OH)_2D_3$), 25-hydroxyvitamin D_3-3-sulfate ($25(OH)D_3$-S), and 25-hydroxyvitamin D_3-3-glucuronide ($25(OH)D_3$-G). In addition, the serum levels of vitamin D binding protein (VDBP) and albumin were quantified and used to estimate the free concentration and the percent unbound of $25(OH)_2D_3$ and $1\alpha,25(OH)_2D_3$. Linear mixed-effects modeling was used to analyze the association between $25(OH)D_3$ and its metabolites with gestational age. Gestational age was associated with a 50% increase in the circulating concentrations of $25(OH)D_3$ ($p < 0.001$) and a 2-fold increase in $1\alpha,25(OH)_2D_3$ ($p < 0.001$). Gestational age was positively associated with changes in $24,25(OH)_2D_3$, $4\beta,25(OH)D_3$, and $25(OH)D_3$-G and negatively associated with $25(OH)D_3$-S. VDBP increased almost 2-fold by 32 weeks of gestation, whereas albumin concentrations

decreased by 24%. Overall, the changes in protein concentrations resulted in a 20% decrease in the fraction unbound of 25(OH)D_3. Postpartum changes were difficult to detect due to limited sample size, however, 25(OH)D_3 concentrations appeared to return to pre-pregnancy levels by 12 weeks postpartum. Our study showed that 25(OH)D_3 metabolism is altered in healthy pregnant women. As vitamin D is a critical nutrient during pregnancy, additional research is warranted to understand how changes in vitamin D metabolism support fetal development and maternal health.

4.2. Introduction

Vitamin D_3 is a fat-soluble prohormone that, in combination with parathyroid hormone (PTH), regulates the transport and absorption of calcium in the gut and kidney. Bioactivation of vitamin D_3 requires two sequential hydroxylation steps (1, 2). The first step is 25-hydroxylation in the liver by cytochrome P450s (CYP) 27A1 and 2R1 (CYP27A1 and CYP2R1) to form 25-hydroxyvitamin D_3 (25(OH)D_3) (3, 4). In the kidney, 25(OH)D_3 undergoes further metabolism by CYP27B1 to form the active moiety of vitamin D_3, 1α,25-dihydroxyvitamin D_3 (1α,25$(OH)_2D_3$) (3, 4). In circulation, 25(OH)D_3 and 1α,25$(OH)_2D_3$ are highly bound to plasma proteins, with approximately 85-90% bound to vitamin D binding protein (VDBP) and the remaining 10-15% bound to albumin (5). Due to the extensive binding, changes in plasma protein levels can greatly influence the unbound 25(OH)D_3 concentrations.

In addition to the active metabolite, 25(OH)D_3 can be catabolized by CYP24A1 in the kidney to the inactive metabolite, 24R,25-dihydroxyvitamin D_3 (24,25$(OH)_2D_3$). In the liver, CYP3A4 converts 25(OH)D_3 to 4β,25-dihydroxyvitamin D_3 (4β,25$(OH)_2D_3$). Conjugated metabolites are formed in the liver, including 25(OH)D_3-(3)-sulfate (25(OH)D_3-S) by sulfotransferase (SULT) 2A1 and 25(OH)D_3-(3)-glucuronide (25(OH)D_3-G) by uridine 5'-diphospho-glucuronosyltransferases (UGT) 1A3 and 1A4 (3, 4, 6-8). While the biological function of the hepatic metabolites is not well understood, it has been hypothesized that

25(OH)D_3-S and 25(OH)D_3-G could be a mechanism to store excess 25(OH)D_3 that can be utilized following deconjugation (9). The metabolic scheme of 25(OH)D_3 and selected metabolites is provided in Figure 4.1.

Although 1α,25$(OH)_2D_3$ is the active hormone form of vitamin D_3, it is a poor biomarker of overall vitamin D exposure because of its short half-life (4-6 hours) and tight regulation of serum concentrations (10). Given the longer half-life of 25(OH)D_3 (~2 weeks), serum 25(OH)D_3 is a better marker of total vitamin D exposure. Vitamin D sufficiency is defined by the Endocrine Society as a total serum 25(OH)D concentration greater than 30 ng/mL, while insufficiency is defined as 25(OH)D concentrations between 20-30 ng/mL, and deficiency is defined as 25(OH)D concentrations less than 20 ng/mL (11). As many as 50-90% of women take prenatal vitamins, which typically contain 400-1000 international units (IU) of vitamin D_3. However, an estimated 45% of white women and 83% of black women in the northeastern United States were classified as vitamin D insufficient or deficient at the time of delivery (12, 13). At birth, only 34% of white and 7.6% of black newborns were vitamin D sufficient (13).

Recent studies reported that vitamin D is critical for maternal and fetal health during pregnancy. Low maternal 25(OH)D_3 levels were associated with pregnancy complications and poor birth outcomes. A case-control study of 50 women with early-onset severe preeclampsia found that a 10 ng/mL increase in 25(OH)D_3 levels was associated with a 63% reduction in the odds of being diagnosed with preeclampsia (14). A recent meta-analysis reported that pregnant women who are vitamin D deficient have an increased risk for a low-birth-weight delivery (15). Additionally, low circulating levels of 25(OH)D_3 are negatively correlated with the duration of oxygen therapy of neonates after birth (16).

Previous studies reported that circulating 1α,25$(OH)_2D_3$ increases two- to three-fold during pregnancy, however the changes in the concentration of other 25(OH)D_3 metabolites are not well understood (17, 18). Many physiological changes that occur during pregnancy (e.g., changes in hepatic and renal enzyme expression, cardiac output, protein binding, and placental

enzyme expression (19)) may contribute to altered concentrations of 25(OH)D_3 and its metabolites (18, 20). In addition, pregnancy is known to affect the circulating concentrations of VDBP and albumin; however, the rate and magnitude of these changes during the first trimester have yet to be established (21, 22). This study aims to characterize the changes in the concentrations of 25(OH)D_3 and its metabolites from pre-pregnancy, through pregnancy, at delivery and up to 12 weeks postpartum. Additionally, we aim to characterize VDBP and albumin to estimate changes in the unbound concentration and fraction unbound of 25(OH)D_3 and 1α,25(OH)$_2D_3$. These data will provide insights into how physiological changes in pregnancy contribute to altered 25(OH)D_3 metabolism.

4.3. Materials and Methods

4.3.1. Chemicals and Materials

25(OH)D_3 and 24,25(OH)$_2D_3$ were purchased from IsoSciences (Ambler, PA). d_7-vitamin D_3, d_6-25(OH)D_3, 4β,25(OH)$_2D_3$, 25(OH)D_3-S, and 25(OH)D_3-G were purchased from Toronto Research Chemicals (North York, Ontario, Canada). 1α,25(OH)$_2D_3$, d_6-1α,25(OH)$_2D_3$, d_6-24,25(OH)$_2D_3$ were purchased from Medical Isotopes, Inc. (Pelham, NH). (Diacetoxyiodo)benzene, 3'-phosphoadenosine-5'-phosphosulfate (PAPS), uridine 5′-diphosphoglucuronic acid trisodium salt (UDPGA), and bovine serum albumin (BSA) were purchased from Sigma-Aldrich Corp. (St. Louis, MO). 4-(4'-dimethylaminophenyl)-1,2,4-triazolidine-3,5-dione was purchased from Santa Cruz Biotechnology, Inc. (Dallas, TX). HPLC-grade acetonitrile, ethyl acetate, methanol, methyl tert-butyl ether (MTBE), heptane, isopropanol, hexanes, formic acid, acetic acid, and dichloromethane were purchased from Fisher Scientific (Pittsburgh, PA). Vitamin D-free serum (Seratrol™) was purchased from Golden West Biologicals, Inc. (Temecula, CA).

4.3.2. Participants

Healthy women who intended to become pregnant in the 12 months following study enrollment or who were less than eight weeks pregnant were recruited to take part in the study. Subjects were 18-45 years of age with a body mass index of 18-30 kg/m^2 at enrollment. Potential participants were excluded if they had an existing major medical condition (e.g., heart disease, liver disease, renal impairment, gastrointestinal disease, hyperthyroidism, diabetes, or metabolic disorders) or if they required chronic medications that would alter drug-metabolizing enzyme or transporter functions. Potential participants were excluded if they were current cigarette smokers, had a prior or present addiction to drugs or alcohol, or if they had had two or more previous miscarriages. The study was approved by the Institutional Review Board at the University of Washington.

4.3.3. Sample Collection

For women who enrolled before becoming pregnant, baseline urine and blood samples were collected every three months for 12 months or until a positive pregnancy test. Upon confirmation of the pregnancy or for women who enrolled during their first trimester, blood and urine samples were collected, along with concomitant medication and health information at selected timepoints until delivery (up to 12 visits). Pregnancy visits were scheduled at 4, 8, 12, 16, 20, 24, 28, 32, 36, 38, 40, and 42 weeks of gestation or until delivery. Gestational age was based on last menstrual period or early ultrasound dating. When possible, maternal and fetal blood and urine were collected at delivery. Blood, urine, and breast milk samples were collected at 3, 6, and 12 weeks postpartum. Up to 18 samples could be collected per subject (4 pre-pregnancy, 12 during pregnancy, 1 at delivery, and 3 postpartum).

4.3.4. Analysis of Vitamin D Metabolites

Plasma concentrations of $25(OH)D_3$, $24,25(OH)_2D_3$, $1\alpha,25(OH)_2D_3$, and $4\beta,25(OH)_2D_3$

were determined as described in Chapter 2. Vitamin D_2 metabolites were not quantified. In brief, 500 µL of serum was transferred into polypropylene micro-centrifuge tubes. Standard curve samples were prepared in bovine serum albumin (BSA). 20 µL of internal standard solution (0.2 ng/µL d_7-vitamin D_3; 0.5 ng/µL d_6-25(OH)D_3; 0.25 ng/µL d_6-24,25(OH)$_2D_3$; 60 pg/µL d_6-1α,25(OH)$_2D_3$) was added to each sample. After equilibration at room temperature for 25 minutes, serum proteins were precipitated with 1 mL of acetonitrile. After centrifugation, the supernatant was transferred and combined with 1.5 mL of 0.1 M phosphate buffer (pH 10.5) before analytes were extracted using two solid phase extraction (SPE) steps. For the first step, SPE Agilent Bond Elut C18 OH SPE cartridges (500 mg, 3 mL) were equilibrated with acetonitrile, methanol, and water. After adding the sample, the cartridge was washed with 70% methanol in water and eluted with 10% isopropanol in hexanes (v/v). The eluent was dried under N_2 gas at 37°C and the residual was reconstituted in 10% dichloromethane in heptane (v/v). For the second SPE step, samples were processed using Agilent Bond Elut SI cartridges (100 mg, 1 mL) conditioned with dichloromethane and heptanes. After adding the sample, the cartridge was washed with 10% dichloromethane in heptane (v/v), 30% dichloromethane in heptane (v/v), and 40% dichloromethane in heptane (v/v). Samples were eluted with 5% isopropanol in MTBE (v/v) into silanized glass culture tubes and dried under N_2 gas at 37°C. The residue was reconstituted in 50 µL of acetonitrile and derivatized with DAPTAD (50 µL) at room temperature for 45 minutes before the reaction was quenched by drying under N_2 gas at 37°C. Samples were reconstituted in 45 µL of methanol and 20 µL of water. The derivatized samples were centrifuged to remove insoluble particulates and excess DAPTAD.

Liquid chromatography-mass spectrometry (LC-MS/MS) analysis was performed on a Sciex QTRAP 6500 hybrid triple quadrupole/linear ion trap mass spectrometer (Framingham, MA) coupled with a Shimadzu liquid chromatography system (Kyoto, Japan). Chromatographic separation was achieved using an Ascentis Express RP-Amide column (2.1 mm x 150 mm x 2.7 µm) (Sigma-Aldrich Corp, St. Louis, MO), attached to a SecurityGuard™ ULTRA cartridge (2.1

mm x 2 µm) guard column (Phenomenex, Torrance, CA). The column temperature was maintained at 20°C with the mobile phase flowing at a rate of 0.275 mL/min. The autosampler was maintained at 4°C and the injection volume was 10 µL. The mobile phase consisted of a mixture of 0.1% formic acid in water (A) and 100% methanol (B). Initial conditions were set to 55% B and increased to 90% B through the 26 minute run time. The electrospray ionization (ESI) source of the mass spectrometer was operated in the positive ion mode. Multiple reaction monitoring (MRM) was used for quantitation. Mass spectrometric conditions are summarized in Table 4.1.

Peak integration was performed using MultiQuant software (version 3.0.2) from AB Sciex. Peak heights of vitamin D_3, 25(OH)D_3, and 24,25$(OH)_2D_3$ were normalized to d_7-vitamin D_3, d_6-25(OH)D_3 and d_6-24,25$(OH)_2D_3$, respectively. Peak heights of 1α,25$(OH)_2D_3$ and 4β,25$(OH)_2D_3$ were normalized to d_6-1α,25$(OH)_2D_3$. A quadratic equation with $1/x^2$ weighting was used to estimate the relationship between the peak height ratio and concentration.

Plasma concentrations of 25(OH)D_3-S and 25(OH)D_3-G were measured as previously described by Gao et al. (23). Briefly, standard curve and quality control samples were prepared in vitamin D-free serum. The proteins from 200 µL of serum were precipitated with 200 µL of acetonitrile and centrifuged at 13,362 *g* for 10 min at 4°C. The supernatant was subjected to SPE using Waters Oasis WAX (1 cc, 30 mg, 60 µm) anion-exchange cartridges and derivatized with DAPTAD. After 1 hour, samples were dried under N_2 gas at 37°C. The residue was reconstituted in 100 µL of 30% acetonitrile in water prior to LC-MS/MS analysis. LC-MS/MS analysis was performed on a Sciex (Framingham, MA) Q-Trap 6500 hybrid triple quadrupole/linear ion trap mass spectrometer with ESI coupled with a Shimadzu (Kyoto, Japan) liquid chromatography system. A Hypersil Gold (2.1 mm × 100 mm, 1.9 µm) column (Thermo Fisher Scientific, Waltham, MA) was used for chromatographic separation. The autosampler was maintained at 4°C and the injection volume was 20 µL. The ESI source of the mass spectrometer was operated in the positive ion mode and MRM was used for quantitation. Mass

spectrometric conditions are summarized in Table 4.1.

Peak integration was performed using Analyst MultiQuant software (version 3.0.2) from AB Sciex. To determine the peak area ratios, the peak areas of 25(OH)D_3-S and 25(OH)D_3-G were normalized to *d_6*-25(OH)D_3-S and *d_6*-25(OH)D_3-G, respectively. A linear equation with $1/x^2$ weighting was fit to estimate the relationship between peak area ratio and concentration for 25(OH)D_3-S and 25(OH)D_3-G.

4.3.5. Calculation of Unbound 25(OH)D_3 and 1α,25(OH)$_2D_3$ Concentrations

VDBP and albumin were measured at selected timepoints (pre-pregnancy, 4, 8, 16, 24, 32 weeks, and the sample collected closest to delivery) by the Department of Laboratory Medicine at the University of Washington. Unbound concentrations of 25(OH)D_3 and 1α,25(OH)$_2D_3$ were estimated using the equations published by Bikle et al. (Equation 4.1) (5, 24).

$$\mathrm{D_{free}} = \frac{\mathrm{D_{total}}}{\left(1 + (\text{binding constant ALB} \cdot [\mathrm{ALB}]) + (\text{binding constant VDBP} \cdot [\mathrm{VDBP}])\right)} \quad (4.2)$$

where D_{free} is the calculated free concentration of either 25(OH)D_3 or 1α,25(OH)$_2D_3$, D_{total} is the measured plasma concentration of 25(OH)D_3 or 1α,25(OH)$_2D_3$, and [ALB] and [VDBP] are the measured plasma albumin and VDBP concentrations. The 25(OH)D_3 binding constants for albumin and VDBP were 6×10^5 M^{-1} and 7×10^8 M^{-1}, respectively (5, 24). The 1α,25(OH)$_2D_3$ binding constants for albumin and VDBP were 5.4×10^4 M^{-1} and 3.7×10^7 M^{-1}, respectively (5, 24). The unbound fractions of 25(OH)D_3 and 1α,25(OH)$_2D_3$ were estimated by dividing the unbound concentration by the total concentration of the respective metabolite (% free D = (D_{free} / D_{total})·100).

4.3.6. Statistical Analysis

To assess changes in 25(OH)D_3 metabolism during pregnancy, data collected pre-

pregnancy and during pregnancy were analyzed using linear, quadratic, and cubic mixed-effects models for each analyte with gestational age as a fixed effect and subject as a random effect. For subjects with multiple pre-pregnancy samples, the concentration of 25(OH)D_3 and its metabolites closest to conception were used for modeling. To compare models, an ANOVA was performed between each model and its reduced form. Additionally, inspection of the predicted model and residual plots were used to assess goodness of fit. Season at conception and season at the time of sample collection were tested as fixed effects. A p-value less than 0.05 was considered significant. Statistical analysis was performed in RStudio (version 3.5.3, r-project.org/).

4.4. Results

4.4.1. Subject Demographics

A total of 34 women were enrolled in the study. Five women did not meet the inclusion criteria, seven failed to conceive within one year, two miscarried, and five withdrew from the study for personal reasons. Of the 15 women included in the analysis, nine women completed study visits pre-pregnancy through postpartum, four enrolled in the first trimester through postpartum, and two enrolled pre-pregnancy but withdrew from the study after delivery. The median number of samples collected from each participant was 14 out of a possible 18 visits. The age of the women at their first visit was 31 ± 4 years. Of the 15 participants included in the analysis, ten were white, four were Asian/Pacific Islander and one was black. Demographic data are presented in Table 4.2.

4.4.2. Changes in the plasma concentration of 25(OH)D_3 and its metabolites

In order to assess trends in the concentration of 25(OH)D_3 and its metabolites during pregnancy, linear, quadratic, and cubic mixed-effects models were fit to each metabolite from the data collected pre-pregnancy through the last sample collected during pregnancy (n = 154

data points). The coefficients of the final model for $25(OH)D_3$ and its metabolites are presented in Table 4.3 and model fits and residuals are shown in Figure 4.2 and Figure 4.3, respectively. The observed values at each visit of $25(OH)D_3$ and its metabolites are presented in Table 4.4 and Figure 4.4 for comparison to model predictions.

Based on $25(OH)D_3$ levels, at baseline (pre-pregnancy), three women were vitamin D sufficient (> 30 ng/mL), five women were vitamin D insufficient (between 20 – 30 ng/mL), and four women were vitamin D deficient (< 20 ng/mL). The concentration of $25(OH)D_3$ was linearly associated with gestational age ($p < 0.001$ compared to null model). The model estimated concentration of $25(OH)D_3$ pre-pregnancy was 25.0 ± 9.5 ng/mL. The model estimated an increase in plasma $25(OH)D_3$ concentrations of 0.314 ng/mL/week (95% CI 0.247 – 0.380), an estimated mean increase of 11.3 ng/mL (95% CI 8.9 – 13.7) by 36 weeks of gestation compared to the observed mean increase of 10.5 ± 12.5 ng/mL. At 36 weeks, nine women were vitamin D sufficient, four women were vitamin D insufficient, and two women were vitamin D deficient. Of the women who were vitamin D insufficient at 36 weeks, one woman was sampled in the summer, and three women were sampled in the fall. Two women were classified as borderline vitamin D deficient at 36 weeks (19.1 and 19.3 ng/mL), and were of Asian/Pacific Islander descent and sampled in the fall. The inclusion of season at conception and at the time of sample collection was assessed as a potential model covariate of $25(OH)D_3$ concentration, however, season did not improve the fit of the model (data not shown).

A quadratic model best described the change in the concentration of $1\alpha,25(OH)_2D_3$ throughout pregnancy ($p < 0.01$ compared to linear model). Pre-pregnancy, the model estimated concentration of $1\alpha,25(OH)_2D_3$ was 39.2 ± 7.0 pg/mL. Plasma concentrations of $1\alpha,25(OH)_2D_3$ rose rapidly in the first trimester, with a model estimated $1\alpha,25(OH)_2D_3$ concentration of 65.5 ± 9.7 pg/mL (67% increase) at 12 weeks of gestation. Serum concentrations of $1\alpha,25(OH)_2D_3$ plateaued early in the third trimester, reaching an estimated 81.7 ± 9.6 pg/mL at 28 weeks of gestation. At 40 weeks, the concentration of $1\alpha,25(OH)_2D_3$ was

estimated to be 2.1-fold higher than pre-pregnancy.

The concentration of 24,25$(OH)_2D_3$ throughout pregnancy was best described by a cubic model ($p < 0.01$ compared to quadratic model). Pre-pregnancy, the mean concentration of 24,25$(OH)_2D_3$ was estimated to be 2.5 ± 0.9 ng/mL. Plasma concentrations of 24,25$(OH)D_3$ were predicted to be at the nadir at 10 weeks of gestation. After the first trimester, concentrations of 24,25$(OH)_2D_3$ gradually increased to a model estimated 2.8 ± 0.9 ng/mL, a 12% increase from baseline.

Changes of the concentrations of 4β,25$(OH)_2D_3$, 25$(OH)D_3$-S, and 25$(OH)D_3$-G throughout pregnancy were best described by linear models ($p< 0.01$, $p < 0.001$, and $p < 0.01$, respectively, compared to null for all models). Pre-pregnancy, the concentration of 4β,25$(OH)_2D_3$ was predicted to be 77.8 ± 44.0 pg/mL. By 36 weeks, the concentration of 4β,25$(OH)_2D_3$ was estimated to increase by 13.6%, reaching an estimated concentration of 88.4 ± 39.3 pg/mL. Similarly, the serum concentration of 25$(OH)D_3$-G increased throughout pregnancy by an estimated 38% from 1.3 ± 1.0 ng/mL pre-pregnancy to 1.8 ± 0.9 ng/mL at 36 weeks of pregnancy. In contrast, the serum concentration of 25$(OH)D_3$-S decreased through pregnancy with concentrations estimated to fall from 42.7 ± 16.4 ng/mL pre-pregnancy to 32.3 ± 15.0 ng/mL at 36 weeks, an overall estimated decrease of 25%.

4.4.3. Changes in VDBP and Albumin and Effects on the Unbound Concentrations of 25(OH)D_3 and 1α,25$(OH)_2D_3$

Serum concentrations of VDBP and albumin were measured at selected time points (pre-pregnancy, 4, 8, 16, 24, 32 weeks, and the sample collected closest to delivery) to estimate the effects of pregnancy on the unbound concentrations of 25$(OH)D_3$ and 1α,25$(OH)_2D_3$. Similar to the serum concentrations of the metabolites, linear and quadratic mixed-effects models were fit to VDBP, albumin, and unbound concentrations and percent unbound of 25$(OH)D_3$ and 1α,25$(OH)_2D_3$ from pre-pregnancy until delivery (n = 86 data points). The coefficients of the final

models are presented in Table 4.5 and model fits and residuals are shown in Figure 4.5 and Figure 4.6, respectively. The summary statistics and the observed values of each metabolite are presented in Table 4.6 and Figure 4.7 for comparison to model predictions.

The serum concentration of VDBP was best fit with a quadratic model ($p < 0.001$ compared to linear model). At baseline, VDBP concentrations were estimated to be 221 ± 42 µg/mL compared to the observed 235 ± 32 µg/mL. The concentration of VDBP increased quickly in the first trimester and was estimated to reach 392 ± 34 µg/mL at 8 weeks of gestation. The concentrations of VDBP continued to rise, reaching peak concentrations in the third trimester. At 32 weeks, the concentration of VDBP was predicted to be 429 ± 40 µg/mL, an estimated increase of nearly 2-fold. The serum concentrations of albumin were best fit with a quadratic model ($p < 0.001$ compared to linear model). In contrast to VDBP, concentrations of albumin decreased during pregnancy. The concentration of albumin decreased from an estimated 4.6 ± 0.1 g/dL pre-pregnancy to 3.4 ± 0.1 g/dL at 32 weeks, a decrease of 26%.

The unbound concentrations of $25(OH)D_3$ and $1\alpha,25(OH)_2D_3$ were estimated using the equation previously published by Bikle et al. (5) The unbound concentration of $25(OH)D_3$ decreased linearly during pregnancy ($p < 0.001$ compared to null model). The model estimated unbound concentration of $25(OH)D_3$ was 19 ± 4 pg/mL pre-pregnancy and decreased to 16 ± 4 pg/mL by 32 weeks of gestation. The change in the percent of unbound $25(OH)D_3$ during pregnancy was best described by a quadratic equation ($p < 0.001$ compared to linear model). The percent unbound of $25(OH)D_3$ pre-pregnancy was estimated to be 0.071 ± 0.006% and decreased 40% by 32 weeks of gestation to 0.043 ± 0.05%.

The changes in the unbound concentration and percent unbound of $1\alpha,25(OH)_2D_3$ were best described by a quadric model ($p < 0.001$ compared linear models for both). The estimated unbound concentration of $1\alpha,25(OH)_2D_3$ was 0.53 ± 0.05 pg/mL pre-pregnancy. The estimated unbound concentration of $1\alpha,25(OH)_2D_3$ increased to 0.63 ± 0.09 pg/mL at 8 weeks of gestation. At 32 weeks, the estimated unbound concentration of $1\alpha,25(OH)_2D_3$ was 0.70 ± 0.082 pg/mL, a

32% increase. The percent unbound of $1\alpha,25(OH)_2D_3$ was estimated to decrease by 36% from 0.50 ± 0.04% pre-pregnancy to 0.32 ± 0.03% at 32 weeks of gestation.

4.4.4. Postpartum Changes in 25(OH)D_3 and its metabolites

Due to sparse data collect postpartum, the postpartum concentrations of $25(OH)D_3$ and its metabolites were compared to the concentration pre-pregnancy and at 36 weeks of gestation. The mean concentration of $25(OH)D_3$ and its metabolites are presented in Table 4.4 and Figure 4.4. By 3 weeks postpartum, serum concentrations of $25(OH)D_3$, $1\alpha,25(OH)_2D_3$, $4\beta,25(OH)_2D_3$, $25(OH)D_3$-S, and $25(OH)D_3$-G were similar to pre-pregnancy values. The mean concentration of $24,25(OH)_2D_3$ at 3 weeks postpartum, 3.62 ± 1.31 ng/mL, was higher than pre-pregnancy concentrations ($p < 0.001$), however concentrations returned to pre-pregnancy levels by 6 weeks postpartum. By 6 weeks postpartum, the serum concentration of VDBP and albumin, 246 ± 33 µg/mL and 4.4 ± 0.2 g/dL, respectively, were comparable to pre-pregnancy values. Similarly, the unbound concentration and percent unbound of $25(OH)D_3$ and $1\alpha,25(OH)_2D_3$ were similar to pre-pregnancy estimates by 6 weeks postpartum.

4.5. Discussion

We used linear mixed-effects modeling to describe pregnancy-induced changes in the serum concentration of $25(OH)D_3$ and its metabolites. We found that the serum concentrations of $25(OH)D_3$ increased by 45% from pre-pregnancy to 36 weeks of gestation. At 36 weeks, 60% of the study participants were vitamin D sufficient compared to 25% of the study participants pre-pregnancy. We observed that $1\alpha,25(OH)_2D_3$ concentrations increased by more than 60% at the end of the first trimester (12 weeks) compared to pre-pregnancy. Serum concentrations of $1\alpha,25(OH)_2D_3$ plateaued early in the third trimester, more than 2-fold above baseline, and remained elevated through delivery. For $24,25(OH)_2D_3$, serum concentrations decreased by 13% by week 8 of pregnancy, however, the concentrations of $24,25(OH)_2D_3$ then increased

throughout the remainder of pregnancy and reached concentrations 27% higher at 36 weeks compared to pre-pregnancy. The circulating concentrations of 4β,25(OH)$_2$D$_3$ and 25(OH)D$_3$-G increased by 14% and 38%, respectively, from pre-pregnancy to 36 weeks of gestation and the serum concentrations of 25(OH)D$_3$-S were 25% lower at 36 weeks compared to pre-pregnancy. Additionally, we found that the concentrations of VDBP increased nearly 2-fold during pregnancy, while the concentrations of albumin decreased by 26%. During pregnancy, the unbound concentrations of 25(OH)D$_3$ decreased by 20% and the unbound concentrations of 1α,25(OH)$_2$D$_3$ increased by 32%. The fraction unbound of both 25(OH)D$_3$ and 1α,25(OH)$_2$D$_3$ decreased by more than 35% throughout pregnancy.

While we observed a 45% increase in the concentrations of 25(OH)D$_3$ from pre-pregnancy to 36 weeks of gestation, in previously published studies, total concentrations of 25(OH)D were reported to have no change (25, 26) or increased during pregnancy (20, 27-30). Understanding the magnitude of change of 25(OH)D$_3$ concentrations during pregnancy is complicated by the numerous inter-individual determinants of 25(OH)D concentration (e.g., sun exposure, amount of vitamin D consumed in diet and supplements, race, and BMI) (13, 31-34). Endogenous formation of vitamin D$_3$ is dependent on sun exposure. Therefore, 25(OH)D$_3$ concentrations can vary significantly between seasons (35, 36). Seasonal variability in the prevalence of maternal vitamin D deficiency and insufficiency has been previously reported by Bodnar et al. and by Best et al., in which they found that the prevalence of maternal vitamin D deficiency and insufficiency at delivery was higher in the winter and spring compared to summer (13, 37). Additionally, both authors reported that the prevalence of vitamin D deficiency and insufficiency was higher in black women compared to white women, even when adjusted for season (13, 20). Although subjects in our study reported taking prenatal vitamins, the dose of vitamin D$_3$ present in the supplements is unknown. However, the endogenous formation of vitamin D$_3$ makes it difficult to assess the “dose” of vitamin D$_3$ on a given day, even when dietary and supplemental sources are recorded (35).

Due to the difficulty in recruiting women to participate in clinical studies early in pregnancy, there is limited information about changes in the concentrations of $25(OH)D_3$ and $1\alpha,25(OH)_2D_3$ in the first trimester. Figueiredo et al. measured the concentrations of $25(OH)D_3$ and $1\alpha,25(OH)_2D_3$ as early as the 5^{th} week of pregnancy. In a dataset including more than 200 women, Figueiredo et al. estimated that concentrations of 25(OH)D increased by approximately 12.2 ng/mL between 5 and 40 weeks of gestation, similar to the 11.3 ng/mL increase in $25(OH)D_3$ observed in our study from pre-pregnancy to 36 weeks of gestation (18). Additionally, Figueiredo et al. reported an average $1\alpha,25(OH)_2D$ concentration in the first trimester of 72.2 ± 32.4 pg/mL, which is in the range of the mean $1\alpha,25(OH)_2D_3$, 62.6 ± 13.9 pg/mL, at 12 weeks of gestation observed in our study.

Similar to previous studies (18, 20, 26, 29, 38-40), we observed that $1\alpha,25(OH)_2D_3$ concentrations increased two- to three-fold in the second and third trimesters compared to non-pregnant women. While CYP27B1 is expressed in the placenta, it is likely that most of the $1\alpha,25(OH)_2D_3$ in circulation during pregnancy is formed by the maternal kidneys (41).However, it is unknown whether CYP27B1 is induced in the kidney during pregnancy (42). It has been suggested that increased $1\alpha,25(OH)_2D_3$ concentrations support increased calcium absorption during pregnancy (37, 41, 43). Others proposed that elevated $1\alpha,25(OH)_2D_3$ modulates the immune system to support maternal tolerance of the developing fetus (41, 43).

In circulation, $25(OH)D_3$ is more than 99% protein bound, mainly by VDBP (~ 85%) and albumin (~15%), and is highly sensitive to changes in plasma protein levels. Concentrations of VDBP increased nearly two-fold, whereas albumin concentrations fell by 25% during pregnancy. Similar changes in VDBP and albumin were observed in previous studies (20, 21, 38-40, 44, 45). However, our study is unique in that we were able to measure VDBP and albumin early in the first trimester. Since VDBP is expressed on the surface of placental trophoblasts, which are in contact with the maternal blood supply, a proposed mechanism of increased VDBP during pregnancy is the release of VDBP from trophoblasts as they undergo cell turnover (22).

Increased 25(OH)D_3 binding to VDBP during pregnancy may lengthen the half-life of 25(OH)D_3 as a mechanism to conserve vitamin D (22). Increased VDBP during pregnancy resulted in an overall 20% decrease in unbound 25(OH)D_3 concentrations and 41% decrease in the fraction unbound of 25(OH)D_3 from pre-pregnancy to 36 weeks of gestation. Best et al. (17) used an enzyme-linked immunosorbent assay (ELISA) to measure the unbound 25(OH)D_3 directly and reported a percent unbound of 0.0158 ± 0.00064% at 40 weeks gestation, a value nearly three-fold lower than the 0.046 ± 0.006% at 32 weeks gestation observed in the current study. Further work will need to be done to determine whether Bikle's formula results in an overestimation of the percent of 25(OH)D_3 unbound, whether analytical issues with the ELISA exist, or if there is a more appropriate methodology for ascertaining free concentrations in pregnancy samples.

Currently, there is limited data reported for 24,25$(OH)_2D_3$ and 25(OH)D_3-S during pregnancy. Best et al. reported that the serum concentrations of 24,25$(OH)_2$D increased between weeks 15 and 40 of pregnancy, however, concentrations before 15 weeks were not reported for comparison (17). Axelson et al. reported the 25(OH)D_3-S concentrations in 20 women at delivery as 10.4 ± 5.2 ng/mL, which is three-fold lower than the 25(OH)D_3-S concentrations observed in our study (46). Lower concentrations of 25(OH)D_3 reported by Axelson et al. may partially explain the lower 25(OH)D_3-S concentrations, as 25(OH)D_3 and 25(OH)D_3-S are highly correlated (8, 46, 47).

We could find no reports of 4β,25$(OH)_2D_3$ and 25(OH)D_3-G concentrations in pregnancy. CYP3A4 and UGT1A4, the enzymes responsible for the formation of 4β,25$(OH)_2D_3$ and 25(OH)D_3-G, respectively, are known to be induced in pregnancy. Hebert et al. reported that CYP3A4-mediated clearance of midazolam was 2-fold higher in the third trimester of pregnancy compared postpartum (48). Similarly, the clearance of lamotrigine, a UGT1A4 probe, was higher in pregnant women as early as the fifth week of pregnancy and continued to increase until delivery (49-51). Despite CYP3A4 and UGT1A4 activity increasing more than two-fold during pregnancy, we only observed a 14% and 38% increase in the concentration of

4β,25(OH)$_2$D$_3$ and 25(OH)D$_3$-G, respectively. Due to the low hepatic extraction ratio of 25(OH)D$_3$, changes in clearance are not only driven by altered hepatic enzyme expression, but also by changes in the percent unbound of 25(OH)D$_3$. As previously discussed, the percent unbound of 25(OH)D$_3$ decreased approximately 40% during pregnancy, which may explain why the increase in 4β,25(OH)$_2$D$_3$ and 25(OH)D$_3$-G concentration was not as significant as expected given the putative increases in CYP3A4 and UGT1A4 expression.

In contrast to the liver situation, Tsuproykov et al. and Chapron et al. provided evidence that 25(OH)D$_3$ does not follow the free-drug hypothesis in the kidney, which assumes that only unbound 25(OH)D$_3$ can distribute into tissues (52, 53). Instead, Chapron et al. (53) used an *in vitro* kidney on-a-chip platform to confirm that 25(OH)D$_3$ bound to VDBP can be endocytosed by megalin and cubilin. We hypothesize that as VDBP concentrations increase through pregnancy, more 25(OH)D$_3$ can be delivered to CYP27B1 in the proximal tubule cells of the kidneys and be converted to 1α,25(OH)$_2$D$_3$. In addition, increased renal blood flow may contribute to increased 1α,25(OH)$_2$D$_3$ formation during pregnancy (45). CYP27B1 and megalin are also expressed in the placenta. Megalin expression increases over the course of placental development, which may lead to a concurrent increase in the uptake of 25(OH)D$_3$ into the placental epithelial cells, and subsequent placenta CYP27B1-mediated conversion to 1α,25(OH)$_2$D$_3$ (54).

We observed that concentrations of 25(OH)D$_3$ and its metabolites postpartum were similar to pre-pregnancy levels. Most notably, 1α,25(OH)$_2$D$_3$, the metabolite most affected by pregnancy, returned to pre-pregnancy levels by three weeks postpartum. Additionally, plasma levels of VDBP and albumin returned to pre-pregnancy levels by six weeks postpartum, though the return to baseline may have occurred sooner. Samples collect at three weeks postpartum were not analyzed for plasma protein levels. Earlier and more frequent sampling postpartum would provide additional insight into how quickly VDBP, albumin, the unbound concentrations and percent unbound of 25(OH)D$_3$ and 1α,25(OH)$_2$D$_3$ return to pre-pregnancy levels.

Longitudinal studies are optimal for studying changes in 25(OH)D$_3$ metabolism during

pregnancy. With the exception of 1α,25(OH)$_2$D$_3$, changes in the concentrations of 25(OH)D$_3$ and its metabolites during pregnancy were small, making them difficult to detect without paired comparisons. Typically, longitudinal studies compare concentrations of 25(OH)D$_3$ and its metabolites during pregnancy to paired postpartum values, rather than paired pre-pregnancy values. Moreover, there are few reports describing when postpartum levels return to baseline and if they are reliable surrogates for pre-pregnancy levels (21, 29, 30, 55). Alternatively, some studies compared concentrations of 25(OH)D$_3$ and 1α,25(OH)$_2$D$_3$ measured in pregnancy to a cohort of healthy, non-pregnant women or to laboratory reference ranges. By recruiting women prior to conception or early in the first trimester, we were able to model changes in the metabolism of 25(OH)D$_3$ through the entirety of pregnancy. Additionally, by collecting up to eleven samples from each participant during pregnancy, these data allow for more statistical power despite the limited sample size.

While the study described herein adds to the overall understanding of vitamin D disposition in pregnancy by monitoring concentrations of binding proteins and 25(OH)D$_3$ metabolites, there are many limitations to this study. First, this study only presents data from 15 pregnant women from the Pacific Northwest. It is unclear whether the changes observed will be reflective of pregnant women in general as the biological variability of vitamin D between individuals is large and the changes in 4β,25(OH)$_2$D$_3$, 25(OH)D$_3$-S and 25(OH)D$_3$-G concentrations were relatively small. Additionally, only healthy women participated in our study, which is likely not representative of women with pregnancy complications, such as preeclampsia and gestational diabetes. Although quantification of VDBP and albumin was limited to a restricted number of timepoints in this study due to cost considerations, we were able to report concentrations at 4 and 8 weeks of gestation which have not previously been described. Postpartum data were extremely limited; thus we were unable to model changes in 25(OH)D$_3$ and its metabolites after delivery. Collection of samples in the first week postpartum may allow for postpartum changes in 25(OH)D$_3$ disposition to be modeled. Finally, larger studies are

needed to confirm the observed changes in the concentrations of 25(OH)D_3 metabolites (e.g., 24,25(OH)$_2D_3$, 4β,25(OH)$_2D_3$, 25(OH)D_3-S, and 25(OH)D_3-G), and to include season and race, confounders of 25(OH)D_3 concentrations, to be included in future models. While describing the changes in the concentrations of 25(OH)D_3 and its metabolites is useful in understanding changes in vitamin D disposition during pregnancy, more data are needed to link these changes to maternal and fetal health outcomes.

4.6. Conclusions

This longitudinal observational study measured changes in 25(OH)D_3 and its metabolites in 15 women sampled prior to pregnancy, throughout pregnancy, at delivery, and postpartum. Serum concentrations of 25(OH)D_3 increased by nearly 50% during pregnancy, with a higher proportion of subjects being vitamin D sufficient in the third trimester compared to pre-pregnancy. As seen in other studies, 1α,25(OH)$_2D_3$ concentrations increased by nearly two-fold compared to pre-pregnancy. However, we were able to confirm that 1α,25(OH)$_2D_3$ concentrations were elevated as early as 4 weeks of pregnancy. Serum levels of VDBP increased by more than two-fold, while albumin concentrations fell by 25% during pregnancy. This resulted in a decrease in the unbound concentrations and percent unbound of both 25(OH)D_3 and 1α,25(OH)$_2D_3$ during pregnancy. The concentrations of 24,25(OH)$_2D_3$ decreased by nearly 15% in the first trimester and then steadily increased to more than 25% above pre-pregnancy levels in the third trimester. Circulating levels of 25(OH)D_3-S decreased by 25% during pregnancy. Circulating concentrations of 4β,25(OH)$_2D_3$ and 25(OH)D_3-G increased by less than 40%, despite presumed 2-fold higher CYP3A4 and UGT1A4 expression during pregnancy, likely due to the decreased fraction unbound of 25(OH)D_3. Concentrations of 25(OH)D_3 and its metabolites, except for 24,25(OH)$_2D_3$, returned to pre-pregnancy levels by three weeks postpartum. The disposition of 25(OH)D_3 and its metabolites was altered during pregnancy and additional studies are required to determine the underlying mechanisms and

significance of these results for maternal and fetal health.

4.7. References

(1) Bikle, D.D. Vitamin D and bone. *Curr Osteoporos Rep* **10**, 151-9 (2012).

(2) Bikle, D.D. & Bouillon, R. Vitamin D and bone and beyond. *Bone Rep* **9**, 120-1 (2018).

(3) Jones, G., Prosser, D.E. & Kaufmann, M. Cytochrome P450-mediated metabolism of vitamin D. *J Lipid Res* **55**, 13-31 (2014).

(4) Sakaki, T., Kagawa, N., Yamamoto, K. & Inouye, K. Metabolism of vitamin D3 by cytochromes P450. *Front Biosci* **10**, 119-34 (2005).

(5) Bikle, D., Bouillon, R., Thadhani, R. & Schoenmakers, I. Vitamin D metabolites in captivity? Should we measure free or total 25(OH)D to assess vitamin D status? *J Steroid Biochem Mol Biol* **173**, 105-16 (2017).

(6) Wang, Z. *et al.* Human UGT1A4 and UGT1A3 conjugate 25-hydroxyvitamin D3: metabolite structure, kinetics, inducibility, and interindividual variability. *Endocrinology* **155**, 2052-63 (2014).

(7) Wang, Z. *et al.* An inducible cytochrome P450 3A4-dependent vitamin D catabolic pathway. *Mol Pharmacol* **81**, 498-509 (2012).

(8) Wong, T. *et al.* Polymorphic Human Sulfotransferase 2A1 Mediates the Formation of 25-Hydroxyvitamin D3-3-O-Sulfate, a Major Circulating Vitamin D Metabolite in Humans. *Drug Metab Dispos* **46**, 367-79 (2018).

(9) Gao, C., Liao, M.Z., Han, L.W., Thummel, K.E. & Mao, Q. Hepatic Transport of 25-Hydroxyvitamin D3 Conjugates: A Mechanism of 25-Hydroxyvitamin D3 Delivery to the Intestinal Tract. *Drug Metab Dispos* **46**, 581-91 (2018).

(10) Jin, S.E., Park, J.S. & Kim, C.K. Pharmacokinetics of oral calcitriol in healthy human based on the analysis with an enzyme immunoassay. *Pharmacological research* **60**, 57-60 (2009).

(11) Holick, M.F. Vitamin D: a d-lightful solution for health. *Journal of investigative medicine : the official publication of the American Federation for Clinical Research* **59**, 872-80 (2011).

(12) Ozias, M.K., Kerling, E.H., Christifano, D.N., Scholtz, S.A., Colombo, J. & Carlson, S.E. Typical prenatal vitamin D supplement intake does not prevent decrease of plasma 25-hydroxyvitamin D at birth. *J Am Coll Nutr* **33**, 394-9 (2014).

(13) Bodnar, L.M., Simhan, H.N., Powers, R.W., Frank, M.P., Cooperstein, E. & Roberts, J.M. High prevalence of vitamin D insufficiency in black and white pregnant women residing in the northern United States and their neonates. *J Nutr* **137**, 447-52 (2007).

(14) Robinson, C.J., Alanis, M.C., Wagner, C.L., Hollis, B.W. & Johnson, D.D. Plasma 25-hydroxyvitamin D levels in early-onset severe preeclampsia. *American journal of obstetrics and gynecology* **203**, 366.e1-6 (2010).

(15) Fang, K., He, Y., Mu, M. & Liu, K. Maternal vitamin D deficiency during pregnancy and Low birth weight: a systematic review and meta-analysis. *The journal of maternal-fetal & neonatal medicine : the official journal of the European Association of Perinatal Medicine, the Federation of Asia and Oceania Perinatal Societies, the International Society of Perinatal Obstet*, 1-161 (2019).

(16) Dinlen, N., Zenciroglu, A., Beken, S., Dursun, A., Dilli, D. & Okumus, N. Association of vitamin D deficiency with acute lower respiratory tract infections in newborns. *The Journal of Maternal-Fetal & Neonatal Medicine* **29**, 928-32 (2016).

(17) Best, C.M., Pressman, E.K., Queenan, R.A., Cooper, E. & O'Brien, K.O. Longitudinal changes in serum vitamin D binding protein and free 25-hydroxyvitamin D in a multiracial cohort of pregnant adolescents. *J Steroid Biochem Mol Biol* **186**, 79-88 (2019).

(18) Figueiredo, A.C.C. *et al.* Changes in plasma concentrations of 25-hydroxyvitamin D and 1,25-dihydroxyvitamin D during pregnancy: a Brazilian cohort. *Eur J Nutr* **57**, 1059-72 (2018).

(19) Isoherranen, N. & Thummel, K.E. Drug metabolism and transport during pregnancy: how does drug disposition change during pregnancy and what are the mechanisms that cause such changes? *Drug Metab Dispos* **41**, 256-62 (2013).

(20) Best, C.M., Pressman, E.K., Queenan, R.A., Cooper, E. & O'Brien, K.O. Longitudinal changes in serum vitamin D binding protein and free 25-hydroxyvitamin D in a multiracial cohort of pregnant adolescents. *The Journal of steroid biochemistry and molecular biology*, (2018).

(21) Zhang, J.Y., Lucey, A.J., Horgan, R., Kenny, L.C. & Kiely, M. Impact of pregnancy on vitamin D status: a longitudinal study. *Br J Nutr* **112**, 1081-7 (2014).

(22) Karras, S.N., Koufakis, T., Fakhoury, H. & Kotsa, K. Deconvoluting the Biological Roles of Vitamin D-Binding Protein During Pregnancy: A Both Clinical and Theoretical Challenge. *Front Endocrinol (Lausanne)* **9**, 259 (2018).

(23) Gao, C. *et al.* Simultaneous quantification of 25-hydroxyvitamin D3-3-sulfate and 25-hydroxyvitamin D3-3-glucuronide in human serum and plasma using liquid chromatography-tandem mass spectrometry coupled with DAPTAD-derivatization. *J Chromatogr B Analyt Technol Biomed Life Sci* **1060**, 158-65 (2017).

(24) Bikle, D.D., Gee, E., Halloran, B., Kowalski, M.A., Ryzen, E. & Haddad, J.G. Assessment of the free fraction of 25-hydroxyvitamin D in serum and its regulation by albumin and the vitamin D-binding protein. *J Clin Endocrinol Metab* **63**, 954-9 (1986).

(25) Yoshikata, H. *et al.* 25-Hydroxyvitamin D profiles and maternal bone mass during pregnancy and lactation in Japanese women. *Journal of bone and mineral metabolism* **38**, 99-108 (2020).

(26) Gustafsson, M.K. *et al.* Alterations in the vitamin D endocrine system during pregnancy: A longitudinal study of 855 healthy Norwegian women. *PLoS One* **13**, e0195041 (2018).

(27) Xia, J. *et al.* Vitamin D status during pregnancy and the risk of gestational diabetes mellitus: A longitudinal study in a multiracial cohort. *Diabetes, obesity & metabolism* **21**, 1895-905 (2019).

(28) Boghossian, N.S., Koo, W., Liu, A., Mumford, S.L., Tsai, M.Y. & Yeung, E.H. Longitudinal measures of maternal vitamin D and neonatal body composition. *Eur J Clin Nutr* **73**, 424-31 (2019).

(29) Lundqvist, A., Sandstrom, H., Stenlund, H., Johansson, I. & Hultdin, J. Vitamin D Status during Pregnancy: A Longitudinal Study in Swedish Women from Early Pregnancy to Seven Months Postpartum. *PLoS One* **11**, e0150385 (2016).

(30) Milman, N., Hvas, A.M. & Bergholt, T. Vitamin D status during normal pregnancy and postpartum. A longitudinal study in 141 Danish women. *J Perinat Med* **40**, 57-61 (2011).

(31) Hollis, B.W. Vitamin D requirement during pregnancy and lactation. *J Bone Miner Res* **22 Suppl 2**, V39-44 (2007).

(32) Moon, R.J. *et al.* Tracking of 25-hydroxyvitamin D status during pregnancy: the importance of vitamin D supplementation. *Am J Clin Nutr* **102**, 1081-7 (2015).

(33) Moon, R.J. *et al.* Determinants of the Maternal 25-Hydroxyvitamin D Response to Vitamin D Supplementation During Pregnancy. *J Clin Endocrinol Metab* **101**, 5012-20 (2016).

(34) Perez-Lopez, F.R. *et al.* Effect of vitamin D supplementation during pregnancy on maternal and neonatal outcomes: a systematic review and meta-analysis of randomized controlled trials. *Fertil Steril* **103**, 1278-88 e4 (2015).

(35) Bikle, D. Vitamin D: Production, Metabolism, and Mechanisms of Action. In: *Endotext* (eds. Feingold, K.R., Anawalt, B., Boyce, A., Chrousos, G., Dungan, K., Grossman, A. *et al.*) (South Dartmouth (MA), 2000).

(36) Klingberg, E., Oleröd, G., Konar, J., Petzold, M. & Hammarsten, O. Seasonal variations in serum 25-hydroxy vitamin D levels in a Swedish cohort. *Endocrine* **49**, 800-8 (2015).

(37) Best, C.M., Pressman, E.K., Queenan, R.A., Cooper, E., Vermeylen, F. & O'Brien, K.O. Gestational Age and Maternal Serum 25-hydroxyvitamin D Concentration Interact to Affect the 24,25-dihydroxyvitamin D Concentration in Pregnant Adolescents. *J Nutr* **148**, 868-75 (2018).

(38) Markestad, T., Ulstein, M., Aksnes, L. & Aarskog, D. Serum concentrations of vitamin D metabolites in vitamin D supplemented pregnant women. A longitudinal study. *Acta Obstet Gynecol Scand* **65**, 63-7 (1986).

(39) Wilson, S.G., Retallack, R.W., Kent, J.C., Worth, G.K. & Gutteridge, D.H. Serum free 1,25-dihydroxyvitamin D and the free 1,25-dihydroxyvitamin D index during a longitudinal study of human pregnancy and lactation. *Clin Endocrinol (Oxf)* **32**, 613-22 (1990).

(40) Ardawi, M.S., Nasrat, H.A. & HS, B.A.A. Calcium-regulating hormones and parathyroid hormone-related peptide in normal human pregnancy and postpartum: a longitudinal study. *Eur J Endocrinol* **137**, 402-9 (1997).

(41) Larqué, E., Morales, E., Leis, R. & Blanco-Carnero, J.E. Maternal and Foetal Health Implications of Vitamin D Status during Pregnancy. *Annals of Nutrition and Metabolism* **72**, 179-92 (2018).

(42) Olmos-Ortiz, A., Avila, E., Durand-Carbajal, M. & Diaz, L. Regulation of calcitriol biosynthesis and activity: focus on gestational vitamin D deficiency and adverse pregnancy outcomes. *Nutrients* **7**, 443-80 (2015).

(43) Hollis, B.W. & Wagner, C.L. New insights into the vitamin D requirements during pregnancy. *Bone Research* **5**, 17030 (2017).

(44) Halhali, A. *et al.* Longitudinal changes in maternal serum 1,25-dihydroxyvitamin D and insulin like growth factor I levels in pregnant women who developed preeclampsia: comparison with normotensive pregnant women. *J Steroid Biochem Mol Biol* **89-90**, 553-6 (2004).

(45) Anderson, G.D. Pregnancy-induced changes in pharmacokinetics: a mechanistic-based approach. *Clin Pharmacokinet* **44**, 989-1008 (2005).

(46) Axelson, M. & Christensen, N.J. Vitamin D metabolism in human pregnancy. Concentrations of free and sulphated 25-hydroxyvitamin D3 in maternal and fetal plasma at term. *J Steroid Biochem* **31**, 35-9 (1988).

(47) Axelson, M. 25-Hydroxyvitamin D3 3-sulphate is a major circulating form of vitamin D in man. *FEBS letters* **191**, 171-5 (1985).

(48) Hebert, M.F. *et al.* Effects of pregnancy on CYP3A and P-glycoprotein activities as measured by disposition of midazolam and digoxin: a University of Washington specialized center of research study. *Clin Pharmacol Ther* **84**, 248-53 (2008).

(49) Deligiannidis, K.M., Byatt, N. & Freeman, M.P. Pharmacotherapy for mood disorders in pregnancy: a review of pharmacokinetic changes and clinical recommendations for therapeutic drug monitoring. *J Clin Psychopharmacol* **34**, 244-55 (2014).

(50) Karanam, A. *et al.* Lamotrigine clearance increases by 5 weeks gestational age: Relationship to estradiol concentrations and gestational age. *Ann Neurol* **84**, 556-63 (2018).

(51) Pennell, P.B., Newport, D.J., Stowe, Z.N., Helmers, S.L., Montgomery, J.Q. & Henry, T.R. The impact of pregnancy and childbirth on the metabolism of lamotrigine. *Neurology* **62**, 292-5 (2004).

(52) Tsuprykov, O., Chen, X., Hocher, C.F., Skoblo, R., Lianghong, Y. & Hocher, B. Why should we measure free 25(OH) vitamin D? *J Steroid Biochem Mol Biol* **180**, 87-104 (2018).

(53) Chapron, B.D. *et al.* Reevaluating the role of megalin in renal vitamin D homeostasis using a human cell-derived microphysiological system. *ALTEX* **35**, 504-15 (2018).

(54) O'Brien, K.O. *et al.* Placental CYP27B1 and CYP24A1 expression in human placental tissue and their association with maternal and neonatal calcitropic hormones. *J Clin Endocrinol Metab* **99**, 1348-56 (2014).

(55) Holmes, V.A., Barnes, M.S., Alexander, H.D., McFaul, P. & Wallace, J.M. Vitamin D deficiency and insufficiency in pregnant women: a longitudinal study. *Br J Nutr* **102**, 876-81 (2009).

4.8. Tables

Table 4.1. Retention time, precursor molecular ion/product ion for quantification of hydroxylated and conjugated metabolites of $25(OH)D_3$.

Analyte	Retention Time (min)	Precursor Ion	Product Ion	DP[a] (V)	CE[c] (V)	LLOD	Standard Curve Range
Hydroxylated Metabolites							
Vitamin D_3	22.2	603.2	163.1	276	53	0.06 ng/mL	0.09 – 22 ng/mL
d_7-vitamin D_3	22.1	610.2	163.1	276	53	-	-
$25(OH)D_3$	18.3	619.2	601.1	196	27	0.1 ng/mL	0.2 – 50 ng/mL
d_6-$25(OH)D_3$	18.2	625.4	341.1	196	31	-	-
$24R,25(OH)_2D_3$	13.9	635.2	341.1	66	35	0.03 ng/mL	0.06 – 15 ng/mL
d_6-$24R,25(OH)_2D_3$	13.7	641.2	341.1	66	35	-	-
$1\alpha,25(OH)_2D_3$	15.7	635.2	357.1	146	33	1.6 pg/mL	2 – 800 pg/mL
$4\beta,25(OH)_2D_3$	15.5	635.2	357.1	146	33	1.6 pg/mL	2 – 800 pg/mL
d_6-$1\alpha,25(OH)_2D_3$	15.6	641.2	357.1	146	33	-	-
Conjugated Metabolites							
$25(OH)D_3$-S	10.78	699.5	323.0	100	45	0.5	2.4 – 96
d_6-$25(OH)D_3$-S	10.72	705.5	323.0	100	45	-	-
$25(OH)D_3$-G	9.59	795.5	341.1	100	42.5	0.2	0.3 – 11.5
d_6-$25(OH)D_3$-G	9.56	801.5	341.1	100	42.5	-	-

[a] declustering potential
[b] collision energy
[c] lower limit of detection

Table 4.2. Demographics of participants at the first study visit.

Parameter	**Value (N = 15)**
Age (years)	31 ± 4
Weight (kg)	60 ± 10
BMI (kg/m^2)	22 ± 3
Race	
White	10
Asian/Pacific Islander	4
Black	1

Table 4.3: Final model estimates (betas) of the effect of gestational age on 25(OH)D_3 and its metabolites during pregnancy.

Metabolite	Model type	Intercept	Gestational Age	(Gestational Age)^2	(Gestational Age)^3	p-value
25(OH)D_3 (ng/mL)	linear	24.5 (19.1, 29.8)	0.314 (0.247, 0.380)	-	-	< 0.001
1α,25(OH)$_2D_3$ (pg/mL)	quadratic	41.7 (33.6, 49.9)	2.24 (1.50, 2.98)	-0.0284 (-0.0467, -0.0103)	-	< 0.01
24,25(OH)$_2D_3$ (ng/mL)	cubic	2.36 (1.81, 2.92)	-0.113 (-0.172, -0.054)	7.14×10^{-3} (3.68×10^{-3}, 1.06×10^{-2})	-1.01×10^{-4} (-1.59×10^{-4}, -4.42×10^{-5})	< 0.001
4β,25(OH)$_2D_3$ (pg/mL)	linear	71.6 (49.2, 93.8)	0.466 (0.142, 0.790)	-	-	< 0.01
25(OH)D_3-S (ng/mL)	linear	40.5 (32.4, 48.5)	-0.228 (-0.304, -0.152)	-	-	< 0.001
25(OH)D_3-G (ng/mL)	linear	1.38 (0.89, 1.87)	0.00117 (0.00421, 0.0192)	-	-	< 0.01

Values = mean (95% Confidence Interval)

Table 4.4. Observed concentrations of 25-hydroxyvitamin D_3 and its metabolites before pregnancy, during pregnancy, at delivery, and postpartum.

Study Day	n	25(OH)D_3 (ng/mL)	1α,25(OH)$_2D_3$ (pg/mL)	24,25(OH)$_2D_3$ (ng/mL)	4β,25(OH)$_2D_3$ (pg/mL)	25(OH)D_3-S (ng/mL)	25(OH)D_3-G (ng/mL)
Pre-pregnancy	12	26.2 ± 7.1	35.8 ±10.5	2.59 ± 0.80	81.5 ± 32.6	43.4± 22.9	1.30 ± 0.81
Pregnancy							
4 weeks	11	24.1 ± 6.8	49.1 ± 13.6*	1.91 ± 0.85	104.3 ± 47.3	41.4 ± 19.5	1.22 ± 0.79
8 weeks	14	26.8 ± 6.6	62.6 ± 21.2**	1.69 ± 0.65**	63.2 ± 24.5	39.3 ± 19.7	1.35 ± 0.92
12 weeks	13	27.4 ± 8.9	62.6 ± 13.9***	1.92 ± 0.80	67.8 ± 33.0	39.0 ± 20.8	1.53 ± 0.72
16 weeks	14	30.3 ± 9.7	71.0 ± 14.8***	2.15 ± 0.80	68.4 ± 31.1	37.5 ± 16.6	1.82 ± 0.92
20 weeks	15	31.0 ± 12.2	74.2 ± 21.3***	2.23 ± 1.10	73.7 ± 43.2	36.0 ± 15.6	1.55 ± 1.01
24 weeks	15	33.3 ± 10.5	77.6 ± 19.9***	2.40 ± 1.13	82.4 ± 49.2	33.2 ± 14.0	1.64 ± 0.96
28 weeks	14	32.1 ± 11.0	77.9 ± 13.1***	2.48 ± 1.18	93.5 ± 56.1	32.3 ± 14.0	1.82 ± 1.18
32 weeks	15	36.1 ± 13.0	92.0 ± 28.7***	2.65 ± 1.17	91.0 ± 44.8	33.2 ± 13.8	2.02 ± 1.13
36 weeks	15	36.1 ± 15.0	81.7 ± 25.1***	2.82 ± 1.40	93.3 ± 52.6	32.3 ± 11.9	1.65 ± 1.34
38 weeks	11	33.2 ± 11	89.6 ± 19.5***	2.65 ± 1.24	87.3 ± 72.4	31.2 ± 11.6	1.75 ± 1.44
40 weeks	6	36.2 ± 18.1	89.2 ± 26.2**	3.17 ± 1.85	99.7 ± 78.6	29.5 ± 8.8	1.69 ± 1.24
Delivery	7	31.5 ± 11.4	82.2 ± 19.3**	2..89 ± 1.63	72.5 ± 42.4	32.5 ± 14.6	1.14 ± 0.61
Postpartum							
3 weeks	13	31.4 ± 11.4	45.7 ± 30$^{\#\#}$	3.62 ± 1.31*	85.2 ± 42.4	33.0 ± 12.8	1.56 ± 1.09
6 weeks	13	28.8 ± 8.2	46.3 ± 26.6$^{\#\#}$	3.22 ± 0.89	81.8 ± 38.0	34.0 ± 11.2	1.51 ± 1.03
12 weeks	12	25.0 ± 7.4	53.5 ± 29.7$^{\#\#}$	2.5 ± 0.7	69.9 ± 23.5	34.3 ± 13.3	1.27 ± 0.79

Values = mean ± standard deviation

* $p < 0.05$, ** $p < 0.01$, *** $p < 0.001$ compared to pre-pregnancy using a Wilcoxson rank-summed test

$^{\#}$ $p < 0.05$, $^{\#\#}$ $p < 0.01$, $^{\#\#\#}$ $p < 0.001$ compared to 36 weeks of gestation using a Wilcoxson rank-summed test

Table 4.5: Final model estimates (betas) of the effect of gestational age on vitamin D binding protein, albumin, and the unbound concentrations of $25(OH)D_3$ and $1\alpha,25(OH)_2D_3$ during pregnancy.

	Model Type	Intercept	Gestational Age	$(\text{Gestational Age})^2$	p-value
VDBP (µg/mL)	quadratic	214 (189, 240)	11.5 (9.7, 13.3)	-0.151 (-0.198, -0.102)	< 0.001
Albumin (g/dL)	quadratic	4.5 (4.4, 4.7)	-0.059 (-0.070, -0.048)	6.9×10^{-4} (4.0×10^{-4}, 9.9×10^{-4})	< 0.001
Unbound $25(OH)D_3$ (pg/mL)	quadratic	20 (17, 22)	-0.37 (-0.54, -0.19)	7.6×10^{-3} (3.0×10^{-3}, 0.012)	< 0.01
Percent Unbound $25(OH)D_3$	quadratic	0.081 (0.077, 0.085)	-2.1×10^{-3} (-2.5×10^{-3}, -1.8×10^{-3})	3.3×10^{-5} (2.4×10^{-5}, 4.1×10^{-5})	< 0.001
Unbound $1\alpha,25(OH)_2D_3$ (pg/mL)	linear	0.60 (0.51, 0.68)	3.5×10^{-3} (4.8×10^{-4}, 6.4×10^{-3})	-	< 0.05
Percent Unbound $1\alpha,25(OH)_2D_3$	quadratic	0.56 (0.53, 0.58)	-0.014 (-0.016, - 0.012)	2.1×10^{-4} (1.5×10^{-4}, 2.6×10^{-4})	< 0.001

Values = mean (95% Confidence Interval)

Table 4.6. Observed concentrations of vitamin D binding protein (VDBP) and albumin, and calculated unbound concentrations and percent unbound of 25-hydroxyvitamin and 1α,25-dihydroxyvitamin D_3.

Study Day (n)	n	VDBP (µg/mL)	Albumin (g/dL)	Unbound $25(OH)D_3$ (pg/mL)	% Unbound $25(OH)D_3$	Unbound $1\alpha,25(OH)_2D_3$ (pg/mL)	% Unbound $1\alpha,25(OH)_2D_3$
Pre-Pregnancy	12	238 ± 33	4.5 ± 0.3	21 ± 4	0.077 ± 0.009	0.46 ± 0.99	0.53 ± 0.06
Pregnancy							
4 weeks	11	239 ± 35	4.4 ± 0.2	19 ± 6	0.077 ± 0.010	0.63 ± 0.19*	0.53 ± 0.06
8 weeks	13	296 ± 45**	4.2 ± 0.3*	17 ± 4	0.064 ± 0.009**	0.69 ± 0.31**	0.45 ± 0.06**
16 weeks	14	371 ± 43***	3.7 ± 0.2***	16 ± 5	0.052 ± 0.005***	0.64 ± 0.16***	0.38 ± 0.04***
24 weeks	15	400 ± 60***	3.5 ± 0.2***	16 ± 5	0.049 ± 0.006***	0.66 ± 0.15***	0.36 ± 0.04***
32 weeks	15	428 ± 56***	3.4 ± 0.2***	16 ± 5	0.046 ± 0.006***	0.73 ± 0.18***	0.34 ± 0.04***
Postpartum							
6 weeks	13	246 ± 33^{ǂǂǂ}	4.4 ± 0.2^{ǂǂǂ}	21 ± 6	0.075 ± 0.009^{ǂǂǂ}	0.58 ± 0.33^{ǂ}	0.52 ± 0.06^{ǂǂǂ}

Values = mean ± standard deviation

* $p < 0.05$, ** $p < 0.01$, *** $p < 0.001$ compared to pre-pregnancy using a Wilcoxson rank-summed test

^{ǂ} $p < 0.05$, ^{ǂǂ} $p < 0.01$, ^{ǂǂǂ} $p < 0.001$ compared to 36 weeks of gestation using a Wilcoxson rank-summed test

4.9. Figures

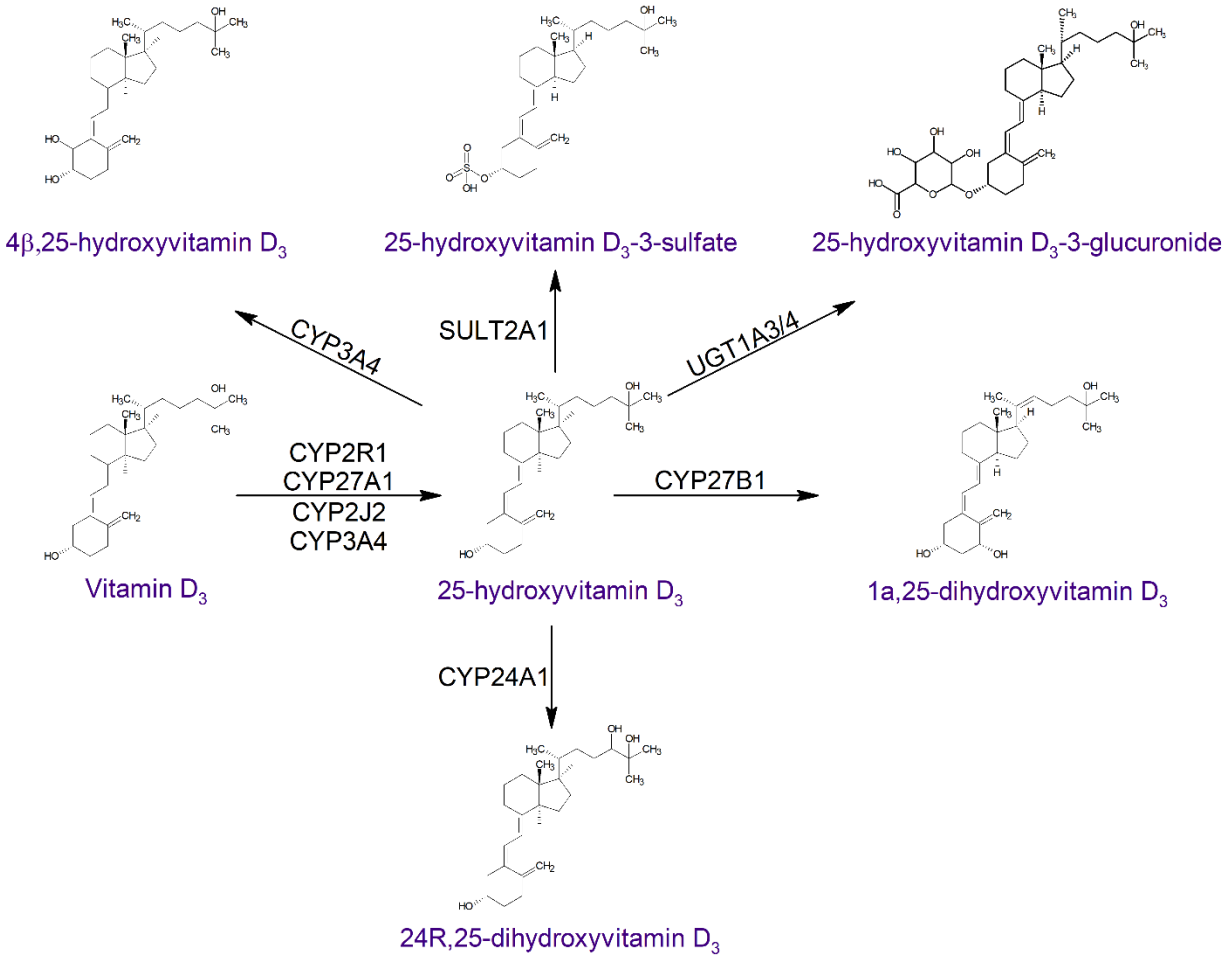

Figure 4.1: Metabolic scheme of vitamin D_3 and selected metabolites.

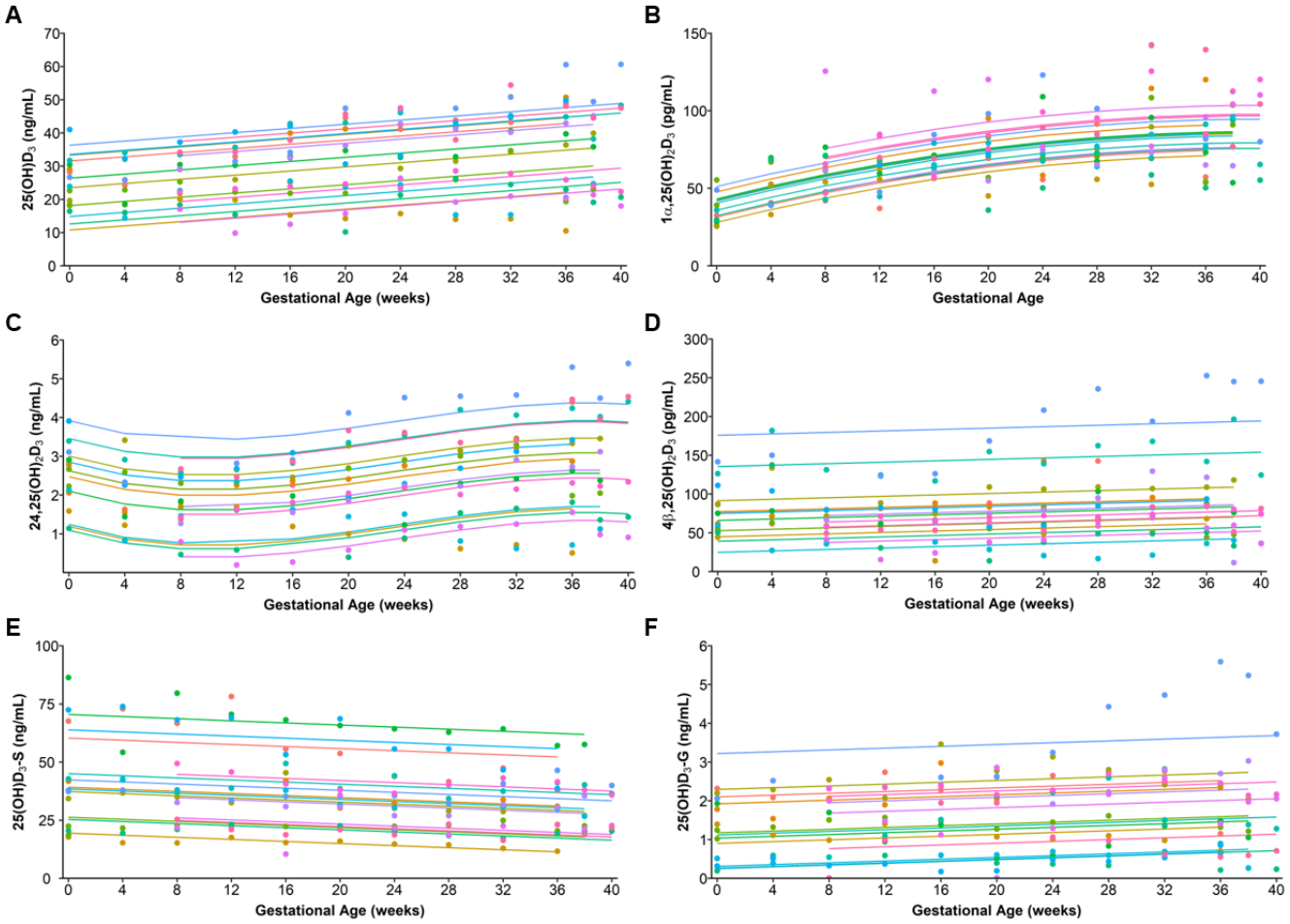

Figure 4.2: Mixed-effects model fits for A) 25-hydroxyvitamin D_3, B) 1α,25-dihydroxyvitamin D_3, C) 24,25-dihydroxyvitamin D_3, D) 4β,25-dihydroxyvitamin D_3, E) 25-hydroxyvitamin D_3-sulfate, and F) 25-hydroxyvitamin D_3-glucuronide from pre-pregnancy through the end of the third trimester. The circles are the observed plasma concentrations of each analyte. The lines represent the final linear mixed-effects fits for each subject. Each color represents one subject.

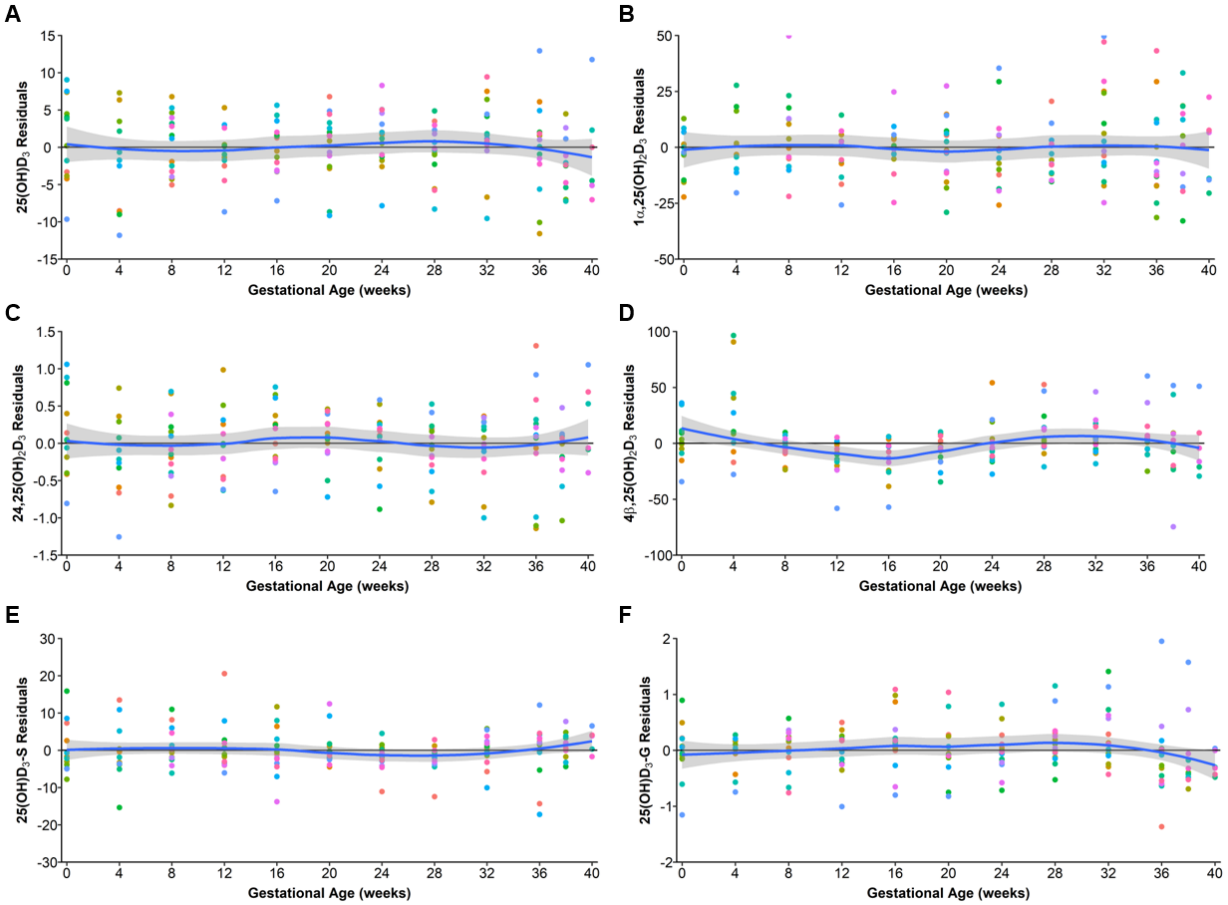

Figure 4.3: Residual plots for A) 25-hydroxyvitamin D_3, B) 1α,25-dihydroxyvitamin D_3, C) 24,25-dihydroxyvitamin D_3, D) 4β,25-dihydroxyvitamin D_3, E) 25-hydroxyvitamin D_3-sulfate, and F) 25-hydroxyvitamin D_3-glucuronide models from pre-pregnancy through the end of the third trimester. The blue lines and shaded regions represent the mean and 95% confidence interval, respectively, of the loess line. Each point represents the residuals for individual data. Each color represents one subject.

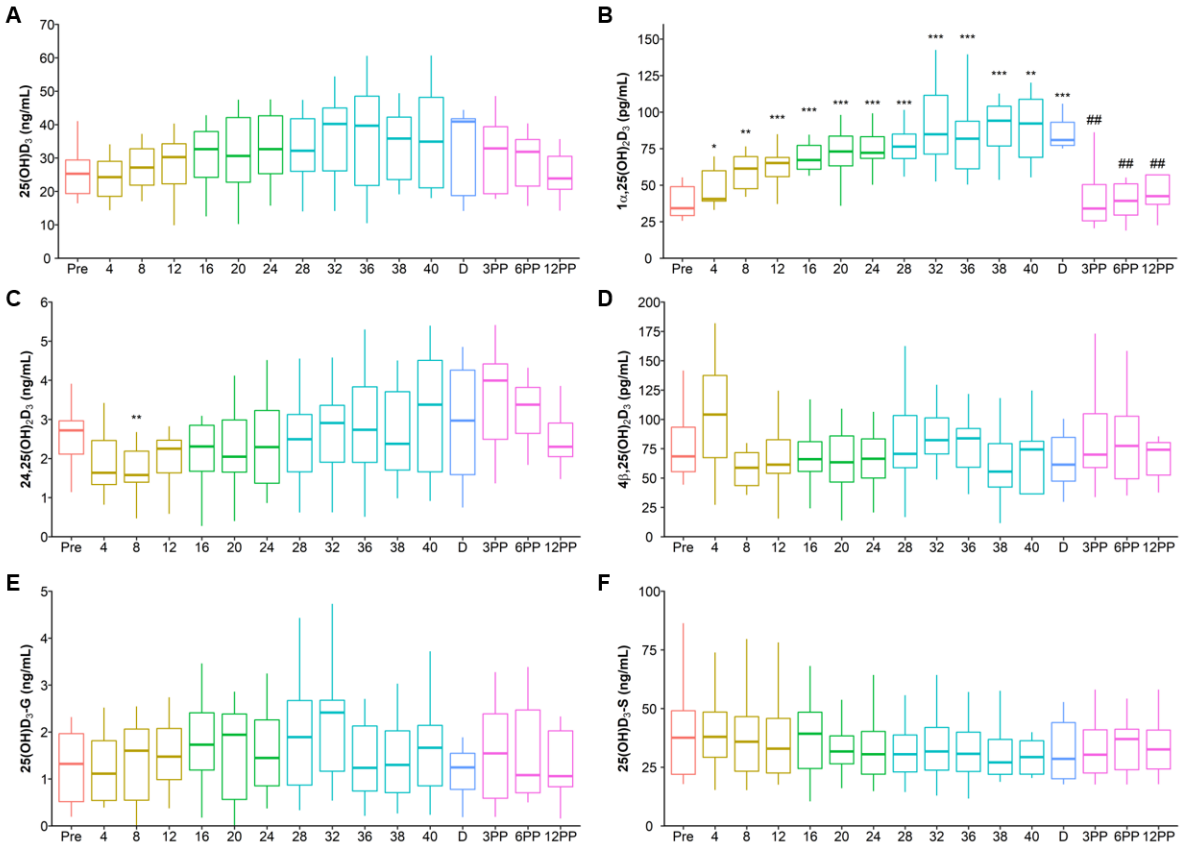

Figure 4.4: Observed concentrations of A) $25(OH)D_3$, B) $1\alpha,25(OH)_2D_3$, C) $24,25(OH)_2D_3$, D) $4\beta,25(OH)_2D_3$, E) $25(OH)D_3$-S, and D) $25(OH)D_3$-G. For each boxplot, the center line represents the median. The boxed region is the 25th to 75th percentile (interquartile range). The whiskers are the largest value within 1.5 times interquartile range above the 75th percentile and smallest value within 1.5 times the interquartile range below the 25th percentile. Box colors: pre-pregnancy (red), first trimester (yellow), second trimester (green), third trimester (blue), and postpartum (purple).

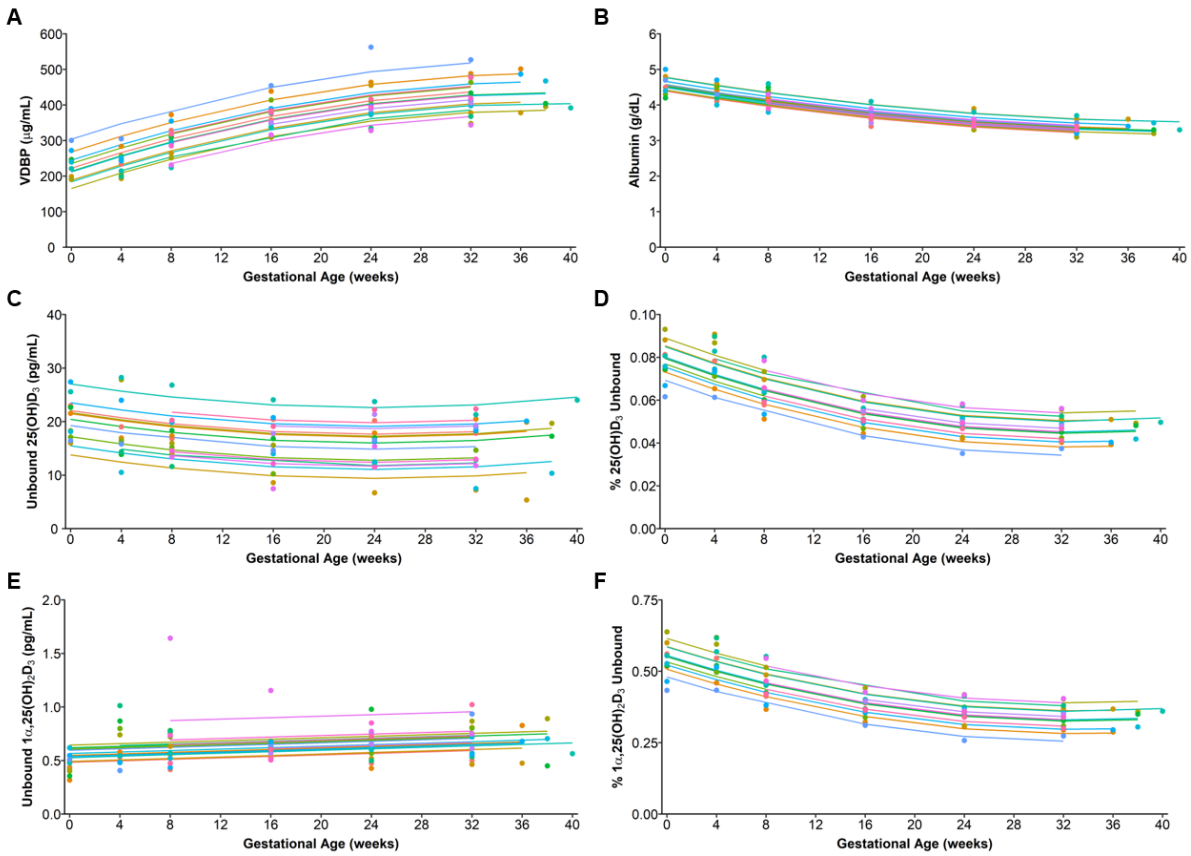

Figure 4.5: Mixed-effects model fits for A) vitamin D binding protein, B) albumin, C) unbound 25-hydroxyvitamin D_3, D) fraction unbound of 25-hydroxyvitamin D_3, E) unbound 1α,25-dihydroxyvitamin $D_3$and F) fraction unbound of 1α,25-dihydroxyvitamin D_3 from pre-pregnancy through the end of the third trimester. The circles are the observed plasma concentrations of each analyte. The lines represent the final mixed-effects model fits for each subject. Each color represents one subject.

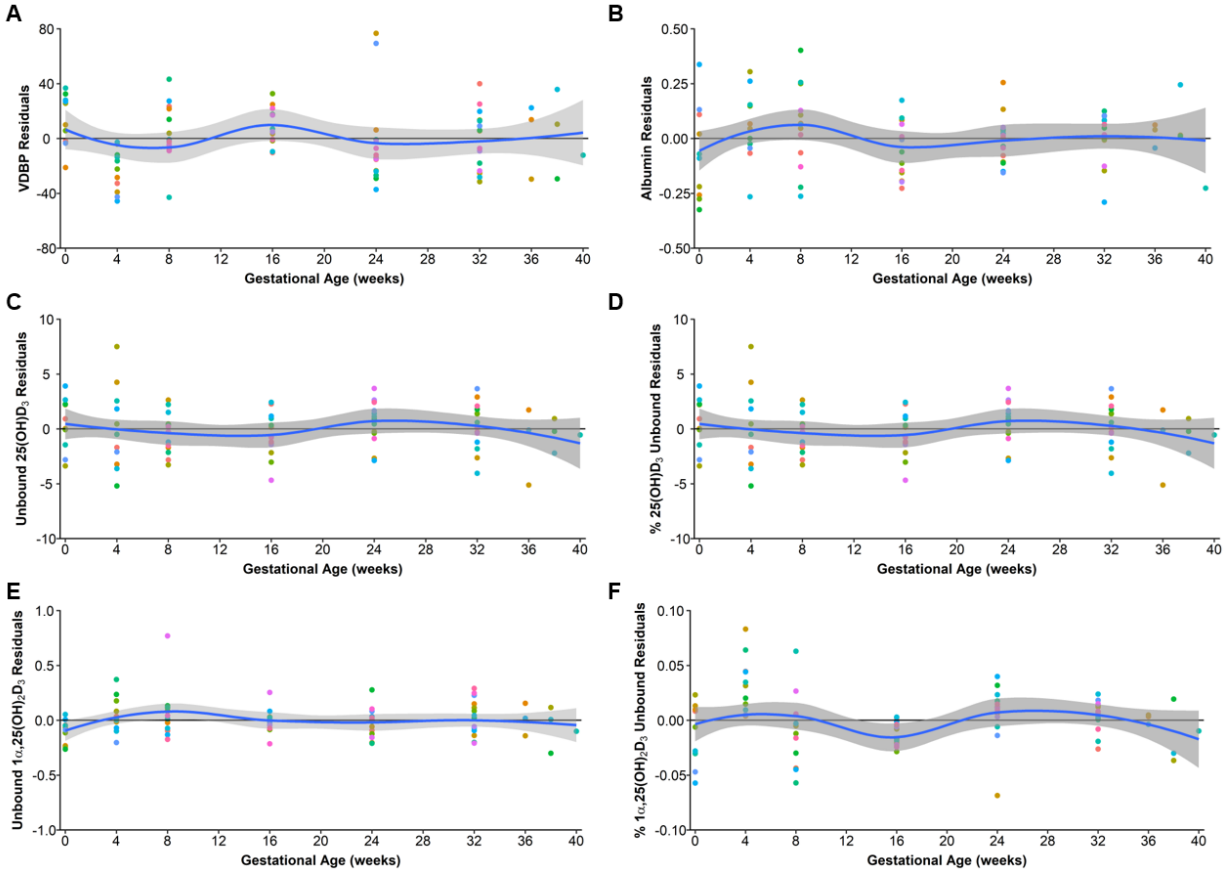

Figure 4.6: Residual plots for A) vitamin D binding protein, B) albumin, C) unbound 25-hydroxyvitamin D_3, D) fraction unbound of 25-hydroxyvitamin D_3 E) unbound 1α,25-dihydroxyvitamin D_3, and F) fraction unbound of 1α,25-dihydroxyvitamin D_3 models from pre-pregnancy through the end of the third trimester. The blue lines and shaded regions represent the mean and 95% confidence interval, respectively, of the loess line. Each point represents the residuals for individual data. Each color represents one subject.

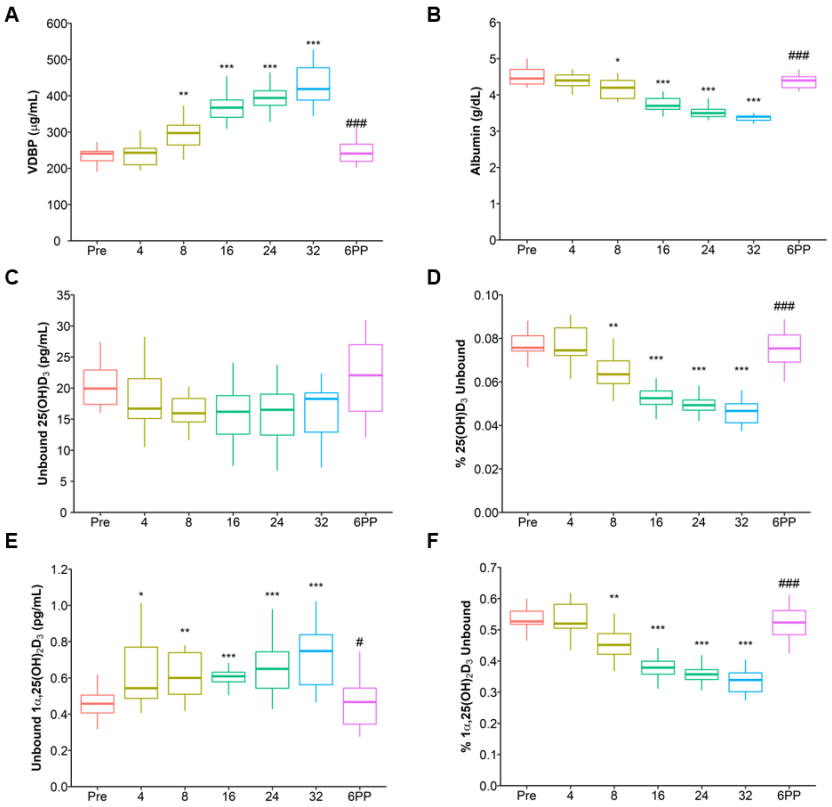

Figure 4.7: Observed concentrations of A) VDBP, B) albumin, C) unbound concentration 25(OH)D_3, D) percent unbound of 25(OH)D_3, E) unbound concentration of 1α,25$(OH)_2D_3$, and D) percent unbound of 1α,25$(OH)_2D_3$. For each boxplot, the center line represents the median. The boxed region is the 25th to 75th percentile (interquartile range). The whiskers are the largest value within 1.5 times interquartile range above the 75th percentile and smallest value within 1.5 times the interquartile range below the 25th percentile. Box colors: pre-pregnancy (red), first trimester (yellow), second trimester (green), third trimester (blue), and postpartum (purple).

Chapter 5.

A Semi-Mechanistic Modeling Approach Evaluating 4β,25-dihydroxyvitamin D_3 as a Potential Biomarker of CYP3A4 Inhibition and Induction

5.1. Abstract

Investigation of the risk of a new molecular entity (NME) to precipitate drug interactions is an essential part of drug development. To study drug-drug interactions in clinical development, NMEs are simultaneously administered with a probe substrate. The endogenous compound, 4β,25-dihydroxyvitamin D_3 (4β,25$(OH)_2D_3$), has been proposed as a biomarker of CYP3A4 activity. To ascertain the utility of 4β,25$(OH)_2D_3$ as an endogenous biomarker, we developed a semi-mechanistic pharmacokinetic-pharmacodynamic (PKPD) model to describe the pharmacokinetics of midazolam, clarithromycin, rifampin, 25-hydroxyvitamin D_3 and 4β,25$(OH)_2D_3$. Midazolam, clarithromycin, and rifampin models were developed using data from published clinical studies. The full PKPD model was fit to data from a healthy volunteer clinical study measuring the changes in 4β,25$(OH)_2D_3$ after treatment with water, 250 mg of clarithromycin twice a day, 600 mg of rifampin daily, or 250 mg of clarithromycin twice a day in combination with 600 mg of rifampin daily for 14 days. To assess the dynamic range of 4β,25$(OH)_2D_3$ as a biomarker, model simulations were conducted for a range of mechanism-based inhibitors (MBIs) and inducers. After 14 days of treatment with an MBI of CYP3A4, a 50%, 75% and 90% reduction in CYP3A4 activity resulted in an estimated 20%, 35% and 45% decrease in the 4β,25$(OH)_2D_3$ concentrations, respectively. After 14 days of treatment with a CYP3A4 inducer, a 1.2-, 2- and 5-fold induction of CYP3A4 activity was predicted to increase 4β,25$(OH)_2D_3$ levels by approximately 10%, 50%, and 200%, respectively. While this model supports that 4β,25$(OH)_2D_3$ has potential as a biomarker of CYP3A4 activity, additional data from clinical studies are required to verify the utility and dynamic range of 4β,25$(OH)_2D_3$.

5.2. Introduction

Characterizing the inhibitory and inductive effects of a new molecular entity (NME) is a critical step in drug development (1, 2). While *in vitro* and animal models are useful tools to investigate potential drug interactions, they frequently do not predict what will happen in human trials (3-5). Currently, drug-drug interactions (DDIs) in humans are assessed by the administration of a probe substrate, such as midazolam for cytochrome P450 3A4 (CYP3A4) activity, with and without the potential precipitant NME in development (6). However, traditional DDI studies require time, resources, and expose additional study participants, usually healthy volunteers, to an investigational drug. (7). Endogenous biomarkers of drug metabolizing enzyme or transporter activity may serve as a useful tool early in clinical development to evaluate the potential of an NME to cause a drug interaction (8).

One of the first reported CYP3A4 biomarkers is 6β-hydroxycortisol, a metabolite of cortisol formed solely by CYP3A4. The advantage of 6β-hydroxycortisol as a biomarker is that the 6β-hydroxycortisol-to-cortisol ratio can be measured in urine, which is a less invasive method of sample collection. Additionally, the short half-life of 6β-hydroxycortisol results in rapid changes in the 6β-hydroxycortisol-to-cortisol ratio in response to enzyme inhibition. One weakness of 6β-hydroxycortisol-to-cortisol ratio is the high degree of intra-individual variability due to diurnal variation in cortisol formation (9). As such, the timing and length of urine collection must be carefully considered when designing clinical studies (9).

A newer proposed endogenous biomarker of CYP3A4 activity is 4β-hydroxycholesterol (4β(OH)C) (2, 7). First reported in 2001, Bodin et al. found that 4β(OH)C concentrations in patients treated with carbamazepine, phenytoin, and phenobarbital (known inducers of cytochrome P450 activity) were 7-8-fold higher compared to 4β(OH)C concentrations in healthy volunteers (10). A screening with recombinant CYP enzymes determined that 4β(OH)C was formed from cholesterol by CYP3A4 (10). Additional studies have been conducted with a range of rifampin doses (10 – 500 mg per day QD) to show dose-dependent increases in 4β(OH)C

concentrations with increasing levels of induction after 14 days of rifampin treatment (11-14). Studies of competitive inhibition of CYP3A4 have shown that 4β(OH)C is also responsive to inhibition by ketoconazole after treatment for 2 weeks (15). Diczfalusy et al. estimated the half-life of 4β(OH)C as 17 days (16). The long half-life of 4β(OH)C is the likely cause of the low intra-individual variability in 4β(OH)C concentrations (2, 9, 16).

Semi-mechanistic and population pharmacokinetic/pharmacodynamic (PK/PD) models have been used to investigate the sensitivity and dynamic range of changes in 4β(OH)C concentrations relative to midazolam area under the concentration-time curve (AUC) (7, 17). Using a semi-mechanistic PK/PD model, Leil et al. predicted that after 14 days of treatment with a potent CYP3A4 inducer, the concentration of 4β-hydroxycholesterol would increase by more than 250% (7). Treatment with weak or moderate inducers would increase 4β(OH)C concentrations by approximately 20 to 100% and could be detected with an adequate sample size (7). 4β(OH)C is not as sensitive for CYP3A4 inhibition, as clinical data and modeling suggest that only strong competitive inhibition is detectable, due to the long half-life of $4\beta,25(OH)_2D_3$ and typical degree of variability in the analytical assay (7, 15). The predicted sample size that would be required to detect weak or moderate competitive inhibition (n = 50 to 80) is likely too large to be practical in Phase 1 clinical studies, which usually include 6 to 20 subjects per dosing group (7).

Recently, 4β,25-dihydroxyvitamin D_3 ($4\beta,25(OH)_2D_3$) has been proposed as a potential endogenous biomarker of CYP3A4 induction and inhibition based on *in vitro* data (18-20). Formed solely by CYP3A4, $4\beta,25(OH)_2D_3$ is a metabolite of 25-hydroxyvitamin D_3 ($25(OH)D_3$), the major circulating form of vitamin D_3 (20, 21). Both *in vitro* and *in vivo* studies showed that treatment with rifampin increased $4\beta,25(OH)_2D_3$ concentrations (18, 20). In a study with 23 healthy volunteers, plasma $4\beta,25(OH)_2D_3$ increased by 60% following oral treatment with 300 mg of rifampin QD for 6 days (20).

In a clinical study of deuterium-labeled d_6-25(OH)D_3 administered intravenously to healthy subjects, the half-life of deuterated 25(OH)D_3 was estimated as 21.9 ± 5.7 days (Simon Hsu, personal communication), similar to previous estimates (22, 23). The half-life of 4β,25$(OH)_2D_3$ is unknown. Wang et al. suggested that low circulating concentrations of 4β,25$(OH)_2D_3$ relative to 24,25-dihydroxyvitamin D_3 (24,25$(OH)_2D_3$), an inactive metabolite of 25(OH)D_3, might indicate that 4β,25$(OH)_2D_3$ elimination is more rapid than 24,25$(OH)_2D_3$ (24). However, in cases where the half-life of the metabolite is shorter than the parent molecule, metabolite elimination is limited by its formation, and the metabolite has the same apparent half-life as the parent (25). Similar to 4β(OH)C, the long half-life of 25(OH)D_3 likely makes it difficult to detect rapid changes in CYP3A4 activity caused by competitive inhibition following a single dose of the precipitant. However, prolonged treatment with a potent competitive inhibitor or a mechanism-based inhibitor (MBI) of CYP3A4, such as clarithromycin, may be detectable. Unlike competitive inhibitors, MBIs irreversibly bind to an enzyme rendering it inactive (26, 27). MBIs reduce the amount of functional enzyme until new enzyme can be synthesized and, therefore, decrease the metabolic clearance of the object drug (26, 27).

Before 4β,25$(OH)_2D_3$ can be applied in clinical drug development as a biomarker of CYP3A4 activity, the dynamic range of 4β,25$(OH)_2D_3$ to CYP3A4 inhibition and induction in comparison to CYP3A4 probe substrates should be well-understood. To assess the sensitivity of 4β,25$(OH)_2D_3$ compared to midazolam, a typical CYP3A4 probe, we developed a semi-mechanistic PK/PD model linking CYP3A4 enzyme levels, the effect of either rifampin or clarithromycin treatment, and the resulting PK of midazolam or 25(OH)D_3 and 4β,25$(OH)_2D_3$. The midazolam, clarithromycin, and rifampin PK/PD models were built using published models, *in vitro* parameters, and clinical PK data. Published midazolam concentration vs. time data were used to verify the effects of clarithromycin and rifampin on CYP3A4 activity. To build the 25(OH)D_3 and 4β,25$(OH)_2D_3$ portions of the model, we used data from a clinical study in which 25(OH)D_3 and 4β,25$(OH)_2D_3$ concentrations were monitored during 14 days of treatment with

clarithromycin, rifampin, or clarithromycin and rifampin in healthy volunteers. Non-linear mixed effects (NLME) modeling with first-order condition estimation (FOCE) was used to optimize PK/PD parameters in MATLAB Simbiology. After verification of the model, we conducted simulations to compare the ability of 4β,25(OH)$_2$D$_3$ vs. midazolam to detect changes in CYP3A4 activity.

5.3. Methods

5.3.1. Overview

A flow chart of model development is presented in Figure 5.1. Semi-mechanistic pharmacokinetic models were developed for midazolam, clarithromycin, rifampin, 25(OH)D$_3$ and 4β,25(OH)$_2$D$_3$. The structural models of midazolam, clarithromycin, and rifampin were adapted from previously published models (28, 29). The structural model of 4β,25(OH)$_2$D$_3$ was adapted from the Leil et al. model of 4β(OH)C-drug interactions (7). Pharmacokinetic parameters were optimized and verified using the data from published clinical studies in healthy adults for midazolam, rifampin and, clarithromycin. Details for the clinical data for the vitamin D model are presented in Section 5.3.3.10.

5.3.2. Simulated Study Population for Model Development

Due to the large proportion of clinical studies with all male participants, the simulated population for model development was built upon a normal distribution of a mean body weight (BW) of 75 ± 15 kg (20% coefficient of variation). Allometric scaling was applied to calculate hepatic blood flow (Q_H) from body weight (Equation 5.1) (30). Portal vein blood flow (Q_{PV}) and hepatic artery blood flow (Q_{HA}) were calculated as 75% and 25% of Q_H, respectively.

$$Q_H = 3.75 \cdot BW^{0.75} \quad (5.1)$$

5.3.3. General Model Development Strategy

Physiological parameters were obtained from literature values (28). Midazolam, clarithromycin, and rifampin models incorporated compartments representing the gut lumen, gut wall, portal vein, and liver. The volume of the gut lumen (V_{GL}) was equivalent to the volume of liquid administered with an oral dose of the drug (250 mL). The volume of the gut wall (V_{GW}, 250 mL), portal vein (V_{PV}, 70 mL), and liver (V_H, 2.8 L) were obtained from previously published semi-mechanistic models (listed in Table 5.1) (31). Additional clinical data such as urinary excretion and fraction unbound were incorporated into model development. Renal clearance of midazolam, clarithromycin, and rifampin (CL_R) were obtained from the mean of literature estimates.

Clearance from the liver (CL_H) was calculated using the well-stirred hepatic clearance model (Equation 5.2), where f_u is the fraction unbound of the drug and $CL_{int,H}$ is the intrinsic clearance in the liver. $CL_{int,H}$ was calculated by the Michaelis-Menten equation (Equation 5.3), where $V_{max,H}$ is the maximum metabolic capacity of the liver, K_m is the Michaelis-Menten constant (concentration at half of $V_{max,H}$), f_u is the fraction unbound and C_H is the total drug concentration in the liver.

$$\mathrm{CL_H} = \frac{\mathrm{Q_H} \cdot \mathrm{f_u} \cdot \mathrm{CL_{int,H}}}{\mathrm{Q_H} + \mathrm{f_u} \cdot \mathrm{CL_{int,H}}} \tag{5.2}$$

$$\mathrm{CL_{int,H}} = \frac{\mathrm{V_{max,H}}}{\mathrm{K_m} + \mathrm{f_u} \cdot \mathrm{C_H}} \tag{5.3}$$

It was assumed that oral doses of midazolam, clarithromycin, and rifampin were instantaneously available in the gut lumen. For midazolam and clarithromycin, metabolism in the gut wall was assumed to be solely by CYP3A4. Intrinsic clearance from the gut ($CL_{int,GW}$) was assumed to follow Michaelis-Menten kinetics, where $V_{max,GW}$ is the maximum metabolic capacity of the gut wall and C_{GW} is the total concentration of drug in the gut wall (Equation 5.4). The K_m is

the Michaelis-Menten constant in the gut and was assumed to be equivalent to the value in the liver.

$$CL_{int,GW} = \frac{V_{max,GW}}{K_m + C_{GW}} \quad (5.4)$$

Parameters were fit to the previously published clinical studies using nonlinear mixed-effects (NLME) modeling with first-order conditional estimation (FOCE). Intravenous, oral, and multiple dosing, when applicable, were fit simultaneously. The final model parameters are presented in Table 5.2.

5.3.3.1. Midazolam Model Development

The structural model for midazolam was previously described by Zhang et al., Chien et al., and Quinney et al. (1, 28, 32). Midazolam is best described by a two-compartment model (Figure 5.2). The mass balance equations are provided by Equations 5.5-5.10, where $A_{GL,MDZ}$, $A_{GW,MDZ}$, $A_{PV,MDZ}$, $A_{H,MDZ}$, $A_{C,MDZ}$, and $A_{P,MDZ}$ are the amounts of midazolam in the gut lumen, gut wall, portal vein, liver, central compartment, and peripheral compartment, respectively; $C_{GL,MDZ}$, $C_{GW,MDZ}$, $C_{PV,MDZ}$, $C_{H,MDZ}$, $C_{C,MDZ}$, and $C_{P,MDZ}$ are the concentrations of midazolam in the gut lumen, gut wall, portal vein, liver, central compartment, and peripheral compartment, respectively; $k_{a,MDZ}$ is the first-order absorption rate constant for midazolam; $CL_{int,GW,MDZ}$ is the intrinsic clearance of midazolam from the gut; $CL_{H,MDZ}$ is the hepatic clearance of midazolam; $CL_{PER,MDZ}$ is the clearance between the central and peripheral compartment of midazolam; and $CL_{R,MDZ}$ is the renal clearance of midazolam. The model assumed that all gut and hepatic metabolism was by CYP3A4.

$$\frac{dA_{GL,MDZ}}{dt} = -C_{GL,MDZ} \cdot V_{GL} \cdot K_{a,MDZ} \quad (5.5)$$

$$\frac{dA_{GW,MDZ}}{dt} = C_{GL,MDZ} \cdot V_{GL} \cdot K_{a,MDZ} - C_{GW,MDZ} \cdot V_{GW} \cdot K_{a,MDZ} - C_{GW,MDZ} \cdot CL_{int,GW,MDZ} \quad (5.6)$$

$$\frac{dA_{PV,MDZ}}{dt} = C_{GW,MDZ} \cdot V_{GW} \cdot k_{a,MDZ} + C_{C,MDZ} \cdot Q_{PV} - C_{PV,MDZ} \cdot Q_{PV} \quad (5.7)$$

$$\frac{dA_{H,MDZ}}{dt} = C_{PV,MDZ} \cdot Q_{PV} + C_{C,MDZ} \cdot Q_{HA} - C_{H,MDZ} \cdot Q_H - C_{H,MDZ} \cdot CL_{H,MDZ} \quad (5.8)$$

$$\frac{dA_{C,MDZ}}{dt} = C_{H,MDZ} \cdot Q_H + C_{P,MDZ} \cdot CL_{PER,MDZ} - C_{C,MDZ} \cdot Q_{HA} - C_{C,MDZ} \cdot Q_{PV} - C_{C,MDZ} \cdot CL_{R,MDZ} - C_{C,MDZ} \cdot CL_{PER,MDZ} \quad (5.9)$$

$$\frac{dA_{P,MDZ}}{dt} = C_{c,MDZ} \cdot CL_{PER,MDZ} - C_{P,MDZ} \cdot CL_{PER,MDZ} \quad (5.10)$$

5.3.3.2. Clarithromycin Model Development

The structural model for clarithromycin was previously described by Quinney et al. (28). Clarithromycin is best described by a one-compartment model (Figure 5.2). The mass balance equations are provided by Equations 5.11-5.15:

$$\frac{dA_{GL,CLAR}}{dt} = -C_{GL,CLAR} \cdot V_{GL} \cdot K_{a,CLAR} \quad (5.11)$$

$$\frac{dA_{GW,CLAR}}{dt} = C_{GL,CLAR} \cdot V_{GL} \cdot K_{a,CLAR} - C_{GW,CLAR} \cdot V_{GW} \cdot K_{a,CLAR} - C_{GW,CLAR} \cdot CL_{int,GW,CLAR} \quad (5.12)$$

$$\frac{dA_{PV,CLAR}}{dt} = C_{GW,CLAR} \cdot V_{GW} \cdot K_{a,CLAR} + C_{C,CLAR} \cdot Q_{PV} - C_{PV,CLAR} \cdot Q_{PV} \quad (5.13)$$

$$\frac{dA_{H,CLAR}}{dt} = C_{PV,CLAR} \cdot Q_{PV} + C_{C,CLAR} \cdot Q_{HA} - C_{H,CLAR} \cdot Q_H - C_{H,CLAR} \cdot CL_{H,CLAR} \quad (5.14)$$

$$\frac{dA_{C,CLAR}}{dt} = C_{H,CLAR} \cdot Q_H - C_{C,CLAR} \cdot Q_{HA} - C_{C,CLAR} \cdot Q_{PV} - C_{C,CLAR} \cdot CL_{R,CLAR} \quad (5.15)$$

where $A_{GL,CLAR}$, $A_{GW,CLAR}$, $A_{PV,CLAR}$, $A_{H,CLAR}$, and $A_{C,CLAR}$ are the amounts of clarithromycin in the gut lumen, gut wall, portal vein, liver and central compartment, respectively; $C_{GL,CLAR}$,

$C_{GW,CLAR}$, $C_{PV,CLAR}$, $C_{H,CLAR}$, and $C_{C,CLAR}$, are the concentrations of clarithromycin in the gut lumen, gut wall, portal vein, liver, and central compartment, respectively; $k_{a,CLAR}$ is the first-order absorption rate constant of clarithromycin; $CL_{int,GW,CLAR}$ is the intrinsic clearance of clarithromycin from the gut; $CL_{H,CLAR}$ is the hepatic clearance of clarithromycin; and $CL_{R,CLAR}$ is the renal clearance of clarithromycin. The model assumed that all gut and hepatic metabolism was by CYP3A4.

5.3.3.3. Rifampin Model Development

The structural model for rifampin was previously described by Smythe et al. (29). Rifampin is best described by a one-compartment model (Figure 5.2). Rifampin auto-induces its own metabolism by arylacetamide deacetylase (AADAC). The differential equation of the amount of AADAC is provided in equation 5.16, where $E_{H,AADAC}$ is the total concentration of AADAC in the liver, $R_{0,AADAC}$ is the rate of AADAC synthesis, $E_{max,AADAC}$ is the maximal increase in the production rate of AADAC, $EC_{50,AADAC}$ is concentration of rifampin required to achieve half of the $E_{max,AADAC,}$ $C_{H,RIF}$ is the concentration rifampin in the liver and $k_{deg,AADAC}$ is the degradation rate of AADAC. Values for $R_{0,AADAC}$ and $k_{deg,AADAC}$ were obtained from Smythe et al. and the $EC_{50,AADAC}$ was obtained from Hanke et al. (29, 33).

$$\frac{dE_{AADAC,H}}{dt} = R_{0,AADAC}\left(1 + \frac{E_{max,AADAC} \cdot C_{H,RIF}}{EC_{50,AADAC} + C_{H,RIF}}\right) - k_{deg,AADAC} \cdot E_{H,AADAC} \quad (5.16)$$

The mass balance equations for rifampin are provided by Equations 5:17-5.22:

$$\frac{dA_{GL,RIF}}{dt} = -C_{GL,RIF} \cdot V_{GL} \cdot K_{a,RIF} \quad (5.17)$$

$$\frac{dA_{TRANS,RIF}}{dt} = C_{GL,RIF} \cdot V_{GL} \cdot k_{a,RIF} - C_{TRANS,RIF} \cdot V_{TRANS} \cdot K_{a,RIF} \quad (5.18)$$

$$\frac{dA_{GW,RIF}}{dt} = C_{TRANS,RIF} \cdot V_{TRANS} \cdot K_{a,RIF} - C_{GW,RIF} \cdot V_{GW} \cdot K_{a,RIF} \quad (5.19)$$

$$\frac{dA_{PV,RIF}}{dt} = C_{GW,RIF} \cdot V_{GW} \cdot K_{a,RIF} + C_{C,RIF} \cdot Q_{PV} - C_{PV,RIF} \cdot Q_{PV} \quad (5.20)$$

$$\frac{dA_{H,RIF}}{dt} = C_{PV,RIF} \cdot Q_{PV} + C_{C,RIF} \cdot Q_{HA} - C_{H,RIF} \cdot Q_{H} - C_{H,RIF} \cdot CL_{H,RIF} \quad (5.21)$$

$$\frac{dA_{C,RIF}}{dt} = C_{H,RIF} \cdot Q_{H} - C_{C,RIF} \cdot Q_{HA} - C_{C,RIF} \cdot Q_{PV} - C_{C,RIF} \cdot CL_{R,RIF} \quad (5.22)$$

where $A_{GL,RIF}$, $A_{TRANS,RIF}$, $A_{GW,RIF}$, $A_{PV,RIF}$, $A_{H,RIF}$, and $A_{C,RIF}$ are the amounts of rifampin in the gut lumen, transit compartment, gut wall, portal vein, liver and central compartment, respectively; $C_{GL,RIF}$, $C_{TRANS,RIF}$, $C_{GW,RIF}$, $C_{PV,RIF}$, $C_{H,RIF}$, and $C_{C,RIF}$, are the concentrations of rifampin in the gut lumen, transit compartment, gut wall, portal vein, liver, and central compartment, respectively; $k_{a,RIF}$ is the first-order absorption rate constant of rifampin; $CL_{H,RIF}$ is the hepatic clearance of rifampin; and $CL_{R,RIF}$ is the renal clearance of rifampin. The model assumed that all hepatic metabolism of rifampin was by AADAC.

5.3.3.4. CYP3A4 enzyme model

In the absence of a CYP3A4 inducer or MBI, the amount of CYP3A4 in the liver and gut at steady-state ($E_{0,CYP3A4}$) is determined by the zero-order formation rate constant ($R_{0,CYP3A4}$) and the first-order degradation constant ($k_{deg,CYP3A4}$) (Equation 5.23). For CYP3A4, $E_{0,CYP3A4}$ represents the baseline normalized levels of CYP3A4, and the half-life ($t_{1/2,CYP3A4}$) was assumed to be 28 hours in the gut and the liver. The value of $k_{deg,CYP3A4}$ was calculated as $\ln(2)/t_{1/2,CYP3A4}$ and was estimated to be 0.025 hr^{-1} (28). At steady-state, the rate of formation is equal to the rate of degradation (Equation 5.24), thus the resulting $R_{0,CYP3A4}$ is 0.025 hr^{-1} when enzyme half-life is converted to a rate constant using the equation $R_{0,CYP3A4} = \ln(2)/t_{1/2,CYP3A4}$.

$$\frac{dE_{0,CYP3A4}}{dt} = R_{0,CYP3A4} - k_{deg,CYP3A4} \cdot E_{0,CYP3A4} \quad (5.23)$$

$$R_{0,CYP3A4} = k_{deg,CYP3A4} \cdot E_{0,CYP3A4} \quad (5.24)$$

5.3.3.5. Incorporating Competitive Inhibition of CYP3A4

Clarithromycin and rifampin are weak competitive inhibitors of CYP3A4, affecting the intrinsic clearance of both midazolam and clarithromycin. Competitive inhibition by clarithromycin and rifampin were incorporated into the intrinsic clearance equations by replacing the K_m with the apparent K_m (Equation 5.25 and 5.26), where $C_{CLAR,GW}$ and $C_{CLAR,H}$ are the concentrations of clarithromycin in the gut wall and liver, respectively; $C_{RIF,GW}$ and $C_{RIF,H}$ are the concentrations of rifampin in the gut wall and liver, respectively; and $K_{i,CLAR}$ and $K_{i,RIF}$ are the reversible inhibitory constants of clarithromycin and rifampin for CYP3A4, respectively. The K_i values were obtained from published *in vitro* studies and were assumed to be equivalent in the gut wall and the liver (28). C_{GW} and C_H are the gut wall and hepatic concentrations of the substrate (e.g., midazolam, rifampin, clarithromycin or 25(OH)D_3).

$$CL_{int,GW} = \frac{V_{max,GW}}{K_m \cdot \left(1 + \frac{C_{GW,CLAR}}{K_{i,CLAR}} + \frac{C_{GW,RIF}}{K_{i,RIF}}\right) + C_{GW}} \quad (5.25)$$

$$CL_{int,H} = \frac{V_{max,H}}{K_m \cdot \left(1 + \frac{C_{H,CLAR}}{K_{i,CLAR}} + \frac{C_{H,RIF}}{K_{i,RIF}}\right) + C_H} \quad (5.26)$$

5.3.3.6. Incorporating Mechanism-Based Inactivation of CYP3A4

Due to mechanism-based inhibition by clarithromycin, the observed degradation rate of CYP3A4 is increased after clarithromycin administration. The resulting $k_{deg,CYP3A4,obs}$, the observed degradation rate of CYP3A4 in the presence of clarithromycin, is calculated by Equation 5.27, where k_{inact} is the maximum rate of inactivation the inhibition constant K_I is the clarithromycin concentration at 50% of k_{inact}, and C_{CLAR} represents the concentrations of clarithromycin in the gut wall or liver. The values of k_{inact} and K_I were obtained from Quinney et al. (28).

$$k_{deg,CYP3A4,obs} = k_{deg,CYP3A4} + \frac{k_{inact} \cdot C_{CLAR}}{K_I + C_{CLAR}} \quad (5.27)$$

The differential equations of CYP3A4 expression in the gut wall in the presence of clarithromycin are presented in Equations 5.28 and 5.29.

$$\frac{dE_{GW,CYP3A4}}{dt} = R_{0,CYP3A4} - \left(k_{deg,CYP3A4} - \frac{k_{inact} \cdot C_{GW,CLAR}}{K_I + C_{GW,CLAR}}\right) \cdot E_{GW,CYP3A4} \quad (5.28)$$

$$\frac{dE_{H,CYP3A4}}{dt} = R_{0,CYP3A4} - \left(k_{deg,CYP3A4} - \frac{k_{inact} \cdot C_{H,CLAR}}{K_I + C_{H,CLAR}}\right) \cdot E_{H,CYP3A4} \quad (5.29)$$

5.3.3.7. Incorporating CYP3A4 Induction

In the presence of the CYP3A4 inducer, rifampin, the synthesis rate of CYP3A4 is increased. The resulting $R_{0,CYP3A4,obs}$, the observed synthesis rate of CYP3A4, in the presence of rifampin is calculated by Equation 5.30; where $E_{max,CYP3A4}$ is the maximum increase in the enzyme synthesis rate, $EC_{50,CYP3A4}$ is the concentration of rifampin at which half of the $E_{max,CYP3A4}$ is reached, and C_{RIF} is the concentration of rifampin in the gut wall or liver. The $EC_{50,CYP3A4}$ was obtained from published *in vitro* studies and were assumed to be equivalent in the gut wall and the liver (33). The estimate for $E_{max,CYP3A}$ was optimized during model development.

$$R_{0,CYP3A4,obs} = R_{0,CYP3A4} \cdot \left(1 + \frac{E_{max,CYP3A4} \cdot C_{RIF}}{EC_{50,CYP3A4} + C_{RIF}}\right) \quad 5.30$$

The differential equations for CYP3A4 expression in the gut wall and liver in the presence of rifampin are presented in Equations 5.31 and 5.32, respectively.

$$\frac{dE_{GW,CYP3A4}}{dt} = R_{0,CYP3A4} \cdot \left(1 + \frac{E_{max,CYP3A4} \cdot C_{GW,RIF}}{EC_{50,CYP3A4} + C_{GW,RIF}}\right) - k_{deg,CYP3A4} \cdot E_{GW,CYP3A4} \quad (5.31)$$

$$\frac{dE_{H,CYP3A4}}{dt} = R_{0,CYP3A4} \cdot \left(1 + \frac{E_{max,CYP3A4} \cdot C_{H,RIF}}{EC_{50,CYP3A4} + C_{H,RIF}}\right) - k_{deg,CYP3A4} \cdot E_{H,CYP3A4,} \quad (5.31)$$

5.3.3.8. Verification of Midazolam, Clarithromycin, and Rifampin Models

Published clinical studies were used to qualitatively and quantitatively evaluate the predictive performance of the midazolam, clarithromycin, and rifampin models. Simulations were performed using MATLAB SimBiology model analyzer (version 2019B), incorporating the dosing data for each study. Each model was evaluated by comparing observed and predicted concentration-time profiles, area under the concentration-time curve, and maximum plasma concentration (C_{max}) values. The PKNCA package in R was used to estimate AUC from the simulated data (version 0.9.1) (34). To quantify the predictive performance of the model the geometric mean fold error (GMFE) was calculated using Equation 5.33:

$$\mathrm{GMFE} = 10^{\left(\frac{\sum \log_{10}\left({}^{\text{pred PK parameter}}/_{\text{obs PK parameter}}\right)}{\mathrm{n}}\right)} \tag{5.33}$$

where pred PK parameter is the model predicted estimate of AUC or C_{max}, obs PK parameter is the reported estimate of AUC or C_{max}, and n is the number of simulations for each drug.

5.3.3.9. Assessment of DDI Predictions

The DDI model performance was evaluated by a comparison of the plasma-concentration time curve of the midazolam alone and in combination with clarithromycin or rifampin. The DDI ratio of the AUC and C_{max} of midazolam were calculated by Equation 5.34 and 5.35. To quantitatively assess the predictive performance of the DDI, the GMFE of the AUC and C_{max} DDI ratios were calculated according the Equation 5.33.

$$\text{AUC DDI ratio} = \frac{\mathrm{AUC}_{\text{MDZ DDI}}}{\mathrm{AUC}_{\text{MDZ alone}}} \tag{5.34}$$

$$\mathrm{C}_{\max}\ \text{DDI ratio} = \frac{\mathrm{C}_{\max,\text{MDZ DDI}}}{\mathrm{C}_{\max,\text{MDZ alone}}} \tag{5.35}$$

5.3.3.10. Vitamin D-Drug Interaction Clinical Study Design

Healthy volunteers were recruited to participate in a randomized open-label clinical study to determine if vitamin D and bone mineral homeostasis are sensitive to changes in intestinal and hepatic CYP3A4 activity caused by rifampin, grapefruit juice and/or clarithromycin treatment. Selected data from the water (200 mL QD), rifampin (600 mg QD), clarithromycin (250 mg BID), and rifampin + clarithromycin (600 mg QD and 250 mg BID, respectively) were used to develop the vitamin D model for this chapter. Three baseline samples were collected on Study Days 1, 4, and 7. Participants received one of the treatments on Days 8 through 21 (samples collected on Study Days 9, 12, 15, 18, 21). Subjects were followed through day 35 (samples collected on Study Days 23, 25, 28, 31, 35). The data used in the PK/PD model included 710 4β,25(OH)$_2$D$_3$ and 25(OH)D$_3$ concentrations.

5.3.3.11. 25-hydroxyvitamin D$_3$ and 4β,25-dihydroxyvitamin D$_3$ Model Development

The proposed model for 25(OH)D$_3$ and 4β,25(OH)$_2$D$_3$ is shown in Figure 5.2. The synthesis rate of 25(OH)D$_3$ ($k_{syn,25(OH)D_3}$) was assumed to be zero-order and constant throughout the study. The elimination of 25(OH)D$_3$ by all pathways except for 4β,25(OH)$_2$D$_3$ were summed as the elimination rate constant ($k_{other,25(OH)D_3}$). The volume of distribution of 25(OH)D$_3$ ($V_{25(OH)D_3}$) was estimated from a clinical study of the deuterium-labeled 25(OH)D$_3$ (Chapter 3). The volume of distribution of 4β,25(OH)$_2$D$_3$ ($V_{4\beta,25(OH)_2D_3}$) was assumed to be equal to that of 25(OH)D$_3$. The formation of 4β,25(OH)$_2$D$_3$ ($CL_{int,4\beta,25(OH)_2D_3}$) was assumed to follow Michaelis-Menten kinetics and incorporated the changes in hepatic CYP3A4 and competitive inhibition by clarithromycin and rifampin (Equation 5.36), where $V_{max,4\beta,25(OH)_2D_3}$ is the maximum metabolic capacity of hepatic CYP3A4, $K_{m,25(OH)D_3}$ is the Michaelis-Menten constant (concentration at half of $V_{max,H}$), $f_{u,25(OH)D_3}$ is the fraction unbound of 25(OH)D$_3$ and $C_{25(OH)D_3}$ is serum concentration of 25(OH)D$_3$. The elimination of 4β,25(OH)$_2$D$_3$ ($k_{deg,\ 4\beta,25(OH)_2D_3}$) was assumed to follow first-order kinetics. The

mass balance equations are provided by Equations 5.37 and 5.38. The model was fit to the data using MATLAB SimBiology (2019B) with FOCE estimation and 1000 iterations.

$$CL_{int,4\beta,25(OH)_2D_3} = \frac{V_{max,4\beta,25(OH)_2D_3} \cdot E_{H,CYP3A4,}}{K_{m,25(OH)D_3} \cdot \left(1 + \frac{f_{u,CLAR} \cdot C_{H,CLAR}}{K_{i,CLAR}} + \frac{f_{u,RIF} \cdot C_{H,RIF}}{K_{i,RIF}}\right) + f_{u,25(OH)D_3} \cdot C_{25(OH)D_3}} \quad (5.36)$$

$$\frac{dA_{25(OH)D_3}}{dt} = k_{syn,25(OH)D_3} - C_{25(OH)D_3} \cdot V_{25(OH)D_3} \cdot k_{other,25(OH)D_3} - C_{25(OH)D_3} \cdot CL_{int,4\beta,25(OH)_2D_3} \quad (5.37)$$

$$\frac{dA_{,4\beta,25(OH)_2D_3}}{dt} = C_{25(OH)D_3} \cdot CL_{int,4\beta,25D3} - C_{,4\beta,25(OH)_2D_3} \cdot k_{deg,4\beta,25(OH)_2D_3} \quad (5.38)$$

5.3.3.12. Evaluation of the PK/PD Model for 4β,25-dihydroxyvitamin D_3

The predictive performance of the model was assessed by generating a virtual population of 1,000 iterations built from individuals with a normal distribution of body weight (75 ± 15 kg) and a log normal distribution of $k_{syn,25(OH)D_3}$, $V_{max,4\beta,25(OH)_2D_3}$, $k_{deg,4\beta,25(OH)_2D_3}$, 25(OH)$D_3$, and 4β,25(OH)$_2D_3$. The virtual population and simulations were generated using MATLAB SimBiology and compared to the observed data.

5.3.4. Simulations of Dynamic Range of DDIs with 4β,25-dihydroxyvitamin D_3 vs. Midazolam

Simulations to compare the dynamic range of 4β,25(OH)$_2D_3$ and MDZ were performed by assuming 14 days of treatment either with an MBI or inducer of CYP3A4. A total of 250 MBI simulations with theoretical inhibitors with k_{inact} ranging from 0 to 10 hr^{-1} were simulated. The MBIs were administered as 250 mg BID with the mean PK parameters of clarithromycin with no competitive inhibition of CYP3A4. A total of 250 simulations with theoretical increase of 0-100-fold in CYP3A4 activity using the mean PK parameters were simulated. The inducers were administered as 600 mg QD with the mean PK parameters of rifampin and without competitive inhibition of CYP3A4. Simulations were conducted in MATLAB SimBiology.

5.4. Results

5.4.1. Model Development and Verification

A schematic of the non-linear mixed effects PK/PD models for CYP3A4 mediated drug interactions are shown in Figure 5.2. The models describe the pharmacokinetics of midazolam, clarithromycin, rifampin, $25(OH)D_3$, and $4\beta,25(OH)_2D_3$, and the inhibition and induction of CYP3A4 activity by clarithromycin and rifampin, respectively.

The PK models of midazolam, clarithromycin, and rifampin were developed using published clinical studies. Midazolam, clarithromycin, and rifampin models were optimized by fitting the structural model to a training data set compiled from published clinical studies. The final midazolam, clarithromycin, and rifampin model parameters are presented in Table 5.1. The model fit was evaluated quantitatively by simulating each dosing regimen and comparing the simulated AUC and C_{max} to reported values. Qualitative assessment of models was performed by visual inspection of model fit to published concentration vs. time curves and the geometric mean fold error (GMFE) was used to provide a quantitative assessment of the predictive performance of the model.

The midazolam model parameters were optimized using 9 dosing regimens (4 IV, 5 PO). The parameters were verified using 11 dosing regimens (6 IV, 5 PO) with IV and oral doses ranging from 0.4 to 5 mg and 1 to 7.5 mg, respectively. A summary of each dosing regimen is presented in Table 5.3. The visual check of the simulations following IV and oral dosing is presented in Figure 5.3 and Figure 5.4, respectively. For the verification datasets, IV data were better described by the proposed model compared to oral data. However, all of the predicted AUCs for IV and oral dosing were within 2-fold of the observed values. The GMFE of AUC and C_{max} for the verification data were 1.11 and 1.01, respectively.

The clarithromycin model parameters were optimized using 11 dosing regimens (1 IV, 10 PO). Multiple dosing regimens with 250 mg and 500 mg clarithromycin were also included in the

training dataset. The model was verified using 9 oral dosing regimens (ranging from 200 to 800 mg) and included data after multiple dosing of 250 and 500 mg twice daily. A summary of each dosing regimen is presented in Table 5.4. The visual check of the simulations is presented in Figure 5.5. The model adequately described the pharmacokinetics of clarithromycin after single and multiple dosing. All simulated AUC and C_{max} were within 2-fold of the observed values. The predicted AUC and C_{max} for the verification dataset were both slightly high with GMFEs of 1.32 and 1.10, respectively.

The rifampin model parameters were optimized using 7 training dosing regimens (3 IV, 4 PO), including data from one multiple dosing study. The parameters were verified using 8 dosing regimens (3 IV, 5 PO) with IV doses ranging from 600 to 1200 mg and an oral dose of 600 mg. The verification data included two multiple dosing studies of 600 mg of rifampin QD for up to 10 days. A summary of each dosing regimen is presented in Table 5.5. The visual check of simulations following IV and oral dosing is presented in Figure 5.6. Although all of the simulated AUC and C_{max} values were within 2-fold of the observed values, the AUC and C_{max} values were underpredicted with the calculated GFME of 0.79 and 0.94, respectively.

The effects of clarithromycin and rifampin on CYP3A4 activity were verified by comparing the simulated midazolam-clarithromycin and midazolam-rifampin drug interactions to published data. The midazolam-clarithromycin interaction was well-predicted with the predicted-to-observed change in midazolam AUC within 2-fold for all 3 studies. The midazolam-rifampin prediction performed better for orally dosed midazolam compared to iv midazolam. A summary of the drug-drug interaction verification results is presented in Table 5.6.

The PK model of 4β,25$(OH)_2D_3$ formation from 25$(OH)D_3$ was fit to data collected from subjects administered water, clarithromycin, rifampin, or clarithromycin and rifampin in combination. All study arms were fit simultaneously. Initial estimates of kinetic parameters were obtained using published *in vitro* data and initial estimates for 25$(OH)D_3$ pharmacokinetic parameters were obtained from subjects administered deuterium-labeled 25$(OH)D_3$. The volume

of distribution of 4β,25(OH)$_2$D$_3$ was assumed to be the same as 25(OH)D$_3$. Additionally, it was assumed that non-4β,25(OH)$_2$D$_3$ clearance pathways of 25(OH)D$_3$ were not affected by clarithromycin or rifampin administration. Due to limited *in vivo* variability data, the pharmacokinetics of midazolam, clarithromycin, rifampin, and change in CYP3A4 enzyme activity were assumed to be identical for all subjects. The objective function and fixed effects parameters converged and reached stationary values based on review of the caterpillar plots (data not shown). The final model parameter values are presented in Table 5.2. The error model was assessed by the plots of the residuals and Q-Q plots (data not shown). The residuals were equally distributed and showed no bias to high or low concentrations of 25(OH)D$_3$ and 4β,25(OH)$_2$D$_3$ (data not shown). The model estimate of the initial concentration of 25(OH)D$_3$ and 4β,25(OH)$_2$D$_3$ ($C_{0,25(OH)D_3}$ and $C_{0,4\beta,25(OH)_2D_3}$) were 20.0 ng/mL (95% CI: 18.5, 21.7 ng/mL) and 59.3 pg/mL (95% CI 54.5, 64.6 ng/mL), respectively, which are similar to the observed values of 21.2 ± 8.23 ng/mL and 62.8 ± 31.3 pg/mL, respectively. The synthesis rate of 25(OH)D$_3$, assuming a 21.9 day half-life of 25(OH)D$_3$, was estimated to be 6.44 µg/day (95% CI: 5.85, 7.08 µg/day). The estimated half-life of 4β,25(OH)$_2$D$_3$ was 11.8 days (95% CI: 10.4, 13.3 days) which is shorter than the assumed half-life of 25(OH)D$_3$.

5.4.2. Evaluation of the PK/PD model for 4β,25-dihydroxyvitamin D$_3$

The predictive performance of the final PK/PD model was evaluated by simulating the treatment of 1,000 virtual subjects with water, clarithromycin, rifampin, or clarithromycin and rifampin in combination for 14 days (Figure 5.7). The predicted 4β,25(OH)$_2$D$_3$ concentration-time profiles and the observed values are shown in Figure 5.8. The simulated 4β,25(OH)$_2$D$_3$ concentrations adequately described the observed clinical data. Treatment with water did not affect 4β,25(OH)$_2$D$_3$ concentrations. The fit of the model following inhibition by clarithromycin appeared to be adequate. While the increasing 4β,25(OH)$_2$D$_3$ concentrations with rifampin treatment was well captured, the rate at which 4β,25(OH)$_2$D$_3$ concentrations returned to

baseline appear to be underestimated. A similar trend was observed for the clarithromycin and rifampin combination treatment. Figure 5.8 shows the predicted change in CYP3A4 activity for each of the treatment arms. For the clarithromycin and rifampin combination, induction of hepatic CYP3A4 outweighed clarithromycin inhibition, though the fold-induction was less than that observed with rifampin treatment alone. In contrast to hepatic CYP3A4, intestinal CYP3A4 activity was reduced with the clarithromycin and rifampin combination.

5.4.3. Evaluation of the Dynamic Range of 4β,25-dihydroxyvitamin D_3 Compared to Midazolam

Simulations using the final semi-mechanistic PK/PD model of CYP3A4 activity were conducted to characterize the dynamic range of 4β,25$(OH)_2D_3$ as a potential biomarker of CYP3A4 activity. Changes in midazolam AUC were simulated for comparison. Figure 5.9A shows the fold-change in midazolam AUC relative to the percent decrease in 4β,25$(OH)_2D_3$ concentrations after 14 days of treatment with theoretical mechanism-based inhibitors with varying k_{inact} values. A 50% decrease in hepatic CYP3A4 activity was predicted to decrease 4β,25$(OH)_2D_3$ by 21% and increase IV midazolam AUC by 60%. Similar to what was observed following 14 days of treatment with clarithromycin, a 33% decrease in 4β,25$(OH)_2D_3$ corresponded to a 2.8-fold increase in midazolam AUC. When CYP3A4 activity was decreased to 10% of baseline, 4β,25$(OH)_2D_3$ was predicted to decrease by 46%, while the midazolam AUC increased by 5.4-fold. While the midazolam AUC would continue to increase with decreasing CYP3A4 activity, simulations suggested that 4β,25$(OH)_2D_3$ concentrations would not decrease by more than 60% of baseline values.

Figure 5.9B shows the change in midazolam AUC relative to the percent increase in the 4β,25$(OH)_2D_3$ concentrations after 14 days of treatment with theoretical inducers with varying CYP3A4 induction potential. For weak inducers, 4β,25$(OH)_2D_3$ appeared to be equally sensitive as midazolam. A 20% increase in CYP3A4 activity resulted in a 10% increase in 4β,25$(OH)_2D_3$

and 9% decrease in midazolam AUC. With a 2-fold increase in CYP3A4 activity, 4β,25$(OH)_2D_3$ concentrations increased by 53%, whereas midazolam AUC decreased by 28%. Following treatment with strong inducers where CYP3A4 activity increased by more than 5-fold (e.g., 600 mg of rifampin), predicted 4β,25$(OH)_2D_3$ concentrations increased by 2-fold, while predicted midazolam AUC decreased by 44%. While the decrease in midazolam AUC did not decreased beyond 60%, 4β,25$(OH)_2D_3$ concentrations are expected to continue to rise with greater CYP3A4 induction.

5.5. Discussion

We developed a semi-mechanistic PK/PD model to evaluate the utility of 4β,25$(OH)_2D_3$ as an endogenous biomarker of CYP3A4 activity in clinical studies. The semi-mechanistic PK/PD model was developed using previously published models and clinical studies for clarithromycin and rifampin. Midazolam was incorporated into the model to verify the inhibitory and inductive effects of clarithromycin and rifampin, respectively, before fitting the model to study data. Additionally, the midazolam model was used to compare the change in 4β,25$(OH)_2D_3$ relative to a “gold standard” probe of CYP3A4 activity. The semi-mechanistic PK/PD model was fit to 25$(OH)D_3$ and 4β,25$(OH)_2D_3$ data from a clinical study in which clarithromycin, rifampin, or clarithromycin and rifampin in combination were given to healthy volunteers.

Due to the limited knowledge about the pharmacokinetics of 25$(OH)D_3$ and 4β,25$(OH)_2D_3$, many assumptions were incorporated during model development. The structural model of 25$(OH)D_3$ metabolism assumed that 25$(OH)D_3$ synthesis was constant throughout the study (i.e., endogenous formation and dietary intake of vitamin D were constant) and that 25$(OH)D_3$ formation was not affected by treatment with an inducer or inhibitor. *In vitro* evidence supports that 25$(OH)D_3$ synthesis by CYP27A1 and CYP2R1 from vitamin D_3 (35, 36), is unaffected by treatment with rifampin (20, 37). In hepatocytes treated with rifampin, no induction

of CYP27A1 or CYP2R1 was observed (20). Furthermore, no 25(OH)D_3 was detected after incubating vitamin D_3 with recombinant CYP3A4 (37). As described in Chapter 4 and other clinical studies, the unbound concentration of 25(OH)D_3 is very sensitive to changes in the concentration of the plasma proteins albumin and vitamin D binding protein (38). Monitoring serum albumin and vitamin D binding protein should be considered when the binding proteins are affected by drug treatment.

Additionally, our model assumed that the formation of 4β,25$(OH)_2D_3$ was the only metabolic pathway altered by treatment with clarithromycin and rifampin. In the clinical study, 24,25$(OH)_2D_3$ concentrations decreased by ~35% after treatment with rifampin and concentrations of other conjugated metabolites of 25(OH)D_3 (i.e., 25-hydroxyvitamin D_3-3-sulfate and 25-hydroxyvitamin D_3-3-glucuronide) were unaffected by treatment with clarithromycin or rifampin (data not shown). Thus, although one metabolic pathway (formation of 24,25$(OH)_2D_3$) may be slightly affected, the overall $CL_{other,25(OH)D_3}$ is likely to be unchanged. Finally, our model assumed that treatment with clarithromycin and rifampin did not alter the catabolism of 4β,25$(OH)_2D_3$. 4β,25$(OH)_2D_3$ is eliminated primarily through glucuronidation, however the uridine 5'-diphospho-glucuronosyltransferase (UGT) isoforms responsible have not yet been identified (24).

An additional impediment to the use of 4β,25$(OH)_2D_3$ as a biomarker is the laborious method of quantification. The assay requires multiple solid phase extraction steps and extensive mass spectrometry resources (Chapter 2). The mass spectrometer must have sufficient sensitivity to detect picomolar concentrations of 4β,25$(OH)_2D_3$ as well as being able to quantify 25(OH)D_3 which has 1000-fold higher concentrations. Higher throughput quantification would be necessary for 4β,25$(OH)_2D_3$ to be a practical endogenous biomarker of hepatic CYP3A4 activity.

Following treatment with strong MBIs, we predicted that once CYP3A4 activity falls below 50% of baseline, 4β,25$(OH)_2D_3$ concentrations would decrease by ~20%. Given the technical challenges of detecting 4β,25$(OH)_2D_3$ concentrations, smaller changes in CYP3A4 activity are unlikely to be detectable using 4β,25$(OH)_2D_3$ as a biomarker due to the low abundance of 4β,25$(OH)_2D_3$ (pg/mL) and the limit of sensitivity of the mass spectrometric assay. A 90% decrease in hepatic CYP3A4 enzyme activity would decrease 4β,25$(OH)_2D_3$ concentrations by 46%. For CYP3A4 induction, 4β,25$(OH)_2D_3$ is likely able to detect moderate and strong inducers. We predicted that 4β,25$(OH)_2D_3$ concentrations would increase by ~10% and ~55% for a 1.2-fold and 2-fold increase in CYP3A4 enzyme activity, respectively. A 5-fold increase in CYP3A4 activity, similar to what is observed with rifampin, would result in a 203% increase in 4β,25$(OH)_2D_3$ concentrations. The ability to detect a 10% change in 4β,25$(OH)_2D_3$ concentrations would be dependent upon the ability of the assay to quantify such a minor change.

The predicted changes in 4β,25$(OH)_2D_3$ concentrations after induction are similar to those predicted for 4β(OH)C (7). The cholesterol-4β(OH)C model by Leil et al. estimated that a 1.2- and 4.6-fold increase in CYP3A4 enzyme activity would result in a 10% and 206% increase in 4β(OH)C concentrations, respectively (7). There are no reports of clinical studies in which the concentration of 4β(OH)C was measured during or after treatment with an MBI. However, Leil et al. proposed that prolonged treatment with a competitive inhibitor could be detected by 4β(OH)C, but the study samples size required would be much larger than those necessary to detect induction (7).

A major limitation of our data is that clarithromycin and rifampin concentrations were not measured in the clinical study. With measured clarithromycin and rifampin concentrations, the model could account for the interindividual variability in the PK of these drugs and refine the parameter estimates for 25$(OH)D_3$ and 4β,25$(OH)_2D_3$ kinetics. The PK/PD model described herein does not allow for interindividual variability in the PK of clarithromycin and rifampin, which

would increase the uncertainty in our estimates of the PK parameters of $25(OH)D_3$ and $4\beta,25(OH)_2D_3$. It may be possible to improve the fit of the model through the incorporation of additional metabolites of $25(OH)D_3$, especially those which change during drug treatment, such as $24,25(OH)_2D_3$.

Compared to 4β(OH)C, the development of $4\beta,25(OH)_2D_3$ as a biomarker of CYP3A4 activity is in its infancy. Many steps must be taken before $4\beta,25(OH)_2D_3$ can be implemented as a biomarker to screen for drug interactions during early clinical studies of NMEs. First, the dynamic range of $4\beta,25(OH)_2D_3$ should be assessed in clinical studies to verify and improve the model predictions. For example, studies should be conducted by treating healthy subjects with a range of rifampin doses for 14 days as was done for 4β(OH)C (11-14). As data regarding the effect of MBIs are limited, a clinical study in which weak or moderate MBIs of CYP3A4 are administered would provide more confidence in the dynamic range of $4\beta,25(OH)_2D_3$ at lower levels of inhibition. If $4\beta,25(OH)_2D_3$ is to be implemented in crossover studies, the half-life of $4\beta,25(OH)_2D_3$ must be known to ensure baseline is reached prior to beginning the next stage of the study. Given the apparent 11.8 day half-life of $4\beta,25(OH)_2D_3$, it is unlikely that it can be used to detect single dose inhibition of CYP3A4. Finally, more data need to be collected to understand the factors which contribute to intra- and inter-subject variability in $4\beta,25(OH)_2D_3$ formation and elimination.

AstraZeneca has incorporated 4β(OH)C into their drug development program, specifically by including 4β(OH)C as a biomarker in multiple ascending dose studies (11). If the change in 4β(OH)C concentrations at the highest dose level is greater than 25%, samples from all dosing levels are analyzed to establish a dose-response relationship (11). In combination with *in vitro* studies, these data will prompt the conduct of a traditional DDI clinical study with midazolam (11). While 4β(OH)C is not approved as a biomarker by regulatory agencies, AstraZeneca states that 4β(OH)C is an integral part of their drug development strategy. The

development of similar guidelines for 4β,25(OH)$_2$D$_3$ would be necessary, prior to implementation in clinical studies.

5.6. Conclusion

Recently, there has been interest in developing 4β,25(OH)$_2$D$_3$ as an endogenous biomarker of CYP3A4 activity. In order to investigate the utility of 4β,25(OH)$_2$D$_3$, we developed a semi-mechanistic PK/PD model of midazolam, clarithromycin, rifampin, 25(OH)D$_3$, and 4β,25(OH)$_2$D$_3$. Using the final model, we simulated the predicted change in 4β,25(OH)$_2$D$_3$ concentration for a range of theoretical MBIs and inducers of CYP3A4 activity. After 14 days of treatment with an MBI of CYP3A4, a 50%, 75% and 90% reduction in CYP3A4 activity results in an estimated 20%, 35% and 45% decrease in the 4β,25(OH)$_2$D$_3$ concentrations, respectively. After 14 days of treatment with a CYP3A4 inducer, a 1.2-, 2- and 5-fold induction of CYP3A4 activity is predicted to increase 4β,25(OH)$_2$D$_3$ levels by approximately 10%, 50%,and 200%, respectively. The predicted increase in 4β,25(OH)$_2$D$_3$ concentrations as a result of CYP3A4 inhibition is similar to the predicted increase in 4β(OH)C, a more-established endogenous biomarker of CYP3A4 activity. Although, more supporting evidence is required before 4β,25(OH)$_2$D$_3$ can be routinely implemented into clinical studies, our modeling suggests that 4β,25(OH)$_2$D$_3$ can be used as endogenous biomarker to detect strong MBIs and moderate or strong inducers of CYP3A4.

5.7. References

(1) Zhang, X., Quinney, S.K., Gorski, J.C., Jones, D.R. & Hall, S.D. Semiphysiologically based pharmacokinetic models for the inhibition of midazolam clearance by diltiazem and its major metabolite. *Drug Metab Dispos* **37**, 1587-97 (2009).

(2) Mangold, J.B., Wu, F. & Rebello, S. Compelling Relationship of CYP3A Induction to Levels of the Putative Biomarker 4beta-Hydroxycholesterol and Changes in Midazolam Exposure. *Clinical pharmacology in drug development* **5**, 245-9 (2016).

(3) Brown, H.S., Ito, K., Galetin, A. & Houston, J.B. Prediction of in vivo drug-drug interactions from in vitro data: impact of incorporating parallel pathways of drug elimination and inhibitor absorption rate constant. *British journal of clinical pharmacology* **60**, 508-18 (2005).

(4) Kremers, P. In vitro Tests for Predicting Drug-Drug Interactions: The Need for Validated Procedures. *Pharmacology & Toxicology* **91**, 209-17 (2002).

(5) Zhang, D., Luo, G., Ding, X. & Lu, C. Preclinical experimental models of drug metabolism and disposition in drug discovery and development. *Acta Pharmaceutica Sinica B* **2**, 549-61 (2012).

(6) Hohmann, N., Haefeli, W.E. & Mikus, G. CYP3A activity: towards dose adaptation to the individual. *Expert opinion on drug metabolism & toxicology* **12**, 479-97 (2016).

(7) Leil, T.A., Kasichayanula, S., Boulton, D.W. & LaCreta, F. Evaluation of 4beta-Hydroxycholesterol as a Clinical Biomarker of CYP3A4 Drug Interactions Using a Bayesian Mechanism-Based Pharmacometric Model. *CPT: pharmacometrics & systems pharmacology* **3**, e120 (2014).

(8) Woolsey, S.J. *et al.* Relationships between Endogenous Plasma Biomarkers of Constitutive Cytochrome P450 3A Activity and Single-Time-Point Oral Midazolam Microdose Phenotype in Healthy Subjects. *Basic & clinical pharmacology & toxicology* **118**, 284-91 (2016).

(9) Mao, J. *et al.* Perspective: 4beta-hydroxycholesterol as an emerging endogenous biomarker of hepatic CYP3A. *Drug metabolism reviews* **49**, 18-34 (2017).

(10) Bodin, K. *et al.* Antiepileptic drugs increase plasma levels of 4beta-hydroxycholesterol in humans: evidence for involvement of cytochrome p450 3A4. *J Biol Chem* **276**, 38685-9 (2001).

(11) Jones, B.C. *et al.* Managing the Risk of CYP3A Induction in Drug Development: A Strategic Approach. *Drug Metab Dispos* **45**, 35-41 (2017).

(12) Bjorkhem-Bergman, L. *et al.* Comparison of endogenous 4beta-hydroxycholesterol with midazolam as markers for CYP3A4 induction by rifampicin. *Drug Metab Dispos* **41**, 1488-93 (2013).

(13) Bjorkhem-Bergman, L. *et al.* Quinine compared to 4beta-hydroxycholesterol and midazolam as markers for CYP3A induction by rifampicin. *Drug Metab Pharmacokinet* **29**, 352-5 (2014).

(14) Kanebratt, K.P. *et al.* Cytochrome P450 induction by rifampicin in healthy subjects: determination using the Karolinska cocktail and the endogenous CYP3A4 marker 4beta-hydroxycholesterol. *Clin Pharmacol Ther* **84**, 589-94 (2008).

(15) Kasichayanula, S. *et al.* Validation of 4beta-hydroxycholesterol and evaluation of other endogenous biomarkers for the assessment of CYP3A activity in healthy subjects. *British journal of clinical pharmacology* **78**, 1122-34 (2014).

(16) Diczfalusy, U., Kanebratt, K.P., Bredberg, E., Andersson, T.B., Bottiger, Y. & Bertilsson, L. 4beta-hydroxycholesterol as an endogenous marker for CYP3A4/5 activity. Stability and half-life of elimination after induction with rifampicin. *British journal of clinical pharmacology* **67**, 38-43 (2009).

(17) Jiang, X., Dutreix, C., Jarugula, V., Rebello, S., Won, C.S. & Sun, H. An Exposure-Response Modeling Approach to Examine the Relationship Between Potency of CYP3A Inducer and Plasma 4beta-Hydroxycholesterol in Healthy Subjects. *Clinical pharmacology in drug development* **6**, 19-26 (2017).

(18) Wang, Z. *et al.* Simultaneous measurement of plasma vitamin D(3) metabolites, including 4beta,25-dihydroxyvitamin D(3), using liquid chromatography-tandem mass spectrometry. *Analytical biochemistry* **418**, 126-33 (2011).

(19) Wang, Z. *et al.* An inducible cytochrome P450 3A4-dependent vitamin D catabolic pathway. *Mol Pharmacol* **81**, 498-509 (2012).

(20) Wang, Z. *et al.* Enhancement of hepatic 4-hydroxylation of 25-hydroxyvitamin D3 through CYP3A4 induction in vitro and in vivo: implications for drug-induced osteomalacia. *J Bone Miner Res* **28**, 1101-16 (2013).

(21) Holick, M.F. Noncalcemic actions of 1,25-dihydroxyvitamin D3 and clinical applications. *Bone* **17**, 107s-11s (1995).

(22) Holick, M.F. Vitamin D: a d-lightful solution for health. *Journal of investigative medicine : the official publication of the American Federation for Clinical Research* **59**, 872-80 (2011).

(23) Holick, M.F. Vitamin D and bone health. *J Nutr* **126**, 1159s-64s (1996).

(24) Wang, Z., Schuetz, E.G., Xu, Y. & Thummel, K.E. Interplay between vitamin D and the drug metabolizing enzyme CYP3A4. *J Steroid Biochem Mol Biol* **136**, 54-8 (2013).

(25) Houston, J.B. & Taylor, G. Drug metabolite concentration-time profiles: influence of route of drug administration. *British journal of clinical pharmacology* **17**, 385-94 (1984).

(26) Zhou, S.F., Xue, C.C., Yu, X.Q., Li, C. & Wang, G. Clinically important drug interactions potentially involving mechanism-based inhibition of cytochrome P450 3A4 and the role of therapeutic drug monitoring. *Therapeutic drug monitoring* **29**, 687-710 (2007).

(27) Kamel, A. & Harriman, S. Inhibition of cytochrome P450 enzymes and biochemical aspects of mechanism-based inactivation (MBI). *Drug discovery today Technologies* **10**, e177-89 (2013).

(28) Quinney, S.K., Zhang, X., Lucksiri, A., Gorski, J.C., Li, L. & Hall, S.D. Physiologically based pharmacokinetic model of mechanism-based inhibition of CYP3A by clarithromycin. *Drug Metab Dispos* **38**, 241-8 (2010).

(29) Smythe, W. *et al.* A semimechanistic pharmacokinetic-enzyme turnover model for rifampin autoinduction in adult tuberculosis patients. *Antimicrobial agents and chemotherapy* **56**, 2091-8 (2012).

(30) Brown, R.P., Delp, M.D., Lindstedt, S.L., Rhomberg, L.R. & Beliles, R.P. Physiological parameter values for physiologically based pharmacokinetic models. *Toxicology and industrial health* **13**, 407-84 (1997).

(31) Quinney, S.K., Haehner, B.D., Rhoades, M.B., Lin, Z., Gorski, J.C. & Hall, S.D. Interaction between midazolam and clarithromycin in the elderly. *British journal of clinical pharmacology* **65**, 98-109 (2008).

(32) Chien, J.Y., Lucksiri, A., Ernest, C.S., 2nd, Gorski, J.C., Wrighton, S.A. & Hall, S.D. Stochastic prediction of CYP3A-mediated inhibition of midazolam clearance by ketoconazole. *Drug Metab Dispos* **34**, 1208-19 (2006).

(33) Hanke, N. *et al.* PBPK Models for CYP3A4 and P-gp DDI Prediction: A Modeling Network of Rifampicin, Itraconazole, Clarithromycin, Midazolam, Alfentanil, and Digoxin. *CPT: pharmacometrics & systems pharmacology* **7**, 647-59 (2018).

(34) Denney, W.S., Duvvuri, S. & Buckeridge, C. Simple, Automatic Noncompartmental Analysis: The PKNCA R Package. Vol. 42 11-107,S65 (2015).

(35) Bikle, D. Vitamin D: Production, Metabolism, and Mechanisms of Action. In: *Endotext* (eds. Feingold, K.R., Anawalt, B., Boyce, A., Chrousos, G., Dungan, K., Grossman, A. *et al.*) (South Dartmouth (MA), 2000).

(36) Bikle, D.D. Vitamin D metabolism, mechanism of action, and clinical applications. *Chem Biol* **21**, 319-29 (2014).

(37) Gupta, R.P., Hollis, B.W., Patel, S.B., Patrick, K.S. & Bell, N.H. CYP3A4 is a human microsomal vitamin D 25-hydroxylase. *J Bone Miner Res* **19**, 680-8 (2004).

(38) Best, C.M., Pressman, E.K., Queenan, R.A., Cooper, E. & O'Brien, K.O. Longitudinal changes in serum vitamin D binding protein and free 25-hydroxyvitamin D in a multiracial cohort of pregnant adolescents. *J Steroid Biochem Mol Biol* **186**, 79-88 (2019).

(39) Svensson, R.J. *et al.* A Population Pharmacokinetic Model Incorporating Saturable Pharmacokinetics and Autoinduction for High Rifampicin Doses. *Clin Pharmacol Ther* **103**, 674-83 (2018).

(40) Haschke, M. *et al.* Pharmacokinetics and pharmacodynamics of nasally delivered midazolam. *British journal of clinical pharmacology* **69**, 607-16 (2010).

(41) Hohmann, N., Kocheise, F., Carls, A., Burhenne, J., Haefeli, W.E. & Mikus, G. Midazolam microdose to determine systemic and pre-systemic metabolic CYP3A activity in humans. *British journal of clinical pharmacology* **79**, 278-85 (2015).

(42) Syed, S. *et al.* Lack of effect of brivanib on the pharmacokinetics of midazolam, a CYP3A4 substrate, administered intravenously and orally in healthy participants. *Journal of clinical pharmacology* **52**, 914-21 (2012).

(43) Burstein, A.H., Modica, R., Hatton, M., Forrest, A. & Gengo, F.M. Pharmacokinetics and pharmacodynamics of midazolam after intranasal administration. *Journal of clinical pharmacology* **37**, 711-8 (1997).

(44) Bui, K.H., Zhou, D., Agbo, F. & Guo, J. Effect of multiple intravenous doses of lanicemine (AZD6765) on the pharmacokinetics of midazolam in healthy subjects. *Journal of clinical pharmacology* **55**, 1024-30 (2015).

(45) Stockis, A., Watanabe, S. & Scheen, A.J. Effect of brivaracetam on CYP3A activity, measured by oral midazolam. *Journal of clinical pharmacology* **55**, 543-8 (2015).

(46) Juif, P.E., Boehler, M., Donazzolo, Y., Bruderer, S. & Dingemanse, J. A pharmacokinetic drug-drug interaction study between selexipag and midazolam, a CYP3A4 substrate, in healthy male subjects. *European journal of clinical pharmacology* **73**, 1121-8 (2017).

(47) Krishna, G. *et al.* Effects of oral posaconazole on the pharmacokinetic properties of oral and intravenous midazolam: a phase I, randomized, open-label, crossover study in healthy volunteers. *Clinical therapeutics* **31**, 286-98 (2009).

(48) Garg, V., Chandorkar, G., Farmer, H.F., Smith, F., Alves, K. & van Heeswijk, R.P. Effect of telaprevir on the pharmacokinetics of midazolam and digoxin. *Journal of clinical pharmacology* **52**, 1566-73 (2012).

(49) Bancke, L.L., Dworak, H.A., Rodvold, K.A., Halvorsen, M.B. & Gidal, B.E. Pharmacokinetics, pharmacodynamics, and safety of USL261, a midazolam formulation optimized for intranasal delivery, in a randomized study with healthy volunteers. *Epilepsia* **56**, 1723-31 (2015).

(50) Veldhorst-Janssen, N.M. *et al.* Pharmacokinetics and tolerability of nasal versus intravenous midazolam in healthy Dutch volunteers: a single-dose, randomized-sequence, open-label, 2-period crossover pilot study. *Clinical therapeutics* **33**, 2022-8 (2011).

(51) Ibrahim, A., Karim, A., Feldman, J. & Kharasch, E. The influence of parecoxib, a parenteral cyclooxygenase-2 specific inhibitor, on the pharmacokinetics and clinical effects of midazolam. *Anesthesia and analgesia* **95**, 667-73, table of contents (2002).

(52) Wermeling, D.P., Record, K.A., Kelly, T.H., Archer, S.M., Clinch, T. & Rudy, A.C. Pharmacokinetics and pharmacodynamics of a new intranasal midazolam formulation in healthy volunteers. *Anesthesia and analgesia* **103**, 344-9, table of contents (2006).

(53) Halama, B., Hohmann, N., Burhenne, J., Weiss, J., Mikus, G. & Haefeli, W.E. A nanogram dose of the CYP3A probe substrate midazolam to evaluate drug interactions. *Clin Pharmacol Ther* **93**, 564-71 (2013).

(54) Johansson, S. *et al.* Effects of Tenapanor on Cytochrome P450-Mediated Drug-Drug Interactions. *Clinical pharmacology in drug development* **6**, 466-75 (2017).

(55) Chu, S.Y., Deaton, R. & Cavanaugh, J. Absolute bioavailability of clarithromycin after oral administration in humans. *Antimicrobial agents and chemotherapy* **36**, 1147-50 (1992).

(56) Chu, S.Y., Sennello, L.T., Bunnell, S.T., Varga, L.L., Wilson, D.S. & Sonders, R.C. Pharmacokinetics of clarithromycin, a new macrolide, after single ascending oral doses. *Antimicrobial agents and chemotherapy* **36**, 2447-53 (1992).

(57) Lappin, G. *et al.* Comparative pharmacokinetics between a microdose and therapeutic dose for clarithromycin, sumatriptan, propafenone, paracetamol (acetaminophen), and phenobarbital in human volunteers. *European journal of pharmaceutical sciences : official journal of the European Federation for Pharmaceutical Sciences* **43**, 141-50 (2011).

(58) Chu, S., Wilson, D.S., Deaton, R.L., Mackenthun, A.V., Eason, C.N. & Cavanaugh, J.H. Single- and multiple-dose pharmacokinetics of clarithromycin, a new macrolide antimicrobial. *Journal of clinical pharmacology* **33**, 719-26 (1993).

(59) Chu, S.Y., Wilson, D.S., Guay, D.R. & Craft, C. Clarithromycin pharmacokinetics in healthy young and elderly volunteers. *Journal of clinical pharmacology* **32**, 1045-9 (1992).

(60) Garey, K.W., Peloquin, C.A., Godo, P.G., Nafziger, A.N. & Amsden, G.W. Lack of effect of zafirlukast on the pharmacokinetics of azithromycin, clarithromycin, and 14-hydroxyclarithromycin in healthy volunteers. *Antimicrobial agents and chemotherapy* **43**, 1152-5 (1999).

(61) Chu, S.Y., Granneman, G.R., Pichotta, P.J., Decourt, J.P., Girault, J. & Fourtillan, J.B. Effect of moderate or severe hepatic impairment on clarithromycin pharmacokinetics. *Journal of clinical pharmacology* **33**, 480-5 (1993).

(62) Sekar, V.J. *et al.* Darunavir/ritonavir pharmacokinetics following coadministration with clarithromycin in healthy volunteers. *Journal of clinical pharmacology* **48**, 60-5 (2008).

(63) Carr, R.A. *et al.* Steady-state pharmacokinetics and electrocardiographic pharmacodynamics of clarithromycin and loratadine after individual or concomitant administration. *Antimicrobial agents and chemotherapy* **42**, 1176-80 (1998).

(64) Nitti, V., Virgilio, R., Patricolo, M.R. & Iuliano, A. Pharmacokinetic study of intravenous rifampicin. *Chemotherapy* **23**, 1-6 (1977).

(65) Padgaonkar, K.A. *et al.* Comparative bioequivalence study of rifampicin and isoniazid combinations in healthy volunteers. *The international journal of tuberculosis and lung disease : the official journal of the International Union against Tuberculosis and Lung Disease* **3**, 627-31 (1999).

(66) Agrawal, S., Kaur, K.J., Singh, I., Bhade, S.R., Kaul, C.L. & Panchagnula, R. Assessment of bioequivalence of rifampicin, isoniazid and pyrazinamide in a four drug fixed dose combination with separate formulations at the same dose levels. *International journal of pharmaceutics* **233**, 169-77 (2002).

(67) Peloquin, C.A., Jaresko, G.S., Yong, C.L., Keung, A.C., Bulpitt, A.E. & Jelliffe, R.W. Population pharmacokinetic modeling of isoniazid, rifampin, and pyrazinamide. *Antimicrobial agents and chemotherapy* **41**, 2670-9 (1997).

(68) Acocella, G., Bonollo, L., Garimoldi, M., Mainardi, M., Tenconi, L.T. & Nicolis, F.B. Kinetics of rifampicin and isoniazid administered alone and in combination to normal subjects and patients with liver disease. *Gut* **13**, 47-53 (1972).

(69) Acocella, G. *et al.* Pharmacokinetic study on intravenous rifampicin in man. *Pharmacological research communications* **16**, 723-36 (1984).

(70) Hao, L.H. *et al.* Comparative bioavailability of rifampicin and isoniazid in fixed-dose combinations and single-drug formulations. *The international journal of tuberculosis and lung disease : the official journal of the International Union against Tuberculosis and Lung Disease* **18**, 1505-12 (2014).

(71) Acocella, G., Nonis, A., Gialdroni-Grassi, G. & Grassi, C. Comparative bioavailability of isoniazid, rifampin, and pyrazinamide administered in free combination and in a fixed triple formulation designed for daily use in antituberculosis chemotherapy. I. Single-dose study. *The American review of respiratory disease* **138**, 882-5 (1988).

(72) la Porte, C.J. *et al.* Pharmacokinetics of adjusted-dose lopinavir-ritonavir combined with rifampin in healthy volunteers. *Antimicrobial agents and chemotherapy* **48**, 1553-60 (2004).

(73) Burger, D.M., Agarwala, S., Child, M., Been-Tiktak, A., Wang, Y. & Bertz, R. Effect of rifampin on steady-state pharmacokinetics of atazanavir with ritonavir in healthy volunteers. *Antimicrobial agents and chemotherapy* **50**, 3336-42 (2006).

(74) Gorski, J.C., Jones, D.R., Haehner-Daniels, B.D., Hamman, M.A., O'Mara, E.M., Jr. & Hall, S.D. The contribution of intestinal and hepatic CYP3A to the interaction between midazolam and clarithromycin. *Clin Pharmacol Ther* **64**, 133-43 (1998).

(75) Gurley, B. *et al.* Assessing the clinical significance of botanical supplementation on human cytochrome P450 3A activity: comparison of a milk thistle and black cohosh product to rifampin and clarithromycin. *Journal of clinical pharmacology* **46**, 201-13 (2006).

(76) Kharasch, E.D. *et al.* The role of cytochrome P450 3A4 in alfentanil clearance. Implications for interindividual variability in disposition and perioperative drug interactions. *Anesthesiology* **87**, 36-50 (1997).

(77) Kharasch, E.D., Walker, A., Hoffer, C. & Sheffels, P. Intravenous and oral alfentanil as in vivo probes for hepatic and first-pass cytochrome P450 3A activity: noninvasive assessment by use of pupillary miosis. *Clin Pharmacol Ther* **76**, 452-66 (2004).

(78) Link, B. *et al.* Pharmacokinetics of intravenous and oral midazolam in plasma and saliva in humans: usefulness of saliva as matrix for CYP3A phenotyping. *British journal of clinical pharmacology* **66**, 473-84 (2008).

(79) Reitman, M.L. *et al.* Rifampin's acute inhibitory and chronic inductive drug interactions: experimental and model-based approaches to drug-drug interaction trial design. *Clin Pharmacol Ther* **89**, 234-42 (2011).

(80) Chung, E., Nafziger, A.N., Kazierad, D.J. & Bertino, J.S., Jr. Comparison of midazolam and simvastatin as cytochrome P450 3A probes. *Clin Pharmacol Ther* **79**, 350-61 (2006).

5.8. Tables

Table 5.1: Model parameters of midazolam, clarithromycin, and rifampin.

Parameter (Units)	Description	Value	Reference
Physiological Volumes			
V_{GL} (L)	Gut lumen volume	0.25	(28)
V_{GW} (L)	Gut wall volume	0.25	(28)
V_{PV} (L)	Portal vein volume	0.07	(28)
V_{H} (L)	Liver volume	2.8	(28)
Enzyme Parameters			
$R_{0,CYP3A4}$ (1/hr)	zero-order synthesis rate of CYP3A4	0.025	(28)
$k_{deg,CYP3A4}$ (1/hr)	first-order degradation rate of CYP3A4	0.025	(28)
$R_{0,AADAC}$ (1/hr)	zero-order synthesis rate of AADAC	0.00603	(39)
$k_{deg,AADAC}$ (1/hr)	first-order degradation rate of AADAC	0.00603	(39)
Midazolam Parameters			
$f_{u,MDZ}$	MDZ fraction unbound	0.04	(28)
$K_{m,MDZ}$ (µg/mL)	MDZ K_m	1.8	(28, 33)
$V_{C,MDZ}$ (L)[a]	MDZ central volume	25.2	-
$V_{P,MDZ}$ (L)[a]	MDZ peripheral volume	54.2	-
$CL_{per,MDZ}$ (L/hr)[a]	MDZ clearance between the central and peripheral compartment	22.7	-
$CL_{R,MDZ}$ (L/hr)	MDZ renal clearance	0.06	(31, 33)
$K_{a,MDZ}$ (1/hr)[a]	MDZ absorption rate	1.32	-
$V_{max,GW,MDZ}$ (mg/hr)[a]	MDZ V_{max} in the gut wall	2.97	-
$V_{max,H,MDZ}$ (mg/hr)[a]	MDZ V_{max} in the liver	1688	-
Clarithromycin Parameters			
$f_{u,CLAR}$	CLAR fraction unbound	0.3	(28, 33)
$K_{m,CLAR}$ (µg/mL)	CLAR K_m	40.8	(28, 33)
$V_{C,CLAR}$ (L)[a]	CLAR central volume	132.3	-
$CL_{R,CLAR}$ (L/hr)	CLAR renal clearance	6.75	(28, 33)
$K_{a,CLAR}$ (1/hr)[a]	CLAR absorption rate	2.0	-

$V_{max,GW,CLAR}$ (mg/hr)[a]	CLAR V_{max} in the gut wall	72.3	-
$V_{max,H,CLAR}$ (mg/hr)[a]	CLAR V_{max} in the liver	4178	-
$K_{i,CLAR}$ (µg/mL)	CLAR reversible inhibition dissociation constant for CYP3A4	224	(28, 33)
$K_{I,CLAR}$ (µg/mL)	CLAR Concentration at 50% of k_{inact}	3.9	(28, 33)
$k_{inact,GW,CLAR}$ (1/hr)	CLAR maximum rate of CYP3A4 inactivation in the gut wall	4.0	(28, 33)
$k_{inact,H,CLAR}$ (1/hr)	CLAR maximum rate of CYP3A4 inactivation in the liver	0.4	(28, 33)
Rifampin Parameters			
$f_{u,RIF}$	RIF fraction unbound	0.17	(33)
$K_{m,RIF}$ (µg/mL)	RIF K_m	160	(29, 33, 39)
$V_{C,RIF}$ (L)[a]	RIF central volume	45.2	-
$V_{TRANS,RIF}$ (L)	Volume of the RIF transit compartment	0.25	(28)
$CL_{R,RIF}$ (L/hr)	RIF renal clearance	1.5	(33)
$K_{a,RIF}$ (1/hr)[a]	RIF absorption rate	2.75	-
$V_{max,AADAC,RIF}$ (mg/hr)	RIF V_{max} of metabolism by AADAC	7267	-
$K_{i,RIF}$ (µg/mL)	RIF reversible inhibition dissociation constant for CYP3A4	1.0	(33)
$EC_{max,AADAC,RIF}$	RIF maximal induction rate of AADAC	2.3	(33)
$E_{50,AADAC,RIF}$ (µg/mL)	RIF concentration at half the $EC_{max,AADAC,RIF}$	0.28	(33)
$EC_{max,H,CYP3A4,RIF}$	RIF maximal induction rate of CYP3A4	13.2	(33)
$EC_{max,G,CYP3A4,RIF}$	RIF maximal induction rate of CYP3A4	13.2	(33)
$E_{50,CYP3A4,RIF}$ (µg/mL)	RIF concentration at half the $EC_{max,CYP3A4,RIF}$	0.28	(33)

[a] Parameters optimized using training data sets

Table 5.2: Final model parameters of 4β,25(OH)$_2$D$_3$ formation from 25(OH)D$_3$.

Parameter (Units)	Description	Estimate (95 % CI)
$V_{25(OH)D_3}$ (L)	25(OH)D$_3$ volume of distribution	9.89
$V_{4\beta,25(OH)_2D_3}$ (L)	4β,25(OH)$_2$D$_3$ volume of distribution	9.89
$k_{other,25(OH)D_3}$ (µg/day)	Non-4β,25(OH)$_2$D$_3$ elimination of 25(OH)D$_3$	0.0355
$C_{0,25(OH)D_3}$ (ng/mL)	Baseline 25(OH)D$_3$ concentrations	20.0 (18.5, 21.7)
$C_{0,4\beta,25(OH)_2D_3}$ (pg/mL)	Baseline 4β,25(OH)$_2$D$_3$ concentrations	59.3 (54.5, 64.6)
$k_{syn,25(OH)D_3}$ (µg/day)	25(OH)D$_3$ synthesis rate	6.44 (5.85, 7.08)
$V_{max,25(OH)D_3,CYP3A4}$ (µg/day)	V_{max} of 4β,25(OH)$_2$D$_3$ formation from 25(OH)D$_3$	5.01 (4.41, 5.69)
$k_{deg,4\beta,25(OH)_2D_3}$ (1/day)	4β,25(OH)$_2$D$_3$ elimination rate constant	0.0587 (0.0519, 0.0664)
IIV $C_{0,25(OH)D_3}$ (%)[a]		31.6 (24.2, 39.2)
IIV $C_{0,4\beta,25(OH)_2D_3}$ (%)[a]		42.6 (33.0, 52.2)
IIV $k_{syn,25(OH)D_3}$ (%)[a]		33.6 (26.3, 40.9)
IIV $_{max,25(OH)D_3,CYP3A4}$ (%)[a]		37.6 (29.8, 45.4)
IIV $k_{deg,4\beta,25(OH)_2D_3}$ (%)[a]		23.1 (17.2, 29.0)
σ	Exponential	0.152

CI, confidence interval; IIV, interindividual variability

[a] Interindividual variability expressed as the percent of the parameter estimate

Table 5.3: Clinical studies with midazolam used for model training and verification.

Dose (mg)	Route	n	Males (%)	Age (years)	Weight (kg)	Pred AUC (ng*hr/mL)	Obs AUC (ng*hr/mL)	AUC Pred/Obs	Pred C_{max} (ng/mL)	Obs C_{max} (ng/mL)	C_{max} Pred/Obs	Reference
Training												
1	IV	7	100	24 ± 3	74 ± 5	47.8	46.7	1.024	39.7	87.6	0.453	(40)
1	IV (5 min)	16	-	-	-	47.8	39	1.226	39.7	37.1	1.07	(41)
1.25	IV	24	83	46	75.4	60.8	46	1.322	49.6	22.3	2.224	(42)
2	IV (2 min)	8	75	30 ± 5	78 ± 17	96.5	52.3	1.845	79.4	115	0.69	(43)
3	PO	16	-	-	-	40.3	24.4	1.652	11	9.99	1.101	(41)
5	PO	24	83	46	75.4	83.6	78.9	1.060	22	26	0.846	(42)
5	PO	46	61	28 ± 10	75 ± 11	83.6	55.9	1.496	22	25.5	0.863	(44)
7.5	PO	14	100	18-55	-	147.4	126.3	1.167	37.8	42.9	0.881	(45)
7.5	PO	18	-	-	-	147.4	118.08	1.248	37.8	39.05	0.968	(46)
							GMFE	**1.31**			**0.93**	
						Within 2-fold		**9/9**			**7/9**	
Verification												
0.4	IV (30 min)	12	92	42.8	80.6	19.2	11.6	1.655	10.3	5.6	1.839	(47)
0.5	IV (2 min)	24	42	37	-	24.1	23.4	1.03	19.8	19.1	1.037	(48)
2.5	IV (15 min)	25	60	30 ± 6.7	77.1 ± 13.4	119.8	142	0.844	76.8	119	0.645	(49)
2.5	IV (10 s)	9	67	34 ± 9	68.6 ± 10.4	121.2	120	1.01	99.2	51.2	1.938	(50)
5	IV (5 min)	13	46	31.5	75 ± 13	239.7	188	1.275	198.4	319	0.622	(51)

5	IV (15 min)	12	-	-	-	239.7	186	1.289	198	167	1.186	(52)
1	PO	5	-	-	-	10.2	9.44	1.081	2.69	4.07	0.661	(53)
2	PO	23	42	37	-	23.6	27.4	0.861	6.37	7.71	0.826	(48)
2	PO	12	92	42.8	80.6	23.6	31.9	0.740	6.37	7	0.910	(47)
3	PO	6	-	-	-	40.3	31.8	1.267	11	12	0.917	(53)
7.5	PO	28	50	29 ± 9	-	147.4	96.2	1.532	37.8	28	1.350	(54)
							GMFE	**1.11**			**1.01**	
							Within 2-fold	**11/11**			**11/11**	
Overall							**GMFE**	**1.19**			**0.97**	
							Within 2-fold	**20/20**			**18/20**	

Table 5.4: Clinical studies with clarithromycin used for model training and verification.

Dose (mg)	Route	n	Males (%)	Age (years)	Weight (kg)	Pred AUC (ng*hr/mL)	Obs AUC (ng*hr/mL)	AUC Pred/Obs	Pred C_{max} (ng/mL)	Obs C_{max} (ng/mL)	C_{max} Pred/Obs	Reference
Training												
250	IV	19	100	29 ± 6	71.5 ± 8.3	10.3	8.63	1.194	1.73	2.78	0.622	(55)
100	PO	39	100	25 ± 4	71.4 ± 9.8	2.09	1.67	1.251	0.28	0.35	0.8	(56)
250	PO	30	100	-	-	6.81	4.91	1.387	0.91	0.958	0.95	(57)
250	PO	17	100	29 ± 6	70.8 ± 84	6.81	4.36	1.562	0.91	0.78	1.167	(58)
400	PO	39	100	25 ± 4	71.4 ± 9.8	11.9	8.55	1.392	1.57	1.13	1.389	(56)
500	PO	17	100	31 ± 6	72.2 ± 6.0	15.6	14.08	1.108	2.01	2.12	0.948	(58)
1200	PO	39	100	25 ± 4	71.4 ± 9.8	43.1	44.6	0.966	5.19	3.97	1.307	(56)
250 BID x 2 days	PO	17	100	29 ± 6	70.8 ± 84	10.1	6.44	1.568	1.41	1.01	1.396	(58)
250 BID x 3 days	PO	17	100	29 ± 6	70.8 ± 84	10.7	6.86	1.56	1.47	1.14	1.289	(58)
500 BID x 2 days	PO	17	100	31 ± 6	72.2 ± 6.0	25.3	19.59	1.291	3.29	2.67	1.232	(58)
500 BID x 7 days	PO	17	100	31 ± 6	72.2 ± 6.0	28.7	20.84	1.377	3.6	2.85	1.263	(58)
							GMFE	**1.32**			**1.09**	
							Within 2-fold	**11/11**			**11/11**	

Verification												
200	PO	39	100	25 ± 4	71.4 ± 9.8	5.16	2.99	1.726	0.69	0.6	1.15	(56)
250	PO	19	100	29 ± 6	71.5 ± 8.3	6.81	4.27	1.595	0.91	0.76	1.197	(59)
500	PO	12	50	39 ± 5	68 ± 12	15.6	20.15	0.774	2.01	2.47	0.814	(60)
600	PO	39	100	25 ± 4	71.4 ± 9.8	15.6	15.44	1.01	2.01	2.03	0.99	(56)
800	PO	39	100	25 ± 4	71.4 ± 9.8	27	24.73	1.092	3.36	2.63	1.278	(56)
250 BID x 2 days	PO	6	100	49 ± 3	66 ± 10	10.1	9.29	1.087	1.41	1.52	0.928	(61)
500 BID x 2 days	PO	12	100	23 ± 2	76.7 ± 7.9	25.3	18.87	1.341	3.29	3.28	1.003	(59)
500 BID x 6 days	PO	18	100	18-46	-	28.7	15.6	1.84	3.61	2.261	1.597	(62)
500 BID x 10 days	PO	24	100	23-40	61-87	28.7	27.4	1.047	3.62	3.27	1.107	(63)
							GMFE	**1.23**			**1.10**	
							Within 2-fold	**9/9**			**9/9**	
Overall							**GMFE**	**1.28**			**1.10**	
							Within 2-fold	**20/20**			**20/20**	

Table 5.5: Clinical studies of rifampin used for model training and verification.

Dose (mg)	Route	n	Males (%)	Age (years)	Weight (kg)	Pred AUC (ng*hr/mL)	Obs AUC (ng*hr/mL)	AUC Pred/Obs	Pred C_{max} (ng/mL)	Obs C_{max} (ng/mL)	C_{max} Pred/Obs	Reference
Training												
300	IV (3 hr)	2	-	-	-	30.1	17.6	1.71	4.9	4.1	1.195	(64)
450	IV (3 hr)	3	-	-	-	45.1	50.5	0.893	7.37	12.4	0.594	(64)
600	IV (3 hr)	6	-	-	-	60	64.1	0.936	9.8	13.5	0.726	(64)
450	PO	12	100	18-30	62.13 ± 4.32	48.4	33.3	1.453	6.71	5.22	1.285	(65)
450	PO	14	-	-	-	49.1	41	1.198	6.71	5.41	1.24	(66)
600	PO	24	100	27 ± 7	76.9 ± 11	65.6	79.79	0.822	8.9	13.61	0.654	(67)
600 QD x 7 days	PO					40.8	-		7.74	-		(68)
							GMFE	**1.13**			**0.91**	
							Within 2-fold	**6/6**			**6/6**	
Verification												
600	IV (2 hr)	6	100	-	-	50.8	52.7	0.964	10.7	8	1.338	(69)
900	IV (2 hr)	6	100	-	-	76.4	92.43	0.827	16	12.5	1.28	(69)
1200	IV (2 hr)	6	100	-	-	101.9	166.08	0.614	21.3	15.8	1.348	(69)
600	PO	6	-	-	-	65.6	-		8.96	-		(68)
600	PO	6	100	18-55	> 50 kg	65.4	96.9	0.675	8.96	13.7	0.654	(70)
600	PO	10	80	25-47	60-72	65.4	77.6	0.843	8.96	11.6	0.772	(71)

600 QD x 5 days	PO	19	58	22-70	60.5-85.4	40.5	79.2	0.511	7.91	14.2	0.557	(72)
600 QD x 10 days	PO					40.8	31.3	1.304	7.74	8	0.968	(73)
							GMFE	**0.79**			**0.94**	
							Within 2-fold	**7/7**			**7/7**	
Overall							**GMFE**	**0.93**			**0.92**	
							Within 2-fold	**13/13**			**13/13**	

Table 5.6: Clinical studies of rifampin used for model development and verification.

Perpetrator	Dose MDZ (mg)	n	Without Perpetrator			With Perpetrator			Pred AUC Ratio	Obs AUC Ratio	AUC Ratio Pred/Obs	Reference
			Pred AUC (ng*hr/mL)	Obs AUC (ng*hr/mL)	AUC Pred/Obs	Pred AUC (ng*hr/mL)	Obs AUC (ng*hr/mL)	AUC Pred/Obs				
Clarithromycin												
500 mg BID x 7 days	3.2 (IV)	8	153	188	0.81	291	333	0.87	1.90	1.77	1.07	(74)
500 mg BID x 7 days	4 (PO)	8	42	55	0.76	294	278	1.06	7.00	5.05	1.39	(74)
500 mg BID x 7 days	8 (PO)	19	120	89.6	1.34	612	752	0.81	5.10	8.39	0.61	(75)
				GMFE	**0.94**			**0.91**			**0.97**	
				Within 2-fold	**3/3**			**3/3**			**3/3**	
Rifampin												
600 mg QD x 5 days	1 (IV)		59	68	1.15	19	26	1.37	0.322	0.378	0.85	(76)
600 mg QD x 7 days	1 (IV)		59	26	2.27	19	14	1.36	0.322	0.521	0.62	(77)
600 mg QD x 7 days	2 (IV)		117	126	0.93	37	82	0.45	0.316	0.655	0.48	(78)
600 mg QD x 28 days	2 (PO)		23	21.4	0.77	1.10	2.64	1.14	0.128	0.123	1.04	(79)

600 mg QD X 9 days	5.5 (PO)	94	49	1.92	12	6.1	1.97	0.128	0.124	1.03	(80)
			GMFE	**1.29**			**1.13**			**0.77**	
			Within 2-fold	**4/5**			**4/5**			**4/5**	

5.9. Figures

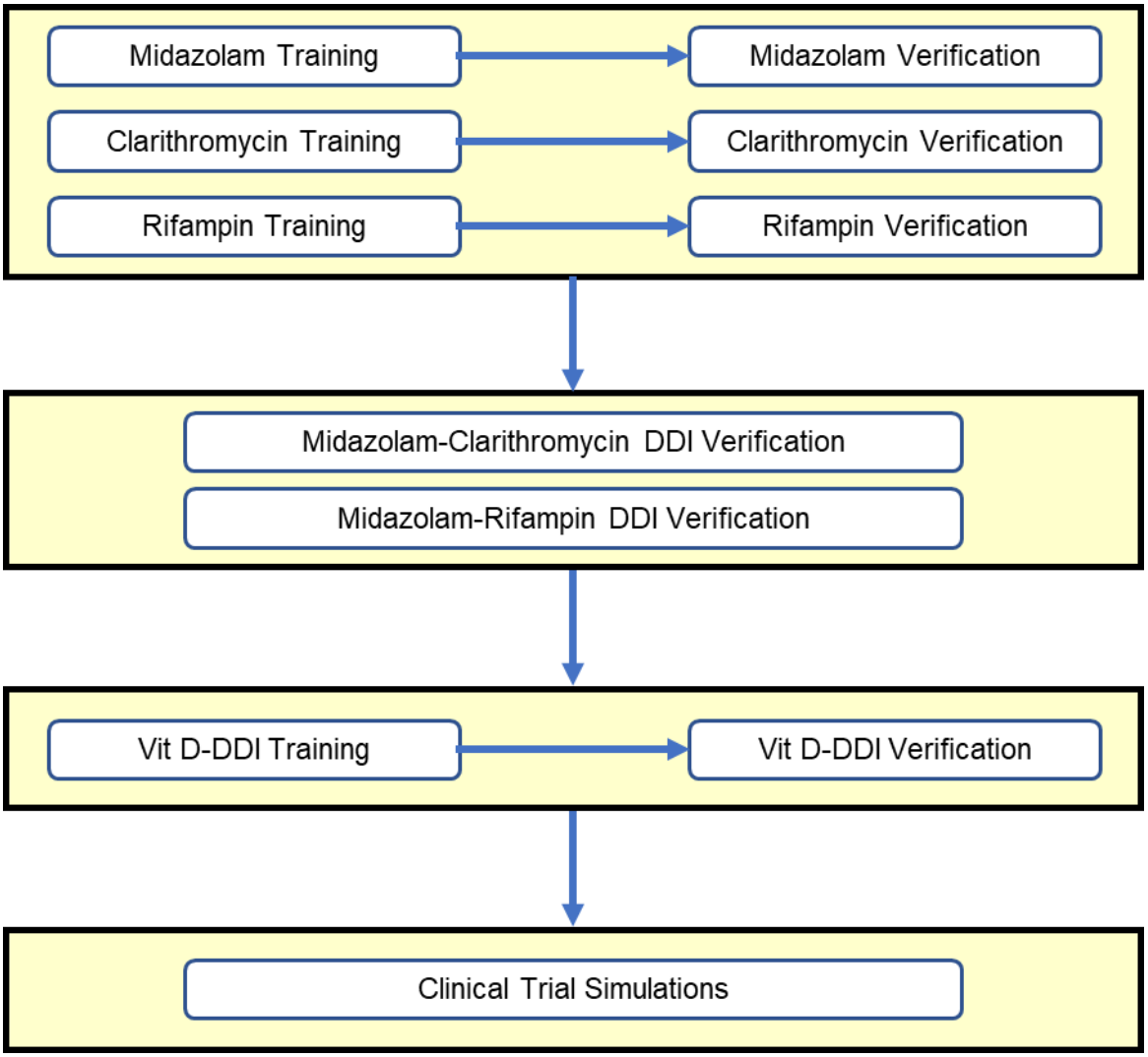

Figure 5.1: Development flowchart for a semi-mechanistic PK/PD model of CYP3A4 enzyme activity. MDZ, midazolam; CLAR, clarithromycin; RIF, rifampin; Vit D, 25-hydroxyvitamin D_3 conversion to 4β,25-dihydroxyvitamin D_3.

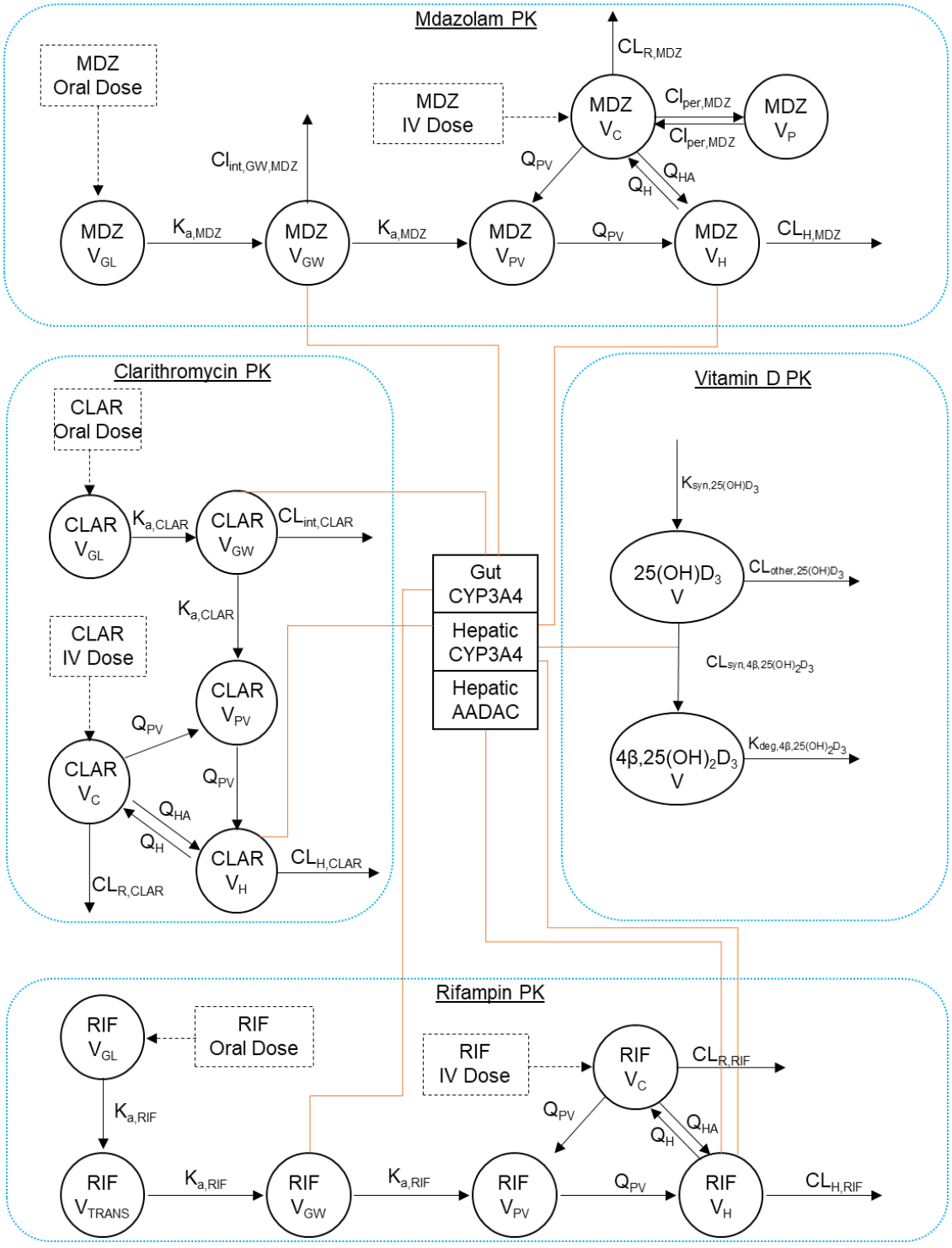

Figure 5.2: Structural model of a semi-mechanistic PK/PD model of CYP3A4 activity including midazolam (MDZ), clarithromycin (CLAR), rifampin (RIF), 25-hydroxyvitamin D_3 ($25(OH)D_3$), and 4β,25-dihydroxyviatmin D_3 ($4β,25(OH)_2D_3$).

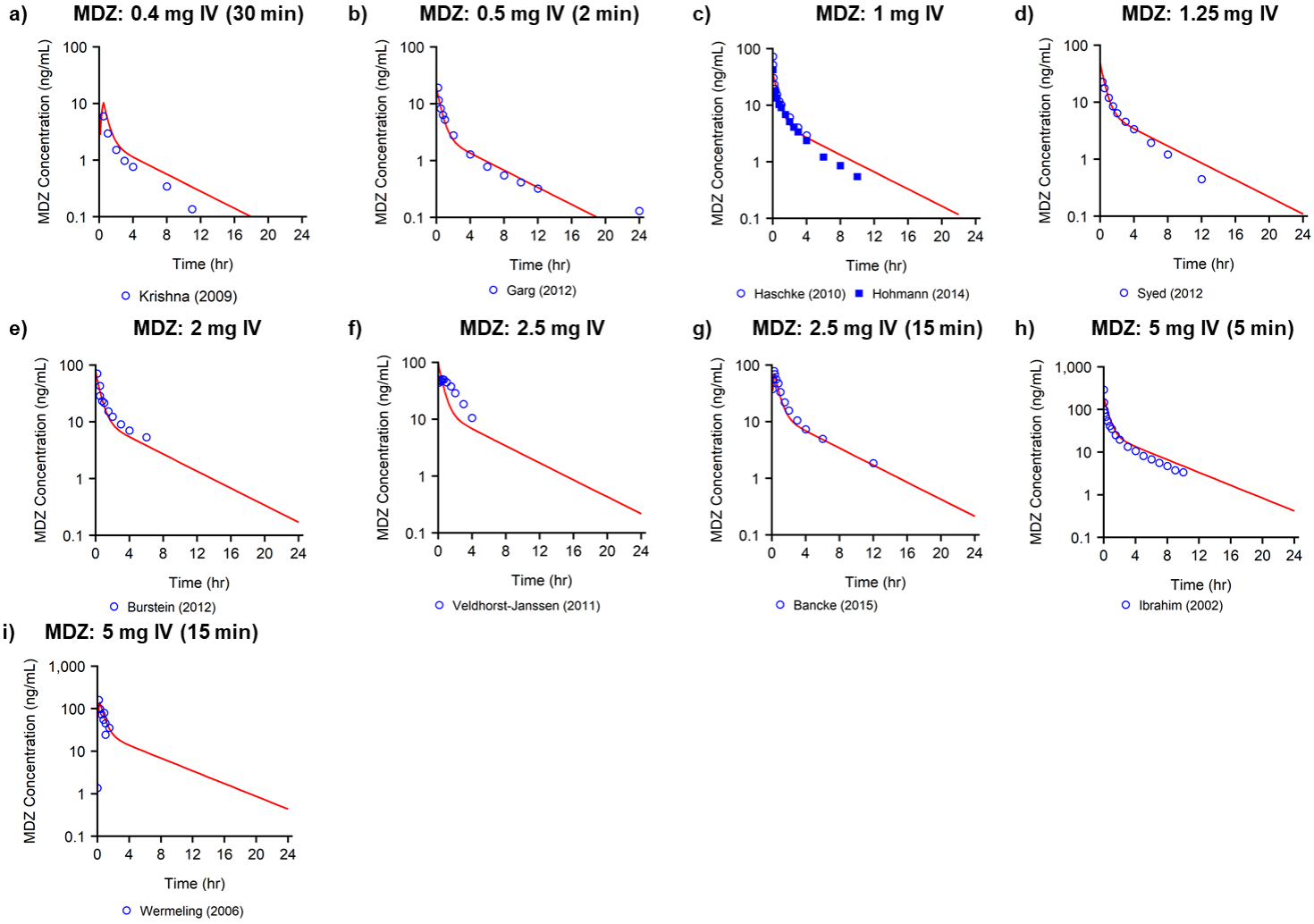

Figure 5.3: Predicted plasma concentration midazolam (MDZ) after IV administration. If MDZ was given as an infusion, the length of infusion is given in parentheses. The red line is the simulated concentration-time profile and the blue circles are the observed concentrations.

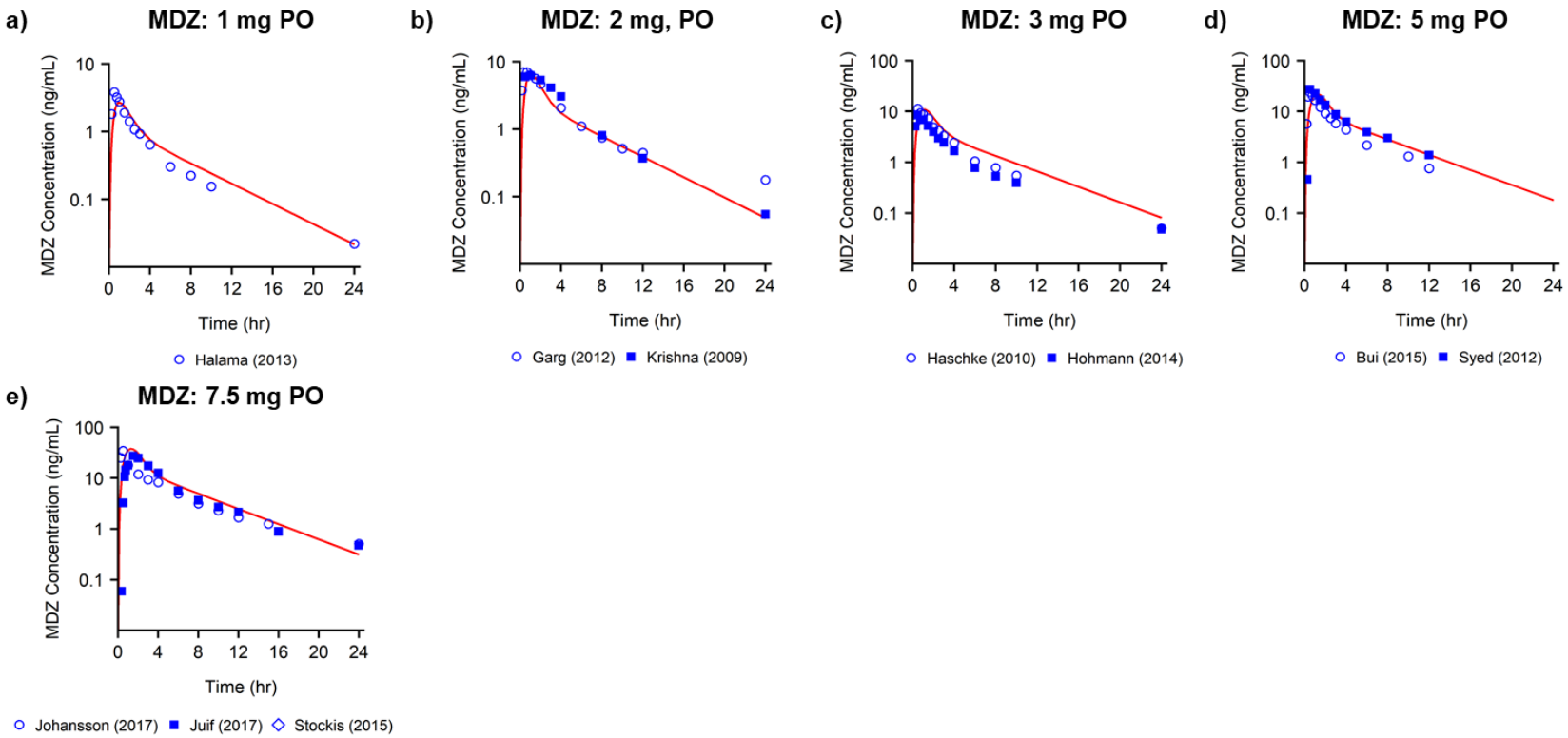

Figure 5.4: Predicted plasma concentration midazolam after oral administration. The red line is the simulated concentration-time profile and the blue circles are the observed concentrations.

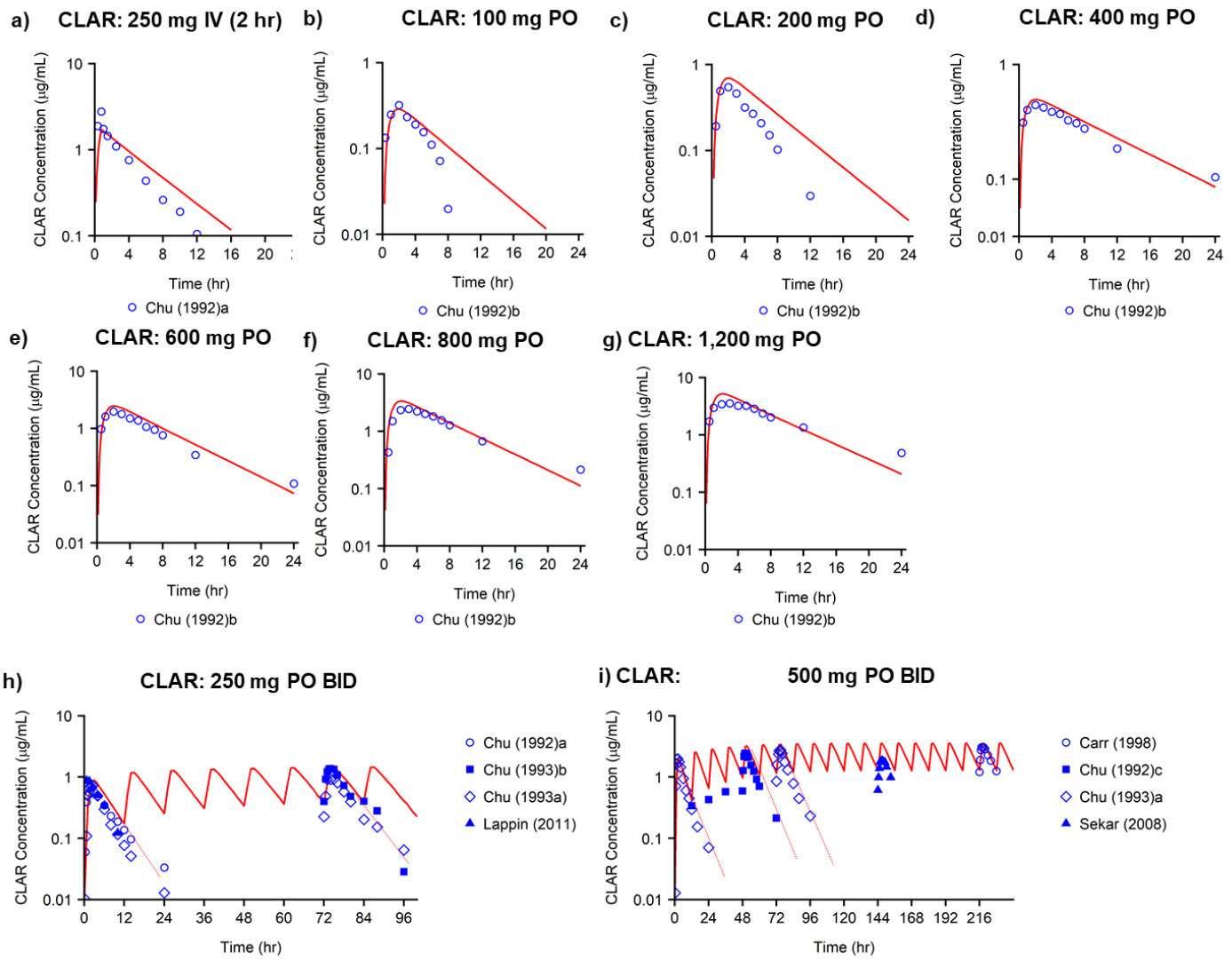

Figure 5.5: Predicted plasma concentration clarithromycin after IV and oral administration. The red line is the simulated concentration-time profile and the blue circles are the observed concentrations.

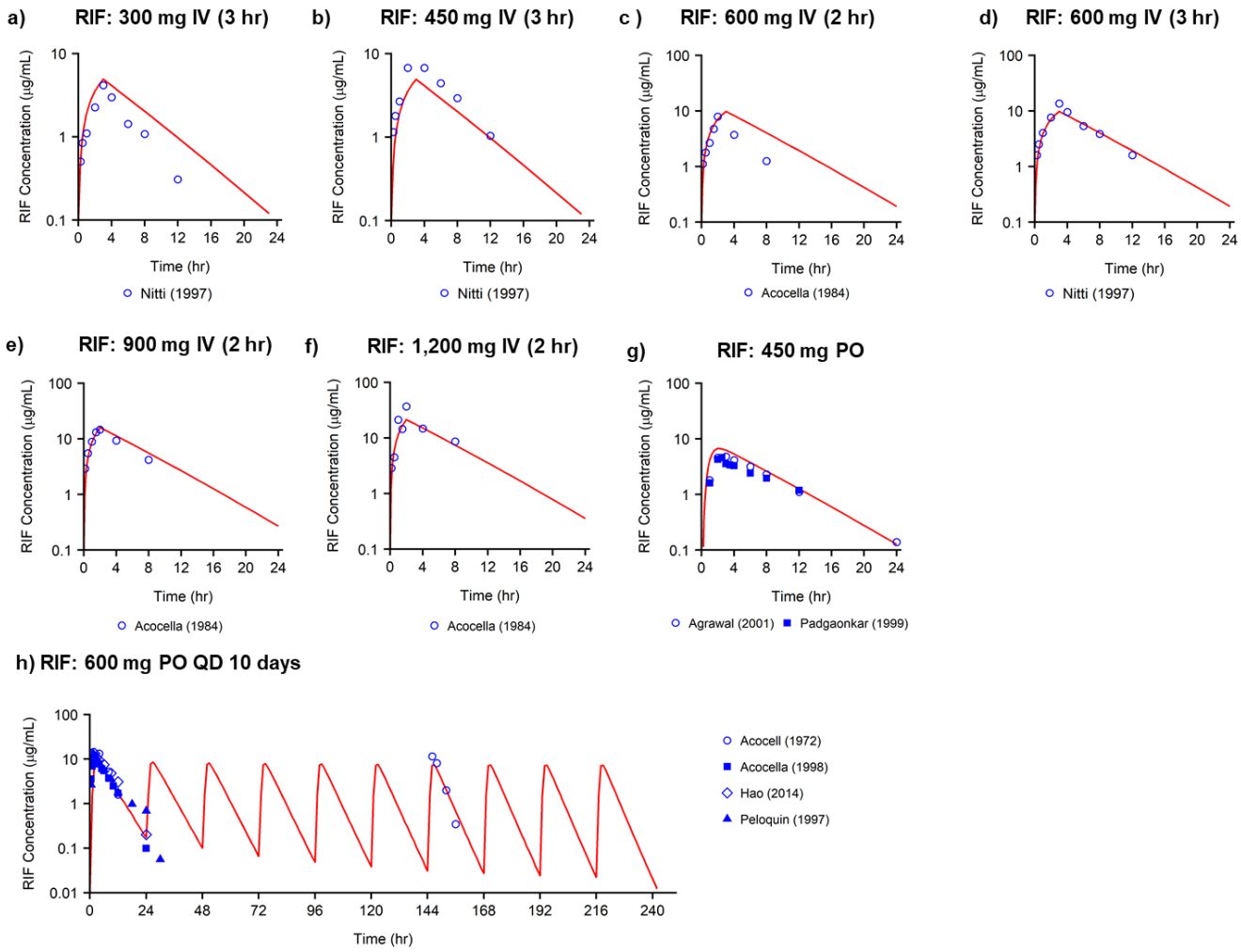

Figure 5.6: Predicted plasma concentration rifampin after IV and oral administration. When RIF was given as an infusion, the length of the infusion is given in the parentheses. The red line is the simulated concentration-time profile and the blue circles are the observed concentrations.

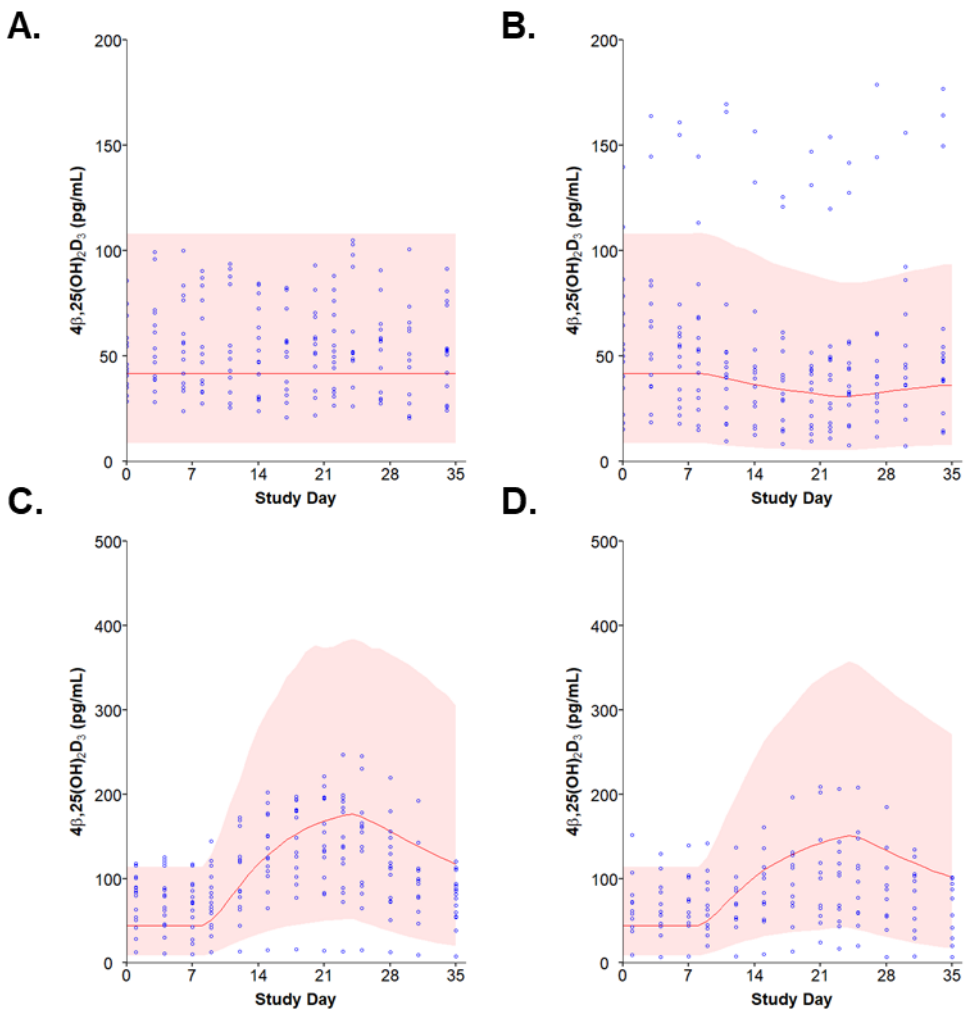

Figure 5.7: Evaluation of the predictive performance of the PK/PD model. Observed and predicted concentrations of 4β,25-dihydroxyvitamin D_3 (4β,25$(OH)_2D_3$) after treatment with A) water, B) 250 mg clarithromycin BID, C) 600 mg rifampin QD, and D) 250 mg clarithromycin BID in combination with 600 mg rifampin QD for 14 days (Study Days 8 – 21). The blue circles are the observed values, the red line and shaded region are the mean and 10^{th} to 90^{th} percentile of 4β,25$(OH)_2D_3$ concentrations, respectively, after simulation with 1,000 virtual subjects.

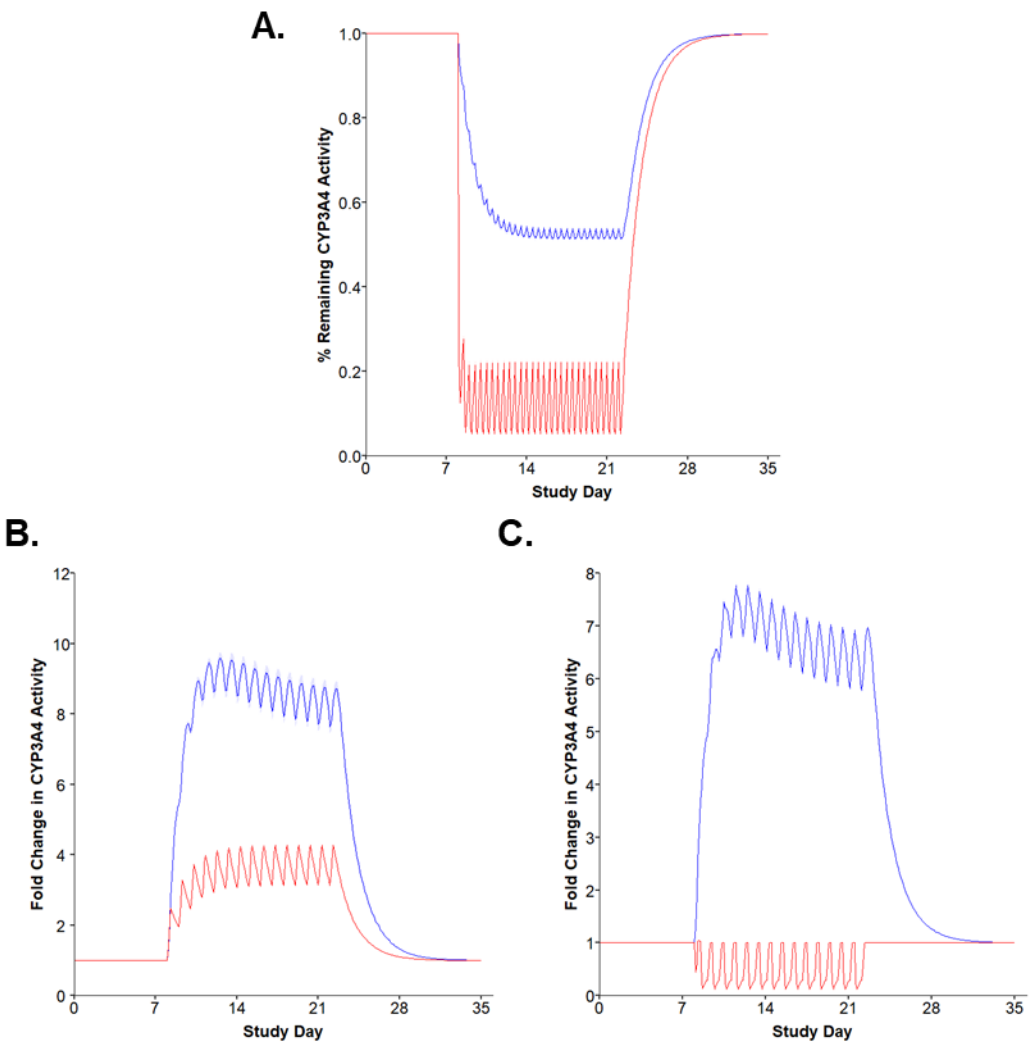

Figure 5.8: Predicted change in CYP3A4 activity treatment with A) 250 mg clarithromycin BID, B) 600 mg rifampin QD, and C) 250 mg clarithromycin BID in combination with 600 mg rifampin QD for 14 days (Study Day 8 – 21). The blue and red lines are the mean predicted change in hepatic and intestinal CYP3A4 activity, respectively.

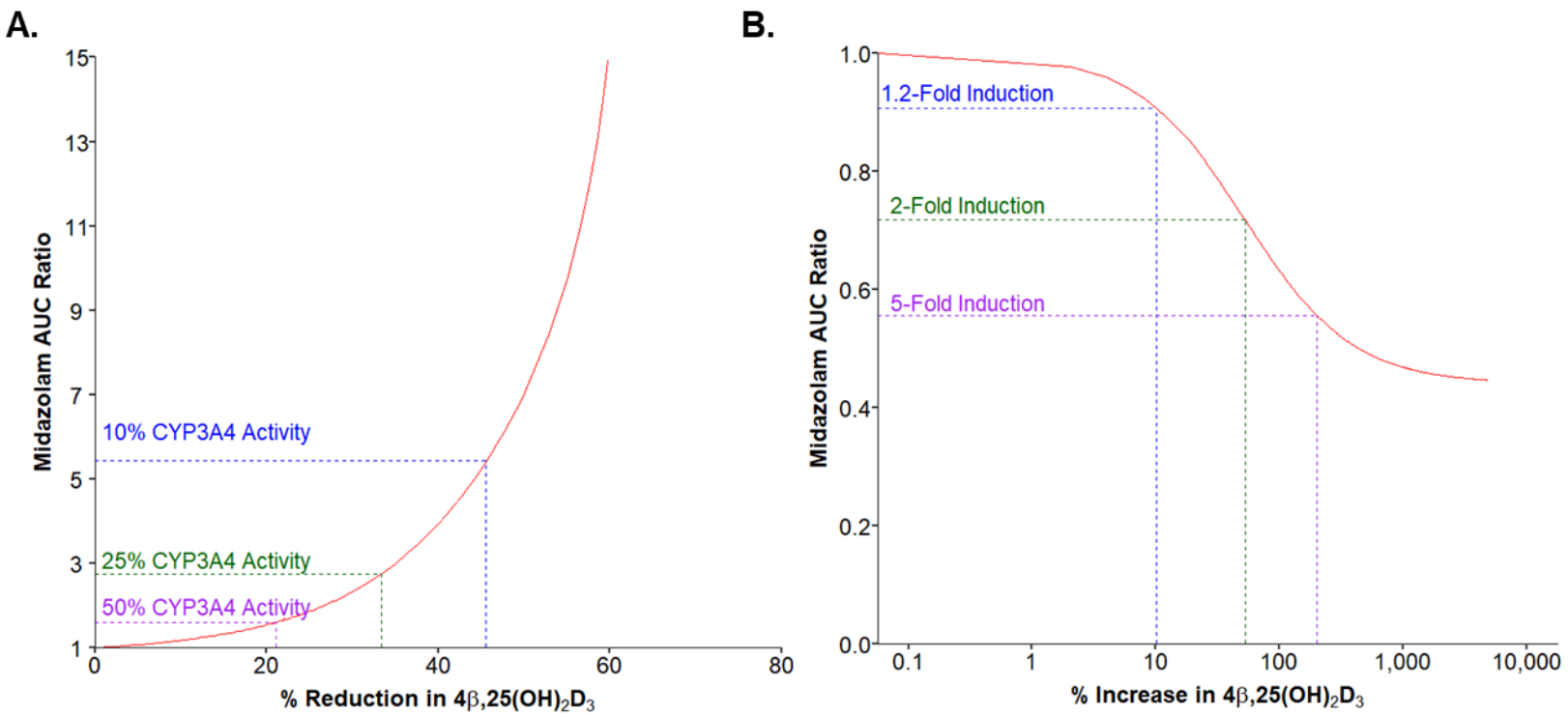

Figure 5.9: Dynamic range of 4β,25-dihydroxyvitamin D_3 (4β,25$(OH)_2D_3$) compared to midazolam after 14 days of treatment with theoretical CYP3A4 mechanism-based inhibitors and inducers. A) Fold increase in midazolam AUC vs. the predicted percent reduction in 4β,25$(OH)_2D_3$ concentration for a range of k_{inact} values. B) Relative decrease in midazolam AUC vs. the predicted percent increase in 4β,25$(OH)_2D_3$ concentration for a range of induction potentials. The red line is the relationship between midazolam AUC and 4β,25$(OH)_2D_3$. The dashed lines are provided as a reference for the change in CYP3A4 enzyme activity.

Chapter 6.

Conclusions

Vitamin D (cholecalciferol or ergocalciferol) is not biologically active and must undergo two sequential enzyme-catalyzed hydroxylations to form the active metabolite, 1α,25-hydroxyvitamin D (1α,25$(OH)_2$D), via the intermediate, 25-hydroxyvitamin D (25(OH)D) (1, 2). In addition to the formation of the 1α,25$(OH)_2D_3$, 25$(OH)D_3$ is metabolized to other metabolites, including 24,25-dihydroxyvitamin D_3 (24,25$(OH)_2D_3$), 4β,25-dihydroxyvitamin D_3 (4β,25$(OH)_2D_3$), 25-hydroxyvitamin D-3-O-sulfate (25$(OH)D_3$-S), and 25-hydroxyvitamin D-3-O-glucuronide (25$(OH)D_3$-G) (1-5). Changes in enzyme expression due to disease, ontogeny, or drug interactions may alter the circulating concentrations of 25$(OH)D_3$ and its metabolites and contribute to an increased risk of vitamin D deficiency. The aim of this dissertation was to explore mechanisms of altered vitamin D homeostasis in various populations.

6.1. Simultaneous Quantification of Vitamin D_2, Vitamin D_3, and Eight Hydroxylated Vitamin D Metabolites in Human Serum and Plasma by LC-MS/MS

In Chapter 2, we developed a method to accurately and reproducibly measure 25$(OH)D_3$ and its metabolites in human plasma and serum. We developed and validated a liquid chromatography-tandem mass spectrometry (LC-MS/MS) method for the simultaneous quantification of vitamin D_2, vitamin D_3, 25$(OH)D_2$, 25$(OH)D_3$, 1α,25$(OH)_2D_2$, 1α,25$(OH)_2D_3$, 24R,25$(OH)_2D_3$, 4β,25$(OH)_2D_3$, 1β,25$(OH)_2D_3$, and 1α,24,25$(OH)_3D_3$. We optimized the chromatographic separation of 1α,25$(OH)_2D_3$ from isomers with similar mass and ion fragmentation patterns. Two solid-phase extraction steps were used to isolate vitamin D metabolites of interest from human plasma and serum samples. The isolated metabolites were derivatized with (4'-dimethylaminophenyl)-1,2,4-triazoline-3,5-dione (DAPTAD) to improve analytical sensitivity. Despite its limitations (i.e., requiring a large sample volume (0.5 mL), time consuming extraction method, lengthy LC-MS/MS run times), this method can be used to

simultaneously quantify vitamin D and multiple metabolites in plasma or serum samples in order to investigate changes in vitamin D disposition. We applied this method to quantify vitamin D_2, vitamin D_3 and its metabolites in patients with cystic fibrosis (CF), healthy women in pregnancy, and to evaluate 4β,25$(OH)_2D_3$ as an endogenous biomarker of cytochrome P450 3A4 (CYP3A4) activity.

6.2. Altered Vitamin D Metabolism in Patients with Cystic Fibrosis

Achieving adequate vitamin D levels (≥ 30 ng/mL) in patients with CF is essential for maintaining bone strength and immune function (6, 7). In Chapter 3, we investigated the hypothesis that altered 25$(OH)D_3$ metabolism in patients with CF contributed to low circulating levels of 25$(OH)D_3$. To test our hypothesis, we measured circulating serum levels of 25$(OH)D_3$ and five metabolites in 83 CF patients and 82 matched healthy controls. Additionally, we assessed the pharmacokinetics of a single intravenous dose of deuterium-labeled 25-hydroxyvitamin D_3 (d_6-25$(OH)D_3$) in 5 patients with CF and 5 healthy controls.

In our study, the prevalence of 25(OH)D deficiency (i.e., 25(OH)D concentrations less than 30 ng/mL) in patients with CF (67%) was similar to the healthy controls (62%) and lower than previously reported rates of 85% to 90% (8, 9). These data suggest that recent efforts to increase vitamin D supplementation in patients with CF have resulted in improved 25(OH)D levels in this cohort. However, basal serum 1α,25$(OH)_2D_2$, 1α,25$(OH)_2D_3$, 4β,25$(OH)_2D_3$, and 25$(OH)D_3$-S concentrations were lower in patients with CF compared to healthy controls ($p < 0.001$). Although albumin concentrations were 9% lower in patients with CF compared to healthy subjects, we found no difference in the unbound concentration of 25$(OH)D_3$, estimated using published equations, between patients with CF and healthy controls. However, the unbound concentration of the biologically active metabolite, 1α,25$(OH)_2D_3$ was 10% lower in patients with CF compared to healthy controls ($p < 0.05$).

The pharmacokinetics of 25(OH)D_3 were ascertained in patients with CF and healthy controls following an intravenous bolus dose of d_6-25(OH)D_3. The estimated half-life of d_6-25(OH)D_3 was 16 days, similar to previous estimates of 2-3 weeks (2, 10). The clearance and volume of distribution of d_6-25(OH)D_3 were comparable between patients with CF and healthy controls. With only five participants in each group, our study was underpowered to detect small changes in these parameters. Although d_6-24,25(OH)D_3 concentrations were measurable, the concentrations were close to the limit of detection resulting in a high degree of variability. From the data available, the plasma d_6-24,25$(OH)_2D_3$ concentration-time profile appeared comparable between the two groups.

In conclusion, we found that patients with CF have lower serum concentrations of 1α,25$(OH)_2$D, 4β,25$(OH)_2D_3$, and 25(OH)D_3-S compared to healthy controls. The decreased 1α,25$(OH)_2$D concentration may have implications in maintaining bone health. Additionally, we found that patients with CF have 25(OH)D_3-normalized levels of 4β,25$(OH)_2D_3$ and 25(OH)D_3-S lower than healthy controls. Studies with a larger number of participants, higher doses of d_6-25(OH)D_3, more sensitive analytical methods, and quantification of other deuterated metabolites are needed to understand the effects of CF on 25(OH)D_3 disposition and metabolism.

6.3. An Observational Study of Longitudinal Changes in 25-Hydroxyvitamin D_3 and its Metabolites During Pregnancy and Postpartum

Biochemical and physiological changes that occur in pregnancy (i.e., changes in enzyme expression, cardiac output, protein binding, and placental enzyme expression) may alter the disposition of 25(OH)D_3 and its metabolites and the effectiveness of vitamin D supplementation therapy (11). In Chapter 4, we measured plasma concentrations of 25(OH)D_3 and five of its metabolites in a cohort of 15 pregnant women studied from pre-pregnancy through delivery and postpartum. Additionally, we characterized the serum vitamin D binding protein (VDBP) and albumin levels to assess changes in free 25(OH)D_3 and 1α,25$(OH)_2D_3$ concentrations over the

course of pregnancy. We used linear mixed-effects modeling to describe pregnancy-related changes in the plasma $25(OH)D_3$ and its metabolites.

Serum $25(OH)D_3$ concentrations increased by 45% from pre-pregnancy to 36 weeks of gestation ($p < 0.001$). Serum $1\alpha,25(OH)_2D_3$ concentrations increased quickly, plateaued early in the third trimester at greater than 2-fold that at baseline, and remained elevated through delivery ($p < 0.001$). $24,25(OH)_2D_3$ concentrations decreased 13% by week 8 of pregnancy and then rebounded until concentrations were 27% higher than baseline at 36 weeks of pregnancy ($p < 0.001$). $4\beta,25(OH)_2D_3$ and $25(OH)D_3$-G concentrations increased by 14% and 36%, respectively, at 36 weeks of gestation compared to pre-pregnancy (< 0.001). $25(OH)D_3$-S concentrations decreased throughout pregnancy (25% lower at 36 weeks compared to pre-pregnancy) ($p < 0.001$). VDBP levels increased nearly 2-fold during pregnancy, whereas albumin levels decreased by 26% ($p < 0.001$). Consequently, unbound $25(OH)D_3$ concentrations decreased by 20% from pre-pregnancy to 36 weeks of gestation, resulting in an overall 41% decrease in the percent unbound of $25(OH)D_3$ ($p < 0.001$).

Despite CYP3A4 and UGT1A4 activity increasing more than two-fold during pregnancy, we only observed a 14% and 38% increase in $4\beta,25(OH)_2D_3$ and $25(OH)D_3$-G concentrations, respectively (12, 13). $25(OH)D_3$ is a low extraction ratio drug, thus changes in hepatic clearance are driven by changes in enzyme expression and the unbound fraction of $25(OH)D_3$. The decrease in free fraction and the unbound concentration of $25(OH)D_3$ may explain why the increases in $4\beta,25(OH)_2D_3$ and $25(OH)D_3$-G concentrations were not as significant as expected, given the expected increase in CYP3A4 and UGT1A4 activity. In contrast, $1\alpha,25(OH)_2D_3$ is formed in the kidney. Unlike the liver, $25(OH)D_3$ distribution to the kidney does not follow the free-drug hypothesis, which assumes that only unbound $25(OH)D_3$ can diffuse through plasma membranes (14, 15). Uptake of $25(OH)D_3$ into tubular epithelial cells is supported by megalin/cubulin-mediated transcytosis of the VDBP-$25(OH)D_3$ complex in urine filtrate. We hypothesize that as VDBP concentrations increase during pregnancy, more $25(OH)D_3$ can be

delivered to CYP27B1 in the proximal tubule cells of the kidneys and be converted to 1α,25$(OH)_2D_3$. In addition, increased renal blood flow and glomerular filtration of VDBP-25$(OH)D_3$ may contribute to increased 1α,25$(OH)_2D_3$ formation during pregnancy (16).

6.4. A Semi-Mechanistic Modeling Approach Evaluating 4β,25-dihydroxyvitamin D_3 as a Potential Biomarker of CYP3A4 Inhibition and Induction

In Chapter 5, we investigated the use of 4β,25$(OH)_2D_3$ as a potential biomarker of CYP3A4 activity by developing a semi-mechanistic model describing CYP3A4 induction and inhibition. Understanding the sensitivity, specificity, and time-scale of a biomarker is essential for implementation into clinical drug development. Plasma concentrations of 4β,25$(OH)_2D_3$ and 25$(OH)D_3$ were measured before, during, and after treatment with water (control arm), rifampin (CYP3A4 inducer), clarithromycin (mechanism-based inhibitor (MBI) of CYP3A4), or rifampin and clarithromycin in combination. The 4β,25$(OH)_2D_3$ and 25$(OH)D_3$ data from this study, along with previously published *in vitro* and *in vivo* data, were used to build semi-mechanistic PKPD models of midazolam, rifampin, clarithromycin, 25$(OH)D_3$ and 4β,25$(OH)_2D_3$. Due to the limited knowledge about the pharmacokinetics of 25$(OH)D_3$ and 4β,25$(OH)_2D_3$, many assumptions were incorporated during model development. These assumptions included a constant synthesis rate of 25$(OH)D_3$ and that treatment with clarithromycin and rifampin did not change non-CYP3A4 clearance or catabolism of 4β,25$(OH)_2D_3$. Midazolam was incorporated into the model to verify the inhibitory and inductive effects of clarithromycin and rifampin, respectively, before fitting the model to study data. Models were verified with published clinical data and midazolam was used to compare the change in 4β,25$(OH)_2D_3$ concentrations relative to a “gold standard” probe of CYP3A4 activity.

Following treatment with strong MBIs, we predicted that at 50% of baseline CYP3A4 activity, 4β,25$(OH)_2D_3$ concentrations would decrease by ~20%. Similarly, a 90% decrease in hepatic CYP3A4 enzyme activity would decrease 4β,25$(OH)_2D_3$ concentrations by nearly 50%.

For CYP3A4 induction, 4β,25(OH)$_2$D$_3$ is likely able to detect moderate and strong inducers. For CYP3A4 induction, we predicted that 4β,25(OH)$_2$D$_3$ concentrations would increase by ~10% and ~50% for a 1.2-fold and 2-fold increase in CYP3A4 enzyme activity, respectively. A 5-fold increase in CYP3A4 activity, similar to what is observed with rifampin, would result in a 2-fold increase in 4β,25(OH)$_2$D$_3$ concentrations. The predicted changes in 4β,25(OH)$_2$D$_3$ concentrations after induction are similar to those predicted for 4β-hydroxycholesterol (4β(OH)C) (17).

Although, more supporting evidence is required before 4β,25(OH)$_2$D$_3$ testing can be routinely implemented into clinical studies, our modeling suggests that 4β,25(OH)$_2$D$_3$ can be used as endogenous biomarker to detect strong MBIs and moderate or strong inducers of CYP3A4.

6.5. Final Conclusions and Future Directions

In this body of work, we demonstrated that the characterization of 25(OH)D$_3$ metabolites in systemic plasma or serum samples is a useful tool for evaluating altered vitamin D metabolism in populations at risk for vitamin D deficiency and insufficiency, including patients with CF and pregnant women. Such data can be used to generate hypotheses of altered 25(OH)D$_3$ metabolic pathways, which can be investigated in future *in vitro* and *in vivo* studies.

Following the IV administration of deuterium-labeled 25(OH)D$_3$, we found only minor differences in its elimination by patients with CF and controls, suggesting that vitamin D deficiency in CF is the result of aberrant pro-hormone absorption. However, more sensitive analytical instrumentation is required to fully characterize the metabolites of deuterium-labeled 25(OH)D$_3$. Moreover, given the long half-life of 25(OH)D$_3$ and its metabolites, sample collection must continue for at least 56 days or possibly longer. Studies in which deuterated vitamin D$_3$ is given intravenously and orally may further our knowledge of the mechanisms for differences in vitamin D disposition in patients with CF, whether it be due to differences in oral bioavailability,

hydroxylation pathways, or other factors. This information could be useful in helping design better supplementation methods for patients with CF to maintain adequate levels of 25(OH)D_3.

As described in our pregnancy study, the unbound concentration of 25(OH)D_3 was very sensitive to changes in the concentration of albumin and VDBP. Because the hepatic intrinsic clearance of 25(OH)D_3 can be altered by changes in enzyme expression and plasma protein binding, routine monitoring of serum albumin and VDBP should be considered as part of vitamin D supplementation therapy during pregnancy and postpartum. Although we were able to analyze VDBP and albumin, and subsequently calculate unbound 25(OH)D_3 and 1α,25$(OH)_2D_3$ concentrations at 6 weeks postpartum, more intensive sampling during the postpartum may allow for improved understanding of the complex interaction of enzyme expression, protein binding and vitamin D metabolism in women after delivery.

We determined that 4β,25$(OH)_2D_3$ has potential as a biomarker of CYP3A4. However, more clinical data and validation are needed before it can be routinely implemented into clinical studies. Specifically, the dynamic range of 4β,25$(OH)_2D_3$ should be assessed in clinical studies to verify and improve the model predictions. For example, studies should be conducted by treating healthy subjects with a range of rifampin doses for 14 days as was done for 4β(OH)C (18-21). If 4β,25$(OH)_2D_3$ is to be implemented in crossover studies, there must be high confidence in the half-life of 4β,25$(OH)_2D_3$ to ensure baseline is reached prior to beginning the next stage of the study. More data need to be collected to understand the factors which contribute to the intra- and inter-subject variability in 4β,25$(OH)_2D_3$ formation and elimination.

Finally, 25(OH)D_3 and its metabolites (i.e., 24,25$(OH)_2D_3$, 4β,25$(OH)_2D_3$, 25(OH)D_3-S, and 25(OH)D_3-G) may be useful endogenous biomarkers of other metabolic pathways. As 25(OH)D_3-G concentrations increased due to UGT1A4 induction during pregnancy, investigation of 25(OH)D_3-G as a biomarker of UGT1A4 activity should be considered. However, it has been hypothesized that 25(OH)D_3-S and 25(OH)D_3-G undergo enterohepatic recirculation and can be deconjugated as an additional source of 25(OH)D_3 (22). Work should be done to understand the

biological role of 25(OH)D_3-S and 25(OH)D_3-G, as loss of the conjugated metabolites could be a cause of low circulating levels of 25(OH)D_3, but also confound their use as endogenous biomarkers. Although there are still many unanswered questions, the research presented in this dissertation furthers our understanding of vitamin D disposition in health and disease and provides more insight into the complexity of vitamin D homeostasis.

6.6. Reference

(1) Bikle, D. Vitamin D: Production, Metabolism, and Mechanisms of Action. In: Endotext (eds. Feingold, K.R., Anawalt, B., Boyce, A., Chrousos, G., Dungan, K., Grossman, A. et al.) (South Dartmouth (MA), 2000).

(2) Bikle, D.D. Vitamin D metabolism, mechanism of action, and clinical applications. Chem Biol 21, 319-29 (2014).

(3) Christakos, S., Ajibade, D.V., Dhawan, P., Fechner, A.J. & Mady, L.J. Vitamin D: metabolism. Endocrinol Metab Clin North Am 39, 243-53, table of contents (2010).

(4) Gallagher, J.C. & Bikle, D.D. Vitamin D: Mechanisms of Action and Clinical Applications. Endocrinol Metab Clin North Am 46, xvii-xviii (2017).

(5) Sakaki, T., Kagawa, N., Yamamoto, K. & Inouye, K. Metabolism of vitamin D3 by cytochromes P450. Front Biosci 10, 119-34 (2005).

(6) Konstantinidis, I. et al. Vitamin D(3) deficiency and its association with nasal polyposis in patients with cystic fibrosis and patients with chronic rhinosinusitis. American journal of rhinology & allergy 31, 395-400 (2017).

(7) Tangpricha, V. et al. The Vitamin D for Enhancing the Immune System in Cystic Fibrosis (DISC) trial: Rationale and design of a multi-center, double-blind, placebo-controlled trial of high dose bolus administration of vitamin D3 during acute pulmonary exacerbation of cystic fibrosis. Contemporary clinical trials communications 6, 39-45 (2017).

(8) West, N.E. et al. Appropriate goal level for 25-hydroxyvitamin D in cystic fibrosis. Chest 140, 469-74 (2011).

(9) Donovan, D.S., Jr. et al. Bone mass and vitamin D deficiency in adults with advanced cystic fibrosis lung disease. American journal of respiratory and critical care medicine 157, 1892-9 (1998).

(10) Bikle, D.D. Vitamin D and bone. Curr Osteoporos Rep 10, 151-9 (2012).

(11) Isoherranen, N. & Thummel, K.E. Drug metabolism and transport during pregnancy: how does drug disposition change during pregnancy and what are the mechanisms that cause such changes? Drug Metab Dispos 41, 256-62 (2013).

(12) Karanam, A. et al. Lamotrigine clearance increases by 5 weeks gestational age: Relationship to estradiol concentrations and gestational age. Ann Neurol 84, 556-63 (2018).

(13) Hebert, M.F. et al. Effects of pregnancy on CYP3A and P-glycoprotein activities as measured by disposition of midazolam and digoxin: a University of Washington specialized center of research study. Clin Pharmacol Ther 84, 248-53 (2008).

(14) Tsuprykov, O., Chen, X., Hocher, C.F., Skoblo, R., Lianghong, Y. & Hocher, B. Why should we measure free 25(OH) vitamin D? J Steroid Biochem Mol Biol 180, 87-104 (2018).

(15) Chapron, B.D. et al. Reevaluating the role of megalin in renal vitamin D homeostasis using a human cell-derived microphysiological system. ALTEX 35, 504-15 (2018).

(16) Anderson, G.D. Pregnancy-induced changes in pharmacokinetics: a mechanistic-based approach. Clin Pharmacokinet 44, 989-1008 (2005).

(17) Leil, T.A., Kasichayanula, S., Boulton, D.W. & LaCreta, F. Evaluation of 4beta-Hydroxycholesterol as a Clinical Biomarker of CYP3A4 Drug Interactions Using a Bayesian Mechanism-Based Pharmacometric Model. CPT: pharmacometrics & systems pharmacology 3, e120 (2014).

(18) Jones, B.C. et al. Managing the Risk of CYP3A Induction in Drug Development: A Strategic Approach. Drug Metab Dispos 45, 35-41 (2017).

(19) Bjorkhem-Bergman, L. et al. Comparison of endogenous 4beta-hydroxycholesterol with midazolam as markers for CYP3A4 induction by rifampicin. Drug Metab Dispos 41, 1488-93 (2013).

(20) Bjorkhem-Bergman, L. et al. Quinine compared to 4beta-hydroxycholesterol and midazolam as markers for CYP3A induction by rifampicin. Drug Metab Pharmacokinet 29, 352-5 (2014).

(21) Kanebratt, K.P. et al. Cytochrome P450 induction by rifampicin in healthy subjects: determination using the Karolinska cocktail and the endogenous CYP3A4 marker 4beta-hydroxycholesterol. Clin Pharmacol Ther 84, 589-94 (2008).

(22) Gao, C. et al. Simultaneous quantification of 25-hydroxyvitamin D3-3-sulfate and 25-hydroxyvitamin D3-3-glucuronide in human serum and plasma using liquid chromatography-tandem mass spectrometry coupled with DAPTAD-derivatization. J Chromatogr B Analyt Technol Biomed Life Sci 1060, 158-65 (2017).